Calcium-aktivierte Kaliumkanäle vom BK_{Ca}- und IK_{Ca}-Typ regulieren radioinduzierte Migration sowie Radiosensitivität von Glioblastomzellen

DISSERTATION

der Mathematisch-Naturwissenschaftlichen Fakultät

der Eberhard Karls Universität Tübingen

zur Erlangung des Grades eines

Doktors der Naturwissenschaften (Dr. rer. nat.)

vorgelegt von

Lena Maria Edalat, geb. Butz

aus Berlin

Tübingen 2016

Gedruckt mit Genehmigung der Mathematisch-Naturwissenschaftlichen Fakultät der Eberhard Karls Universität Tübingen.

Tag der mündlichen Qualifikation:	04.05.2016
Dekan:	Prof. Dr. rer. nat. Wolfgang Rosenstiel
1. Berichterstatter:	Prof. Dr. rer. nat. Peter Ruth
2. Berichterstatter:	Prof. Dr. rer. nat. Stephan M. Huber

Die Wissenschaft fängt eigentlich erst da an, interessant zu werden, wo sie aufhört.

Justus von Liebig

Inhaltsverzeichnis

Abkürzungsverzeichnis

AMD3100	CXCR4 Inhibitor, Plerixafor
AQP	Aquaporin
BK_{Ca}	Calcium-aktivierter Kaliumkanal mit großer Leitfähigkeit („big conductance“)
Ca^{2+}	Calciumion
CaMKII	Calcium/Calmodulin-abhängige Proteinkinase II
cAMP	cyclisches Adenosinmonophosphat
CD133	Prominin-1, Krebsstammzellmarker
cdc2	„cell division cycle protein 2 homolog“
cGMP	cyclisches Guanosinmonophophat
Cl^-	Chloridion
ClC-3	Chloridkanal
CO	Kohlenstoffmonoxid
CXCL12	SDF-1, „stromal cell derived factor 1“
CXCR4	CXC-Motiv-Chemokinrezeptor 4, „stromal cell derived factor 1 recetor“
DNA	Desoxyribonukleinsäure
EdU	5-Ethynyl-2’-Desoxyuridin
EGFR	„epidermal growth factor receptor“
E_K	Kalium-Gleichgewichtspotential
ELISA	„enzyme-linked immunosorbent assay“
ER	Endoplasmatisches Retikulum
gBK	glioma BK
γH_2AX	phosphoryliertes Histon H_2AX
Gy	Gray
H^+	Wasserstoffion
H_2O	Wasser
HIF-1α	Hypoxie-induzierter-Faktor-1α“
ICA 17043	Senicapoc
IDH1	Isocitrat-Dehydrogenase 1

IK1	Calcium-aktivierter Kaliumkanal mit mittlerer Leitfähigkeit („intermediate conductance“)
IK_{Ca}	Calcium-aktivierter Kaliumkanal mit mittlerer Leitfähigkeit („intermediate conductance“)
i.p.	intraperitoneal
IP_3	Inositoltrisphophat
IR	„ionizing radiation“
IUPHAR	„International Union of Basic and Clinical Pharmacology“
K^+	Kaliumion
KCl	Kaliumchlorid
K_{Ca}	Calcium-aktivierter Kaliumkanal
K_{Ca}1.1	Calcium-aktivierter Kaliumkanal mit großer Leitfähigkeit („big conductance“)
K_{Ca}3.1	Calcium-aktivierter Kaliumkanal mit mittlerer Leitfähigkeit („intermediate conductance“)
KG	Körpergewicht
MaxiK	Calcium-aktivierter Kaliumkanal mit großer Leitfähigkeit („big conductance“)
Mg^{2+}	Magnesiumion
MGMT	O6-Methylguanin-DNA-Methyltransferase
MMP-2	Matrixmetalloprotease 2
MMP-9	Matrixmetalloprotease 9
mRNA	**„**messenger“ Ribonukleinsäure
n	Anzahl
Na^+	Natriumion
NaCl	Natriumchlorid
NKCCl	$Na^+/K^+/Cl^-$-Kotransporter
NS1608	BK_{Ca}-Kanalaktivator
NS1619	BK_{Ca}-Kanalaktivator
NSG	NOD-*scid* IL2Rgamma^{null} Maus
Orai1	calcium release-activated calcium channel protein 1
OS	„overall survival“, Gesamtüberleben
PFS	„progression free survival“, progressionsfreies Überleben

pH	negativ dekadischer Logarithmus der Wasserstoffionenaktivität
PIP_2	Phophatidylinositol-4,5-bisphophonat
PLC	Phospholipase C
qRT-PCR	„quantitative real time polymerase chain reaction“, quantitative Echtzeit Polymerase-Kettereaktion
RCK1	regulatory of conductance of K^+
SDF-1	CXCL12, „stromal cell derived factor 1“
shRNA	„small hairpin“ Ribonukleinsäure
SK4	Calcium-aktivierter Kaliumkanal mit mittlerer Leitfähigkeit („intermediate conductance“)
Slo1	Calcium-aktivierter Kaliumkanal mit großer Leitfähigkeit („big conductance“)
STIM	„stromal interaction molecule“, Calciumsensor
SVGA	embryonale Astrozytenzelllinie
T98G	humane Glioblastomzellline
TCGA	„Cancer Genome Atlas“
TRAM34	IK_{Ca}-Kanalinhibitor, 1-[(2-Chlorophenyl)diphenylmethyl]-1*H*-pyrazol
TRPC1	**„**transient receptor potential channel subfamily C member 1“
TRPM8	„transient receptor potential channel subfamily M member 8“
U-87MG	humane Glioblastomzelllinie
U-87MG-Kat	humane Glioblastomzelllinie transfiziert mit rotem Fluoreszenzprotein Katushka
WHO	„World Health Organization“

Zusammenfassung

Glioblastome gehören zu den häufigsten und bösartigsten primären Hirntumoren beim Erwachsenen. Dies ist vor allem auf den stark migrativen und invasiven Phänotyp der Glioblastomzellen zurückzuführen. Bereits bei einem kleinen Tumor kann man davon ausgehen, dass sich einzelne Tumorzellen im ganzen Gehirn verteilt haben. Den Tumor vollständig durch eine Operation bzw. Strahlentherapie zu entfernen ist durch die Streuung praktisch unmöglich. Es ist bekannt, dass hauptsächlich die Zellvolumenänderungen der Glioblastomzellen für die Migration der Tumorzellen durch das Gehirn verantwortlich sind. Um zu schrumpfen, pumpen die Zellen einen Großteil des ungebundenen Zellwassers aus der Zelle heraus. Damit Wasser osmotisch über Aquaporine herausströmt, muss zuvor Kaliumchlorid die Zelle verlassen. Vor allem BK_{Ca}-Kanäle sind an der Volumenregulation der Zellen beteiligt. Bisher war bekannt, dass *in vitro* sowohl die Offenwahrscheinlichkeit der BK_{Ca}-Kanäle als auch die Migration der Zellen nach Bestrahlung erhöht ist. Der erste Teil der vorliegenden Arbeit beschäftigt sich mit dem zugrundeliegenden Mechanismus der radioinduzierten Migration nach BK_{Ca}-Kanalaktivierung und ob diese BK_{Ca}-Kanalabhängige radioinduzierte Migration auch in einem orthotopen Mausmodell zu sehen ist. Es konnte gezeigt werden, dass Bestrahlung zu einer verstärkten Expression des SDF-1-Proteins führte, was wiederum intrazelluläres Ca^{2+} ansteigen lässt. Zusätzlich resultierte daraus eine Ca^{2+}-aktivierte BK_{Ca}-Kanalaktivierung. Sowohl SDF-1 als auch konditioniertes Medium bestrahlter Zellen führte in unbestrahlten Zellen, wie die Bestrahlung an sich, zu einer verstärkten Migration der Zellen. Die radioinduzierte Migration konnte durch eine BK_{Ca}-Kanalblockade mit Paxillin gehemmt werden. In einem orthotopen Glioblastommausmodell ließ sich nach Bestrahlung eine verstärkte Migration der Glioblastomzellen durch das Gehirn beobachten, die auch hier mit Paxillin blockiert werden konnte.

Nicht nur BK_{Ca}-Kanäle sondern auch IK_{Ca}-Kanäle sind an der Tumorgenese bzw. Malignität der Glioblastome beteiligt. Es ist bekannt, dass IK_{Ca}-Kanäle in Glioblastomen hochreguliert sind und dass diese Tatsache mit einem schlechteren Überleben der Patienten einhergeht. Im zweiten Teil dieser Arbeit wurde daher die Funktion der IK_{Ca}-Kanäle bei der Radioresistenz von Glioblastomzellen näher untersucht. Wie schon bei den BK_{Ca}-Kanälen beobachtet, führte Bestrahlung auch bei IK_{Ca}-Kanälen zu einer erhöhten

Offenwahrscheinlichkeit, die aus dem Anstieg der intrazellulären Ca^{2+}-Spiegel resultierte. Die verstärkte Aktivierung der IK_{Ca}-Kanäle führte dann zu einem vorübergehenden G_2/M-Arrest der Zellen. Durch die Blockade der IK_{Ca}-Kanäle mit TRAM-34 konnte der G_2/M-Arrest weitestgehend unterbunden werden. TRAM-34 erhöhte zusätzlich die residualen DNA-Doppelstrangbrüche nach Bestrahlung und führte zu einer Radiosensitivierung der Glioblastomzellen. Der Effekt von TRAM-34 während der Bestrahlung konnte durch eine retrovirale Herunterregulation der IK_{Ca}-Kanäle bestätigt werden. Vor allem konnte die Kombination der IK_{Ca}-Kanalblockade mit der fraktionierten Bestrahlung das Glioblastomwachstum in einem ektopen Mausmodell verlangsamen.

Zusammenfassend machen diese Daten deutlich, dass IK_{Ca}- und BK_{Ca}-Kanäle eine Schlüsselrolle in Bezug auf das Überleben von Glioblastompatienten bzw. die Ausbreitung des Tumors nach Bestrahlung einnehmen. IK_{Ca}- und BK_{Ca}-Kanäle könnten also neue, vielversprechende Zielstrukturen in der Glioblastomtherapie werden.

Summary

Glioblastoma multiforme is the most frequent and most aggressive primary brain tumor in adults. This is probably due to the highly migratory and invasive phenotype of the glioblastoma cells. Already in small tumors one can assume that glioblastoma cells have spread throughout the brain at the time of diagnosis. Therefore, elimination of the whole tumor by surgery and radiotherapy is not possible in the vast majority of patients. Migration and brain invasion of glioblastoma cells requires efficient cell volume changes. Glioblastoma cells accomplish regulatory volume decrease by loss of K^+ and Cl^- ions and osmotically obliged water. In particular, BK_{Ca} channels are involved in the volume decrease of glioblastoma cells.

A previous report suggested that irradiation leads to an increase of the open probability of BK_{Ca} channels followed by enhanced migration of glioblastoma cells *in vitro*. The first part of the doctoral thesis analyzed the underlying mechanisms of radiation-induced migration after BK_{Ca} channel activation. In addition, this project addressed the question whether or not radiation-induced and BK_{Ca} channel-dependent migration also occurs *in vivo* in an orthotopic glioblastoma mouse model. As a result, irradiation increased the expression of SDF-1 which led to an increase of intracellular Ca^{2+}. The increased Ca^{2+} levels in turn stimulated activation of BK_{Ca} channels. SDF-1 as well as conditioned medium from irradiated cells stimulated migration of unirradiated cells similar as irradiation does. Radiation-induced migration could be blocked with the BK_{Ca} channel inhibitor paxilline. In the orthotopic glioblastoma mouse model ionizing radiation stimulated and BK_{Ca} channel targeting by paxilline inhibited infiltration of the brain by glioblastoma cells similarly to the radiation-induced migration observed *in vitro*.

Besides BK_{Ca}, IK_{Ca} channels are involved in the tumorigenesis and malignancy of glioblastomas. Reportedly, IK_{Ca} channels are upregulated in glioblastomas and overexpression correlates with a poor prognosis of glioblastoma patients. The second part of the doctoral thesis addressed the potential role of IK_{Ca} channels in radioresistance of glioblastoma cells. Similar to BK_{Ca}, ionizing radiation increased the open probability of IK_{Ca} channels. Again, the activation of these channels resulted from increased intracellular levels of Ca^{2+}. Increased IK_{Ca} channel activity, in turn, contributed to a transient G_2/M arrest of the

irradiated glioblastoma cells. TRAM-34, an IK_{Ca} channel inhibitor, overrode the G_2/M arrest and increased the number of residual double strand breaks in irradiated glioblastoma cells leading to radiosensitization. Retroviral down regulation of IK_{Ca} channels mimicked the effect of TRAM-34. Notably, IK_{Ca} channel targeting combined with fractionated radiation delayed glioblastoma growth in the orthotopic mouse model.

Together, these data suggest a pivotal function of IK_{Ca} and BK_{Ca} channels for survival and spreading of irradiated glioblastoma cells, respectively. Therefore, targeting of IK_{Ca} and BK_{Ca} channels might be a promising new strategy for anti-glioblastoma therapy.

Liste der Publikationen der Dissertation

Bei der vorliegenden Arbeit handelt es sich um eine kumulative Dissertation. Übersichtsarbeiten und Forschungsergebnisse sind bereits in folgenden Fachzeitschriften veröffentlicht:

1. **Edalat L, Stegen B, Klumpp L, Haehl E, Schilbach K, Lukowski R, Kühnle M, Bernhardt G, Buschauer A, Zips D, Ruth P, Huber SM (2016).**
   BK K^+ channel blockade inhibits radiation-induced migration/brain infiltration of glioblastoma cells. *Oncotarget* 7423.

2. **Stegen B, Butz L, Klumpp L, Zips D, Dittmann K, Ruth P, Huber SM (2015).**
   Ca^{2+}-Activated IK K^+ Channel Blockade Radiosensitizes Glioblastoma Cells.
   Mol Cancer Res 13:1283-1295.

3. **Huber SM, Butz L, Stegen B, Klumpp L, Klumpp D, Eckert F (2014).**
   Role of ion channels in ionizing radiation-induced cell death.
   Biochim Biophys Acta 1848:2657-2664.

4. **Huber SM, Butz L, Stegen B, Klumpp D, Braun N, Ruth P, Eckert F (2013).**
   Ionizing radiation, ion transports, and radioresistance of cancer cells.
   Front Physiol 4:212.

Beschreibung der Bedeutung der Eigenanteile

Lena Edalat, Benjamin Stegen, Lukas Klumpp, Erik Haehl, Karin Schilbach, Robert Lukowski, Matthias Kühnle, Günther Bernhardt, Armin Buschauer, Daniel Zips, Peter Ruth and Stephan M. Huber (2016).

BK K^+ channel blockade inhibits radiation-induced migration/brain infiltration of glioblastoma cells. *Oncotarget* 7423.

Die gesamte Arbeit entstand unter der Leitung von Stephan M. Huber und Peter Ruth. Die Zelllinie U-87MG wurde von Matthias Kühnle unter der Leitung von Armin Buschauer und Günther Bernhardt im Rahmen seiner Doktorarbeit mit dem Fluoreszenzprotein Katushka transfiziert und charakterisiert. Die Mäuse wurden uns von Karin Schilbach zur Verfügung gestellt. Patch-Clamp-Messungen, Koloniebildungsassays, Calciummessungen, ELISAs und Western Blots wurden von Benjamin Stegen mit teilweiser Unterstützung der technischen Assistenten Ilka Müller und Heidrun Faltin durchgeführt. Die Messungen zur Untersuchung der *in vitro* Migration und die Immunfluoreszenzfärbungen von Zellen habe ich teilweise mit Unterstützung von Benjamin Stegen und Erik Haehl ausgeführt und ausgewertet. Die mRNA-Expressionsanalysen wurden von mir in Zusammenarbeit mit Lukas Klumpp angefertigt. Alle *in vivo* Experimente (orthotopes Glioblastommausmodell) habe ich unter Anleitung von Stephan M. Huber, Peter Ruth und Hilfe von Armin Buschauer und Günther Bernhardt etabliert und ausgeführt. Die Auswertung der ausgewanderten Zellen und die Immunfluoreszenzfärbungen der Gehirnkryoschnitte erfolgten ebenfalls durch mich. Robert Lukowski und Daniel Zips leisteten ihren Beitrag durch wissenschaftliche Diskussion, Design und Korrektur der Arbeit.

Benjamin Stegen, Lena Butz, Lukas Klumpp, Daniel Zips, Klaus Dittmann, Peter Ruth and Stephan M. Huber (2015).

Ca^{2+}-Activated IK K^+ Channel Blockade Radiosensitizes Glioblastoma Cells. *Mol Cancer Res* 13:1283-1295.

Die gesamte Arbeit entstand unter der Leitung von Stephan M. Huber und Peter Ruth. Die Patch-Clamp-Messungen, Calciummessungen, Western Blots, Koloniebildungsassays und Durchflusszytometrie wurden von Benjamin Stegen mit Unterstützung der technischen

Assistenten Ilka Müller und Heidrun Faltin durchgeführt. Die γH_2AX-Foci Bestimmungen wurden unter Anleitung von Klaus Dittmann angefertigt. Des Weiteren war Klaus Dittmann an Diskussion und Korrektur beteiligt. Die lentivirale Herunterregulation des IK_{Ca}-Kanals wurde von Lukas Klumpp ausgeführt und charakterisiert. Die Immunfluoreszenzfärbungen und die *in vivo* Versuche (ektopes Glioblastommausmodell) habe ich etabliert, durchgeführt und ausgewertet. Daniel Zips leistete seinen Beitrag durch wissenschaftliche Diskussion, Design und Korrektur der Arbeit.

1 Einleitung

1.1 Glioblastom

Glioblastome sind die häufigste und bösartigste Form von Hirntumoren im Erwachsenenalter. Die Inzidenz beträgt drei bis vier Neuerkrankungen pro Jahr auf 100.000 Einwohner. Das durchschnittliche Erkrankungsalter bei primären Glioblastomen liegt bei 62 Jahren. Dagegen treten Glioblastome, die sekundär aus anderen Hirntumorarten entstehen, schon bei Patienten mit durchschnittlich 45 Jahren auf (Louis et al., 2007).

Glioblastome gehören zu den Astrozytomen und stammen von Vorläuferzellen der Gliazellen ab. Sie entstehen überwiegend in den supratentoriellen Regionen des Gehirns (Frontal-, Temporal-, Parietal- und Okzipitallappen) und werden von der „World Health Organization“ (WHO) als Grad IV Tumoren klassifiziert (siehe Tabelle 1) (Thakkar et al., 2014). Das bedeutet, dass Glioblastome äußerst bösartige Tumoren sind, und Patienten, die an einem Glioblastom erkrankt sind, mit einer deutlichen Reduktion ihrer Lebenserwartung rechnen müssen. Unter primären Glioblastomen versteht man Glioblastome, die de novo entstehen. Sie sind die häufigere Variante des Glioblastoms. Bei einem sekundären Glioblastom handelt es sich hingegen um ein Glioblastom, welches sich mit der Zeit aus einem niedriggradigeren Astrozytom oder Oligodendrogliom entwickelt. Diese machen lediglich 5 % aller Glioblastome aus (Ohgaki et al., 2004).

Betrachtet man die Risikofaktoren des Glioblastoms genauer, so wird deutlich, dass es eine Vielzahl von genetischen als auch äußeren Faktoren gibt, die eine Entstehung des Tumors beeinflussen können. Es zeichnet sich jedoch ab, dass bis heute kein Risikofaktor bekannt ist, der hauptsächlich für die Erkrankung an einem Glioblastom verantwortlich ist (Wrensch et al., 2002).

Astrozytäre Tumoren	I	II	III	IV
Subependymales Riesenzellastrozytom	x			
Pilozystisches Astrozytom	x			
Pilomyxoides Astrozytom		x		
Diffuses Astrozytom		x		
Pleomorphes Xanthoastrozytom		x		
Anaplastisches Astrozytom			x	
Glioblastom				X
Riesenzellglioblastom				X
Gliosarkom				X

Tabelle 1 WHO Klassifikation astrozytärer Tumoren (Louis et al., 2007)

1.1.1 Therapie und Prognose des Glioblastoms

Neu diagnostizierte Glioblastome werden, bei Patienten unter 70 Jahren, standardmäßig reseziert. Da sich Glioblastome jedoch durch ein stark invasives und infiltratives Wachstum auszeichnen, ist die vollständige Entfernung des Tumors in der Praxis nicht möglich. Postoperativ sollte daher immer eine Bestrahlung der Operationsränder mit einer zusätzlichen systemischen Chemotherapie mit Temozolomid (Temodal®) folgen.

Am besten profitieren Patienten mit einem methylierten MGMT-Promoter von der Kombination aus Radiotherapie und Temozolomid (Stupp et al., 2009). Bei MGMT handelt es sich um die O6-Methylguanin-DNA-Methyltransferase, einem Protein, das der Reparatur von DNA-Schäden dient. Da die zytostatische Wirkung von Temozolomid hauptsächlich auf eine Schädigung der DNA durch Methylierung der O6-Position des Guanins beruht, ist bei Patienten mit methyliertem MGMT-Promoter (d.h. einer verringerten MGMT-Expression) die DNA-Reparaturaktivität im Tumorgewebe verringert. Der methylierte MGMT-Promoter ist in ca. 50 % aller Glioblastome zu finden (Thakkar et al., 2014).

Zusätzlich zu einer Antitumortherapie muss immer auch eine gute Supportivtherapie erfolgen. Viele Patienten leiden unter epileptischen Anfällen, die mit Antiepileptika therapiert werden müssen. Des Weiteren ist aber auch mit behandlungsbedürftigen Ödemen, venösen Thromboembolien, Fatigue und kognitiver Dysfunktion zu rechnen. Ebenfalls sind die Nebenwirkungen der durchgeführten Therapien zu berücksichtigen und entsprechend zu behandeln (Wen et al., 2006).

Die Prognose, der an einem Glioblastom erkrankten Patienten, ist trotz aller Therapien und ständiger Forschung auf diesem Gebiet sehr schlecht. Nur sehr wenige Patienten überleben 2,5 Jahre nach Diagnosestellung und weniger als 5 % überleben fünf Jahre.
Die mittlere Überlebensdauer eines Patienten mit vollständiger Antitumortherapie beträgt 15 Monate (Stupp et al., 2009).
Vergleicht man das jedoch mit der mittleren Überlebensdauer von unbehandelten Patienten, die nur drei Monate beträgt, erkennt man den deutlichen Vorteil der Tripeltherapie (Operation, Bestrahlung, Chemotherapie).
Die Prognose der Patienten mit einem Glioblastom wird jedoch von vielen verschiedenen Faktoren beeinflusst, wie dem Alter, dem präoperativen „performance status“, der Tumorlokalisation und dem Umfang der erfolgten Tumorresektion. Ältere Patienten weisen zum Beispiel ein signifikant schlechteres Überleben auf als jüngere. Aber auch spezielle genetische Veränderungen des Tumors, wie die Methylierung des bereits genannten MGMT-Promotors oder die Überexpression des humanen epidermalen Wachstumsfaktorrezeptors (EGFR) und Mutationen des Enzyms Isocitrat-Dehydrogenase (IDH1) können als prognostische Marker angesehen werden (Thakkar et al., 2014).

1.1.2 Migration von Glioblastomzellen

Wie zuvor erwähnt, besitzen Glioblastomzellen einen sehr invasiven und infiltrativen Charakter, auf den die schlechte Prognose dieser Erkrankung zurückzuführen ist. Die Zellen haben so die Möglichkeit gesundes Gewebe zu infiltrieren und sich diffus über das ganze Gehirn zu verteilen (Holland, 2000). Es bilden sich Mikrosatelliten aus denen zeitnah nach erfolgreicher Behandlung der primären Läsion Rezidive entstehen können.
Glioblastomzellen können in kurzer Zeit weite Strecke durch das Gehirn zurücklegen. Sie erreichen Durchschnittsgeschwindigkeiten von 12 µm/h und migrieren vor allem entlang von Nervenfasern und Blutgefäßen (Johnson et al., 2009; Zagzag et al., 2008). Dies verleiht ihnen die Fähigkeit, sich ständig mit Sauerstoff und Nährstoffen zu versorgen (Montana and Sontheimer, 2011).
Um durch die engen Zwischenräume im Gehirn zu gelangen, müssen die Zellen schrumpfen. Hierfür können sie ihr gesamtes ungebundenes Zellwasser nach außen abgeben und erreichen somit eine maximale Zellvolumenverringerung (Watkins and Sontheimer, 2011).

Als Osmolyten benutzen die Zellen Chlorid (Cl^-). Die ungewöhnlich hohen intrazellulären Cl^--Konzentrationen (100 mM) werden über den $Na/K^+/2Cl^-$-Kotransporter NKCCl aufrechterhalten (Haas and Sontheimer, 2010).

Durch das Ausströmen von Cl^- und K^+ (Kalium) entlang des elektrochemischen Gradienten kann Wasser (H_2O) osmotisch bedingt über Aquaporine (AQP) die Zelle verlassen. An dem Ausströmen von Cl^-- und K^+-Ionen sind vor allem ClC-3-Chloridkanäle bzw. $2Cl^-/H^+$-Antiporter (Cuddapah and Sontheimer, 2010; Olsen et al., 2003), Calcium-aktivierte Kaliumkanäle mit hoher Leitfähigkeit (BK_{Ca}) (Ransom and Sontheimer, 2001) und Calcium-aktivierte Kaliumkanäle mit mittlerer Leitfähigkeit (IK_{Ca}) (D'Alessandro et al., 2013; Sciaccaluga et al., 2010) beteiligt (siehe Abbildung 1).

Um nun das Zellvolumen nach Passage der engen Zwischenräume wieder zu erhöhen, erfolgt eine osmotisch bedingte Aufnahme von Wasser über Aquaporine. Das Wasser fließt dabei osmotisch der Aufnahme von NaCl über den NKCCl-Kotransporter nach (siehe Abbildung 1).

Des Weiteren konnte gezeigt werden, dass ionisierende Strahlung (IR) die Offenwahrscheinlichkeit von BK_{Ca}- und IK_{Ca}-Kanälen erhöht und damit die Migration der Zellen fördern kann (siehe Abbildung 1). Näheres hierzu in Kapitel 1.3.2.

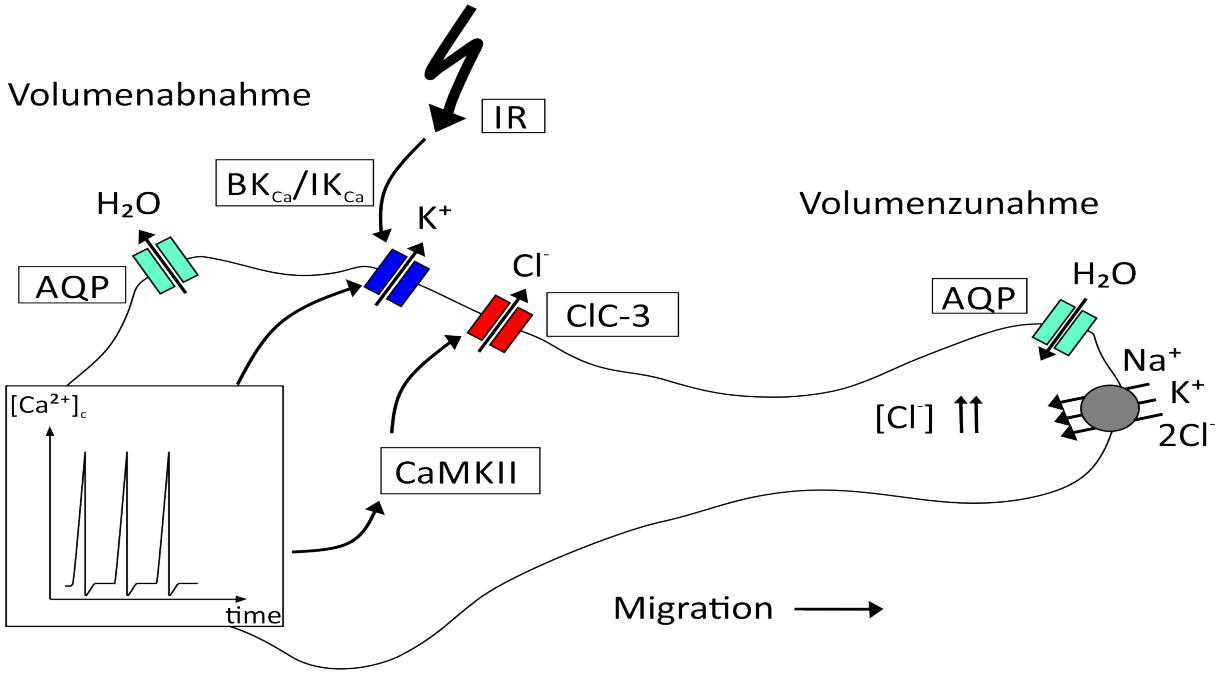

Abbildung 1 Migration von Glioblastomzellen durch Ionenverschiebung modifiziert nach (Huber et al., 2013): Ionisierende Strahlung (IR) aktiviert BK_{Ca}/IK_{Ca}-Kanäle. Es strömt verstärkt K^+ aus der Zelle. Steigende intrazelluläre Ca^{2+}-Konzentrationen führen ebenfalls zur Aktivierung von BK_{Ca}/IK_{Ca}-Kanälen und indirekt über die CaMKII (Calcium/Calmodulin-abhängige Proteinkinase II) zur Aktivierung von ClC-3-Kanälen. Das Ausströmen von K^+- und Cl^--Ionen führt zu osmotisch bedingtem Ausströmen von H_2O über AQP. Erhöhte cytoplasmatische Cl^--Konzentrationen werden durch den NKCCl-Kotransporter aufrechterhalten.

1.2 Strahlentherapie des Glioblastoms

Strahlentherapie ist eine wichtige Säule in der Tumortherapie. Die Hälfte aller Krebspatienten bekommen eine Strahlentherapie und wiederum die Hälfte werden durch Therapien, die die Bestrahlung enthalten, geheilt (Beckmann, 2014). In der Therapie des Glioblastoms hat die Bestrahlung neben der Operation und der Chemotherapie einen wichtigen Stellenwert erreicht. Der Standard in der Primärtherapie des Glioblastoms ist eine Dosis von 54-60 Gy in 1,8-2 Gy Fraktionen (Laperriere et al., 2002). Dadurch kann eine Verlängerung der mittleren Überlebensdauer von sechs Monaten erreicht werden. Bei älteren Patienten oder Patienten mit einer schlechteren Prognose kann auch eine Verkürzung der Behandlung in Betracht gezogen werden. Hierbei wird eine Gesamtdosis von 30-45 Gy auf 2,5-3 Gy Fraktionen verteilt (Weller, 2015).

Die Strahlentherapie schädigt Tumorzellen in erster Regel über Doppelstrangbrüche in der DNA. Die Anzahl der Doppelstrangbrüche steigt linear mit der absorbierten Strahlendosis (Huber et al., 2013). Tumorzellen haben dann die Möglichkeit die Doppelstrangbrüche durch homologe Rekombination bzw. nicht-homologes „end-joining“ zu reparieren (Kanaar et al., 1998). Die homologe Rekombination spielt in der späten S- bzw. G_2-Phase des Zellzyklus eine Rolle, wobei das nicht homologe „end-joining“ in allen Zellzyklusphasen zu beobachten ist. Nicht reparierbare Doppelstrangbrüche können über Apoptose oder Nekrose zum Zelltod führen. Die Radioresistenz der Tumorzellen hängt von verschiedenen Faktoren ab. In mehreren Experimenten konnte beobachtet werden, dass Zellen je nach dem in welcher Zellzyklusphase sie sich gerade befinden resistenter bzw. sensibler auf ionisierende Strahlung reagieren. Zellen in der M- und G_2-Phase reagieren am empfindlichsten auf Bestrahlung weniger empfindlich sind Zellen in der G_1-Phase. Zellen in der späten S-Phase zeigen die größte Resistenz (Pawlik and Keyomarsi, 2004).

Einen weiteren Einfluss hat jedoch auch das Mikromilieu. Hypoxische Areale sind zum Beispiel relativ strahlenresistent. Dies ist darauf zurückzuführen, dass Strahlung zu einer Radikalbildung im DNA-Rückgrat führt, welche in einer sauerstoffreichen Umgebung zu Strangbrüchen aufoxidiert. In hypoxischen Arealen jedoch, können Thiole mit den DNA-Radikalen reagieren und es kommt quasi zur chemischen Reparatur der DNA (Huber et al., 2013). Durch fraktionierte Bestrahlung kann eine Reoxygenierung des Tumors erreicht werden. Je größer der Tumor, desto schlechter ist seine Blutversorgung und desto mehr

hypoxische Areale gibt es im Tumor. Wird der Tumor nun mit einer Dosis von 2 Gy bestrahlt, gehen eine signifikante Anzahl an Tumorzellen zu Grunde und der restliche Tumor kann wieder besser durch die Blutgefäße versorgt werden. Dieses führt wiederum dazu, dass die nächste Strahlendosis durch eine bessere Sauerstoffversorgung einen größeren Effekt hat (Narita et al., 2012; Thorwarth et al., 2007). Ein weiterer Vorteil fraktionierter Bestrahlung ist, dass vor allem p53-mutierte Tumorzellen bereits durch geringe Strahlendosen in der G_2/M-Zellzyklusphase arretieren. Die Zellen werden dadurch mit der Zeit auf eine sehr strahlensensitive Phase des Zellzyklus synchronisiert und die einzelnen Bestrahlungsfraktionen werden effektiver (Geldof et al., 2003).

Tumorzellen haben zusätzlich die Möglichkeit, in Abhängigkeit des Tumormikromilieus von einem „Grow"- in einen „Go"-Phänotyp überzugehen. Sobald die Tumormasse eine bestimmte Größe erreicht hat, ist die Versorgung des Tumors mit Sauerstoff und Nährstoffen über die Blutgefäße nicht mehr ausreichend. Es kommt zu Hypoxie, Nährstoffmangel und einem niedrigen pH-Wert in den minderversorgten Tumorarealen. Diese Faktoren werden als Trigger für einen Übergang in den „Go"-Phänotyp angesehen. Die Tumorzellen haben dadurch die Möglichkeit die minder versorgten Areale zu verlassen und sich an anderer Stelle mit besseren Bedingungen niederzulassen. Sie gehen anschließend wieder in den „Grow"-Phänotyp über und bilden Mikrosatelliten bzw. durch Eindringen der Tumorzellen in die Blut- oder Lymphgefäße auch Metastasen. Bestrahlung ist ebenfalls ein Stressfaktor, der einen solchen Phänotyp-Wechsel induzieren kann. Während der Bestrahlung haben die Zellen so die Möglichkeit aus dem Bestrahlungsareal auszuwandern und sich vor den schädigenden Einflüssen der Strahlung zu schützen (Huber et al., 2013; Stock and Schwab, 2009).

Diese strahlungsinduzierte Migration konnte in verschiedenen Tumorentitäten wie Kopf-Halstumoren (Pickhard et al., 2011), Lungentumoren (Jung et al., 2007) und Glioblastomen (Steinle et al., 2011; Vanan et al., 2012; Wild-Bode et al., 2001) bereits nachgewiesen werden.

1.3 Calcium-aktivierte Kaliumkanäle vom BK_{Ca}- und IK_{Ca}-Typ

Calcium-aktivierte Kaliumkanäle (K_{Ca}-Kanäle) sind Ionenkanäle mit einer spezifischen Durchlässigkeit für K^+-Ionen. Sie vermitteln in der Regel einen Efflux der K^+-Ionen, können aber vor allem unter experimentellen Bedingungen auch einen K^+-Influx generieren. Die Richtung wird dabei durch den elektrochemischen Gradienten bestimmt.

Es werden eine Vielzahl von biologischen Prozessen innerhalb einer Zelle über K_{Ca}-Kanäle reguliert. Sie sind sowohl bei erregbaren als auch nicht erregbaren Zellen von großer Bedeutung und nahezu in allen Zellen des Organismus exprimiert.

K_{Ca}-Kanäle können in drei verschiedene Gruppen eingeteilt werden. Diese Einteilung erfolgt aufgrund der unterschiedlichen Einzelleitfähigkeit der verschiedenen Kanäle. Der Kanal mit der höchsten Leitfähigkeit ist der BK_{Ca}-Kanal („big conductance“), des Weiteren gibt es noch den IK_{Ca}-Kanal („intermediate conductance“) mit einer mittleren Leitfähigkeit und die SK_{Ca}-Kanäle („small conductance“) mit kleiner Leitfähigkeit.

Um eine funktionierende Pore zu bilden, lagern sich vier *alpha*-Untereinheiten, die aus jeweils sechs bzw. sieben Transmembrandomänen bestehen zu einem Tetramer zusammen. Zusätzlich zu den *alpha*-Untereinheiten können gewebeabhängig auch noch regulatorische *beta*-Untereinheiten angelagert oder die Kanäle durch Phosphorylierung moduliert werden (Gueguinou et al., 2014).

Der BK_{Ca}-Kanal verfügt über Leitfähigkeiten von 100-300 pS. Er ist auch bekannt als MaxiK, Slo1 oder $K_{Ca}1.1$ Kanal. Das kodierende Gen der porenformenden *alpha*-Untereinheit des BK_{Ca}-Kanals ist das *KCNMA1* Gen beim Menschen. BK_{Ca}-Kanäle sind sowohl im zentralen Nervensystem als auch im peripheren Gewebe in erregbaren und nicht erregbaren Zellen vorhanden. Aufgrund ihrer hohen Leitfähigkeit führt die Öffnung der BK_{Ca}-Kanäle in nicht erregbaren Zellen, wie den Tumorzellen, zu einem raschen Ausströmen an K^+-Ionen und somit zu einer Hyperpolarisation der Zelle. BK_{Ca}-Kanäle sind dadurch an der Regulation des Ionengleichgewichtes, der Calciumsignalkaskade sowie an der Regulation von Volumenänderungen beteiligt (Yang et al., 2015).

Des Weiteren konnte ein Zusammenhang zwischen dem BK_{Ca}-Kanal und Tumorerkrankungen gefunden werden. BK_{Ca}-Kanäle sind zum Beispiel an der Entstehung und Verbreitung von Mamma-, Pankreaskarzinomen (Bloch et al., 2007; Khaitan et al., 2009; Oeggerli et al., 2012) und Glioblastomen beteiligt (Sontheimer, 2008; Weaver et al., 2004). Oeggerli und seine

Gruppe konnten zeigen, dass die BK_{Ca}-Kanalexpression in Brusttumoren signifikant mit starker Tumorzellproliferation und mit schlechterem Überleben der Patienten korreliert. Näheres zum Zusammenhang zwischen BK_{Ca}-Kanalexpression und Glioblastomen in Kapitel 1.3.1.

Der BK_{Ca}-Kanal kann über Spannungsänderungen und Änderung der intrazellulären Ca^{2+}-Konzentrationen aktiviert werden. Mit zunehmend zytosolisch freier Ca^{2+} Konzentration aktivieren BK_{Ca}-Kanäle bei zunehmend negativer Spannung (Stefani et al., 1997). Spannungsänderungen werden dabei über den Spannungssensor wahrgenommen und es kommt zu einer allosterischen Konformationsänderung des Kanals (Horrigan and Aldrich, 1999).

Die Ca^{2+}-Konzentrationen werden direkt über eine Bindung von Ca^{2+} an der C-terminalen Region der *alpha*-Untereinheit des Kanals detektiert. Hier existieren zwei Bindungsstellen; eine ist die „Ca^{2+}-bowl“ (Schreiber and Salkoff, 1997) eine weitere befindet sich in der RCK1-Domäne des Kanals (Xia et al., 2002).

Zusätzlich können auch weitere Liganden wie zum Beispiel Magnesium (Mg^{2+}), Kohlenstoffmonoxid (CO) und Protonen (H^{+}) die Aktivität des BK_{Ca}-Kanals regulieren (Hou et al., 2008a; Hou et al., 2008b; Shi and Cui, 2001). Auch Serin/Threonin und Tyrosin-Phosphorylierung bestimmter Sequenzbereiche der *alpha*-Untereinheit des BK_{Ca}-Kanals spielen bei der Regulierung der Aktivität eine große Rolle (Schubert and Nelson, 2001; Tian et al., 2004; Zhou et al., 2001).

Die Sensitivität der *alpha*-Untereinheit des BK_{Ca}-Kanals auf die eben beschriebenen Liganden und Proteinkinasen kann durch unterschiedliche Spleißvarianten in den verschiedenen Geweben nochmals variiert werden (Chen and Shipston, 2008). Glioblastomzellen exprimieren zum Beispiel eine Spleißvariante mit 34 zusätzlichen Aminosäuren im C-terminalen Ende des Kanals (gBK-Variante), die eine höhere Ca^{2+}-Sensitivität und eine langsamere Aktivierung des Kanals bedingen (Liu et al., 2002).

BK_{Ca}-Kanäle können durch verschiedene Toxine wie Paxillin und Iberiotoxin blockiert werden. Bei Paxillin handelt es sich um ein Indolalkaloid aus dem Pilz *Penicillium paxilli* und einen sehr spezifischen BK_{Ca}-Kanalblocker (Knaus et al., 1994; Sanchez and McManus, 1996) ebenso Iberiotoxin, welches aus dem Skorpion Mesobuthus tamulus isoliert wurde. Des Weiteren werden BK_{Ca}-Kanäle bereits durch geringe Mengen an Tetraethylammoniumsalzen

sowie durch Charybdotoxin gehemmt. Diese Blockaden sind jedoch nicht BK_{Ca}-Kanal spezifisch, vielmehr werden durch diese Substanzen viele andere Kaliumkanäle blockiert (Wei et al., 2005). Zu den Aktivatoren zählen die Substanzen NS1608 und NS1619 (Wei et al., 2005).

Der IK_{Ca}-Kanal besitzt eine Leitfähigkeit von 20-80 pS (Vergara et al., 1998). Weitere Namen sind auch Gardos-Kanal, KCa3.1, SK4 und IK1. Er wird über das Gen *KCNN4* codiert. Im Gegensatz zu dem BK_{Ca}-Kanal wird der IK_{Ca}-Kanal nur durch Ca^{2+} aktiviert, wobei seine Sensitivität auf Ca^{2+} höher ist als die des BK_{Ca}-Kanals. IK_{Ca}-Kanäle sind nicht ubiquitär exprimiert. Sie konnten vor allem in Erythrozyten, Immunzellen, Speicheldrüsen, der Placenta und der Lunge nachgewiesen werden. Besonders werden die Kanäle von Blut-, Epithel- und Endothelzellen exprimiert (Jensen et al., 1998). Eine erstmalige Beschreibung der Kanäle erfolgte 1958 von Gardos und seiner Gruppe im Rahmen der Erforschung von Membraneigenschaften roter Blutkörperchen (Gardos, 1958). Später konnte gezeigt werden, dass IK_{Ca}-Kanäle bei der Sichelzellenanämie von Bedeutung sind. Sie sind hauptverantwortlich für die Dehydrierung der roten Blutkörperchen, da es durch das Ausströmen von K^+ über IK_{Ca}-Kanäle zu einem osmotischen Verlust von Wasser kommt (McNaughton-Smith et al., 2008). Aus diesem Grund wurde Senicapoc als spezifischer IK_{Ca}-Kanalblocker in verschiedenen Studien bei der Sichelzellenanämie getestet (Castro et al., 2011). Des Weiteren spielen die IK_{Ca}-Kanäle auch bei der Tumorentstehung und Metastasierung eine große Rolle. Wie die BK_{Ca}-Kanäle sind sie an der Proliferation von Prostatakarzinomen beteiligt (Lallet-Daher et al., 2009). Lallet-Daher konnte zeigen, dass eine Inhibition der IK_{Ca}-Kanäle zu einer verminderten Proliferation von Prostatakarzinomzellen führt. Aber auch bei der Entstehung von Lungenkrebs und Mammakarzinomen konnte ein Zusammenhang mit IK_{Ca}-Kanälen gezeigt werden (Bulk et al., 2015; Haren et al., 2010). Näheres zur Rolle von IK_{Ca}-Kanälen im Glioblastom in Kapitel 1.3.1.

Die Ca^{2+}-abhängige Öffnung des Kanals erfolgt nicht über die direkte Bindung von Ca^{2+} sondern indirekt über das Protein Calmodulin, das in Bereichen des cytoplasmatischen C-Terminus an die *alpha*-Untereinheiten bindet. Im Anschluss daran wird Ca^{2+} gebunden und es kommt zu einer Konformationsänderung, die die Öffnung des Kanals bedingt (Fanger et al., 1999).

Es sind eine Reihe pharmakologischer Inhibitoren des IK_{Ca}-Kanals bekannt wobei auch hier die Toxine wieder eine Rolle spielen. Eine sehr spezifische Blockade kann zum Beispiel mit dem Maurotoxin erzielt werden, eher unspezifisch wirkt hingegen das bereits erwähnte Charybdotoxin. Als niedermolekulare Inhibitoren sind vor allem Clotrimazol und TRAM-34 bekannt. Clotrimazol diente bei der Entwicklung von IK_{Ca}-Kanalblockern als Leitstruktur. Durch Abwandlungen des Clotrimazols konnten selektivere Inhibitoren wie das TRAM-34 synthetisiert werden (Wulff et al., 2000).

1.3.1 Bedeutung von BK_{Ca}- und IK_{Ca}-Kanälen für das Glioblastom

Ionenkanäle spielen eine große Rolle in der Tumorgenese. Sie haben durch die Steuerung des Ruhemembranpotentials zum Beispiel einen Einfluss auf die Zellproliferation. Mit Iberiotoxin, einem BK_{Ca}-Kanalblocker, konnte gezeigt werden, dass Gliomazellen in der S-Phase des Zellzyklus arretieren (Weaver et al., 2004). Zusätzlich sind sie wie bereits in Kapitel 1.1.2 erwähnt, auch an der Invasion und Migration von Tumorzellen beteiligt.

In Tumorbiopsien aus Gliomapatienten konnte eine Überexpression von BK_{Ca}-Kanälen im Vergleich zu normalem Hirngewebe nachgewiesen werden, die mit der Malignität des Tumors korreliert (Ransom and Sontheimer, 2001). Des Weiteren gibt es mehrere Publikationen, die zeigen, dass eine Hemmung bzw. Aktivierung des BK_{Ca}-Kanals in direktem Zusammenhang mit der Migration von Gliomazellen stehen (Kraft et al., 2003; Soroceanu et al., 1999; Weaver et al., 2006; Wondergem and Bartley, 2009). Die Datenlage ist hier jedoch nicht eindeutig. Während Weaver und Soroceanu in ihren Publikationen eine Inhibition der Migration durch Hemmung des BK_{Ca}-Kanals bestätigen konnten und Wondergem und seine Gruppe eine verstärkte Migration nach indirekter Aktivierung des BK_{Ca}-Kanals durch Menthol zeigen konnten, hat Kraft in seiner Publikation gezeigt, dass eine direkte Aktivierung des Kanals durch NS1619 und Phloretin zu einer Hemmung der Migration führt. Es muss allerdings berücksichtigt werden, dass die gewählten Migrationsmodelle in den Publikationen unterschiedlich waren (Catacuzzeno et al., 2015).

Wie bereits erwähnt, gibt es auch einen Zusammenhang zwischen einer durch Strahlentherapie induzierten Migration und BK_{Ca}-Kanälen (Huber et al., 2013; Huber et al., 2015). Dieses wird in Kapitel 1.3.2 näher beschrieben.

IK_{Ca}-Kanäle konnten im menschlichen Gehirn nur in den Microglia nachgewiesen werden. (Ifuku et al., 2007; Ishii et al., 1997). In Glioblastomzelllinien und Biopsien sind die Kanäle jedoch funktionell exprimiert (Fioretti et al., 2006; Turner et al., 2014). Zusätzlich konnte gezeigt werden, dass die IK_{Ca}-Kanalexpression signifikant mit einem schlechterem Überleben der Patienten korreliert (Turner et al., 2014). Das Hochregulieren dieser Kanäle während der neoplastischen Transformation und malignen Progression des Glioms deutet auf eine bedeutende Funktion der IK_{Ca}-Kanäle in der Tumorgenese hin (Ruggieri et al., 2012). Zahlreiche Publikationen konnten zeigen, dass sie sowohl an der Proliferation (Khalid et al., 1999; Khalid et al., 2005) als auch an der Migration (Catacuzzeno et al., 2011; Catacuzzeno et al., 2012; D'Alessandro et al., 2013; Fioretti et al., 2006; Ruggieri et al., 2012; Sciaccaluga et al., 2010) von Glioblastomzellen beteiligt sind. Ebenfalls konnte ein Zusammenhang zwischen der IK_{Ca}-Kanalaktivität und der Radioresistenz gezeigt werden (Huber et al., 2013; Huber et al., 2015). Näheres hierzu in Kapitel 1.3.2.

1.3.2 Einfluss von BK_{Ca}- und IK_{Ca}-Kanälen auf die Strahlentherapie des Glioblastoms

Der BK_{Ca}-Kanal scheint bei der strahlungsinduzierten Migration eine Schlüsselrolle einzunehmen. Bestrahlung führt in Glioblastomzellen zu einer erhöhten Offenwahrscheinlichkeit von BK_{Ca}-Kanälen. Durch die erhöhte Aktivität dieser Kanäle kommt es über den bereits in Kapitel 1.1.2 beschriebenen Mechanismus zu einer erhöhten Migration, die mit Hilfe des selektiven BK_{Ca}-Kanalblockers Paxillin inhibiert werden kann (siehe Abbildung 1). Es kommt zusätzlich zu einer BK_{Ca}-Kanal abhängigen Aktivierung der Calcium/Calmodulin-abhängigen Proteinkinase II (CaMKII), welche ebenfalls in die Zellvolumenregulation eingreift (siehe Abbildung 1) (Steinle et al., 2011). Da, wie bereits in Kapitel 1.1.2 erwähnt, auch die IK_{Ca}-Kanäle an der für die Migration nötigen Zellvolumenregulation beteiligt sind, ist auch bei ihnen ein Zusammenhang mit der strahlungsinduzierten Migration zu erwarten.

Des Weiteren ist bekannt, dass über die Regulierung von Kaliumkanälen eine Radiosensitivierung von Tumorzellen erzielt werden kann (Huber et al., 2015). Interessanterweise wirkt auch Clotrimazol über einen G_1-Arrest der Zellen radiosensitivierend (Liu et al., 2010). Da Clotrimazol, wie bereits in Kapitel 1.3 beschrieben,

unter anderem auch IK_{Ca}-Kanäle blockiert, liegt die Vermutung nahe, dass bei diesem Mechanismus zusätzlich eine Beteiligung von IK_{Ca}-Kanälen vorliegen könnte.

2 Zielsetzung der vorliegenden Arbeit

Glioblastome sind äußerst therapieresistent und daher ist die Forschung auf diesem Gebiet von essenzieller Bedeutung. Es ist wichtig, die Mechanismen zu verstehen, über die es den Tumorzellen gelingt, sich vor der schädigenden Chemo- bzw. Strahlentherapie zu schützen. Wie bereits in Kapitel 1.3.2 erwähnt, gibt es mehrere Arbeiten die eine strahlungsinduzierte Migration sowohl *in vitro* als auch *in vivo* zeigen. Aber auch hier ist die Datenlage widersprüchlich. Es gibt ebenso eine Publikation, in der in einem drei dimensionalen *in vitro* Modell, die verstärkte Migration von Tumorzellen nach Bestrahlung nicht nachgewiesen werden konnte (Eke et al., 2012)**.** Ist die radioinduzierte Migration nun in großem Ausmaße nach fraktionierter Bestrahlung vorhanden, kann dies die Verbreitung der Tumorzellen im ganzen Gehirn während fraktionierter Strahlentherapie sogar noch begünstigen. Zielsetzung der vorliegenden Arbeit war die radioinduzierte Migration von Glioblastomzellen in Abhängigkeit von der BK_{Ca}-Kanalaktivität sowohl *in vitro* als auch in einem orthotopen *in vivo* Mausmodell zu untersuchen. Um eine möglichst auf den Patienten übertragbare Situation in unserem *in vivo* Mausmodell zu schaffen, wurden die Mäuse fraktioniert an fünf aufeinanderfolgenden Tagen mit 2 Gy gezielt am Tumor bestrahlt. Des Weiteren wurde die Bedeutung des SDF-1/CXCR4-Chemokinsignalweges bei der radioinduzierten Migration beschrieben, da in verschiedenen Publikationen bereits gezeigt werden konnte, dass das SDF-1/CXCR4-„Signaling“ sowohl einen Einfluss auf die Migration von Glioblastomzellen haben kann als auch nach Bestrahlung hochreguliert wird (Sciaccaluga et al., 2010; Tabatabai et al., 2006; Zhou et al., 2013).

Im zweiten Teil dieser Arbeit wurde versucht, die intrinsische Radioresistenz der Glioblastomzellen über eine Blockade des IK_{Ca}-Kanals zu erniedrigen. Diese Untersuchungen erfolgten ebenfalls *in vitro* und in einem ektopen *in vivo* Mausmodell. Dem liegt zu Grunde, dass Bestrahlung eine Aktivierung von Kaliumkanälen, insbesondere von IK_{Ca}- und BK_{Ca}-Kanälen, und Ca^{2+}-Kanälen zur Folge hat, was zu einem veränderten Ca^{2+}-„Signaling“ und dadurch bedingt zu einem verändertem Zellzyklus bzw. zum Zellzyklusarrest führt. In einer anderen Publikation konnte eine Beteiligung von Kaliumkanälen an der Regulation des Zellzyklus nach Bestrahlung bereits gezeigt werden (Palme et al., 2013).

3 BK_{Ca}-Kanalblockade inhibiert die radioinduzierte Migration bzw. Gehirninvasion von Glioblastomzellen

Der Inhalt dieses Kapitels ist in folgender Arbeit veröffentlicht:

Lena Edalat, Benjamin Stegen, Lukas Klumpp, Erik Haehl, Karin Schilbach, Robert Lukowski, Matthias Kühnle, Günther Bernhardt, Armin Buschauer, Daniel Zips, Peter Ruth and Stephan M. Huber (2016). BK K^+ channel blockade inhibits radiation-induced migration/brain infiltration of glioblastoma cells. Oncotarget 7423

In der vorliegenden Publikation wurde eine quantitative Analyse der radioinduzierten Migration von humanen Glioblastomzellen in einem orthotopen Mausmodell durchgeführt. Zusätzlich wurde getestet, ob die Blockade des BK_{Ca}-Kanals mit Paxillin die verstärkte Migration nach Bestrahlung *in vivo* unterbindet.

Hierfür wurde einen humane Glioblastomzelllinie (U-87MG), welche zuvor stabil mit dem roten Fluoreszenzprotein Katushka transfiziert wurde (U-87MG-Kat), stereotaktisch in das rechte Striatum einer immundefizienten NOD/SCID/IL2γ^{null} (NSG) Maus injiziert. Nach dem Anwachsen des Tumors folgte die fraktionierte Bestrahlung der Mäuse kombiniert mit einer zusätzlichen Gabe von Paxillin. Die Auswertung erfolgte mittels Immunfluoreszenzmikroskopie. Die Anzahl und Migrationsstrecke aller aus dem Tumor ausgewanderten Zellen (rot fluoreszierend) wurde bestimmt. Darüber hinaus wurde auch die Bedeutung der SDF-1-Signalkaskade in diesem Zusammenhang näher untersucht.

Da es sich bei den U-87MG-Zellen um eine sehr abgekapselte wenig invasiv wachsende Zelllinie handelt, eignete sie sich besonders gut für diese Untersuchungen.

Zunächst musste allerdings genau charakterisiert werden, ob sich die mit Katushka transfizierten Zellen hinsichtlich Wachstumskinetik und Chemosensitivität von den Wildtyp Zellen unterscheiden. Hier konnten keine Unterschiede gefunden werden (Suppl. Fig IA-C).

3.1 Ergebnisse

3.1.1 *In vitro* Untersuchungen zur BK_{Ca}-Kanalexpression und zum Einfluss von Paxillin auf das klonogene Überleben

Essentiell für alle weiteren Experimente waren BK_{Ca}-Kanalexpressionsanalysen in U-87MG-Kat-Zellen und der Einfluss des BK_{Ca}-Kanalinhibitors Paxillin auf das klonogene Überleben der Zellen. Da eine Blockade des mit dem BK_{Ca}-Kanal verwandten IK_{Ca}-Kanals bekanntermaßen zu einer Radiosensibilisierung führt (näheres hierzu in Kapitel 4) liegt die Vermutung nahe, dass auch Paxillin einen solchen Effekt haben könnte. Würde Paxillin an sich bereits radiosensibilisierend auf U-87MG-Kat-Zellen wirken, wäre die Interpretation der Migration und Gehirninfiltration *in vivo* deutlich erschwert und der Effekt müsste bei der Auswertung mit berücksichtigt werden.

U-87MG-Kat Zellen exprimieren funktionell intakte BK_{Ca}-Kanäle, was mit „Whole-cell“ Patch-Clamp-Experimenten gezeigt werden konnte. Die Experimente wurden mit Kaliumgluconat in der Pipette und Natriumchlorid (NaCl) in der Badlösung durchgeführt. In Abbildung 1A sind starke Auswärtsströme im Bereich von mehreren Nanoampere (nA) zu sehen, welche auswärtsrektifizierend sind (Abb. 1B) und mit Paxillin blockiert werden konnten (Abb. 1A-B). Dies lässt auf die Expression funktioneller BK_{Ca}-Kanäle schließen.

Um die radiosensibilisierenden Effekte einer BK_{Ca}-Kanalblockade mit Paxillin näher zu untersuchen, wurden „Delayed plating“-Koloniebildungsassays mit bestrahlten T98G- und U-87MG-Kat-Zellen durchgeführt. Abbildung 1C und D zeigen, dass Paxillin in beiden Zelllinien keinen Einfluss auf das klonogene Überleben hatte. Das heißt, die Fähigkeit der Zellen Kolonien zu bilden, wurde durch Paxillin nicht beeinträchtigt und die Effekte der Strahlentherapie wurden nicht verstärkt. Zusätzlich konnten mit Paxillin bei Konzentrationen bis zu 10 µM keine antiproliferativen Eigenschaften auf U87MG-Kat-Zellen nachgewiesen werden (Suppl. Fig 1D)

3.1.2 *In vitro* Charakterisierung der BK_{Ca}-Kanalaktivität und Chemotaxis nach Bestrahlung

„Cell-Attached“ Patch-Clamp-Messungen an U-87MG-Kat-Zellen mit Kaliumchlorid (KCl) in der Pipette und NaCl in der Badlösung zeigten, dass die Aktivität der BK_{Ca}-Kanäle mit zunehmend positiver Spannung ansteigt (Abb. 2A). Bei bestrahlten Zellen (2 Gy, 2-4,5 h nach IR) konnte man die charakteristischen Ströme jedoch bereits bei viel niedrigeren Spannungen sehen (Abb. 2A-D). Legt man im „Cell-Attached“ Modus eine Spannungsklemme von 0 mV zwischen Pipette und Badlösung an, können die Transmembranströme unter physiologischen Bedingungen gemessen werden. In Abbildung 2C ist zu sehen, dass der BK_{Ca}-Kanal in bestrahlten U-87MG-Kat-Zellen bereits unter physiologischen Membranpotentialen aktiv war, wohingegen bei unbestrahlten Zellen eine Aktivität des BK_{Ca}-Kanals erst ab einer Klemmspannung von über +50 mV messbar war (Abb. 2D). Zusammenfassend kann man sagen, dass die Auswärtsströme der bestrahlten Zellen die der unbestrahlten Zellen um das Zweifache überstiegen (Abb. 2E-F). Fügte man bei den Messungen Paxillin hinzu, konnte man eine Verringerung der nach Bestrahlung erhöhten Auswärtsströme auf das Niveau der Auswärtsströme in unbestrahlten Zellen erreichen. In unbestrahlten Zellen hatte Paxillin hingegen keinen Einfluss (Abb. 2E-F). Betrachtet man die Paxillin-sensitive Fraktion, erkennt man die typischen BK_{Ca}-Auswärtsströme (Abb. 2G).

Die erhöhte BK_{Ca}-Kanalaktivität nach Bestrahlung wurde von einer verstärkten Chemotaxis begleitet, was mit Hilfe eines Transfiltermigrationsassays ermittelt werden konnte (Abb. 2H-I). Paxillin hat hier ebenfalls die durch Bestrahlung erhöhte Migration gehemmt, wobei es keinen Einfluss auf die basale Migration von U-87MG-Kat-Zellen hatte. Es scheint also einen Zusammenhang zwischen der erhöhten Migration von U-87MG-Kat-Zellen und der BK_{Ca}-Kanalaktivität nach Bestrahlung zu geben.

Um bereits publizierte Daten (Steinle et al., 2011) zur Paxillin-sensitiven radioinduzierten Migration zu bestätigen, wurden die gleichen Versuche auch mit der humanen Glioblastomzelllinie T98G wiederholt. „Cell-Attached“ Messungen zeigten auch hier ähnlich wie bei den U-87MG-Kat-Zellen, dass die spannungsabhängige Aktivierung des BK_{Ca}-Kanals in bestrahlten Zellen bei niedrigeren Spannungsklemmen möglich war als in unbestrahlten T98G-Zellen (Abb. 3A-C). Ebenfalls wurden nach Bestrahlung wieder auswärtsrektifizierende Paxillin-sensitive „Cell-Attached“ Ströme generiert (Abb. 3D-F), was für eine

strahlungsinduzierte Aktivierung von BK_{Ca}-Kanälen spricht. Transfiltermigrationsassays konnten eine verstärkte Migration nach Bestrahlung bestätigen. Die radioinduzierte Migration war BK_{Ca}-Kanal abhängig, da BK_{Ca}-Knockdownzellen diese nicht zeigten. Wie in den U-87MG-Kat-Zellen (BK_{Ca}-Kanalblockade mit Paxillin) hat der Knockdown des BK_{Ca}-Kanals auch in den T98G-Zellen keinen Einfluss auf die basale Migration unbestrahlter Zellen (Abb. 3G-H).

3.1.3 mRNA-Expressionsanalysen, Proteinabundanzbestimmungen und Immunfluoreszenzfärbungen zur Untersuchung der Invasion nach Bestrahlung

Um herauszufinden, ob die radioinduzierte Migration auch mit einem erhöhten invasiven Phänotyp zusammenhängt wurden mittels qRT-PCR-Analysen die mRNA-Expressionen verschiedener Invasionsmarker bestimmt. Es wurden fraktioniert bestrahlte (5 x 2 Gy) und unbestrahlte (5 x 0 Gy) U-87MG-Kat-Zellen miteinander verglichen. Besonders die Matrixmetalloproteasen 2 und 9 (MMP-2, MMP-9) und SDF-1 wurden hierbei als Invasionsmarker untersucht. Bei allen drei stieg die mRNA-Expression nach Bestrahlung signifikant an (Abb. 4A). Weiterhin war interessant, inwieweit sich die mRNA-Expression des SDF-1-Rezeptors (CXCR4) nach Bestrahlung veränderte. Hier konnte kein Unterschied zu den unbestrahlten Zellen gesehen werden. Das gleiche gilt für den BK_{Ca}-Kanal. Auch hier konnte nach fraktionierter Bestrahlung kein signifikanter Unterschied in der mRNA-Expression detektiert werden (Abb. 4A).

Es ist bekannt, dass der Hypoxie-induzierte-Faktor-1α (HIF-1α) für eine Hochregulation von CXCR4 und SDF-1 verantwortlich sein kann (Greenfield et al., 2010). In Westernblotanalysen konnte eine Stabilisierung des HIF-1α Proteins nach einmaliger Bestrahlung (1 x 2 Gy, 2 h nach IR) gezeigt werden (Abb. 4B-C). In Übereinstimmung mit den mRNA-Expressionsanalysen führte die Stabilisierung von HIF-1α zwar nicht zu einem strahlungsinduzierten Anstieg des CXCR4-Proteins (Abb. 4B-C) jedoch zu einer signifikant ansteigenden SDF-1-Immunfluoreszenz in U-87MG-Kat-Zellen (Abb. 4D-E). Gleiches ergaben SDF-1-Immunfluoreszenzfärbungen in T98G-Zellen (Abb. 5A-C).

3.1.4 Analyse der SDF-1-Signalkaskade im Zusammenhang mit der radioinduzierten BK_{Ca}-Kanalaktivierung mittels Ca^{2+}-Imaging und Patch-Clamp-Messungen

In der Literatur wird postuliert, dass SDF-1 über CXCR4, die Phospholipase C (PLC) und die Bildung von Inositol-1,4,5-trisphosphat (IP_3) eine Ca^{2+}-Freisetzung aus den intrazellulären Speichern stimuliert. Ebenso weiß man, dass an Kontaktstellen zwischen Endoplasmatischem Retikulum (ER) und Plasmamembran BK_{Ca}-Kanäle in sogenannten „lipid rafts“ an IP_3-Rezeptoren gekoppelt sind, so dass auf ein direktes Signaling über SDF-1, CXCR4, PLC, IP_3, Ca^{2+}-„release“ durch IP_3-Rezeptoren im ER und Aktivierung der benachbarten BK_{Ca}-Kanäle in der Plasmamembran geschlossen werden kann (Peng et al., 2004; Weaver et al., 2007). Um diesen Zusammenhang im Modell dieser Arbeit zu untersuchen, wurden intrazelluläre Ca^{2+}-Konzentrationen in U-87MG-Kat-Zellen nach Zugabe von konditioniertem Medium in Abhängigkeit von einer CXCR4-Blockade mit AMD3100 bestimmt. Das konditionierte Medium wurde sowohl aus bestrahlten als auch unbestrahlten U-87MG-Kat-Zellen (2 h nach IR) gewonnen. Die Ca^{2+}-Messungen zeigten einen signifikant höheren intrazellulären Ca^{2+}-Anstieg in den Zellen, die mit dem konditionierten Medium von bestrahlten Zellen versetzt wurden (Abb. 4F-G). Interessanterweise konnte dieser Effekt mit dem CXCR4-Antagonist AMD3100 komplett gehemmt werden (Abb. 4G). Das gleiche konnte auch in T98G-Zellen beobachtet werden (Abb. 5E-F). Zusätzlich konnten im konditionierten Medium von bestrahlten T98G Zellen mittels ELISA erhöhte SDF-1-Konzentrationen detektiert werden (Abb. 5D). Dies spricht dafür, dass Bestrahlung zu einer Anreicherung von Faktoren führt, die die CXCR4-Signalkaskade stimulieren. Ob es hierbei den vermuteten Zusammenhang mit den durch Bestrahlung aktivierten BK_{Ca}-Kanälen gibt, wurde mittels Patch-Clamp-Messungen untersucht. Es wurden „Cell-Attached“ Messungen unter Zugabe von AMD3100 durchgeführt. Abbildungen 4H und I zeigen, dass die radioinduzierte Aktivierung von BK_{Ca}-Kanälen in U-87MG-Kat-Zellen durch die Zugabe eines CXCR4-Inhibitors vollständig blockiert werden konnte. Zusammenfassend bestätigen diese Ergebnisse den Zusammenhang der BK_{Ca}-Kanalaktivierung durch Bestrahlung mit einer verstärkten SDF-1/CXCR4-Signalkaskade.

3.1.5 Einfluss von SDF-1 auf intrazelluläre Ca^{2+}-Konzentrationen, BK_{Ca}-Kanalaktivität und Migration *in vitro*

Bereits beschriebene Daten legen dar, dass Bestrahlung die SDF-1-Expression induzieren kann. In folgenden Versuchen wurde nun ermittelt, ob nach alleiniger Zugabe von SDF-1, ähnliche Effekte wie nach Bestrahlung erzielt werden können. Zu diesem Zweck wurden in U-87MG-Kat-Zellen intrazelluläre Ca^{2+}-Konzentrationen unter Zugabe von SDF-1 gemessen. Es konnte ein lang anhaltender Anstieg der Ca^{2+}-Spiegel gemessen werden (Abb. 6A-B). Zusätzlich wurden in „Cell-Attached" Patch-Clamp-Messungen, nach Zugabe von SDF-1, Paxillin-sensitive Ströme generiert (Abb. 6C). Die Ströme waren auswärtsrektifizierend und ähnelten den radioinduzierten Strömen (vergl. Abb. 2G mit Abb. 6D-F). Da Bestrahlung, wie bereits erwähnt, über eine BK_{Ca}-Kanalaktivierung auch die Migration stimuliert, sollte dies im Folgenden auch für SDF-1 analysiert werden. Wir konnten die vermutete Induktion in der Migration nicht nur mit Bestrahlung sondern auch mit SDF-1 bestätigen (Abb. 6G). Durch Zugabe von Paxillin konnte die verstärkte Migration gehemmt werden. Paxillin hatte jedoch auch hier wieder keinen Einfluss auf die basale Migration (Abb. 6H).

Zur Bestätigung dieser Ergebnisse wurden das Ca^{2+}-Imaging und die Patch-Clamp-Messungen mit T98G-Zellen wiederholt. Es konnte durch SDF-1 sowohl ein intrazellulärer Anstieg an Ca^{2+} erzielt werden (Abb. 7A-B) als auch ein Anstieg der Auswärtsströme gemessen werden (Abb. 7C-D). Die Einzelkanal-Analyse (Abb. 7E) zeigte wiederum BK_{Ca} ähnliche Kanäle, welche durch ansteigende Spannungen verstärkt aktiviert werden konnten. Durch SDF-1 konnte, wie durch Bestrahlung, eine Aktivierung bereits bei niedrigeren Spannungen erreicht werden (Abb. 7F-G).

Zusammenfassend lässt sich feststellen, dass SDF-1, wie auch ionisierende Strahlung, die Migration der Glioblastomzellen über eine BK_{Ca}-Kanalaktivierung stimuliert.

3.1.6 Generierung eines orthotopen Glioblastommausmodells

Für die Generierung eines orthotopen Glioblastommausmodells wurden 30.000 U-87MG-Kat-Zellen (Abb. 8A) stereotaktisch in das rechte Striatum von NSG-Mäusen injiziert (Abb. 8B). Es bildeten sich rot fluoreszierende abgekapselte Tumoren (Abb. 8C) mit einer exponentiellen Wachstumskurve während der ersten 21 Tage (Abb. 8D). An Tag 7-11 wurden die Mäuse den verschiedenen Behandlungen (Paxillin-Injektionen, IR) unterzogen. Bei der

Bestrahlung wurden nur die rechten tumortragenden Gehirnhemisphären der Mäuse (Abb. 8E) fraktioniert mit 2 Gy bestrahlt. Hierfür wurden die mit Isofluran betäubten Mäuse in einer Maushalterung im Bestrahlungsfeld platziert. Die Körper der Mäuse wurden mit einem 8 cm dicken Bleiblock und dem „Multileaf"-Kollimator im Bestrahlungskopf des Linearbeschleunigers abgeschirmt. Lediglich durch eine kleine Öffnung über dem Tumorareal konnte die Strahlung durch den Bleiblock auf die Maus treffen (Abb. 8F). Durch Filmdosimetrie konnte die Größe des Bestrahlungsareal (50 % Isodosis) von 0,8 cm x 0,5 cm = 0,4 cm^2 bestätigt werden (Abb. 8G). Die Bestrahlung wurde durch die Abschirmung der Maus sehr gut toleriert. Die Mäuse litten nur unter einer geringen Gewichtsabnahme während der Therapie. Mäuse aus der Paxillin-Behandlungsgruppe zeigten höhere Gewichtsabnahmen, die sich jedoch nach Beendigung der Injektionen wieder normalisierten (Abb. 8H). Nach 21 Tagen wurden die Mäuse aller Behandlungsgruppen getötet, die Gehirne entnommen und für histologische Untersuchungen eingefroren. Um das Modell für alle weiteren Untersuchungen verwenden zu können, war es von großer Bedeutung, dass die Tumoren auch nach Anwachsen noch BK_{Ca}-Kanäle exprimieren. Dies konnte mittels Immunfluoreszenzfärbungen bestätigt werden (Abb. 8I-K).

3.1.7 SDF-1/CXCR4-Expression und radioinduzierte Migration *in vivo*

Die Tumoren aus humanen U-87MG-Kat-Zellen exprimieren zusätzlich zu BK_{Ca}-Kanälen auch SDF-1, was mittels Immunfluoreszenzfärbungen aus Tumorkryoschnitten gezeigt werden konnte. Es war erkennbar, dass die SDF-1-Expression neun Tage nach Ende der Bestrahlung stark erhöht war (Abb. 9A-B) und vor allem Zellen an der Invasionsfront des Tumors (Abb. 9B) bzw. einzelne migrierende Zellen starke Färbungen aufwiesen (Abb. 9C). Die gleichen Färbungen wurden auch mit einem CXCR4 spezifischen Antikörper durchgeführt. Hier bestätigten sich die *in vitro* Ergebnisse. Die CXCR4 Expression war sowohl in den unbestrahlten als auch den bestrahlten Tumoren gleich (Abb. 9D-F). Bei höherer Auflösung konnte eine Lokalisation von CXCR4 in der Plasmamembran und im Zytosol der Zellen abgeleitet werden (Abb. 9G).

Um die Migration der Glioblastomzellen im Gehirn einer NSG-Maus zu analysieren wurden die Gehirne entnommen und Kryoschnitte des Tumors angefertigt. Es wurden alle aus dem Tumor ausgewanderten Zellen gezählt und deren Migrationsstrecken bestimmt (Abb. 10A-

B). Vergleicht man in Abbildung 10A die Tumorränder eines unbestrahlten Tumors mit denen eines bestrahlten Tumors in Abbildung 10B so erkennt man, dass bestrahlte Tumoren eher ausgefranste und diffuse Tumorränder aufweisen (Abb. 10B). In Abbildung 10C und D sind die Migrationsstrecken der ausgewanderten Zellen aufgetragen, wobei die Mäuse in Abbildung 10D zusätzlich zur Bestrahlung einer Paxillin-Behandlung unterzogen wurden. Den Mäusen wurde jeweils 6 h vor und nach jeder Bestrahlung 8 mg/kg KG Paxillin i.p. injiziert. Die Migrationsstrecken waren bei beiden Behandlungsgruppen annähernd gleich. Die Anzahl der ausgewanderten Zellen unterschied sich allerdings. Es wanderten fast doppelt so viele Zellen aus einem bestrahlten Tumor wie aus einem unbestrahlten Tumor aus (Abb. 10E). Paxillin konnte diesen Effekt auch *in vivo* blockieren und hatte auch hier keinen Einfluss auf die basale Migration (Abb. 10E). Zusätzlich hatte Paxillin keinen Effekt auf das Tumorvolumen (Abb. 10F).

3.2 Diskussion

Wie bereits erwähnt, ist die radioinduzierte Migration ein kontrovers diskutiertes Thema. Mit dieser Arbeit konnten wir die Frage, ob eine radioinduzierte Migration in der *in vivo* Situation überhaupt auftritt, quantitativ auf zellulärer Ebene beantworten. Es zeigte sich, dass bereits fünf Fraktionen mit der klinisch relevanten Dosis von 2 Gy ausreichend waren, um die Anzahl der das Gehirn infiltrierenden Zellen um das Doppelte zu erhöhen. Ebenfalls scheint der BK_{Ca}-Kanal eine Schlüsselrolle bei der radioinduzierten Migration einzunehmen, da diese bei einer BK_{Ca}-Kanalblockade mit Paxillin vollständig unterdrückt werden konnte. Zusätzlich zeigten die Experimente, dass das durch Bestrahlung induzierte SDF-1/CXCR4-„Signaling“ für die Aktivierung der BK_{Ca}-Kanäle verantwortlich zu sein scheint.

In unserem *in vivo* Glioblastommausmodell verwendeten wir U-87MG-Kat Zellen, welche bekanntermaßen sehr abgekapselte Glioblastome in Mausgehirnen bilden. Dies repräsentiert natürlich nicht den Großteil der Glioblastome, die normalerweise hoch infiltrativ wachsen. Andererseits war es nur durch dieses abgekapselte Wachstum möglich die aus dem Tumor auswandernden Zellen quantitativ zu erfassen. Weitere Vorteile dieser Zelllinie sind, dass sie hoch tumorigen ist, sehr schnell Tumoren in reproduzierbarer Größe bildet und die radioinduzierte Migration auch *in vitro* zeigt.

Ein limitierender Faktor in unseren Untersuchungen ist, dass das Bestrahlungsprotokoll von 5 x 2 Gy natürlich nicht der trimodalen Therapie (Operation, 30 x 2 Gy, Temozolomid) von Glioblastompatienten entspricht. Es gibt einige Arbeitsgruppen die bereits *in vivo* Untersuchungen zur radioinduzierten Migration durchführten, jedoch unterscheiden diese sich erheblich in der Durchführung der Experimente. In zwei Publikationen wurden, um den Bestrahlungseffekt auf Zellen zu untersuchen, bereits bestrahlte Zellen in Mäuse injiziert (Desmarais et al., 2015; Wild-Bode et al., 2001). In anderen Publikationen wurden Ganzhirnbestrahlungen mit einer Einzeldosis von 8 Gy (Tabatabai et al., 2006), Teilhirnbestrahlungen mit Einzeldosierungen von 8 und 15 Gy (Wang et al., 2013) und stereotaktische Bestrahlungen mit einer Einzeldosis von 50 Gy (Shankar et al., 2014) durchgeführt. Das von uns gewählte Modell einer fraktionierten, relativ Tumor gezielten Bestrahlung wurde in der Form noch nicht untersucht. Es handelt sich hierbei also um ein Mausmodell, das trotz seiner Grenzen noch am genauesten die Situation eines Patienten simuliert, da gerade die Folgen der fraktionierten Bestrahlung bei der Patientenbehandlung von Interesse sind.

Ob nun die radioinduzierte Migration von Glioblastomzellen auch für die hohe Radioresistenz der Glioblastome verantwortlich ist, bleibt zu klären. In den meisten Fällen kommt es nach einer erfolgreichen Radiochemotherapie innerhalb kürzester Zeit zu einem Rezidiv. Interessanterweise liegen die Rezidive vorzugsweise im Bestrahlungsareal bzw. am Rand der Bestrahlungsfelder (Minniti et al., 2010; Weber et al., 2009). Es liegt nun der Gedanke nahe, dass die aus dem Tumor migrierenden Zellen eher weniger zur Rezidivbildung beitragen. Berücksichtigt man jedoch die Hypothese, dass Zellen nach der Auswanderung aus dem primären Tumorareal vorzugsweise in das bestrahlte nekrotische Tumorareal zurückkehren, da hier der nötige Platz für die nachfolgende Proliferation vorhanden ist, erkennt man die Bedeutung der radioinduzierten Migration bei der Bildung von Rezidiven.

Des Weiteren konnten wir zeigen, dass erhöhte intrazelluläre Ca^{2+}-Spiegel nach Bestrahlung bzw. Zugabe von SDF-1 zu einer erhöhten Migration führten. Dass die Ca^{2+}-Signalkaskade einen wichtigen Einfluss auf die Migration hat, konnte bereits durch verschiedene Arbeitsgruppen dargelegt werden (Huber, 2013; Huber et al., 2015). Ebenfalls ist bekannt, dass Bestrahlung die Ca^{2+}-Signalkaskade in Leukämiezellen induziert (Heise et al., 2010;

Palme et al., 2013) und SDF-1 über den G-Protein-gekoppelten-Rezeptor CXCR4 zu einer Induktion der intrazellulären Ca^{2+}-Signalkaskade führt und darüber eine verstärkte Migration bzw. Invasion sowohl in Glioblastomen (Sciaccaluga et al., 2010; Zagzag et al., 2008) als auch Pankreaskarzinomen auslöst (Saur et al., 2005).

SDF-1 ist ein HIF-1α-Zielgen und wird vor allem in hypoxischen Arealen verstärkt exprimiert. Im Rahmen dieser Arbeit konnte gezeigt werden, dass die SDF-1-Expression auch nach Bestrahlung erhöht wird. Dies könnte auf die verstärkte Zerstörung der Vaskularisierung und die daraus resultierende Hypoxie zurückzuführen sein (Greenfield et al., 2010). Da aber Zellen in den *in vitro* Experimenten ebenfalls eine erhöhte SDF-1-Expression nach Bestrahlung aufweisen, liegt die Vermutung nahe, dass Bestrahlung auch direkt mit der Expression von SDF-1 interferieren kann. Dies wurde sowohl aus den hier gezeigten Experimenten als auch aus Daten einer anderen Arbeitsgruppe ersichtlich (Tabatabai et al., 2006).

Wie bereits erwähnt konnte die radioinduzierte Migration *in vivo* in der vorliegenden Arbeit effektiv durch eine Blockade des BK_{Ca}-Kanals mit Paxillin blockiert werden. Paxillin ist ein Neurotoxin aus dem Pilz *Penicillium paxilli* welches z.B. für die Weidelgrastaumelkrankheit („ryegrass stagger“) in Schafen verantwortlich ist. Hierbei wird das Toxin über das Weidelgras von den Schafen aufgenommen und es kommt zu Ataxien und unkontrollierbarem Tremor bei den Tieren. Die Symptome der Weidelgrastaumelkrankheit sind vor allem auf die hohe Expression der BK_{Ca}-Kanäle im Cerebellum und deren Blockade durch das Neurotoxin zurückzuführen (Imlach et al., 2008). Paxillin ist ein sehr spezifischer BK_{Ca}-Kanalinhibitor und wirkt bereits im nanomolaren Bereich (Knaus et al., 1994). Der genaue Wirkmechanismus dahinter ist jedoch unbekannt. Es wird vermutet, dass Paxillin als allosterischer Inhibitor den geschlossenen Zustand des Kanals stabilisiert (Zhou and Lingle, 2014). In dieser Arbeit wurde Paxillin in einer Dosierung von 8 mg/kg KG eingesetzt, um ausreichend hohe Plasmaspiegel für eine Blockade der BK_{Ca}-Kanäle zu erreichen. In dieser Dosierung sind außer der transienten Ataxie keine weiteren Nebenwirkungen aufgetreten. Die Ataxie ist ein Indiz dafür, dass Paxillin über die Blut-Hirn-Schranke in das Gehirn gelangt ist.

Wie bereits in Kapitel 1.1.2 beschrieben sind jedoch nicht nur BK_{Ca}-Kanäle sondern auch IK_{Ca}-Kanäle an der Migration von Glioblastomzellen beteiligt. Es stellte sich daher auch die Frage,

ob die radioinduzierte Migration ebenso mit TRAM-34 unterbunden werden kann. Um dies zu testen, wurden die Mäuse dem gleichen Behandlungsschema unterzogen wie in Kapitel 3.1.6 beschrieben. Es wurde lediglich Paxillin durch TRAM-34 ersetzt. Bei TRAM-34 war auf Grund der guten Pharmakokinetik eine einmal tägliche Gabe von 120 mg/kg Körpergewicht (KG) in Mygliol ausreichend (D'Alessandro et al., 2013). Die Mäuse wurden sechs Stunden vor jeder Bestrahlungsfraktion i.p. injiziert. Interessanterweise zeigte sich hier das gleiche Bild wie bei der Behandlung der Mäuse unter Paxillin. Die radioinduzierte Migration konnte vollständig unterdrückt werden während sich das Tumorvolumen nicht änderte (siehe Abbildung 2 (Edalat et al., MS in preparation)).

Die Ergebnisse dieser Versuche bestätigen, dass BK_{Ca}- und IK_{Ca}-Kanäle gleichermaßen für die Migration der Tumorzellen nach Bestrahlung verantwortlich sind.

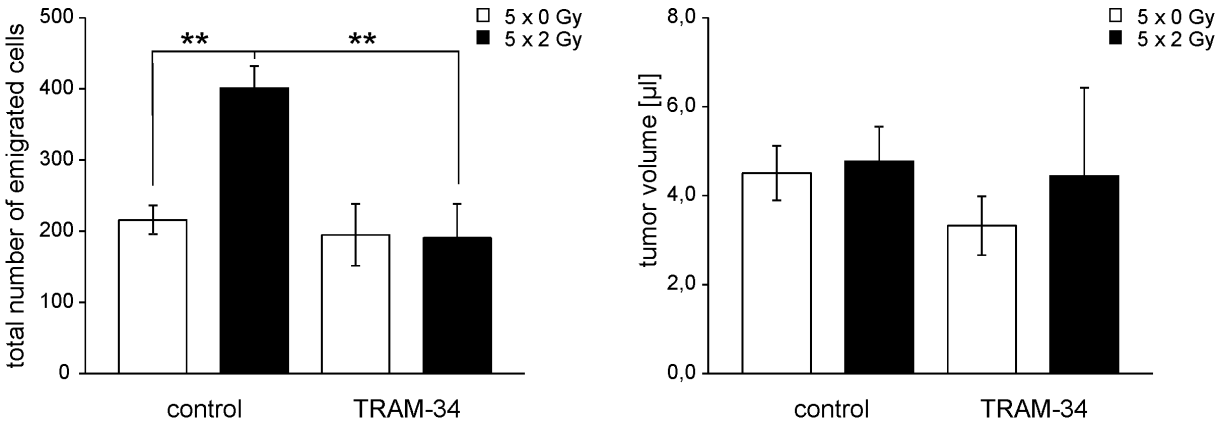

Abbildung 2 Blockade der radioinduzierten Migration *in vivo* durch TRAM-34: Anzahl der migrierten Zellen aus dem Tumor (links) und das mittlere Tumorvolumen (rechts) von fraktioniert bestrahlten Tumoren (5 x 0 Gy (unausgefüllte Säulen) oder 5 x 2 Gy (ausgefüllte Säulen)) in Kontroll- bzw. TRAM-34 behandelten Mäusen, n = 6-11. ** steht für $p \leq 0{,}01$ (ANOVA).

Zusammenfassend konnte durch diese Arbeit geklärt werden, dass die Bestrahlung von Glioblastomzellen *in vivo* zu einer verstärkten Migration der Zellen führt. Dieses Phänomen könnte während einer Strahlentherapie eine Streuung des Tumors zur Folge haben was wiederum zu einem Versagen der Therapie führen könnte. Da die radioinduzierte Migration sowohl durch gesteigerte Aktivität von BK_{Ca}- als auch IK_{Ca}-Kanälen stimuliert wird, stellt die Blockade dieser Kanäle eine geeignete Therapieoption während der Bestrahlung dar.

4 Radiosensibilisierung von Glioblastomzellen durch IK_{Ca}-Kanalblockade

Der Inhalt dieses Kapitels ist in folgender Arbeit veröffentlicht:

Benjamin Stegen, Lena Butz, Lukas Klumpp, Daniel Zips, Klaus Dittmann, Peter Ruth and Stephan M. Huber (2015). Ca^{2+}-Activated IK K^+ Channel Blockade Radiosensitizes Glioblastoma Cells. Molecular Cancer Research 13:1283-1295.

In dieser Publikation wurde der Effekt von IK_{Ca}-Kanälen auf die Strahlensensitivität von Glioblastomzellen näher untersucht. Wie bereits in Kapitel 1.3 dargestellt, sind IK_{Ca}-Kanäle normalerweise wenig bis fast gar nicht in normalen Astrozyten exprimiert und werden bei der Tumorgenese hochreguliert. Zusätzlich korreliert die IK_{Ca}-Kanalexpression mit einem signifikant schlechteren Überleben, was darauf hindeutet, dass der IK_{Ca}-Kanal einen Einfluss auf die Progression und das Therapieansprechen von Glioblastomen hat. In der vorliegenden Arbeit werden die IK_{Ca}-Kanäle sowohl mit TRAM-34 blockiert als auch mit shRNA genetisch herunterreguliert. Nach Bestrahlung werden dann die Unterschiede der verschiedenen Bedingungen auf das Ca^{2+}-„Signaling“, den Zellzyklus, die residualen Doppelstrangbrüche, das klonogene Überleben und das Tumorwachstum analysiert. Die Versuche wurden mit den humanen Glioblastomzelllinien T98G und U-87MG durchgeführt.

4.1 Ergebnisse

4.1.1 Analyse der IK_{Ca}-Kanalexpression mittels Immunfluoreszenzfärbungen und Patch-Clamp-Messungen

Als erstes wurden Untersuchungen zur IK_{Ca}-Kanalexpression mittels Immunfluoreszenzfärbungen durchgeführt. Es wurde die Expression in der embryonalen Astrozytenzelllinie SVGA mit der in der humanen Glioblastomzelllinie T98G verglichen. Wie zu erwarten, zeigen die Färbungen eine höhere IK_{Ca}-Kanalexpression in der Glioblastomzelllinie (Abb. 1A). Die Funktionalität der IK_{Ca}-Kanäle wurde mit Patch-Clamp-Messungen analysiert. Es wurden hierbei die Zelllinien SVGA, T98G und U-87MG näher betrachtet. Die Messungen wurden im „Whole-cell“ Modus mit physiologischer Bad- und Pipettenlösung durchgeführt. Es wurden Ströme vor und nach Ca^{2+}-Permeabilisierung mit

dem Ionophor Ionomycin gemessen. Um die durch Ca^{2+}-stimulierten Ströme voneinander zu unterscheiden, wurden nacheinander der BK_{Ca}- bzw. IK_{Ca}-Kanalinhibitor Paxillin bzw. TRAM-34 zu der Badlösung hinzugefügt. Abbildung 1D und E zeigen, dass die Zugabe von Ionomycin bei allen Spannungen, die größer als das Gleichgewichtspotential von K^+ sind (E_K -90 mV), Auswärtsströme in T98G-Zellen aktiviert. Nach Zugabe von Paxillin wurden ca. 80 % der Auswärtsströme inhibiert. Durch die zusätzliche Zugabe von TRAM-34 konnten die durch Ionomycin aktivierten Ströme nahezu vollständig blockiert werden. Betrachtet man die TRAM-34-sensitiven Stromfraktion, erkennt man einwärtsrektifizierende Ströme mit einem Umkehrpotential nahe dem K^+-Gleichgewichtspotential (Abb. 1F). In Astrozyten konnten wir hingegen durch die Zugabe von Ionomycin keine charakteristischen Auswärtsströme bei Spannungen unter -20 mV generieren. Was für das Fehlen von IK_{Ca}-Kanälen in den Astrozyten spricht. Durch die Zugabe von TRAM-34 konnte dies bestätigt werden. Es gab hier keine Inhibition der Ionomycin generierten Strömen (Abb. 1B-C).

4.1.2 Einfluss der Bestrahlung auf die Aktivität der IK_{Ca}-Kanäle und die intrazellulären Ca^{2+}-Konzentrationen

Um zu untersuchen, welchen Einfluss die Bestrahlung auf die Aktivität der IK_{Ca}-Kanäle hat, wurden T98G-Zellen zwei bis sechs Stunden nach Bestrahlung mittels „Cell-Attached“ Patch-Clamp-Messungen analysiert (Abb. 2A). Bestrahlung führte bei den Zellen zu einer Erhöhung der einwärtsgerichteten und auswärtsgerichteten Ströme (Abb. 2B-C). Wurde zusätzlich TRAM-34 in die Pipette gegeben, war die einwärtsgerichtete Stromfraktion nicht mehr sichtbar, was für durch Bestrahlung aktivierte IK_{Ca}-Kanäle spricht (Abb. 2B-E).

Um die den IK_{Ca}-Kanälen vorangeschalteten Signalwege näher zu untersuchen, wurde mittels Ca^{2+}-„Imaging“ der Effekt von Bestrahlung auf die intrazellulären Ca^{2+}-Konzentrationen in T98G-Zellen getestet. In Abbildungen 3B und C konnte gezeigt werden, dass mit der Bestrahlung ein Anstieg an intrazellulärem Ca^{2+} einhergeht. Die Aktivierung der IK_{Ca}-Kanäle nach Bestrahlung war also vermutlich auf die erhöhten Ca^{2+}-Spiegel zurückzuführen und nicht auf eine erhöhte Expression von IK_{Ca}-Kanälen, wie es der Western Blot in Abbildung 3A zeigt. Messungen im „Steady state“ zeigten einen signifikanten Anstieg an intrazellulärem Ca^{2+} nach Bestrahlung. Nach Entfernen von Ca^{2+} und anschließender Wiederzugabe konnte man ein stärkeres Absinken der Ca^{2+}-Spiegel und einen stärkeren Wiederanstieg bei den

bestrahlten Zellen erkennen (Abb. 2B-C). Dieses Phänomen könnte auf ein verändertes Geleichgewicht zwischen passiver Ca^{2+}-Aufnahme und aktiver Ca^{2+}-Extrusion in der Plasmamembran zurückzuführen sein.

4.1.3 Analyse der Veränderungen in der Zellzykluskontrolle durch Bestrahlung und TRAM-34

Es ist bereits bekannt, dass bestrahlungsinduzierte Kaliumkanäle den Zellzyklus von Tumorzellen beeinflussen können (Palme et al., 2013). Mittels Durchflusszytometrie wurde daher der Einfluss von Bestrahlung auf den Zellzyklus von T98G-Zellen untersucht. Hierfür wurde innerhalb der ersten sechs Stunden nach Bestrahlung die Aufnahme des Thymidinanalogons EdU (5-Ethynyl-2'-Desoxyuridin) in bestrahlten und unbestrahlten Zellen analysiert. In Abbildung 4A ist jeweils die Aufnahme von EdU in Abhängigkeit vom DNA-Gehalt dargestellt. Der DNA-Gehalt wurde mit Propidiumiodid, einem DNA spezifischen Fluoreszenzfarbstoff, bestimmt. Bestrahlung führte zu einem Anstieg der Zellpopulationen in der G_1-, S-, G_2-Phase mit einer geringen EdU-Fluoreszenzintensität (Abb. 4B). Dies deutet darauf hin, dass Bestrahlung zu einem Zellzyklusarrest der Zellen in der G_1- und S-Phase bzw. in dem G_2-M-Übergang führte. Bestrahlung erniedrigte vor allem das Verhältnis von Zellpopulationen in der S_{high}-Phase und $G_{1\ low}$-Phase (high und low steht für die Aufnahme von EdU) und das Verhältnis zwischen der $G_{1\ low}$-und $G_{2\ low}$-Phase (Abb. 4B). Dies spricht für eine Inhibition des G_1-S-Übergangs und der Mitose in bestrahlten T98G-Zellen.

Um die Funktion der IK_{Ca}-Kanäle in diesem Zusammenhang zu ermitteln, wurde der DNA-Gehalt 24 und 48 Stunden nach Bestrahlung (0, 2, 4 oder 6 Gy) in Kombination mit einer IK_{Ca}-Kanalblockade (TRAM-34) mittels Propidiumiodid durchflusszytometrisch vermessen (Abb. 4C). Abbildung 4D zeigt, dass 24 Stunden nach Bestrahlung (2 und 4 Gy) die Zellpopulationen in der G_1-Phase abnahmen und in der S- und G_2-Phase zunahmen. Der vorher durch die EdU-Aufnahme detektierte G_1-Arrest scheint also nur von kurzer Dauer zu sein. Im Gegensatz hierzu zeigten die mit 6 Gy bestrahlten Zellen eine prozentual kleinere Akkumulation in der S- und G_2-Phase als die mit 2 und 4 Gy bestrahlten Zellen. Dies deutet auf einen anhaltenden G_1-Arrest in einem Teil der Zellen, die mit einer höheren Strahlendosis behandelt wurden hin. 48 Stunden nach Bestrahlung hingegen nahmen die Populationen in der G_1-Phase linear mit der Strahlendosis ab bzw. in der G_2-Phase mit der Strahlendosis zu (Abb. 4D), was den

nur vorübergehenden G_1-Arrest bestätigt. TRAM-34 verhindert nun die strahleninduzierte Abnahme der Zellpopulationen in der G_1-Phase und Akkumulation der Zellen in der G_2-Phase (Abb. 4D). Durch diese Daten wird eine Beteiligung der IK_{Ca}-Kanäle an der Zellzykluskontrolle bestätigt. Da TRAM-34 jedoch kaum einen Einfluss auf den Zellzyklus unbestrahlter Zellen hat, scheinen IK_{Ca}-Kanäle eine besondere Rolle in der Zellzykluskontrolle nach Bestrahlung zu spielen.

4.1.4 Bestimmung der residualen Doppelstrangbrüche und des klonogenen Überlebens nach Bestrahlung und IK_{Ca}-Kanalblockade

Die Analyse der residualen Doppelstrangbrüche in T98G-Zellen erfolgte durch die Bestimmung der Anzahl der γH_2AX-Foci mittels Immunfluoreszenzmikroskopie (Abb. 5A). Die Foci wurden 24 Stunden nach Bestrahlung ausgewertet. TRAM-34 erhöhte die DNA-Doppelstrangbrüche nach Bestrahlung signifikant (Abb. 5A-B). Abbildung 5C zeigt, dass die Anzahl der Zellkerne mit niedriger, mittlerer und hoher Foci-Anzahl in beiden Gruppen ähnlich ist und es lediglich eine Rechtsverschiebung bei den mit TRAM-34 behandelten Zellen gibt. Das bedeutet, dass es bei einer zusätzlichen Behandlung mit TRAM-34 in der Regel zu mehr Foci pro Zellkern kommt. Diese Rechtsverschiebung könnte mit einer Verzögerung in der DNA Reparatur erklärt werden.

TRAM-34 alleine scheint bereits Doppelstrangbrüche in T98G-Zellen zu begünstigen was auf einen genotoxischen Effekt des TRAM-34 hindeuten könnte. Um dies zu untersuchen wurden „Delayed plating“-Koloniebildungsassays durchgeführt. Hier gab es jedoch keinen Unterschied in der „Plating efficacy“ verglichen mit der Lösungsmittelkontrolle (Abb. 6A). Der Versuch wurde mit U-87MG-Zellen wiederholt und es zeigten sich die gleichen Ergebnisse (Abb. 6B). Sobald beide Zelllinien zusätzlich zur Bestrahlung mit TRAM-34 behandelt wurden nahm das klonogene Überleben der Zellen signifikant um den Faktor 1,4 (T98G) bzw. 1,3 (U-87MG) ab (Abb. 6A-B). Diese Daten zeigen einen ähnlichen radiosensitivierenden Effekt von TRAM-34 auf zwei verschiedene Zelllinien, obwohl sich die intrinsische Strahlensensitivität beider Zelllinien deutlich unterschieden (Abb. 6A-B).

4.1.5 Knockdown der IK_{Ca}-Kanäle mittels shRNA

Zusätzlich zur IK_{Ca}-Kanalblockade durch TRAM-34 wurden die Kanäle in T98G-Zellen mittels shRNAs herunterreguliert (Abb. 7A-B). Mit diesen Experimenten sollte die Spezifität von TRAM-34 verifiziert werden. Klon 3 zeigte dabei die größte stabile Herunterregulation von IK_{Ca}-Kanälen (Abb. 7A-B). Mit Hilfe der Durchflusszytometrie wurde deutlich, dass sich bei Klon 3 ein größerer prozentualer Anteil der Zellen in der G_1-Phase des Zellzyklus befand als bei dem Kontrollklon 2. Dies deutet auf unterschiedliche Verdopplungszeiten der zwei Klone hin (Abb. 7C). Nach Bestrahlung der beiden Klone nahm der prozentuale Anteil der Zellen in der G_1-Phase linear mit der Dosis ab wohingegen die Akkumulation der Zellen in der G_2-Phase zunahm. Wie erwartet konnte TRAM-34 die Veränderungen im Zellzyklus bei Klon 3 regulieren bei dem Kontrollklon 2 jedoch nicht (Abb. 7C).

Auch bei der Bestimmung der residualen Doppelstrangbrüche konnten zuvor beschriebene Ergebnisse bestätigt werden. Die Analyse folgte wie in Kapitel 4.1.4. Es wurden die Anzahl der γH_2AX-Foci in den beiden Klonen verglichen. Abbildungen 7D und E zeigen, dass Klon 3 sowohl bestrahlt als auch unbestrahlt eine höhere Anzahl an γH_2AX-Foci im Vergleich zum Kontrollklon 2 aufweist. Die Tendenz, dass unbestrahlte Zellen nach IK_{Ca}-Kanalblockade mehr residuale Doppelstrangbrüche zeigen wurde ebenfalls bereits in Kapitel 4.1.4 beschrieben. Zur weiteren Untersuchung des genotoxischen Effekts einer IK_{Ca}-Kanaldefizienz wurden auch hier „Delayed plating"-Koloniebildungsassays durchgeführt. Interessanterweise waren beide Klone radioresistenter als die unbehandelten T98G-Zellen (vergleiche Abb. 7F mit 6A). Zusätzlich war aber auch in diesem Versuch der Klon 3 radiosensitiver als der Kontrollklon 2 und TRAM-34 hatte nur auf den Kontrollklon 2 einen radiosensibilisierenden Effekt (Abb. 7F). Zusammenfassend kann man sagen, dass sowohl die pharmakologische als auch genetische Herunterregulierung von IK_{Ca}-Kanälen radiosensibilisierende Effekte in Glioblastomzellen zeigten und TRAM-34 als spezifischer IK_{Ca}-Kanalblocker genutzt werden konnte.

4.1.6 Wirkung von TRAM-34 auf die Radiosensibilität von Glioblastomzellen *in vivo*

Um den Effekt von TRAM-34 auf die Radiosensibilität auch *in vivo* zu untersuchen, wurde ein ektopes Glioblastommausmodell verwendet. Es wurden humane U-87MG-Zellen in den rechten Hinterlauf immunsupprimierter Nacktmäuse injiziert. Sobald die ektopen

Glioblastome ein Volumen von 150 µl erreicht hatten, begann die Behandlung (Tag 0). Die Mäuse wurden hierfür in vier Behandlungsgruppen eingeteilt. In Abbildung 8A sind die Tumorvolumina der Mäuse aus den unterschiedlichen Gruppen an Tag 0 aufgeführt. Je nach Gruppe wurden die Hinterläufe der Mäuse fraktioniert an fünf aufeinanderfolgenden Tagen mit 0 bzw. 4 Gy Fraktionen bestrahlt und/oder zusätzlich sechs Stunden vor jeder Bestrahlung mit TRAM-34 behandelt (Kontrolle, n = 5; TRAM-34, n = 4; IR n = 9; TRAM-34/IR n = 6). Die Tumorvolumina wurden auf das Startvolumen normalisiert und vor während bzw. nach der Behandlung dokumentiert (Abb. 8B-C). Drei Mäuse zeigten unter Behandlung eine komplette Tumorremission. Hiervon bekam eine Maus eine Kombination aus Bestrahlung und TRAM-34 und zwei Mäuse eine Strahlentherapie alleine. Der Zeitraum bis zur Tumorprogression ist Abbildung 8D aufgeführt. Die Mäuse, die zusätzlich zur Bestrahlung mit TRAM-34 behandelt wurden, weisen signifikant längere Zeiträume auf als die unbehandelten Mäuse. Da es bei einer Maus zu keiner Tumorprogression mehr kam, konnte diese in der Grafik nicht berücksichtigt werden (Abb. 8F).

In Abbildungen 8E und F wurde das Tumorvolumen logarithmisch aufgetragen. Aus diesen Abbildungen ist das exponentielle Wachstum der Tumoren deutlich ersichtlich. Im Folgenden wurden dann die Steigungen der logarithmisch aufgetragenen Tumorvolumina in Abhängigkeit von der Zeit berechnet. Abbildungen 8G und E zeigen die Steigungen vor Therapiebeginn bzw. während der Therapie. In Abbildung 8I ist der Rückgang der Steigungen unter der Therapie aufgeführt. Es ist ersichtlich, dass nur die Kombination von Bestrahlung und TRAM-34 zu einem signifikanten Rückgang des exponentiellen Tumorwachstums führte. TRAM-34 zeigte also auch *in vivo* einen radiosensibilisierenden Effekt auf humane Glioblastomzellen.

4.1.7 Analyse des Einflusses von IK_{Ca}-Kanälen auf die Therapieresistenz in der Klinik

Um die mögliche Funktion der IK_{Ca}-Kanäle auf die Therapieresistenz von Glioblastompatienten bzw. Patienten mit niedriggradigen Gliomen in der Klinik zu untersuchen, wurden Datenbanken auf einen Zusammenhang gescreent. Patientendaten aus „Cancer Genome Atlas“ (TCGA) zeigten, dass erhöhte IK_{Ca}-Kanal mRNA-Expressionen, sowohl bei Glioblastompatienten (Abb. 9C, D), als auch bei Patienten mit niedriggradigen

Gliomen (Abb. 9A, B) mit einem schlechteren progressionsfreien Überleben (PFS) (Abb. 9A, C) und Gesamtüberleben (OS) (Abb. 9B, D) assoziiert ist.

4.2 Diskussion

In der vorliegenden Arbeit konnte gezeigt werden, dass Bestrahlung die Ca^{2+}-Signalkaskade induziert und IK_{Ca}-Kanäle aktiviert. Die IK_{Ca}-Kanäle sind wiederum verantwortlich für Veränderungen im Zellzyklus der Glioblastomzellen. Dass IK_{Ca}-Kanäle das Überleben der Zellen nach Bestrahlung fördern, konnte aus der Radiosensibilisierung durch Blockade der Kanäle mit TRAM-34 geschlossen werden.

Auch in einigen anderen Tumorentitäten wurde ein Zusammenhang zwischen Bestrahlung und Veränderungen in der Ca^{2+}-Signalkaskade bzw. Kaliumkanalaktivität beobachtet. In einem Adenokarzinom der Lunge sind Kaliumkanäle beispielsweise für eine verstärkte Glukoseaufnahme in bestrahlten Zellen verantwortlich. Die hohen Glukosespiegel werden benötigt, um den erhöhten Energiebedarf der Zellen durch die DNA-Schädigungen zu decken (Huber et al., 2012). In Leukämiezellen wurde beobachtet, dass Bestrahlung sowohl Ca^{2+}-permeable-Kanäle als auch Kaliumkanäle aktiviert. Dies führt zu Ca^{2+}-Signalen, die zu einem Zellzyklusarrest führen. Zusätzlich wird über die CaMKII das, für den Zellzyklus essentielle, cdc2-Protein gehemmt. Die Blockade von Kaliumkanälen führt hier zu einer Aufhebung des Zellzyklusarrests und damit zu einer Radiosensibilisierung der Leukämiezellen (Palme et al., 2013).

In Kapitel 4.1.2 wurde deutlich, dass die intrazellulären Ca^{2+}-Spiegel im „Steady state“ in den bestrahlten Zellen fast doppelt so hoch waren wie in den unbestrahlten Zellen (Abb. 3B-C). Aus der Literatur ist bekannt, dass Glioblastomzellen sowohl STIM1/Orai1 Ca^{2+}-Kanäle (Motiani et al., 2013), als auch TRPC1 und TRPM8 Ca^{2+}-permeable nicht selektive Kationenkanäle (Bomben and Sontheimer, 2010; Wondergem et al., 2008) exprimieren. Diese Kanäle könnten für den Anstieg von intrazellulärem Ca^{2+} in bestrahlten Zellen verantwortlich sein. In unserer Arbeitsgruppe konnten wir bereits zeigen, dass es durch eine Herunterregulierung von TRPM8 zu einer Beeinträchtigung der Radioresistenz und der Migration von Glioblastomzellen kommt (Klumpp et al, manuscript submitted).

Doch IK_{Ca}-Kanäle sind auch an der Migration beteiligt. In Kapitel 3 wurde bereits beschrieben, dass eine radioinduzierte Aktivierung von BK_{Ca}-Kanälen zu einer verstärkten

Migration von Glioblastomzellen führt. IK_{Ca}-Kanäle sind bekanntermaßen bei einer durch Serum-, Bradykinin- und SDF-1-induzierten Migration von Glioblastomzellen involviert (Catacuzzeno et al., 2011; Cuddapah et al., 2013; Sciaccaluga et al., 2010). In Übereinstimmung mit diesen *in vitro* Daten konnte in einer weiteren Publikation durch die Inhibition von IK_{Ca}-Kanälen mit TRAM-34 die Gehirninfiltration von Glioblastomzellen in einem orthotopen Mausmodell vermindert werden (D'Alessandro et al., 2013).

Des Weiteren ist bekannt, dass eine erhöhte IK_{Ca}-Kanalexpression vor allem in Glioblastomstammzellen zu finden ist (Ruggieri et al., 2012). Da Glioblastomstammzellen eine erhöhte Migration zeigen, sind diese vermutlich hauptverantwortlich für die Gehirninvasion (Nakada et al., 2013). Tatsächlich vermitteln bei der Gehirnentwicklung IK_{Ca}-Kanäle die Migration neuronaler Vorläuferzellen zur Kopfvorderseite um Interneurone im Bulbus olfactorius zu bilden (Turner and Sontheimer, 2014).

Glioblastomstammzellen gelten zusätzlich auch als therapieresistenter im Vergleich zu den relativ differenzierten Glioblastomzellen (Huber, 2013; Huber et al., 2013; Huber et al., 2015). Die *in vitro* und *in vivo* Experimente der vorliegenden Arbeit zeigen, dass IK_{Ca}-Kanäle, neben der bereits beschriebenen Gehirninvasion, auch an der Strahlenresistenz von Glioblastomzellen über eine Kontrolle des Zellzyklus beteiligt sind. Dies konnte in einer anderen Publikation ebenfalls gezeigt werden (Liu et al., 2010). IK_{Ca}-Kanäle haben somit eine doppelte Funktion für die Biologie des Glioblastoms.

Kürzlich veröffentlichte retrospektive klinische Daten aus der REMBRANDT-Datenbank des „National Cancer Institute“ bestätigen, dass in mehr als 30 % aller Proben die IK_{Ca}-Kanäle um das 1,5 fache im Vergleich zu Normalgewebe hochreguliert sind, und deren Expression mit einem schlechteren Überleben der Patienten korreliert ist (Turner et al., 2014). Ähnliches konnte im Rahmen dieser Arbeit mit Hilfe der Daten aus der TCGA-Datenbank gezeigt werden. Hier korreliert die IK_{Ca}-Kanal-mRNA-Expression sowohl mit einem schlechteren progressionsfreien Überleben (PFS) als auch mit einem schlechteren Gesamtüberleben (OS). Leider konnten mit Hilfe der beiden Datenbanken keine Aussagen über z.B. die Tumorgröße, das Ausmaß der Tumorresektion, das Therapieregime und weitere Details gemacht werden, was eine vollständige Interpretation der Daten erschwert. Die meisten Patienten erhalten allerdings eine Strahlentherapie was bedeutet, dass diese Daten einen Hinweis auf einen radioprotektiven Effekt der IK_{Ca}-Kanäle geben. IK_{Ca}-Kanäle stellen aus diesem Grund ein

interessantes Target für die Antitumortherapie von Glioblastomen dar. Bei Erkrankungen wie der Anämie (Foller et al., 2010; Lang et al., 2003), im Besonderen der Sichelzellanämie (Ataga et al., 2006; Ataga et al., 2011; Ataga et al., 2008; Ataga and Stocker, 2009), Alzheimer (Maezawa et al., 2012) oder weiteren inflammatorischen Erkrankungen (Lam and Wulff, 2011) sind IK_{Ca}-Kanäle als Zielstruktur bereits im Gespräch. Zusätzlich ist Senicapoc (ICA-17043), ein IK_{Ca}-Kanalinhibitor welcher potenter als TRAM-34 und oral bioverfügbar ist, und in klinischen Studien bereits auf seine Verträglichkeit getestet worden ist. Eine tägliche Dosierung von 10 mg Senicapoc führt zu Plasmaspiegeln von 100 ng/ml. Tracer flux Experimente haben gezeigt, dass mit diesen Plasmaspiegeln bis zu 70 % der IK_{Ca}-Kanäle inhibiert werden (Ataga et al., 2008). Da bei Glioblastompatienten die Blut-Hirn-Schranke in ihrer Funktion beeinträchtigt ist, stellt auch die Überwindung der Blut-Hirn-Schranke bei den Inhibitoren kein Hindernis dar (Cheng et al., 2013; Wang et al., 2010). Alles in Allem zeigen die Untersuchungen, dass IK_{Ca}-Kanäle eine sehr geeignete Zielstruktur darstellen. Sie regulieren die Mechanismen in Glioblastomzellen, die hauptverantwortlich für ein Versagen der Therapie sind. Eine Kombination von IK_{Ca}-Kanalinhibitoren mit Chemotherapie und Bestrahlung könnte also ein geeignetes Therapieregime bedeuten. Ein noch größerer Effekt könnte durch eine intrakranielle Gabe der Inhibitoren erreicht werden. Hierbei könnten höhere Spiegel mit weniger Nebenwirkungen realisiert werden.

5 Literaturverzeichnis

Ataga, K.I., E.P. Orringer, L. Styles, E.P. Vichinsky, P. Swerdlow, G.A. Davis, P.A. Desimone, and J.W. Stocker. 2006. Dose-escalation study of ICA-17043 in patients with sickle cell disease. *Pharmacotherapy*. 26:1557-1564.

Ataga, K.I., M. Reid, S.K. Ballas, Z. Yasin, C. Bigelow, L.S. James, W.R. Smith, F. Galacteros, A. Kutlar, J.H. Hull, J.W. Stocker, and I.C.A.S. Investigators. 2011. Improvements in haemolysis and indicators of erythrocyte survival do not correlate with acute vaso-occlusive crises in patients with sickle cell disease: a phase III randomized, placebo-controlled, double-blind study of the Gardos channel blocker senicapoc (ICA-17043). *Br J Haematol*. 153:92-104.

Ataga, K.I., W.R. Smith, L.M. De Castro, P. Swerdlow, Y. Sauntharajah, O. Castro, E. Vichinsky, A. Kutlar, E.P. Orringer, G.C. Rigdon, J.W. Stocker, and I.C.A. Investigators. 2008. Efficacy and safety of the Gardos channel blocker, senicapoc (ICA-17043), in patients with sickle cell anemia. *Blood*. 111:3991-3997.

Ataga, K.I., and J. Stocker. 2009. Senicapoc (ICA-17043): a potential therapy for the prevention and treatment of hemolysis-associated complications in sickle cell anemia. *Expert Opin Investig Drugs*. 18:231-239.

Beckmann, I.-A. 2014. Die blauen Ratgeber - Strahlentherapie. D. Krebshilfe, editor. Deutsche Krebshilfe.

Bloch, M., J. Ousingsawat, R. Simon, P. Schraml, T.C. Gasser, M.J. Mihatsch, K. Kunzelmann, and L. Bubendorf. 2007. KCNMA1 gene amplification promotes tumor cell proliferation in human prostate cancer. *Oncogene*. 26:2525-2534.

Bomben, V.C., and H. Sontheimer. 2010. Disruption of transient receptor potential canonical channel 1 causes incomplete cytokinesis and slows the growth of human malignant gliomas. *Glia*. 58:1145-1156.

Bulk, E., A.S. Ay, M. Hammadi, H. Ouadid-Ahidouch, S. Schelhaas, A. Hascher, C. Rohde, N.H. Thoennissen, R. Wiewrodt, E. Schmidt, A. Marra, L. Hillejan, A.H. Jacobs, H.U. Klein, M. Dugas, W.E. Berdel, C. Muller-Tidow, and A. Schwab. 2015. Epigenetic dysregulation of KCa 3.1 channels induces poor prognosis in lung cancer. *Int J Cancer*. 137:1306-1317.

Castro, O.L., V.R. Gordeuk, M.T. Gladwin, and M.H. Steinberg. 2011. Senicapoc trial results support the existence of different sub-phenotypes of sickle cell disease with possible drug-induced phenotypic shifts. *Br J Haematol*. 155:636-638.

Catacuzzeno, L., F. Aiello, B. Fioretti, L. Sforna, E. Castigli, P. Ruggieri, A.M. Tata, A. Calogero, and F. Franciolini. 2011. Serum-activated K and Cl currents underlay U87-MG glioblastoma cell migration. *J Cell Physiol*. 226:1926-1933.

Catacuzzeno, L., M. Caramia, L. Sforna, S. Belia, L. Guglielmi, M.C. D'Adamo, M. Pessia, and F. Franciolini. 2015. Reconciling the discrepancies on the involvement of large-conductance Ca(2+)-activated K channels in glioblastoma cell migration. *Front Cell Neurosci*. 9:152.

Catacuzzeno, L., B. Fioretti, and F. Franciolini. 2012. A theoretical study on the role of Ca(2+)-activated K+ channels in the regulation of hormone-induced Ca2+ oscillations and their synchronization in adjacent cells. *J Theor Biol*. 309:103-112.

Chen, L., and M.J. Shipston. 2008. Cloning of potassium channel splice variants from tissues and cells. *Methods Mol Biol*. 491:35-60.

Cheng, L., Z. Huang, W. Zhou, Q. Wu, S. Donnola, J.K. Liu, X. Fang, A.E. Sloan, Y. Mao, J.D. Lathia, W. Min, R.E. McLendon, J.N. Rich, and S. Bao. 2013. Glioblastoma stem cells generate vascular pericytes to support vessel function and tumor growth. *Cell*. 153:139-152.

Cuddapah, V.A., and H. Sontheimer. 2010. Molecular interaction and functional regulation of ClC-3 by Ca2+/calmodulin-dependent protein kinase II (CaMKII) in human malignant glioma. *J Biol Chem*. 285:11188-11196.

Cuddapah, V.A., K.L. Turner, S. Seifert, and H. Sontheimer. 2013. Bradykinin-induced chemotaxis of human gliomas requires the activation of KCa3.1 and ClC-3. *J Neurosci*. 33:1427-1440.

D'Alessandro, G., M. Catalano, M. Sciaccaluga, G. Chece, R. Cipriani, M. Rosito, A. Grimaldi, C. Lauro, G. Cantore, A. Santoro, B. Fioretti, F. Franciolini, H. Wulff, and C. Limatola. 2013. KCa3.1 channels are involved in the infiltrative behavior of glioblastoma in vivo. *Cell Death Dis*. 4:e773.

Desmarais, G., G. Charest, D. Fortin, R. Bujold, D. Mathieu, and B. Paquette. 2015. Cyclooxygenase-2 inhibitor prevents radiation-enhanced infiltration of F98 glioma cells in brain of Fischer rat. *Int J Radiat Biol*. 91:624-633.

Eke, I., K. Storch, I. Kastner, A. Vehlow, C. Faethe, W. Mueller-Klieser, G. Taucher-Scholz, A. Temme, G. Schackert, and N. Cordes. 2012. Three-dimensional invasion of human glioblastoma cells remains unchanged by X-ray and carbon ion irradiation in vitro. *Int J Radiat Oncol Biol Phys*. 84:e515-523.

Fanger, C.M., S. Ghanshani, N.J. Logsdon, H. Rauer, K. Kalman, J. Zhou, K. Beckingham, K.G. Chandy, M.D. Cahalan, and J. Aiyar. 1999. Calmodulin mediates calcium-dependent activation of the intermediate conductance KCa channel, IKCa1. *J Biol Chem*. 274:5746-5754.

Fioretti, B., E. Castigli, M.R. Micheli, R. Bova, M. Sciaccaluga, A. Harper, F. Franciolini, and L. Catacuzzeno. 2006. Expression and modulation of the intermediate-conductance Ca2+-activated K+ channel in glioblastoma GL-15 cells. *Cell Physiol Biochem*. 18:47-56.

Foller, M., D. Bobbala, S. Koka, K.M. Boini, H. Mahmud, R.S. Kasinathan, E. Shumilina, K. Amann, G. Beranek, U. Sausbier, P. Ruth, M. Sausbier, F. Lang, and S.M. Huber. 2010. Functional significance of the intermediate conductance Ca2+-activated K+ channel for the short-term survival of injured erythrocytes. *Pflugers Arch*. 460:1029-1044.

Gardos, G. 1958. The function of calcium in the potassium permeability of human erythrocytes. *Biochim Biophys Acta*. 30:653-654.

Geldof, A.A., M.A. Plaizier, I. Duivenvoorden, M. Ringelberg, R.T. Versteegh, D.W. Newling, and G.J. Teule. 2003. Cell cycle perturbations and radiosensitization effects in a human prostate cancer cell line. *J Cancer Res Clin Oncol*. 129:175-182.

Greenfield, J.P., W.S. Cobb, and D. Lyden. 2010. Resisting arrest: a switch from angiogenesis to vasculogenesis in recurrent malignant gliomas. *J Clin Invest*. 120:663-667.

Gueguinou, M., A. Chantome, G. Fromont, P. Bougnoux, C. Vandier, and M. Potier-Cartereau. 2014. KCa and Ca(2+) channels: the complex thought. *Biochim Biophys Acta*. 1843:2322-2333.

Haas, B.R., and H. Sontheimer. 2010. Inhibition of the Sodium-Potassium-Chloride Cotransporter Isoform-1 reduces glioma invasion. *Cancer research*. 70:5597-5606.

Haren, N., H. Khorsi, M. Faouzi, A. Ahidouch, H. Sevestre, and H. Ouadid-Ahidouch. 2010. Intermediate conductance Ca2+ activated K+ channels are expressed and functional in breast adenocarcinomas: correlation with tumour grade and metastasis status. *Histol Histopathol*. 25:1247-1255.

Heise, N., D. Palme, M. Misovic, S. Koka, J. Rudner, F. Lang, H.R. Salih, S.M. Huber, and G. Henke. 2010. Non-selective cation channel-mediated Ca2+-entry and activation of Ca2+/calmodulin-dependent kinase II contribute to G2/M cell cycle arrest and survival of irradiated leukemia cells. *Cell Physiol Biochem*. 26:597-608.

Holland, E.C. 2000. Glioblastoma multiforme: the terminator. *Proc Natl Acad Sci U S A*. 97:6242-6244.

Horrigan, F.T., and R.W. Aldrich. 1999. Allosteric voltage gating of potassium channels II. Mslo channel gating charge movement in the absence of Ca(2+). *J Gen Physiol*. 114:305-336.

Hou, S., R. Xu, S.H. Heinemann, and T. Hoshi. 2008a. The RCK1 high-affinity Ca2+ sensor confers carbon monoxide sensitivity to Slo1 BK channels. *Proc Natl Acad Sci U S A*. 105:4039-4043.

Hou, S., R. Xu, S.H. Heinemann, and T. Hoshi. 2008b. Reciprocal regulation of the Ca2+ and H+ sensitivity in the SLO1 BK channel conferred by the RCK1 domain. *Nat Struct Mol Biol*. 15:403-410.

Huber, S.M. 2013. Oncochannels. *Cell Calcium*. 53:241-255.

Huber, S.M., L. Butz, B. Stegen, D. Klumpp, N. Braun, P. Ruth, and F. Eckert. 2013. Ionizing radiation, ion transports, and radioresistance of cancer cells. *Front Physiol*. 4:212.

Huber, S.M., L. Butz, B. Stegen, L. Klumpp, D. Klumpp, and F. Eckert. 2015. Role of ion channels in ionizing radiation-induced cell death. *Biochim Biophys Acta*. 1848:2657-2664.

Huber, S.M., M. Misovic, C. Mayer, H.P. Rodemann, and K. Dittmann. 2012. EGFR-mediated stimulation of sodium/glucose cotransport promotes survival of irradiated human A549 lung adenocarcinoma cells. *Radiother Oncol*. 103:373-379.

Ifuku, M., K. Farber, Y. Okuno, Y. Yamakawa, T. Miyamoto, C. Nolte, V.F. Merrino, S. Kita, T. Iwamoto, I. Komuro, B. Wang, G. Cheung, E. Ishikawa, H. Ooboshi, M. Bader, K. Wada, H. Kettenmann, and M. Noda. 2007. Bradykinin-induced microglial migration mediated by B1-bradykinin receptors depends on Ca2+ influx via reverse-mode activity of the Na+/Ca2+ exchanger. *J Neurosci*. 27:13065-13073.

Imlach, W.L., S.C. Finch, J. Dunlop, A.L. Meredith, R.W. Aldrich, and J.E. Dalziel. 2008. The molecular mechanism of "ryegrass staggers," a neurological disorder of K+ channels. *J Pharmacol Exp Ther*. 327:657-664.

Ishii, T.M., C. Silvia, B. Hirschberg, C.T. Bond, J.P. Adelman, and J. Maylie. 1997. A human intermediate conductance calcium-activated potassium channel. *Proc Natl Acad Sci U S A*. 94:11651-11656.

Jensen, B.S., D. Strobaek, P. Christophersen, T.D. Jorgensen, C. Hansen, A. Silahtaroglu, S.P. Olesen, and P.K. Ahring. 1998. Characterization of the cloned human intermediate-conductance Ca2+-activated K+ channel. *Am J Physiol*. 275:C848-856.

Johnson, J., M.O. Nowicki, C.H. Lee, E.A. Chiocca, M.S. Viapiano, S.E. Lawler, and J.J. Lannutti. 2009. Quantitative analysis of complex glioma cell migration on electrospun polycaprolactone using time-lapse microscopy. *Tissue Eng Part C Methods*. 15:531-540.

Jung, J.W., S.Y. Hwang, J.S. Hwang, E.S. Oh, S. Park, and I.O. Han. 2007. Ionising radiation induces changes associated with epithelial-mesenchymal transdifferentiation and increased cell motility of A549 lung epithelial cells. *Eur J Cancer*. 43:1214-1224.

Kanaar, R., J.H. Hoeijmakers, and D.C. van Gent. 1998. Molecular mechanisms of DNA double strand break repair. *Trends Cell Biol*. 8:483-489.

Khaitan, D., U.T. Sankpal, B. Weksler, E.A. Meister, I.A. Romero, P.O. Couraud, and N.S. Ningaraj. 2009. Role of KCNMA1 gene in breast cancer invasion and metastasis to brain. *BMC Cancer*. 9:258.

Khalid, M.H., S. Shibata, and T. Hiura. 1999. Effects of clotrimazole on the growth, morphological characteristics, and cisplatin sensitivity of human glioblastoma cells in vitro. *J Neurosurg*. 90:918-927.

Khalid, M.H., Y. Tokunaga, A.J. Caputy, and E. Walters. 2005. Inhibition of tumor growth and prolonged survival of rats with intracranial gliomas following administration of clotrimazole. *J Neurosurg*. 103:79-86.

Knaus, H.G., O.B. McManus, S.H. Lee, W.A. Schmalhofer, M. Garcia-Calvo, L.M. Helms, M. Sanchez, K. Giangiacomo, J.P. Reuben, A.B. Smith, 3rd, and et al. 1994. Tremorgenic indole alkaloids potently inhibit smooth muscle high-conductance calcium-activated potassium channels. *Biochemistry*. 33:5819-5828.

Kraft, R., P. Krause, S. Jung, D. Basrai, L. Liebmann, J. Bolz, and S. Patt. 2003. BK channel openers inhibit migration of human glioma cells. *Pflugers Arch*. 446:248-255.

Lallet-Daher, H., M. Roudbaraki, A. Bavencoffe, P. Mariot, F. Gackiere, G. Bidaux, R. Urbain, P. Gosset, P. Delcourt, L. Fleurisse, C. Slomianny, E. Dewailly, B. Mauroy, J.L. Bonnal, R. Skryma, and N. Prevarskaya. 2009. Intermediate-conductance Ca2+-activated K+ channels (IKCa1) regulate human prostate cancer cell proliferation through a close control of calcium entry. *Oncogene*. 28:1792-1806.

Lam, J., and H. Wulff. 2011. The Lymphocyte Potassium Channels Kv1.3 and KCa3.1 as Targets for Immunosuppression. *Drug Dev Res*. 72:573-584.

Lang, P.A., S. Kaiser, S. Myssina, T. Wieder, F. Lang, and S.M. Huber. 2003. Role of Ca2+-activated K+ channels in human erythrocyte apoptosis. *Am J Physiol Cell Physiol*. 285:C1553-1560.

Laperriere, N., L. Zuraw, G. Cairncross, and G. Cancer Care Ontario Practice Guidelines Initiative Neuro-Oncology Disease Site. 2002. Radiotherapy for newly diagnosed malignant glioma in adults: a systematic review. *Radiother Oncol*. 64:259-273.

Liu, H., Y. Li, and K.P. Raisch. 2010. Clotrimazole induces a late G1 cell cycle arrest and sensitizes glioblastoma cells to radiation in vitro. *Anticancer Drugs*. 21:841-849.

Liu, X., Y. Chang, P.H. Reinhart, H. Sontheimer, and Y. Chang. 2002. Cloning and characterization of glioma BK, a novel BK channel isoform highly expressed in human glioma cells. *J Neurosci*. 22:1840-1849.

Louis, D.N., H. Ohgaki, O.D. Wiestler, and W.K. Cavenee. 2007. WHO classification of tumours of the central nervous system. IARC, Lyon.

Maezawa, I., D.P. Jenkins, B.E. Jin, and H. Wulff. 2012. Microglial KCa3.1 Channels as a Potential Therapeutic Target for Alzheimer's Disease. *Int J Alzheimers Dis*. 2012:868972.

McNaughton-Smith, G.A., J.F. Burns, J.W. Stocker, G.C. Rigdon, C. Creech, S. Arrington, T. Shelton, and L. de Franceschi. 2008. Novel inhibitors of the Gardos channel for the treatment of sickle cell disease. *J Med Chem*. 51:976-982.

Minniti, G., D. Amelio, M. Amichetti, M. Salvati, R. Muni, A. Bozzao, G. Lanzetta, S. Scarpino, A. Arcella, and R.M. Enrici. 2010. Patterns of failure and comparison of

different target volume delineations in patients with glioblastoma treated with conformal radiotherapy plus concomitant and adjuvant temozolomide. *Radiother Oncol*. 97:377-381.

Montana, V., and H. Sontheimer. 2011. Bradykinin promotes the chemotactic invasion of primary brain tumors. *J Neurosci*. 31:4858-4867.

Motiani, R.K., M.C. Hyzinski-Garcia, X. Zhang, M.M. Henkel, I.F. Abdullaev, Y.H. Kuo, K. Matrougui, A.A. Mongin, and M. Trebak. 2013. STIM1 and Orai1 mediate CRAC channel activity and are essential for human glioblastoma invasion. *Pflugers Arch*. 465:1249-1260.

Nakada, M., E. Nambu, N. Furuyama, Y. Yoshida, T. Takino, Y. Hayashi, H. Sato, Y. Sai, T. Tsuji, K.I. Miyamoto, A. Hirao, and J.I. Hamada. 2013. Integrin alpha3 is overexpressed in glioma stem-like cells and promotes invasion. *Br J Cancer*. 108:2516-2524.

Narita, T., H. Aoyama, K. Hirata, S. Onodera, T. Shiga, H. Kobayashi, J. Murata, S. Terasaka, S. Tanaka, and K. Houkin. 2012. Reoxygenation of glioblastoma multiforme treated with fractionated radiotherapy concomitant with temozolomide: changes defined by 18F-fluoromisonidazole positron emission tomography: two case reports. *Jpn J Clin Oncol*. 42:120-123.

Oeggerli, M., Y. Tian, C. Ruiz, B. Wijker, G. Sauter, E. Obermann, U. Guth, I. Zlobec, M. Sausbier, K. Kunzelmann, and L. Bubendorf. 2012. Role of KCNMA1 in breast cancer. *PLoS One*. 7:e41664.

Ohgaki, H., P. Dessen, B. Jourde, S. Horstmann, T. Nishikawa, P.L. Di Patre, C. Burkhard, D. Schuler, N.M. Probst-Hensch, P.C. Maiorka, N. Baeza, P. Pisani, Y. Yonekawa, M.G. Yasargil, U.M. Lutolf, and P. Kleihues. 2004. Genetic pathways to glioblastoma: a population-based study. *Cancer research*. 64:6892-6899.

Olsen, M.L., S. Schade, S.A. Lyons, M.D. Amaral, and H. Sontheimer. 2003. Expression of voltage-gated chloride channels in human glioma cells. *J Neurosci*. 23:5572-5582.

Palme, D., M. Misovic, E. Schmid, D. Klumpp, H.R. Salih, J. Rudner, and S.M. Huber. 2013. Kv3.4 potassium channel-mediated electrosignaling controls cell cycle and survival of irradiated leukemia cells. *Pflugers Arch*. 465:1209-1221.

Pawlik, T.M., and K. Keyomarsi. 2004. Role of cell cycle in mediating sensitivity to radiotherapy. *Int J Radiat Oncol Biol Phys*. 59:928-942.

Peng, H., Y. Huang, J. Rose, D. Erichsen, S. Herek, N. Fujii, H. Tamamura, and J. Zheng. 2004. Stromal cell-derived factor 1-mediated CXCR4 signaling in rat and human cortical neural progenitor cells. *J Neurosci Res*. 76:35-50.

Pickhard, A.C., J. Margraf, A. Knopf, T. Stark, G. Piontek, C. Beck, A.L. Boulesteix, E.Q. Scherer, S. Pigorsch, J. Schlegel, W. Arnold, and R. Reiter. 2011. Inhibition of radiation induced migration of human head and neck squamous cell carcinoma cells by blocking of EGF receptor pathways. *BMC Cancer*. 11:388.

Ransom, C.B., and H. Sontheimer. 2001. BK channels in human glioma cells. *J Neurophysiol*. 85:790-803.

Ruggieri, P., G. Mangino, B. Fioretti, L. Catacuzzeno, R. Puca, D. Ponti, M. Miscusi, F. Franciolini, G. Ragona, and A. Calogero. 2012. The inhibition of KCa3.1 channels activity reduces cell motility in glioblastoma derived cancer stem cells. *PLoS One*. 7:e47825.

Sanchez, M., and O.B. McManus. 1996. Paxilline inhibition of the alpha-subunit of the high-conductance calcium-activated potassium channel. *Neuropharmacology*. 35:963-968.

Saur, D., B. Seidler, G. Schneider, H. Algul, R. Beck, R. Senekowitsch-Schmidtke, M. Schwaiger, and R.M. Schmid. 2005. CXCR4 expression increases liver and lung metastasis in a mouse model of pancreatic cancer. *Gastroenterology*. 129:1237-1250.

Schreiber, M., and L. Salkoff. 1997. A novel calcium-sensing domain in the BK channel. *Biophys J*. 73:1355-1363.

Schubert, R., and M.T. Nelson. 2001. Protein kinases: tuners of the BKCa channel in smooth muscle. *Trends Pharmacol Sci*. 22:505-512.

Sciaccaluga, M., B. Fioretti, L. Catacuzzeno, F. Pagani, C. Bertollini, M. Rosito, M. Catalano, G. D'Alessandro, A. Santoro, G. Cantore, D. Ragozzino, E. Castigli, F. Franciolini, and C. Limatola. 2010. CXCL12-induced glioblastoma cell migration requires intermediate conductance Ca2+-activated K+ channel activity. *Am J Physiol Cell Physiol*. 299:C175-184.

Shankar, A., S. Kumar, A.S. Iskander, N.R. Varma, B. Janic, A. deCarvalho, T. Mikkelsen, J.A. Frank, M.M. Ali, R.A. Knight, S. Brown, and A.S. Arbab. 2014. Subcurative radiation significantly increases cell proliferation, invasion, and migration of primary glioblastoma multiforme in vivo. *Chin J Cancer*. 33:148-158.

Shi, J., and J. Cui. 2001. Intracellular Mg(2+) enhances the function of BK-type Ca(2+)-activated K(+) channels. *J Gen Physiol*. 118:589-606.

Sontheimer, H. 2008. An unexpected role for ion channels in brain tumor metastasis. *Exp Biol Med (Maywood)*. 233:779-791.

Soroceanu, L., T.J. Manning, Jr., and H. Sontheimer. 1999. Modulation of glioma cell migration and invasion using Cl(-) and K(+) ion channel blockers. *J Neurosci*. 19:5942-5954.

Stefani, E., M. Ottolia, F. Noceti, R. Olcese, M. Wallner, R. Latorre, and L. Toro. 1997. Voltage-controlled gating in a large conductance Ca2+-sensitive K+channel (hslo). *Proc Natl Acad Sci U S A*. 94:5427-5431.

Steinle, M., D. Palme, M. Misovic, J. Rudner, K. Dittmann, R. Lukowski, P. Ruth, and S.M. Huber. 2011. Ionizing radiation induces migration of glioblastoma cells by activating BK K(+) channels. *Radiother Oncol*. 101:122-126.

Stock, C., and A. Schwab. 2009. Protons make tumor cells move like clockwork. *Pflugers Arch*. 458:981-992.

Stupp, R., M.E. Hegi, W.P. Mason, M.J. van den Bent, M.J. Taphoorn, R.C. Janzer, S.K. Ludwin, A. Allgeier, B. Fisher, K. Belanger, P. Hau, A.A. Brandes, J. Gijtenbeek, C. Marosi, C.J. Vecht, K. Mokhtari, P. Wesseling, S. Villa, E. Eisenhauer, T. Gorlia, M. Weller, D. Lacombe, J.G. Cairncross, R.O. Mirimanoff, R. European Organisation for, T. Treatment of Cancer Brain, G. Radiation Oncology, and G. National Cancer Institute of Canada Clinical Trials. 2009. Effects of radiotherapy with concomitant and adjuvant temozolomide versus radiotherapy alone on survival in glioblastoma in a randomised phase III study: 5-year analysis of the EORTC-NCIC trial. *The Lancet. Oncology*. 10:459-466.

Tabatabai, G., B. Frank, R. Mohle, M. Weller, and W. Wick. 2006. Irradiation and hypoxia promote homing of haematopoietic progenitor cells towards gliomas by TGF-beta-dependent HIF-1alpha-mediated induction of CXCL12. *Brain*. 129:2426-2435.

Thakkar, J.P., T.A. Dolecek, C. Horbinski, Q.T. Ostrom, D.D. Lightner, J.S. Barnholtz-Sloan, and J.L. Villano. 2014. Epidemiologic and molecular prognostic review of glioblastoma. *Cancer epidemiology, biomarkers & prevention : a publication of the*

American Association for Cancer Research, cosponsored by the American Society of Preventive Oncology. 23:1985-1996.

Thorwarth, D., S.M. Eschmann, F. Paulsen, and M. Alber. 2007. A model of reoxygenation dynamics of head-and-neck tumors based on serial 18F-fluoromisonidazole positron emission tomography investigations. *Int J Radiat Oncol Biol Phys*. 68:515-521.

Tian, L., L.S. Coghill, H. McClafferty, S.H. MacDonald, F.A. Antoni, P. Ruth, H.G. Knaus, and M.J. Shipston. 2004. Distinct stoichiometry of BKCa channel tetramer phosphorylation specifies channel activation and inhibition by cAMP-dependent protein kinase. *Proc Natl Acad Sci U S A*. 101:11897-11902.

Turner, K.L., A. Honasoge, S.M. Robert, M.M. McFerrin, and H. Sontheimer. 2014. A proinvasive role for the Ca(2+) -activated K(+) channel KCa3.1 in malignant glioma. *Glia*. 62:971-981.

Turner, K.L., and H. Sontheimer. 2014. KCa3.1 modulates neuroblast migration along the rostral migratory stream (RMS) in vivo. *Cereb Cortex*. 24:2388-2400.

Vanan, I., Z. Dong, E. Tosti, G. Warshaw, M. Symons, and R. Ruggieri. 2012. Role of a DNA damage checkpoint pathway in ionizing radiation-induced glioblastoma cell migration and invasion. *Cell Mol Neurobiol*. 32:1199-1208.

Vergara, C., R. Latorre, N.V. Marrion, and J.P. Adelman. 1998. Calcium-activated potassium channels. *Curr Opin Neurobiol*. 8:321-329.

Wang, R., K. Chadalavada, J. Wilshire, U. Kowalik, K.E. Hovinga, A. Geber, B. Fligelman, M. Leversha, C. Brennan, and V. Tabar. 2010. Glioblastoma stem-like cells give rise to tumour endothelium. *Nature*. 468:829-833.

Wang, S.C., C.F. Yu, J.H. Hong, C.S. Tsai, and C.S. Chiang. 2013. Radiation therapy-induced tumor invasiveness is associated with SDF-1-regulated macrophage mobilization and vasculogenesis. *PLoS One*. 8:e69182.

Watkins, S., and H. Sontheimer. 2011. Hydrodynamic cellular volume changes enable glioma cell invasion. *J Neurosci*. 31:17250-17259.

Weaver, A.K., V.C. Bomben, and H. Sontheimer. 2006. Expression and function of calcium-activated potassium channels in human glioma cells. *Glia*. 54:223-233.

Weaver, A.K., X. Liu, and H. Sontheimer. 2004. Role for calcium-activated potassium channels (BK) in growth control of human malignant glioma cells. *J Neurosci Res*. 78:224-234.

Weaver, A.K., M.L. Olsen, M.B. McFerrin, and H. Sontheimer. 2007. BK channels are linked to inositol 1,4,5-triphosphate receptors via lipid rafts: a novel mechanism for coupling [Ca(2+)](i) to ion channel activation. *J Biol Chem*. 282:31558-31568.

Weber, D.C., N. Casanova, T. Zilli, F. Buchegger, M. Rouzaud, P. Nouet, H. Vees, O. Ratib, G. Dipasquale, and R. Miralbell. 2009. Recurrence pattern after [(18)F]fluoroethyltyrosine-positron emission tomography-guided radiotherapy for high-grade glioma: a prospective study. *Radiother Oncol*. 93:586-592.

Wei, A.D., G.A. Gutman, R. Aldrich, K.G. Chandy, S. Grissmer, and H. Wulff. 2005. International Union of Pharmacology. LII. Nomenclature and molecular relationships of calcium-activated potassium channels. *Pharmacol Rev*. 57:463-472.

Weller, M. 2015. Leitlinie Gliome. Deutsche Gesellschaft für Neurologie.

Wen, P.Y., D. Schiff, S. Kesari, J. Drappatz, D.C. Gigas, and L. Doherty. 2006. Medical management of patients with brain tumors. *Journal of neuro-oncology*. 80:313-332.

Wild-Bode, C., M. Weller, A. Rimner, J. Dichgans, and W. Wick. 2001. Sublethal irradiation promotes migration and invasiveness of glioma cells: implications for radiotherapy of human glioblastoma. *Cancer research*. 61:2744-2750.

Wondergem, R., and J.W. Bartley. 2009. Menthol increases human glioblastoma intracellular Ca2+, BK channel activity and cell migration. *J Biomed Sci*. 16:90.

Wondergem, R., T.W. Ecay, F. Mahieu, G. Owsianik, and B. Nilius. 2008. HGF/SF and menthol increase human glioblastoma cell calcium and migration. *Biochem Biophys Res Commun*. 372:210-215.

Wrensch, M., Y. Minn, T. Chew, M. Bondy, and M.S. Berger. 2002. Epidemiology of primary brain tumors: current concepts and review of the literature. *Neuro-oncology*. 4:278-299.

Wulff, H., M.J. Miller, W. Hansel, S. Grissmer, M.D. Cahalan, and K.G. Chandy. 2000. Design of a potent and selective inhibitor of the intermediate-conductance Ca2+-activated K+ channel, IKCa1: a potential immunosuppressant. *Proc Natl Acad Sci U S A*. 97:8151-8156.

Xia, X.M., X. Zeng, and C.J. Lingle. 2002. Multiple regulatory sites in large-conductance calcium-activated potassium channels. *Nature*. 418:880-884.

Yang, H., G. Zhang, and J. Cui. 2015. BK channels: multiple sensors, one activation gate. *Front Physiol*. 6:29.

Zagzag, D., M. Esencay, O. Mendez, H. Yee, I. Smirnova, Y. Huang, L. Chiriboga, E. Lukyanov, M. Liu, and E.W. Newcomb. 2008. Hypoxia- and vascular endothelial growth factor-induced stromal cell-derived factor-1alpha/CXCR4 expression in glioblastomas: one plausible explanation of Scherer's structures. *Am J Pathol*. 173:545-560.

Zhou, W., Y. Xu, G. Gao, Z. Jiang, and X. Li. 2013. Irradiated normal brain promotes invasion of glioblastoma through vascular endothelial growth and stromal cell-derived factor 1alpha. *Neuroreport*. 24:730-734.

Zhou, X.B., C. Arntz, S. Kamm, K. Motejlek, U. Sausbier, G.X. Wang, P. Ruth, and M. Korth. 2001. A molecular switch for specific stimulation of the BKCa channel by cGMP and cAMP kinase. *J Biol Chem*. 276:43239-43245.

Zhou, Y., and C.J. Lingle. 2014. Paxilline inhibits BK channels by an almost exclusively closed-channel block mechanism. *J Gen Physiol*. 144:415-440.

6 Danksagung

Die vorliegende Arbeit wurde von April 2012 bis März 2016 unter wissenschaftlicher Anleitung von Prof. Dr. Peter Ruth und Prof. Dr. Stephan Huber am Pharmazeutischen Institut der Universität Tübingen angefertigt.

Mein besonderer Dank gilt Prof. Dr. Peter Ruth und Prof. Dr. Stephan Huber für das Überlassen des sehr interessanten Themas, das mir entgegengebrachte Vertrauen und die Unterstützung während der Anfertigung dieser Arbeit. Ich hatte die Möglichkeit interessante Kongresse zu besuchen, den Freiraum wissenschaftliche Fragestellungen selbstständig mit eigenen Ideen und Lösungsvorschlägen zu bearbeiten und konnte mich bei Problemen immer auf ein offenes Ohr und Unterstützung verlassen.

Weiterer Dank gilt Prof. Dr. Daniel Zips für den wissenschaftlichen Austausch und die Unterstützung in dieser Zeit. Ebenfalls möchte ich JProf. Dr. Robert Lukowski für seine Hilfsbereitschaft, die wissenschaftlichen Diskussionen und die Abnahme der Prüfung danken sowie Prof. Dr. Stefan Laufer für die Bereitschaft als weiterer Prüfer zu fungieren.

Prof. Dr. Armin Buschauer und Prof. Dr. Günther Bernhardt aus Regensburg danke ich für die freundliche Kooperation und das Interesse an meiner Arbeit.
Prof. Dr. Karin Schilbach und Dr. Franziska Eckert danke ich für die Bereitstellung der Mäuse und ihre Hilfsbereitschaft hierbei.

Bei meinen Kollegen Angelina, Anne, Christina, Corinna, Friederike, Juli, Julia, Lucas, Marc, Markus, Rebekka und Sandra möchte ich mich ganz herzlich für die schöne Zeit, den Spaß und aber auch für die private und wissenschaftliche Unterstützung in den letzten vier Jahren bedanken. Ich werde viele schöne Erinnerungen und neue Freundschaften aus dieser Zeit mitnehmen. Ein besonderer Dank gilt Anne, von der ich methodisch sehr viel lernen konnte und Marc, der mich in dieses Thema eingearbeitet hat.

Bei meinen Kollegen Benni, Dominik, Lukas, Erik, Ivan, Efe, Heidi und Ilka aus der Radioonkologie möchte ich mich ebenfalls für die angenehme Arbeitsatmosphäre und die großartige Zusammenarbeit bedanken. Vor allem danke ich Benni. Wir haben uns auf diesem Projekt perfekt ergänzt.

Den technischen Assistenten Isolde, Clement, Michael und Katrin danke ich für ihren unermüdlichen Einsatz im Labor und ihre ständige Hilfsbereitschaft. Loni danke ich für die Unterstützung bei der Versorgung der Mäuse. Frau Weber und Frau Leitermann danke ich für die Verwaltung der Unterlagen.

Ebenfalls möchte ich mich bei allen weiteren Mitarbeitern der 7. und 9. Ebene für die angenehme Arbeitsatmosphäre bedanken.

Ein ganz besonderer Dank gilt meiner Familie, die mich auf all meinen Wegen begleitet und unterstützt hat. Vor allem möchte ich mich hierbei bei meinen Eltern und meinem Mann Armin für ihre Geduld, ihren Rückhalt, die aufbauenden Worte in schwierigen Zeiten und die dadurch entstandene Geborgenheit bedanken.

7 Veröffentlichungen

7.1 Wissenschaftliche Publikationen

Edalat L, Stegen B, Klumpp L, Haehl E, Schilbach K, Lukowski R, Kühnle M, Bernhardt G, Buschauer A, Zips D, Ruth P, Huber SM (2016). BK K^+ channel blockade inhibits radiation-induced migration/brain infiltration of glioblastoma cells. *Oncotarget* 7423.

Stegen B, **Butz L**, Klumpp L, Zips D, Dittmann K, Ruth P, Huber SM (2015). Ca^{2+}-Activated IK K^+ Channel Blockade Radiosensitizes Glioblastoma Cells. *Mol Cancer Res* 13:1283-1295.

Huber SM, **Butz L**, Stegen B, Klumpp L, Klumpp D, Eckert F (2014). Role of ion channels in ionizing radiation-induced cell death. *Biochim Biophys Acta* 1848:2657-2664.

Huber SM, **Butz L**, Stegen B, Klumpp D, Braun N, Ruth P, Eckert F (2013). Ionizing radiation, ion transports, and radioresistance of cancer cells. *Front Physiol* 4:212.

7.2 Kongressbeiträge und Tagungsbeiträge

20. – 22. Juni 2015, 14th International Wolfsberg Meeting on Molecular Radiation Biology/Oncology, Ermatingen, Schweiz

Targeting of ionizing radiation-induced hypermigration of glioblastoma cells *in vivo*

L. Butz, B. Stegen, D. Zips, P. Ruth, S.M. Huber

SDF-1 triggers hypermigration of irradiated glioblastoma cells by modifying the Ca^{2+}-signaling which results in activation of K^+ and Cl^- channels

B. Stegen, **L. Butz**, D. Zips, P. Ruth, S.M. Huber

26. – 28. Februar 2015, 24. Symposium Experimentelle Strahlentherapie und Klinische Strahlenbiologie, Hamburg

Ionizing radiation induced-glioblastoma cell migration *in vivo*

L. Butz, B. Stegen, D. Zips, P. Ruth, S.M. Huber

SDF-1 gesteuerte Hypermigration von bestrahlten Glioblastomzellen durch Modifizierung des Ca^{2+}-Signaling und Aktivierung von K^+ und Cl^- Kanälen

B. Stegen, **L. Butz**, D. Zips, P. Ruth, S.M. Huber

29. September – 01. Oktober 2014, 17th Annual Meeting of the Society for Biological Radiation Research - GBS, Tübingen

Ionizing radiation-induced glioblastoma cell migration *in vivo*

L. Butz, B. Stegen, D. Zips, P. Ruth, S.M Huber

SDF-1 triggers hypermigration of irradiated glioblastoma cells by modifying the Ca^{2+}-signaling which results in activation of BK K^+ and Cl^- channels

B. Stegen, **L. Butz**, D. Zips, P. Ruth, S.M. Huber

24. – 26. September 2014, Jahrestagung Deutsche Pharmazeutische Gesellschaft (DPhG), Frankfurt

Ionizing radiation-induced glioblastoma cell migration *in vivo*

L. Butz, B. Stegen, D. Zips, A. Buschauer, S.M. Huber, P. Ruth

04. – 08. April 2014, ESTRO 33, European Society for Radiotherapy & Oncology, Wien, Österreich

Ionizing radiation-induced glioblastoma cell migration *in vivo*

L. Butz, B. Stegen, D. Zips, P. Ruth, S.M. Huber

BK K^+ channels regulate migration of irradiated glioblastoma cells by modifying the Ca^{2+} signaling

D. Klumpp, B. Stegen, M. Misovic, **L. Butz**, S.N. Reichel, D. Zips, P. Ruth, S.M. Huber

TRAM-34 an inhibitor of the Ca^{2+}-activated IK K^+ channel radiosensitizes glioblastoma cells *in vitro*

B. Stegen, **L. Butz**, K. Dittmann, D. Zips, P. Ruth, S.M. Huber

27. Februar – 01. März 2014, 23. Symposium Experimentelle Strahlentherapie und Klinische Strahlenbiologie, Tübingen

Fractionated radiation stimulates glioblastoma brain infiltration

L. Butz, B. Stegen, S. Tsitsekidis, D. Zips, S.M. Huber, P. Ruth

TRAM-34 radiosensitizes glioblastoma cells by inhibiting Ca^{2+}-activated IK K^+ channels

B. Stegen, **L. Butz**, D. Zips, K. Dittmann, P. Ruth, S.M. Huber.

04. – 06. August 2013, 12th III-Bern Summer School, Jongny, Schweiz

Accelerated migration of glioblastoma cell lines upon ionizing radiation as a function of Ca^{2+}-dependent activation of BK K^+ and Cl^- channels

L. Butz, B. Stegen, R. Lukowski, S.M. Huber, P. Ruth

22. – 23. Februar 2013, 22. Symposium Experimentelle Strahlentherapie und Klinische Strahlenbiologie, Dresden

Ionizing radiation induces cell migration of glioblastoma cells by Ca^{2+}-dependent activation of K^+ and Cl^- channels

B. Stegen, **L. Butz**, M. Steinle, P. Ruth, S.M. Huber.

8 Lebenslauf

Auf einen Lebenslauf wurde in der elektronischen Fassung aus Datenschutzgründen verzichtet.

9 Anhang – Publikationen

Liste der Publikationen

1. Edalat L, Stegen B, Klumpp L, Haehl E, Schilbach K, Lukowski R, Kühnle M, Bernhardt G, Buschauer A, Zips D, Ruth P, Huber SM (2016).
BK K^+ channel blockade inhibits radiation-induced migration/brain infiltration of glioblastoma cells. *Oncotarget* 7423.

2. Stegen B, Butz L, Klumpp L, Zips D, Dittmann K, Ruth P, Huber SM (2015).
Ca^{2+}-Activated IK K^+ Channel Blockade Radiosensitizes Glioblastoma Cells.
Mol Cancer Res 13:1283-1295.

3. Huber SM, Butz L, Stegen B, Klumpp L, Klumpp D, Eckert F (2014).
Role of ion channels in ionizing radiation-induced cell death.
Biochim Biophys Acta 1848:2657-2664.

4. Huber SM, Butz L, Stegen B, Klumpp D, Braun N, Ruth P, Eckert F (2013).
Ionizing radiation, ion transports, and radioresistance of cancer cells.
Front Physiol 4:212.

BK K^+ channel blockade inhibits radiation-induced migration/brain infiltration of glioblastoma cells

Lena Edalat[1,2,*], Benjamin Stegen[2,*], Lukas Klumpp[2,5], Erik Haehl[2], Karin Schilbach[3], Robert Lukowski[1], Matthias Kühnle[4], Günther Bernhardt[4], Armin Buschauer[4], Daniel Zips[2], Peter Ruth[1], Stephan M. Huber[2]

[1]Department of Pharmacology, Toxicology and Clinical Pharmacy, University of Tübingen, Tübingen, Germany

[2]Department of Radiation Oncology, University of Tübingen, Tübingen, Germany

[3]Department of General Pediatrics, Oncology/Hematology, University of Tübingen, Tübingen, Germany

[4]Department of Pharmaceutical/Medicinal Chemistry II, University of Regensburg, Regensburg, Germany

[5]Dr. Margarete Fischer-Bosch-Institute of Clinical Pharmacology, University of Tübingen, Tübingen, Germany

[*]These authors contributed equally to this work

Correspondence to: Peter Ruth, **e-mail:** peter.ruth@uni-tuebingen.de
Stephan M Huber, **e-mail:** stephan.huber@uni-tuebingen.de

Keywords: *glioma, radiation therapy, patch-clamp recording, fura-2 Ca2⁺ imaging, transfilter migration*

Received: *October 20, 2015* ***Accepted:*** *January 29, 2016* ***Published:*** *February 16, 2016*

ABSTRACT

Infiltration of the brain by glioblastoma cells reportedly requires Ca^{2+} signals and BK K^+ channels that program and drive glioblastoma cell migration, respectively. Ionizing radiation (IR) has been shown to induce expression of the chemokine SDF-1, to alter the Ca^{2+} signaling, and to stimulate cell migration of glioblastoma cells. Here, we quantified fractionated IR-induced migration/brain infiltration of human glioblastoma cells *in vitro* and in an orthotopic mouse model and analyzed the role of SDF-1/CXCR4 signaling and BK channels. To this end, the radiation-induced migratory phenotypes of human T98G and far-red fluorescent U-87MG-Katushka glioblastoma cells were characterized by mRNA and protein expression, fura-2 Ca^{2+} imaging, BK patch-clamp recording and transfilter migration assay. In addition, U-87MG-Katushka cells were grown to solid glioblastomas in the right hemispheres of immunocompromised mice, fractionated irradiated (6 MV photons) with 5 × 0 or 5 × 2 Gy, and SDF-1, CXCR4, and BK protein expression by the tumor as well as glioblastoma brain infiltration was analyzed in dependence on BK channel targeting by systemic paxilline application concomitant to IR. As a result, IR stimulated SDF-1 signaling and induced migration of glioblastoma cells *in vitro* and *in vivo*. Importantly, paxilline blocked IR-induced migration *in vivo*. Collectively, our data demonstrate that fractionated IR of glioblastoma stimulates and BK K^+ channel targeting mitigates migration and brain infiltration of glioblastoma cells *in vivo*. This suggests that BK channel targeting might represent a novel approach to overcome radiation-induced spreading of malignant brain tumors during radiotherapy.

INTRODUCTION

Glioblastoma multiforme consists of cells with a highly migratory phenotype that may "travel" long distances throughout the brain [1]. Primary foci of glioblastoma usually show a characteristic diffuse and net-like brain infiltration which represents a major challenge for surgical tumor resection as well as for adequate coverage by radiotherapy [2]. This migratory phenotype in concert with a pronounced resistance to radiotherapy and chemotherapy probably contributes to frequent therapy failure and bad prognosis observed in the vast majority of patients with glioblastoma.

Sublethal IR has been demonstrated *in vitro* and/or in rodent tumor models to induce migration, metastasis, invasion and spreading of a variety of tumor entitites. In

particular, a plethora of *in vitro* and *in vivo* studies suggest that IR induces migration of glioblastoma cells (for review see [3, 4]). Three-dimensional-glioblastoma *in vitro* models, however, could not confirm this phenomenon [5] and whether or not IR induces migration of glioblastoma cells *in vivo* is still under debate.

If IR-induced migration, however, reaches relevant levels during fractionated radiotherapy of glioblastoma patients it might boost glioblastoma brain infiltration and - in the worst case - evasion of glioblastoma cells from the target volume of the radiotherapy. Along those lines, the chemokine SDF-1 (stromal cell-derived factor-1, CXCL12) via its receptor CXCR4 [6–8] stimulates migration of glioblastoma cells [9]. IR reportedly induces the expression of SDF-1 in different tumor entities including glioblastoma [10–13] as well as in normal brain tissue [7].

Collectively, these findings suggest that IR-induced migration may contribute to therapy resistance of glioblastoma. The present study, therefore, aimed to provide a quantitative analysis of IR-induced migration/brain infiltration in an orthotopic *xeno*graft model of human glioblastoma. Importantly, a previous *in vitro* study of our group disclosed IR-induced BK K^+ channel activation as a key event in IR-induced migration. Since BK channel blockade by paxilline, a toxin of the fungus *Penicillium paxilli*, suppresses IR-induced migration *in vitro* [14] the present study further tested whether glioma BK channel targeting with paxilline might be a powerful strategy to suppress IR-induced migration of glioblastoma cells *in vivo*. Our data strongly suggest that fractionated IR stimulates glioblastoma migration/infiltration *in vivo* via auto-/paracrine SDF-1 signaling and subsequent BK channel activation.

RESULTS

Studies using human U-87MG glioblastoma cells to generate orthotopic mouse models report encapsulated and low brain infiltrative tumor growth [15]. Therefore, U-87MG glioblastoma seemed excellently suited for quantitative analysis of number and migration distances of individual glioblastoma cells. We used the U-87MG-Katushka clone stably transfected with the far-red fluorescent protein Katushka for histological glioblastoma cell tracking. The Katushka protein-expressing U-87MG cells were comparable to the wild type cells regarding growth kinetics and chemosensitivity against standard cytostatic drugs as shown in Supplementary Figure S1A–S1C. The BK inhibitor paxilline had no significant antiproliferative activity on U-87MG-Katushka cells upon long-term exposure at concentrations of up to 10 µM (Supplementary Figure S1D).

First, we studied *in vitro* both BK channel expression in U-87MG-Katushka cells and putative radiosensitizing effects of the BK channel inhibitor paxilline. Issuing the latter was plausible since pharmacological blockade of the BK-related Ca^{2+}-activated IK channels reportedly radiosensitizes T98G and U-87MG glioblastoma cells [16]. Similar radiosensitizing action of paxilline would complicate the interpretation of any paxilline *in vivo* effect on tumor cell migration and brain infiltration.

As described for T98G and the parental U-87MG cells [14], the U-87MG-Katushka clone functionally expressed BK channels. This was evident from whole-cell patch-clamp recordings with K-gluconate in the pipette and NaCl in the bath. U-87MG-Katuska cells exhibited large outward currents in the range of several nano-amperes (Figure 1A, left). These currents were outwardly rectifying and blocked by the BK channel inhibitor paxilline (Figure 1A right and 1B) indicative of functional expression of BK channels. To test for a radiosensitizing action of BK channel targeting, the influence of paxilline on clonogenic survival of irradiated U-87MG-Katushka and T98G cells was determined by delayed plating colony formation assays. In contrast to IK channel targeting [16], BK channel blockade by paxilline did not radiosensitize either glioblastoma cell models (Figure 1C and 1D).

Reportedly, IR stimulates *in vivo* the expression of the chemokine SDF-1 by the glioma invasion front [13]. Therefore, U-87MG-Katushka and T98G were tested *in vitro* for IR-induced BK channel activity, transfilter migration and the role of SDF-1 signaling herein in order to define radiation-induced signaling events upstream of BK channel activation. In on-cell patch-clamp recordings (KCl pipette- and NaCl bath solution) from U-87MG-Katushka cells (Figure 2A), large conductance ion channels (unitary conductance, $g \approx 200$ pS, Figure 2B) became increasingly active with increasing positive voltage. In irradiated cells (2 Gy, 2–4.5 h after IR), channel activity was observed at highly significantly lower clamp-voltage than in non-irradiated cells (Figure 2 A, right, Figure 2C, closed triangles and Figure 2D, closed bar). In on-cell mode, a clamp-voltage between pipette and bath solution of 0 mV is recording the transmembrane currents at physiological membrane potential. Therefore, the current transitions at 0 mV observed in irradiated cells indicated the activity of the large conductance ion channel at physiological membrane potential. In unirradiated control cells, in contrast, channel activity was triggered only by clamp-voltages above +50 mV (Figure 2D, open bar). Accordingly, mean macroscopic on-cell outward currents in irradiated cells exceeded significantly that of control cells by twofold (Figure 2E, black symbols and Figure 2F, open bars). Notably, paxilline (5 µM; Figure 2E, grey symbols and Figure 2F, closed bars) blocked about half of the outward current in irradiated cells while having no effect in control cells. The paxilline-sensitive current fractions of irradiated cells showed typical outward rectification (Figure 2G, closed triangles). In combination, voltage-dependence of open probability, high unitary conductance and paxilline-sensitivity defined the large conductance channel as BK K^+ channel. Importantly, BK channels were active in irradiated cells at physiological membrane potential suggesting their functional significance for the irradiated glioblastoma cells.

BK channel activation in irradiated U-87MG-Katushka cells was paralleled by significantly faster chemotaxis when compared to unirradiated control cells as determined by FCS gradient-stimulated transfilter migration assays (Figure 2H and 2I, open bars). The BK channel inhibitor paxilline (5 μM) did not affect the basal fraction of migrating cells, whereas the IR-induced migration was completely abolished (Figure 2I, closed bars). Together, these data indicate radiation-induced migration in U-87MG-Katushka cells depending on IR-induced BK channel activity.

To confirm previously published data on paxilline-sensitive IR-induced migration [14], irradiated (0 or 2 Gy, 2–4.5 h after IR) T98G cells were on-cell patch-clamp recorded with KCl in the pipette and NaCl bath solution. Similar to the U-87MG-Katushka model, irradiated T98G glioblastoma cells showed voltage-dependent activity of large conductance (g ≈ 200 pS) channels (Figure 3A–3C). Channels were active in irradiated T98G cells at physiological membrane potential (i.e., 0 mV clamp-voltage, Figure 3B) and generated an outwardly rectifying macroscopic on-cell current (Figure 3D, black closed

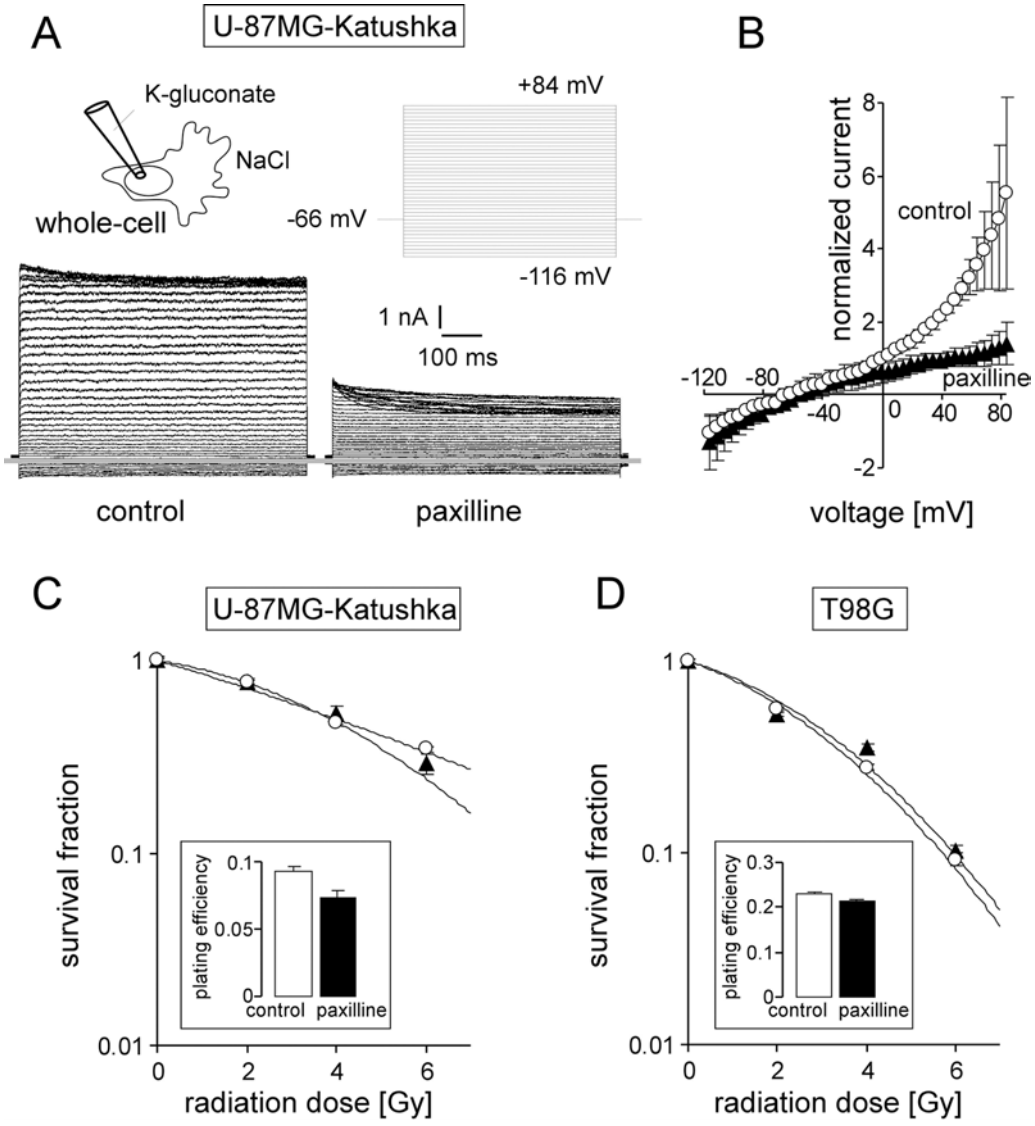

Figure 1: The glioblastoma cell lines T98G and U-87MG-Katushka functionally express BK Ca^{2+}-activated K^+ channels which, in contrast to IK channels, do not modulate radioresistance. (**A**) Whole-cell current tracings recorded from the cell rear of a migrating U-87MG-Katushka cell before (left) und during (right) bath application of the BK channel inhibitor paxilline. Records were obtained in voltage-clamp mode with K-gluconate pipette- and NaCl bath solution. The applied pulse protocol is shown in the upper right, the grey line indicates zero current level. (**B**) Mean (± SE, *n* = 3) whole-cell current densities of migrating U-87MG-Katushka cells recorded as in (A) before (circles) and during paxilline administration (triangles). (**C, D**) Mean survival (± SE, *n* = 12–36) fraction of irradiated (0–6 Gy) U-87MG-Katushka (C) and T98G cells (D) as determined by delayed plating colony formation assay. Cells were irradiated and post-incubated (24 h) in the absence (open bars) or presence (closed triangles) of paxilline. The inserts show the plating efficiencies of both cell lines in the absence (open bars) or presence of paxilline (closed bars).

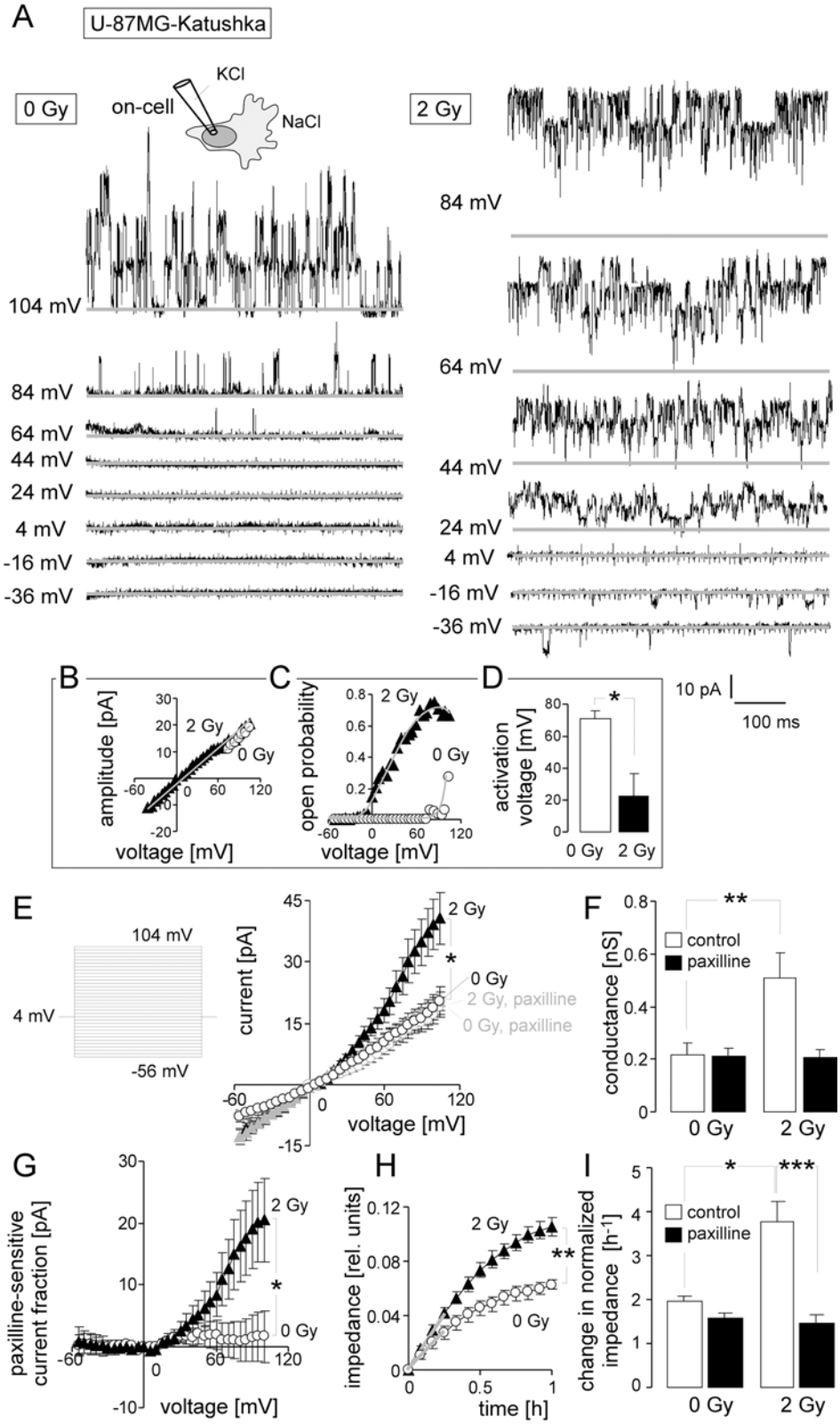

Figure 2: Ionizing radiation (IR) stimulates BK K^+ channel-dependent migration of U-87MG-Katushka cells. (**A**) Single channel current transitions recorded in on-cell mode at different holding potentials (as indicated) with KCl pipette- and NaCl bath solutions from a control (left) and an irradiated (3 h after 2 Gy) U-87MG-Katushka cell. The voltage-dependent increase in open probability is shifted towards more negative potentials in the irradiated as compared to the control cell. (**B, C**) Dependence of the mean unitary current transition (B) and open probability (P_o, C) on the voltage of the channels recorded in the control (open circles) and the irradiated cell (closed triangle) shown in (A). The channels exhibiting a unitary conductance of g ≈ 200 pS and a depolarization-induced increase of P_o typically

for BK channels. (**D**) Mean (± SE, $n = 9$) minimal depolarizing voltage evoking BK channel activity in 0 Gy- (open bar) or 2 Gy-irradiated (closed bar) U-87MG-Katushka cells. (**E**) Mean (± SE, $n = 8–15$) macroscopic on-cell currents recorded as in (A) from control (open circles) and irradiated (2 Gy, closed triangles) U-87MG-Katushka cells. Records were obtained in the absence (black symbols) or presence (grey symbols) of the BK inhibitor paxilline. (**F**) Mean (± SE) conductance of the clamped membrane patch as calculated from (E) for the outward currents for control and irradiated cells in the absence (open bars) or presence (closed bars) of paxilline. (**G**) Mean (± SE) paxilline-sensitive current fractions of control (open circles) and irradiated cells (closed triangles, data from E). (**H**) Mean (± SE, $n = 4$) impedance as measure of transfilter migration of cells irradiated with 0 Gy (open circles) or 2 Gy (closed triangles). The experiment started at 2 h after IR. (**I**) Mean (± SE, $n = 9–24$) normalized migration velocity as calculated for the first 0.25 h of transfilter migration (slopes in H shown by the grey lines) in control (0 Gy) and irradiated (2 Gy) cells recorded in the absence (open bars) or presence of the BK inhibitor paxilline (closed bars). *, ** and *** indicate $p \leq 0.05$, $p \leq 0.01$, and $p \leq 0.001$, respectively, ANOVA (E, F, I) or two-tailed Welch corrected *t*-test (D, H).

triangles, and Figure 3E, 3rd bar) that was significantly larger than that of the unirradiated T98G control cells (Figure 3D, black open circles, and Figure 3E, 1st bar). The BK inhibitor paxilline blocked the IR-induced outward current (Figure 3D, grey closed triangles and Figure 3E, 4th bar) and the paxilline-sensitive current fraction showed typical outward rectification (Figure 3F, closed triangles) indicative of IR-induced BK channel activation. Unirradiated T98G control cells, in contrast, did not exhibit significant paxilline-sensitive outward currents even at high clamp voltages (Figure 3D, open circles, Figure 3E, 1st and 2nd bar, and Figure 3F, open circles).

IR-induced migration (Figure 3G, black symbols and Figure 3H, 1st and 2nd bar) required BK activation, because shRNA-mediated knockdown of BK (Figure 3G, insert) significantly decreased migration velocity of irradiated cells to the control values while not affecting basal migration of unirradiated control cells (Figure 3H, grey symbols and Figure 3H, 3rd and 4th bar). These results suggest that the previously reported IR-induced and paxilline-sensitive migration of T98G cells [14] is mediated by IR-induced BK channel activation.

To estimate, whether IR-induced migration might be associated with an hyperinvasive phenotype and to identify radiation-triggered signaling events, abundances of selected mRNAs were compared between fractionated irradiated (5 × 2 Gy) and control (5 × 0 Gy) U-87MG-Katushka cells. Specifically, mRNAs encoding for BK, the matrix metalloproteinases MMP-2 and MMP-9, the chemokine SDF-1 (CXCL12) and the SDF-1 receptor CXCR4 were analyzed. As shown in Figure 4A, fractionated IR did not alter BK or CXCR4 mRNA but significantly increased the abundance of MMP-2, MMP-9, and SDF-1 mRNA collectively pointing towards an IR-induced hyperinvasive phenotype.

The transcription factor hypoxia-inducible factor-1α (HIF-1α) has been reported to up-regulate CXCR4 and SDF-1 expression (for review see [6]). In U-87MG-Katushka, IR (1 × 2 Gy, 2 h after IR) stabilized HIF-1α protein as shown by immunoblotting (Figure 4B, upper blot and Figure 4C, left). In accordance with the mRNA data (Figure 4A), HIF-1α stabilization was not associated with an IR-induced increase in CXCR4 chemokine receptor protein abundance (immunoblot in Figure 4B, middle and Figure 4C, right) but was paralleled by a significantly elevated SDF-1 immunofluorescence (Figure 4D, 4E).

To estimate the functional significance of SDF-1 signaling in IR-induced BK activation and migration, the effect of conditioned medium harvested from control and irradiated U-87MG-Katushka cells (2 h after IR) on Ca^{2+} signaling was determined in the presence and absence of the CXCR4 antagonist AMD3100 (1 μM). In fura-2 Ca^{2+} imaging experiments, conditioned medium from irradiated cells evoked a significantly faster rise in cytosolic $_{free}[Ca^{2+}]_i$ than conditioned medium from unirradiated control cells (Figure 4F and 4G, open bars). Importantly, AMD3100, when washed-in together with the conditioned medium, completely abolished the IR effect on $_{free}[Ca^{2+}]_i$ (Figure 4G, closed bars). This suggests that IR induces enrichment of factors stimulating the CXCR4 signaling in the medium. Likewise, AMD3100 significantly blocked the BK channel activation by IR when applied before on-cell patch-clamp recording (Figure 4H, 4I). Together, these data suggest the involvement of SDF-1/CXCR4 signaling in IR-induced BK channel activation of U-87MG-Katushka cells.

Similarly to U-87MG-Katushka cells, T98G cells expressed CXCR4 and SDF1 mRNA and protein (RT-PCR and immunoblot data not shown). IR (2 Gy, 2 h after IR) induced a significant increase in SDF-1 protein abundance in T98G cells as determined by immunofluorescence microscopy (Figure 5A–5C). Conditioned medium from irradiated (2 Gy, 2 h after IR) T98G cells exhibited significantly higher SDF-1 concentrations than control cells as determined by ELISA (Figure 5D). Accordingly, superfusion of conditioned medium from irradiated T98G cells (2 Gy, 2 h after IR) stimulated a significant increase in $_{free}[Ca^{2+}]_i$ in T98G cells while medium from control cells did not (Figure 5E and 5F, open bars). The CXCR4 antagonist AMD3100 (1 μM) prevented the Ca^{2+} signals in T98G cells elicited by conditioned medium from irradiated cells (Figure 5F, closed bars). Together, these data suggest IR-induced SDF-1 signaling also in T98G cells.

To test, whether SDF-1 can mimic IR-induced BK channel activation and migration in U-87MG-Katushka cells, $_{free}[Ca^{2+}]_i$ was recorded during wash-in of SDF-1 (Figure 6A, 6B). Acute application of SDF-1 (50 nM) stimulated a significant long-lasting increase in $_{free}[Ca^{2+}]_i$. In addition, acute application of SDF-1 induced significant paxilline-sensitive outward currents in on-cell patch-clamp recordings (Figure 6C–6F). Remarkably, the SDF-1-stimulated current fraction was outwardly rectifying

(Figure 6E) and closely resembled the radiation-induced currents (compare Figure 6E with Figure 2G, closed triangles) in voltage-dependence and absolute values. Finally, SDF-1 (50 nM) significantly increased transfilter migration of U-87MG-Katushka cells (Figure 6G and 6H, open bars). The BK channel inhibitor paxilline (5 μM) blocked the SDF-1 induced augmentation of transfilter migration without significantly inhibiting basal migration (Figure 6H, closed bars). In summary, SDF-1 very similarly to radiation stimulates migration that depends on BK channel activation.

Analogous to U-87MG-Katushka, acute application of SDF-1 (50 nM) induced in T98G cells a long-lasting increase in $_{free}[Ca^{2+}]_i$, (Figure 7A, 7B) and an activation of macroscopic outward current in on-cell patch-clamp recordings (Figure 7C, 7D). Single channel analysis

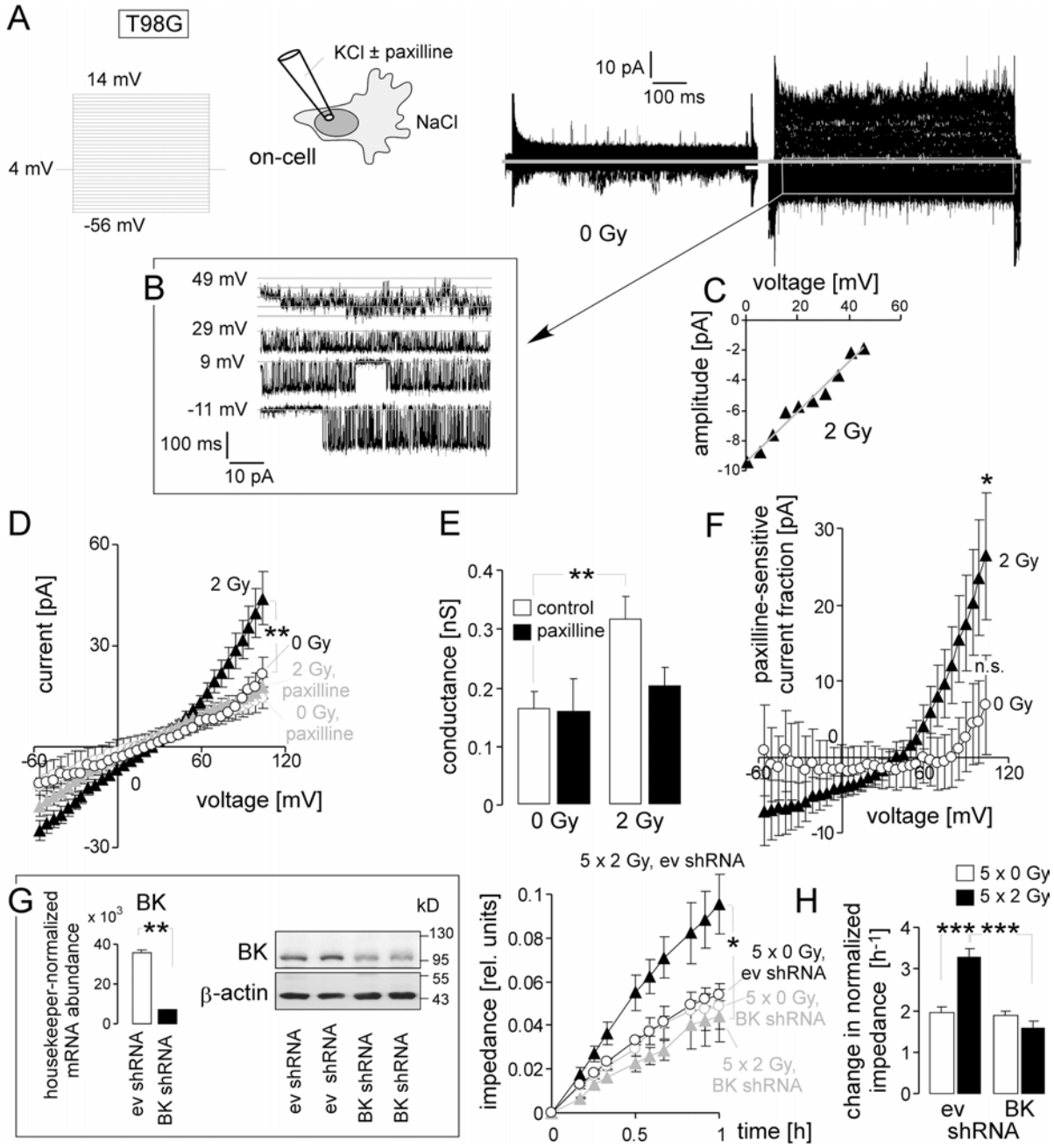

Figure 3: IR stimulates BK channel activity and BK channel-dependent migration of human T98G glioblastoma cells. (**A**) Macroscopic on-cell currents recorded at different voltages (as indicated) with KCl pipette- and NaCl bath solutions from a control (left) and an irradiated T98G cell. (**B, C**) Single channel current transitions at different holding potentials (B) and dependence of the current amplitude on voltage (C) extracted from the current tracings in (A, right) indicate a voltage-dependent activation and a unitary conductance characteristic for BK channels. (**D**) Mean (± SE, n = 8–34) macroscopic on-cell currents recorded as in (A) from control (open circles) and irradiated (2 Gy, closed triangles) T98G cells. Records were obtained in the absence (black) or presence (grey) of the BK inhibitor paxilline.

(**E**) Mean (± SE) conductance of the clamped membrane patch as calculated from (D) for the outward currents for control and irradiated cells in the absence (open bars) or presence (closed bars) of paxilline. (**F**) Mean (± SE) paxilline-sensitive current fractions of control (open circles) and irradiated (closed triangles) cells (data from D). (**G**) Knockdown of BK channels in T98G cells abrogates radiation-induced migration. Mean (± SE, $n = 4$) impedance as measure of transfilter migration of empty vector control (ev, black) or BK-specific shRNA-expressing T98G cells (grey) irradiated with 5 × 0 Gy (open circles) or 5 × 2 Gy (closed triangles). The experiment started 24 h after the last IR fraction. The insert (left) shows the housekeeper-normalized BK-encoding mRNA abundance (left) as well as BK and β-actin protein abundances of T98G cells stably transduced with empty vector control (ev) or BK-specific shRNA. (**H**) Mean (± SE, $n = 8$) normalized migration velocity as calculated from the data in (G) for the first 0.25 h of transfilter migration in control (0 Gy, open bars) and irradiated (2 Gy, closed bars) cells expressing non or BK-specific shRNA. *, ** and *** indicate $p \leq 0.05$, $p \leq 0.01$, and $p \leq 0.001$, respectively, ANOVA (D, G, H) or Welch corrected *t*-test (G). * and n. s. in Figure F indicate significantly ($p \leq 0.05$) and not significantly different from 0, respectively, two-tailed one-sample *t*-test.

(Figure 7E) revealed BK-like large conductance channels (p ≈ 170 pS; Figure 7F) that activated increasingly with increasing voltage (Figure 7G). In summary, the *in vitro* data on the U-87MG-Katushka clone demonstrated IR-induced BK K^+ channel-dependent migration similar to that observed in the present study and/or reported previously for T98G and the parental U-87MG cells [14]. Moreover, these *in vitro* experiments strongly suggest that IR-induced SDF-1 signaling is triggering upstream of BK at least part of the IR-induced migration.

For generation of orthotopic glioblastoma, U-87MG-Katushka (Figure 8A) cells were stereotactically inoculated into the right striatum of NSG mice (Figure 8B). Inoculation resulted in the formation of solid and most widely encapsulated glioblastoma (Figure 8C) that grew exponentially during the first 3 weeks after tumor challenge (Figure 8D). As illustrated in Figure 8E, 8F, the glioblastoma-bearing right hemisphere of isofluran-anaesthesized mice was fractionated irradiated (6 MV photons) on days 7–11 with daily fractions of 2 Gy by the use of mouse holders mounted in the radiation beam of a linear accelerator. The mouse torso and head outside the radiation field were shielded by multileaf collimator and/or an 8 cm thick on-body lead block. The film dosimetry revealed steep dose decline outside the radiation field restricting the area bounded by the 50% isodose line to about 0.8 cm × 0.5 cm = 0.4 cm^2 (with about 1/3 of this field outside the animal (Figure 8F, 8G). Fractionated IR (5 × 2 Gy) was well tolerated by the mice as deduced from the only minute IR-associated decline of body weight (Figure 8H, black symbols). The mice receiving paxilline developed mild and transient ataxia and showed a body weight loss of some 10–15% as compared to the respective control groups (Figure 8H, pink symbols). After end of paxilline treatment, mice recovered completely. On day 21, mice of the 4 treatment groups were sacrificed and brains excised for histological analysis. Importantly, U-87MG-Katushka cells continued to express BK channels when grown in mouse brain as demonstrated by immunohistochemistry (Figure 8I–8K).

Besides BK (see Figure 8I–8J), orthotopic U-87MG-Katuska cells expressed SDF-1 protein as evident from immunofluorescence microscopy. In particular, fractionated IR (5 × 2 Gy) induced marked up-regulation of SDF-1 protein expression 9 days after end of radiotherapy (Figure 9A, 9B). Specifically, brain invading cells at the glioblastoma margin (Figure 9B) and emigrated tumor cells that infiltrate healthy brain parenchyma were SDF-1 positive (Figure 9C) while unirradiated glioblastoma showed only weak SDF-1-specific staining (Figure 9A).

In addition to SDF-1, unirradiated and fractionated irradiated orthotopic U-87MG-Katushka cells expressed CXCR4 chemokine receptor protein (Figure 9D, 9E). CXCR4 protein abundance was similar in fractionated irradiated (Figure 9F) and in unirradiated tumors and localized in the plasma membrane (green fluorescence) and the cytoplasm (merged yellow fluorescence due to colocalization with the far-red Katushka protein, Figure 9G).

To quantify the emigration activity of untreated and irradiated tumors, the number of evaded glioblastoma cells was counted and the migration distances determined. The margin of untreated tumors was usually clearly delimited with tangentially oriented glioblastoma cells at the tumor surface (Figure 10A). Irradiated tumors (Figure 10B), in contrast, exhibited zones where glioblastoma cells invaded in the adjacent brain parenchyma giving the tumor margin a fringed appearance. Figure 10C depicts numbers and emigration distances of glioblastoma cells emigrated from unirradiated (5 × 0 Gy, open circles) and fractionated irradiated (5 × 2 Gy, closed triangles) glioblastoma. IR regimes were applied in the absence (Figure 10C) or presence (Figure 10D) of systemic paxilline administration (8 mg/kg B.W. i.p., 6 h prior to and 6 h after each IR fraction). IR significantly stimulated emigration from the tumor (Figure 10E, left) and paxilline administration prevented this IR-induced migration but did not affect basal emigration (Figure 10E, right). Importantly, neither IR nor paxilline changed the glioblastoma volume (Figure 10F).

In summary, our data on IR-induced migration of glioblastoma cells acquired *in vitro* by the use of the 2D-cultures and those obtained *in vivo* in an orthotopic glioblastoma mouse model strikingly coincided. The IR-induced induction of migration possibly occurs via IR-induced stabilization of HIF-1α. The subsequent up-regulation of the HIF-1α target gene SDF-1 was observed *in vitro* and *in vivo,* suggesting that SDF-1 can stimulate Ca^{2+} transients that lead to BK K^+ channel

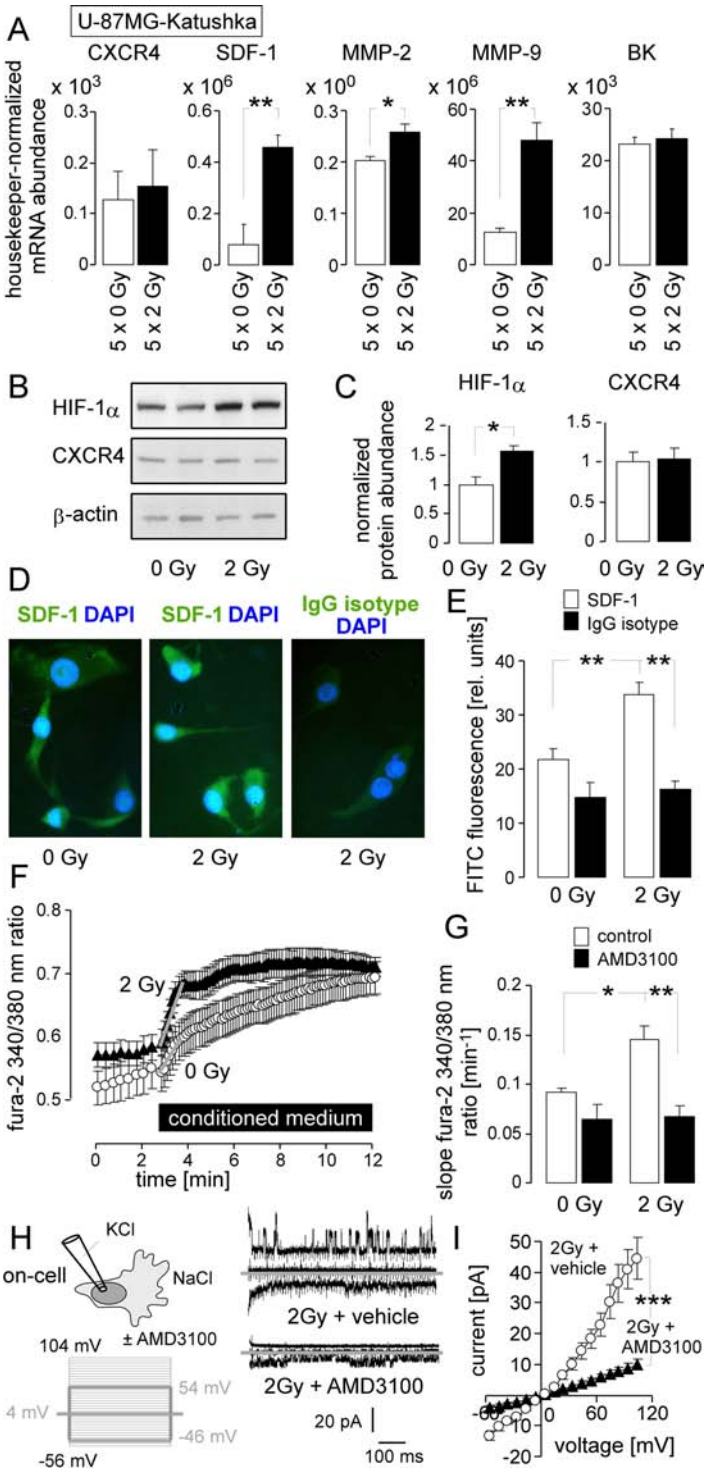

Figure 4: IR stimulates a migratory and invasive phenotype in U-87MG-Katushka cells probably via stabilization of HIF-1α, upregulation of SDF-1, CXCR4-mediated Ca^{2+} signaling and BK channel activation. (**A**) Mean (± SE, n = 5) mRNA abundances of U-87MG-Katushka cells fractionated irradiated with 5 × 0 Gy (open bars) or 5 × 2 Gy (closed bar, mRNA was extracted 24 h after the last IR fraction). Shown are the mRNAs encoding for the chemokine receptor CXCR4, the chemokine SDF-1 (CXCL12), the matrix metalloproteinase MMP-2 and MMP-9, as well as for the BK channel. (**B**) Immunoblots of two lysates each prepared from U-87MG-Katuskha cells irradiated with a single dose of 0 Gy (left) or 2 Gy (2 h after IR, right) probed against HIF-1α, CXCR4 and the loading control β-actin. (**C**) Mean (± SE, n = 4) β-actin-normalized HIF-1α (left) and CXCR4 (right) protein abundance in 0 Gy (open bars) or 2 Gy (2 h after IR, closed bars) U-87MG-Katushka cells. (**D**) Immunofluorescence micrographs of 0 Gy- (left) or 2 Gy (2 h after IR, middle and right) stained with an anti-SDF-1 (left and middle) or the IgG isotype control antibody (right) as detected with a FITC-coupled secondary antibody (green) and co-stained with the DNA-specific dye DAPI (blue). (**E**) Mean (± SE) FITC fluorescence intensity

of anti-SDF-1 (open bars; n = 286–364) or IgG isotype antibody-stained cells from 0 Gy (left, n = 42–75) or 2 Gy irradiated U-87MG-Katushka cells. (**F**) Mean (± SE, n = 36–60) fura-2 340/380 nm fluorescence ratio as measure of cytosolic free Ca^{2+} concentration ($_{free}[Ca^{2+}]_i$) recorded in U-87MG-Katushka cells before and during superfusion with conditioned medium harvested from U-87MG-Katushka cultures 2 h after IR with 0 Gy (open circles) or 2 Gy (closed triangles). (**G**) Mean (± SE, n = 24–60) increase in $_{free}[Ca^{2+}]_i$ as determined by the slope (grey lines in F) of the conditioned medium-evoked rise in the 340/380 nm ratio. The conditioned medium harvested from 0 Gy (left) or 2 Gy (right) irradiated U-87MG-Katushka cells was administered without (open bars) or together with the CXCR4 antagonist AMD3100 (closed bars). (**H**) AMD3100 prevents IR-induced induction of BK channel activity in U-87MG-Katushka cells. On-cell current tracings of irradiated cells (2 Gy, 2 h after IR) irradiated and post-incubated in the absence (top) or presence of AMD3100. Macroscopic on-cell currents were obtained with KCl pipette- and NaCl bath solutions in the absence of AMD3100 as described in Figure 2. Only currents evoked by voltage sweeps to -46, 4, and 54 mV are shown. (**I**) Dependence of mean (± SE, n = 16) macroscopic on-cell currents on voltage recorded as in (H) from vehicle- (open circles) or AMD3100-pretreated (closed triangles) irradiated U-87MG-Katushka cells. *, ** and *** indicate $p \leq 0.05$, $p \leq 0.01$, and $p \leq 0.001$, respectively, two-tailed (Welch)-corrected t-test in (A, C, I) and ANOVA in (G, E).

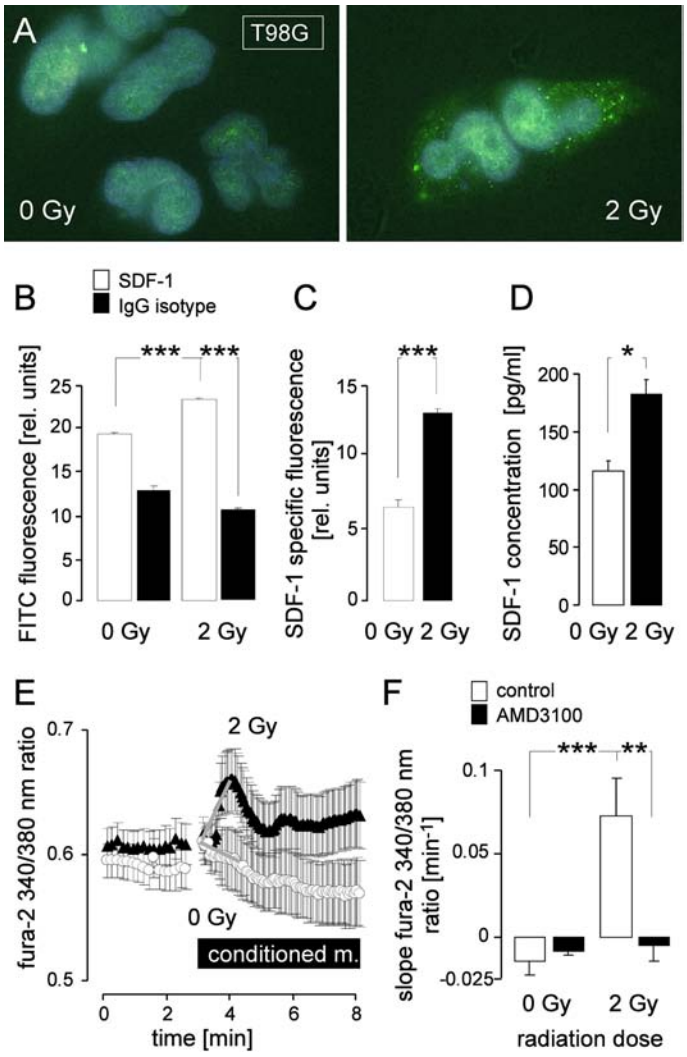

Figure 5: IR induces SDF-1 signaling of T98G cells. (**A**) Immunofluorescence micrographs of 0 Gy (left) or 2 Gy (2 h after IR, right) irradiated cells stained with an anti-SDF-1 antibody and a FITC-coupled secondary antibody (green). (**B**) Mean (± SE) FITC fluorescence intensity of anti-SDF-1 (open bars, n = 286–364) or IgG isotype antibody-stained (closed bars, n = 42–75) cells and (**C**) SDF-1-specific fluorescence from 0 Gy (open bar) or 2 Gy irradiated T98G cells (closed bar). (**D**) Mean (± SE, n = 4) SDF-1 concentration in the medium of T98G cells 2 h after irradiaton with 0 Gy (open bar) or 2 Gy (closed bar). (**E-F**) CXCR4 chemokine receptor antagonist AMD3100 prevents IR-induced Ca^{2+} signaling. (E) Mean (± SE, n = 7–27) fura-2 340/380 nm fluorescence ratio as measure of cytosolic $_{free}[Ca^{2+}]_i$ recorded in T98G cells before and during superfusion with conditioned medium harvested from T98G cultures 2 h after IR with 0 Gy (open circles) or 2 Gy (closed triangles). (F) Mean (± SE) increase in $_{free}[Ca^{2+}]_i$ as determined by the slope (grey lines in E) of the conditioned medium-evoked rise in the 340/380 nm ratio. The conditioned media were administered without (open bars) or together with the CXCR4 antagonist AMD3100 (closed bars). *, **, and *** indicate $p \leq 0.05$, $p \leq 0.01$, and $p \leq 0.001$, respectively, ANOVA in (B) and (F) and Welch-corrected t-test in C and (D).

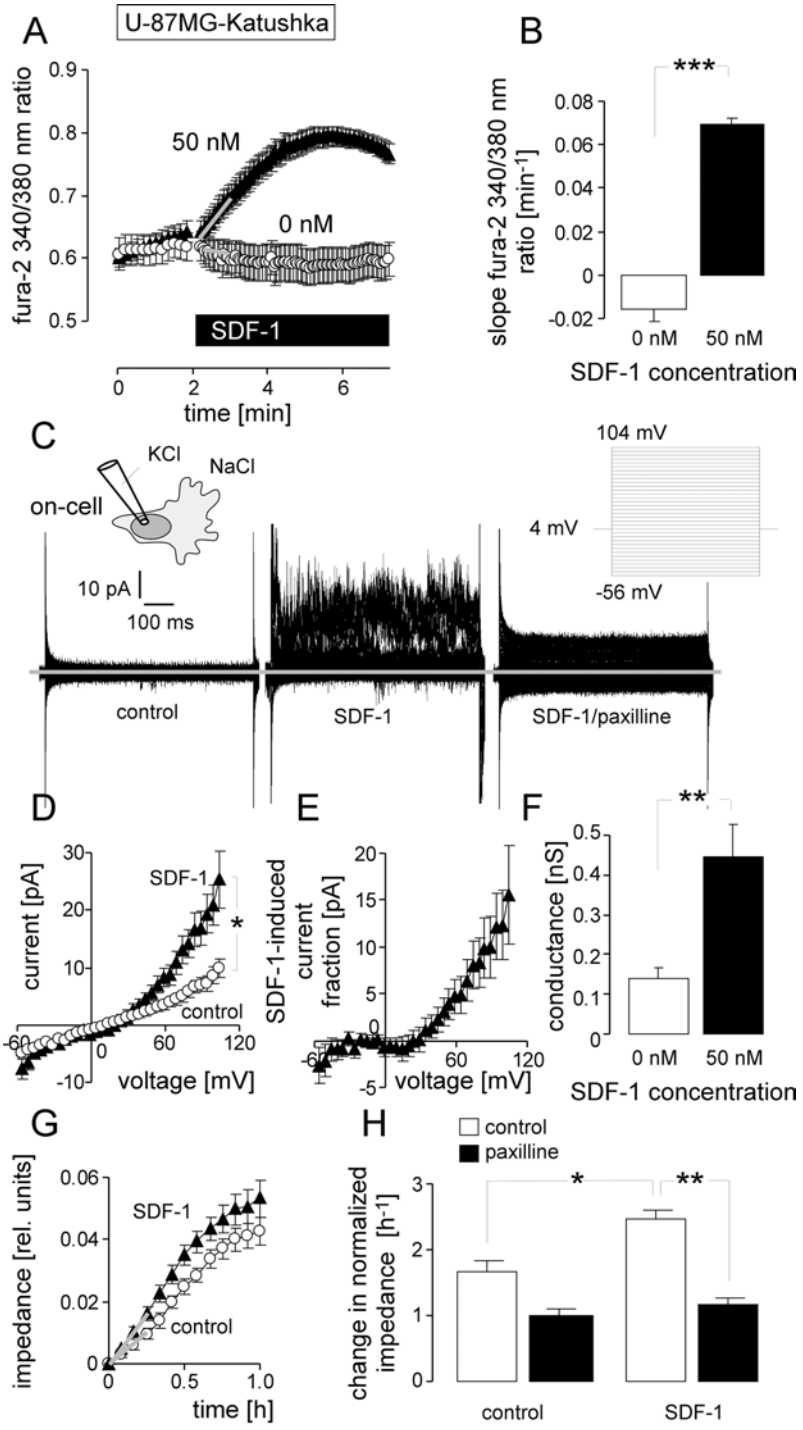

Figure 6: Stimulation with the chemokine SDF-1 mimics the effect of IR on BK channel activity and transfilter migration in U-87MG-Katushka cells. (**A**) Mean (± SE, n = 19–23) fura-2 340/380 nm fluorescence ratio before and during superfusion with SDF-1 or control solution. (**B**) Mean (± SE) change in $_{free}$ $[Ca^{2+}]_i$ as determined by the slope (grey lines in A) of the SDF-1- or control solution-evoked change in the 340/380 nm ratio. (**C**) On-cell current tracings recorded with KCl pipette- and NaCl bath solution from a U-87MG-Katuska cell before (left) and during bath application of SDF-1 (middle) and the BK inhibitor paxilline (right). (**D**) Mean (± SE, n = 10) macroscopic on-cell currents recorded as in (C) before (open circles) and during administration of SDF-1 (closed triangles). (**E**) Mean (± SE) SDF-1-stimulated current fraction (data from C). (**F**) Mean (± SE) conductance of the clamped membrane patch as calculated from (C) for the outward currents recorded in the absence (open bars) and presence of SDF-1 stimulation (closed bars). (**G**) Mean (± SE, n = 4) impedance as measure of transfilter migration of control (open circles) and SDF-1-stimulated (closed triangles) U-87MG-Katushka cells. (**H**) Mean (± SE, n = 9–24) normalized migration velocity in control and SDF-1-stimulated U-87MG-Katushka cells recorded in the absence (open bars) or presence (closed bars) of the BK inhibitor paxilline. *, ** and *** indicate $p \leq 0.05$, $p \leq 0.01$, and $p \leq 0.001$, respectively, two-tailed Welch-corrected t-test in (B, D, F), ANOVA in (H).

activation. *In vitro* and *in vivo*, BK channel targeting prevented IR-induced migration indicating that BK is functionally involved in the stress response of irradiated glioblastoma cells.

DISCUSSION

Whether or not IR-induced glioblastoma cell migration occurs *in vivo* is highly controversially debated and of relevance for the radiotherapy. Our study was conceptualized to get a quantitative answer to this question on cellular resolution. The new findings of our study are that in an orthotopic glioblastoma mouse model only 5 fractions of irradiation with the clinical relevant dose of 2 Gy were sufficient to increase the number of cells infiltring the brain parenchyma by factor of two. Thereby, IR-induced BK channel activity seemed to be a key event since BK blockage by paxilline abrogated IR-induced brain infiltration. Finally, our *in vivo* and *in vitro* experiments strongly suggest that IR-induced auto-/paracrine SDF-1/CXCR4 signaling contribute to BK channel activation.

Our *in vivo* glioblastoma model, U-87MG-Katushka, develops largely encapsulated gliomas in mouse brain. One might say that U-87MG cells, therefore, do not represent the majority of glioblastoma that grow highly infiltative, which certainly limits the generalization of our findings. On the other hand, the encapsulated growth of U-87MG cells only enabled us to quantitatively analyze number and migration distances of cells that emigrated out of the primary tumor lesion and infiltrated the brain. Moreover, U-87MG cells have the advantages to be tumorigenic, to quickly generate tumor mass with highly reproducible tumor volumes, to exhibit IR-induced migration *in vitro* and to express all components required for IR-induced migration as defined so far.

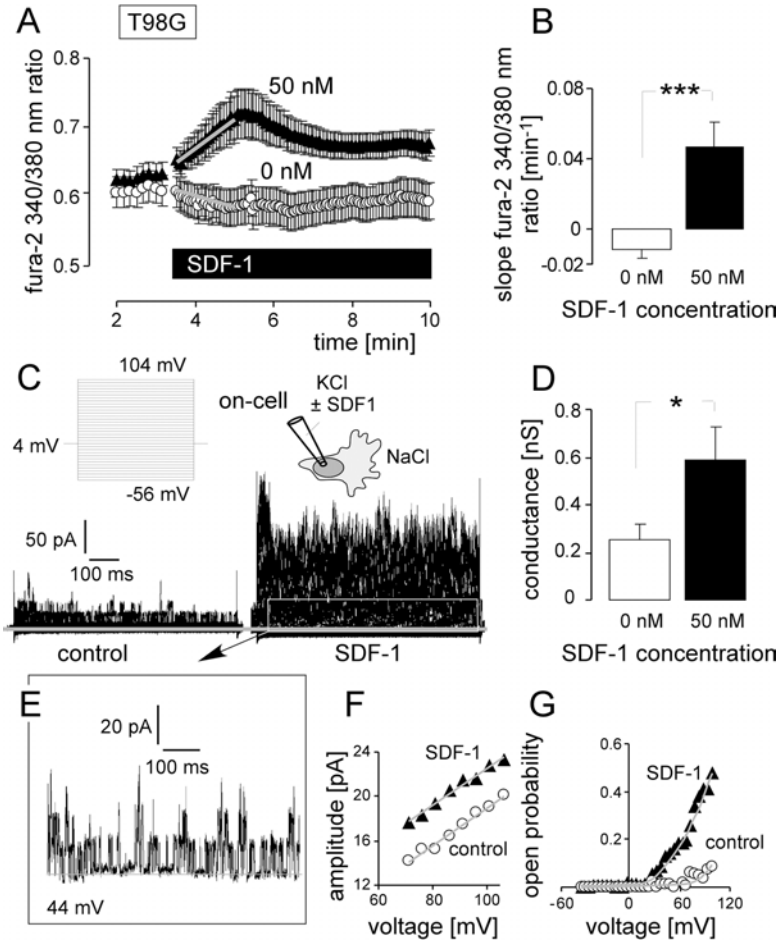

Figure 7: SDF-1 elicits Ca^{2+} signals and mimics the effect of IR on BK channel activity and migration in T98G cells. (**A**) Mean (± SE, n = 21–36) fura-2 340/380 nm fluorescence ratio before and during superfusion with SDF-1 or control solution. (**B**) Mean (± SE) change in $_{free}$ $[Ca^{2+}]_i$ as determined by the slope (grey lines in A) of the SDF-1- or control solution-evoked change in the 340/380 nm ratio. (**C**) On-cell current tracings recorded with KCl pipette- and NaCl bath solution from a control (left) and SDF-1-stimulated T98G cell (right). (**D**) Mean (± SE; n = 11) conductance of the clamped membrane patch as calculated from (C) for the outward currents. (**E-G**) Single channel current transitions (E) and dependence of the current amplitude on voltage (F) and open probability (G) of the control (open circles) and SDF-1-stimulated current tracings (closed triangles) shown in (C). * and *** indicate $p \leq 0.05$ and 0.001, Welch-corrected t-test, respectively.

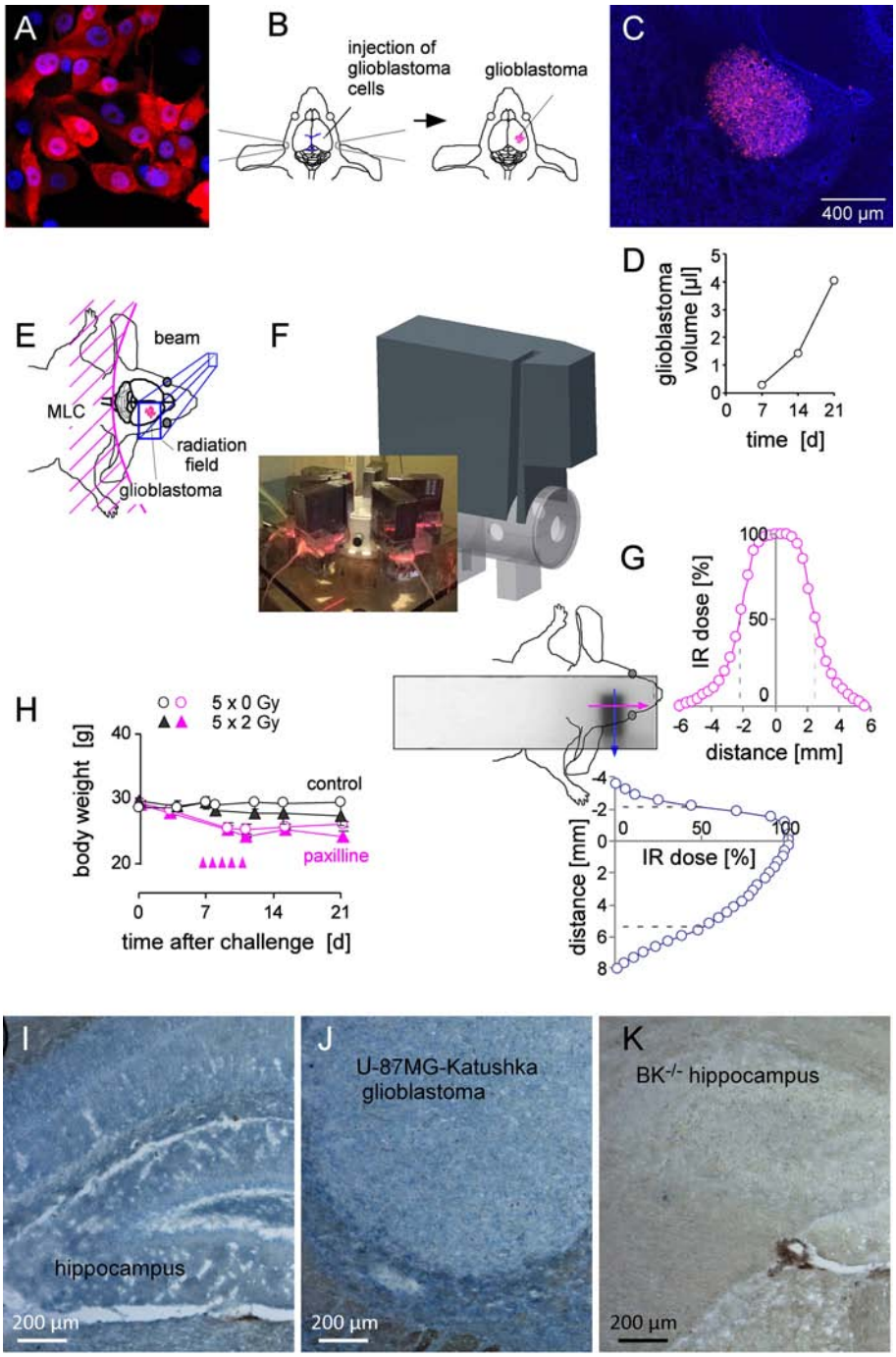

Figure 8: Fractionated IR of human glioblastoma *xeno*grafted orthotopically in NSG mice. (**A**) Fluorescence micrograph of human U-87MG-Katushka glioblastoma cells grown *in vitro* (red and blue fluorescence indicate the Katushka protein and the DNA-specific DAPI fluorochrome, respectively). (**B**) Scheme illustrating the stereotactic transplantation of U-87MG-Katushka cells in mouse right striatum. The blue lines (left drawing) indicate bregma (top) and lambda (bottom). (**C**) Fluorescence micrograph of a U-87MG-Katushka glioblastoma in mouse brain 7 d after tumor cell challenge into the right striatum (DAPI-stained cryosection). (**D**) Time-dependent intracranial growth of U-87MG-Katushka glioblastoma. (**E**) Cartoon illustrating the radiation field. On-body lead shielding has been left out for better clarity (MLC: multileaf collimator). (**F**) Drawing of the mouse holder with mounted on-body leaf shielding. The photography on the lower left shows 6 mice during radiotherapy. (**G**) Dosimetry film and densitometrically analyzed dose distribution in y- (blue) and x-axis (pink) across the radiation field and adjacent shielded brain area. The site of dose deposition is indicated by the superimposed drawing of the mouse head. The dashed lines in the dose distribution plots indicate the 50% isodose. (**H**) Mean (± SE, n = 3) body weight of control (open circles) and fractionated irradiated NSG mice (closed triangles) during the first 3 weeks after intracranial challenge with U-87MG-Katushka cells. Control (black symbols) and mice receiving paxilline (pink symbols) are shown. IR fractions (2 Gy each) are indicated by the pink arrow heads. (**I, J**) BK protein expression (blue) in hippocampus and *xeno*grafted U-87MG-Katushka tumor of NSG mice. (**K**) Hippocampus of $BK^{+/-}$ mice served as negative control.

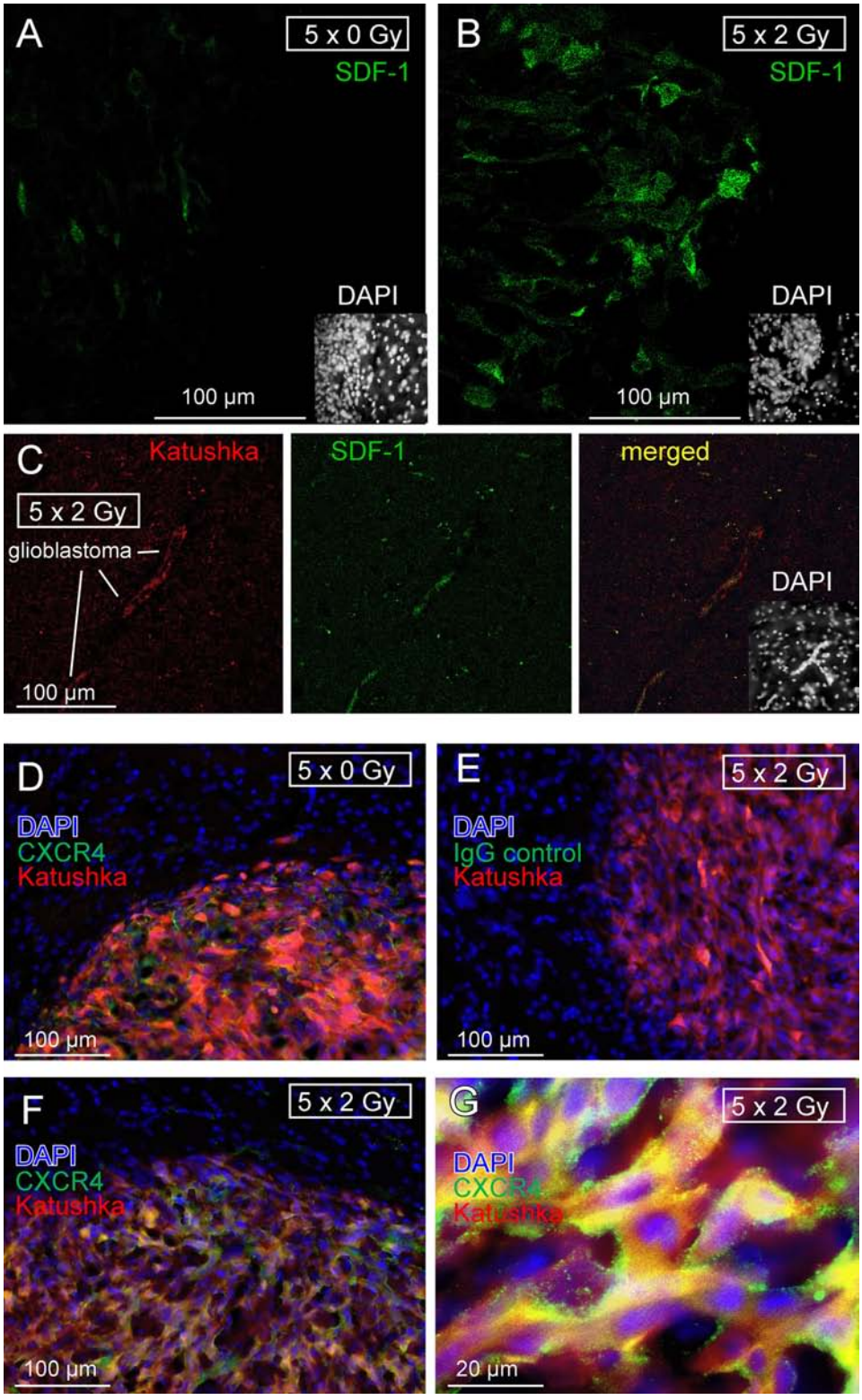

Figure 9: Fractionated IR stimulates *in vivo* SDF-1 protein expression by glioblastoma cells. (**A, B**) SDF-1 specific immunofluorescence (green) of (A) control (5 × 0 Gy) and (B) fractionated irradiated (5 × 2 Gy) U-87MG-Katushka glioblastoma and surrounding normal brain tissue. (**C**) U-87MG-Katushka cells (red) migrating through mouse brain and expressing SDF-1 protein (green). The inserts in the lower right show the corresponding DAPI staining (white) of the nuclei in lower power. The glioblastoma in (A) and (B) can be easily identified by the dense array of nuclei. (**D–G)** U-87MG-Katushka glioblastoma expresses chemokine receptor CXCR4. CXCR4-specific immunofluorescence (green) in control (5 × 0 Gy, D) and fractionated irradiated (5 × 2 Gy) tumors (F, G; Katushka: red, DAPI: blue). CXCR4 was detectable in plasma membrane and cytoplasma of the glioblastoma cells (merged yellow Katushka and CXCR4-specific fluorescence, G). The IgG isotope control did not show green fluorescence (E).

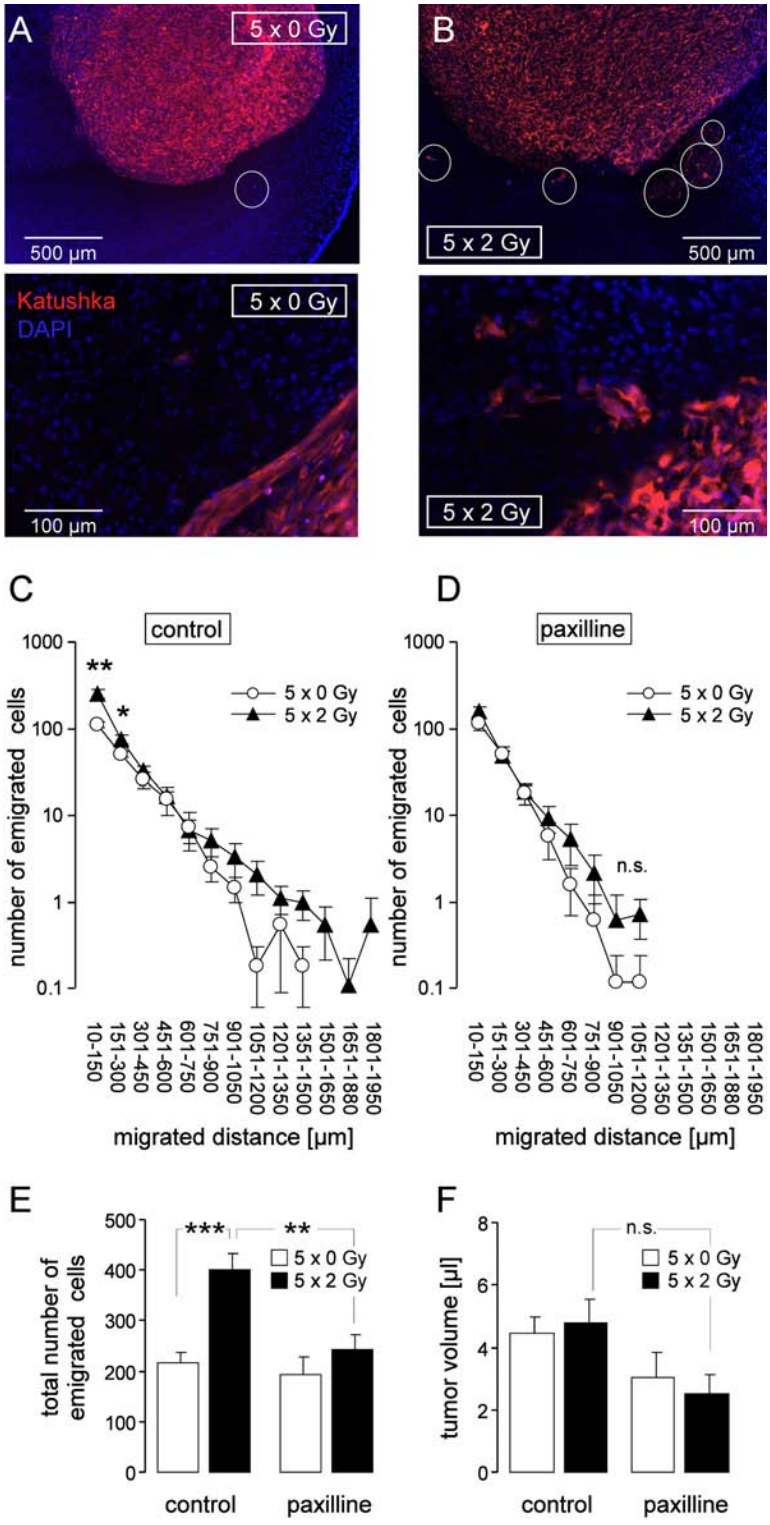

Figure 10: Fractionated IR stimulates migration of glioblastoma cells *in vivo*. (**A, B**) Fluorescence micrographs of control (5 × 0 Gy, A) and fractionated irradiated (5 × 2 Gy, B) U-87MG-Katushka glioblastoma in low (top) and high (bottom) magnification. The nuclei are stained with DAPI (blue), some emigrating U-87MG-Katushka cells are highlighted by white circles. (**C, D**) Number of emigrated cells per tumor (mean ± SE, n = 8–11) as function of the migrated distance of glioblastoma cells fractionated irradiated (5 × 0 Gy, open circles or 5 × 2 Gy, closed triangles) in the absence (C) or presence (D) of concomitant BK channel targeting with paxilline. (**E, F**) Mean (± SE, n = 8–11) total number of emigrated glioblastoma cells (E) and mean (± SE) corresponding glioma volume (F) of fractionated irradiated glioma (5 × 0 Gy, open bars or 5 × 2 Gy, closed bars) of control mice or mice receiving concomitant paxilline chemotherapie. ***, *, **, and n.s. indicate $p \leq 0.05$, $p \leq 0.01$, $p \leq 0.001$ and not significantly different, respectively, two-tailed Welch-corrected t-test in (C, D) and ANOVA in (E, F).

Another limitation of our *in vivo* study is that the applied glioblastoma treatment protocol (5 × 2 Gy) only partially reflects the trimodal therapy (surgery, 30 × 2 Gy radiotherapy and temozolomide chemotherapy) of glioblastoma patients [17]. Previously reported *in vivo* data on IR-induced migration of glioblastoma were acquired with cells or brains pre-irradiated prior to transplantation [18, 19], whole brain irradiation with a single dose of 8 Gy [10], partial brain irradiation with large irradiation fields (1 cm^2) and single doses of 8 and 15 Gy [13], or stereotactical glioblastoma irradiation with a single dose of 50 Gy [20]. Although, each of these studies has the above mentioned limitations, these pieces of evidence combined strongly suggest that IR-induced migration is a general phenomenon and may occur during fractionated radiation therapy of glioblastoma patients.

Does IR-induced migration/infiltration contribute to the apparent high radioresistance of glioblastoma? After clinical radio(chemo)therapy, most (70–90%) volume of the recurrent glioblastoma reportedly lays within the IR target volume [2, 21, 22]. At a first glance, this suggests that the overall contribution of target volume-emigrated tumor cells on tumor recurrence - if existent - is low. On the other hand, one might argue that recurrent glioblastoma preferentially and much faster re-expand into irradiated and necrotic brain volumes than infiltrating intact brain parenchyma. Along those lines, detailed imaging analysis has suggested that significant volume of the recurrent glioblastoma lays in the outermost zone of the IR target volume, i.e., outside the initial gross tumor volume or biological target volume as defined by MRI or PET [2]. This might fit to the idea of re-settling the IR-target volume by glioblastoma cells that formerly emigrated from the gross tumor volume.

Glioblastoma migration is programmed by Ca^{2+} signaling involving CaMKII (for review see [3, 4]). Besides glioblastoma, IR-stimulated Ca^{2+} signaling has been described in leukemia [23–25] suggesting IR-induced Ca^{2+} signaling as a general phenomenon. Like IR, SDF-1 occupation of the G protein coupled chemokine receptor CXCR4 induces Ca^{2+} signaling and migration/invasion in glioblastoma [9, 26] and pancreatic cancer [27]. In particular, SDF-1 has been shown to induce Ca^{2+} release from the Ca^{2+} stores via activation of phospholipase C, and formation of inositol 1, 4, 5-trisphosphate [28]. Notably, the Ca^{2+}-activated BK channels have been demonstrated to be directly linked to inositol 1, 4, 5-triphosphate receptors via lipid rafts [29]. The present study identified BK channel targeting as effective *in vivo* strategy to prevent IR-induced migration. BK channels reportedly fullfil a dual function in glioblastoma migration. They contribute, both, to cell volume changes that motorize migration (for review see [3]) and to Ca^{2+} signaling that trigger migration [14].

BK channels are expressed in neurons of the central nervous system, e.g., in hippocampus, where they can be found in pre- and postsynaptic membranes [30]. The BK channel blocker paxilline, applied in the present study, is a neurotoxin produced by the endophytic fungus *Penicillium paxilli* and causes "ryegrass staggers" in sheep which is characterized by ataxia and uncontrollable tremors [31]. Paxilline is a very specific BK channel inhibitor which works in the nanomolar range [32] .The mechanism of BK blockage is largely unknown. Paxilline has been proposed to be an allosteric inhibitor which stabilizes the closed conformation of the channel [33]. Systemic paxilline administration in our *in vivo* experiments (8 mg/kg BW, twice per day) provoked ataxia due to the blockade of BK channels in the cerebellum [31] indicating that paxilline crosses the blood-brain barrier and reached effectiv concentrations in the brain.

Paxilline at the applied dose induced besides reversible ataxia no severe side effects and was well tolerated by the mice. This might suggest that BK channel targeting might be applied in glioblastoma patients. As a matter of fact, drugs with BK channel modulating side effects are already in clinical use. Classical neuroleptics such as haloperidol or chlorpromazine inhibit BK channels with an IC_{50} in the low micromolar range [34]. Reportedly, haloperidol may accumulate in the human brain up to micromolar [35] and chlorpromazine up to several ten micromolar concentrations [36] suggesting that the therapeutic concentrations of the classical neuroleptics affect BK channel activity.

In conclusion, fractionated radiation stimulates migration of glioblastoma cells *in vivo*. This phenomenon might lead to enhanced tumor spreading during fractionated radiotherapy and might contribute to therapy failure. Radiation-induced BK K^+ channel activation triggers and BK channel blockage suppresses IR-induced migration suggesting BK channel targeting as useful-tool to overcome IR induced migration during radiotherapy.

MATERIALS AND METHODS

Cell culture

Human T98G and U-87MG glioblastoma cells were from ATCC (Bethesda, Maryland, USA) and were grown in 10% fetal calf serum (FCS)-supplemented RPMI-1640 medium as described [14]. The human U-87MG glioblastoma cells were transfected with the far-red Katushka fluorescent protein expression vector pTurboFP635-N (BioCat, Heidelberg, Germany) using the transfection reagent FUGENE HD (Roche Diagnostics GmbH, Mannheim, Germany) according to the manufacturer's instruction. Stably transfected cells were grown in 10% FCS-supplemented RPMI-1640 selection medium containing G418 (750 µg/ml). Exponential growing T98G and U-87MG-Katushka cells were irradiated with 6 MV photons (IR, single dose of 0, 2, 4 and 6 Gy) or five daily fractions of 0 or 2 Gy (fractionated IR) by using a linear accelerator (LINAC SL25 Philips) at a dose rate of 4 Gy/min at room temperature. Following

IR, cells were post-incubated in RPMI-1640/10% FCS medium for 2–4.5 h (immunoblot, patch-clamp, fura-2 Ca^{2+}-imaging, transfilter migration, immunofluorescence microscopy), 24 h (RT-PCR, transfilter migration), or 2–3 weeks (colony formation assay). In some experiments, cells were pre-incubated (0.5 h) and post-incubated after IR with the BK channel inhibitor paxilline (5 μM, Sigma-Aldrich, Taufkirchen, Germany) or the CXCR4 chemokine receptor antagonist AMD3100 (1 μM, Sigma-Aldrich) or vehicle alone (0.1% DMSO). shRNA-transfected T98G cells were grown in RPMI-1640/10% FCS selection medium containing puromycin (2 μg/ml).

Patch-clamp recording

Whole-cell and on-cell currents were evoked by 41 (whole-cell) or 33 (on-cell) voltage square pulses (700 ms each) from -66 mV (whole-cell) or 4 mV holding potential (on-cell) to voltages between -116 (whole-cell) or -56 mV (on-cell) and 84 (whole-cell) or +104 mV (on-cell) delivered in 5 mV increments. The liquid junction potentials between the pipette and the bath solutions were estimated as described [16], and data were corrected for the estimated liquid junction potentials. Cells were superfused at 37°C temperature with NaCl solution (in mM: 125 NaCl, 32 N-2-hydroxyethylpiperazine-N-2-ethanesulfonic acid (HEPES), 5 KCl, 5 D-glucose, 1 $MgCl_2$, 1 $CaCl_2$, titrated with NaOH to pH 7.4). In the whole-cell experiments shown in Figure 1, a K-D-gluconate pipette solution was used containing (in mM): 140 K-D-gluconate, 5 HEPES, 5 $MgCl_2$, 1 K_2-EGTA, 1 K_2-ATP, titrated with KOH to pH 7.4. Paxilline (5 μM) was added to the bath solution.

For the on-cell experiments (Figures 2–4, 6–7) the pipette solution contained (in mM) 0 or 0.005 paxilline in 0.1% DMSO, 130 KCl, 32 HEPES, 5 D-glucose, 1 $MgCl_2$, 1 $CaCl_2$, titrated with KOH to pH 7.4. We used a high K^+-containing pipette solution in order to have a direct quantitative measure for IK channel activity by analyzing the inward currents at highly negative voltages (since BK currents are negligible at these negative voltages). IK channel activity is also induced by radiation [16]. In some experiments, the chemokine stromal cell-derived factor-1 (SDF-1, CXCL12, 50 nM, Immuno Tools, Friesoythe, Germany) and paxilline (5 μM) was added to the bath solution. Whole-cell and macroscopic on-cell currents were analyzed by averaging the currents between 100 and 700 ms of each square pulse. Applied voltages refer to the cytoplasmic face of the membrane with respect to the extracellular space. In the current tracings (whole-cell and macroscopic on-cell currents), the individual current sweeps recorded at the different clamp-voltages are superimposed. Outward currents, defined as flow of positive charge (here: K^+) from the cytoplasmic to the extracellular membrane face, are positive currents and depicted as upward deflections of the original current tracings.

Colony formation assay

To test for clonogenic survival, U-87MG-Katushka and T98G cells were preincubated (0.5 h), irradiated (0, 2, 4 or 6 Gy) and post-incubated (24 h) in RPMI-1640/10% FCS medium additionally containing paxilline (0 or 5 μM in 0.1% DMSO). 24 h after IR, cells were detached, 300 and 600 cells were re-seeded in inhibitor-free medium on 3 cm wells and grown for further 2–3 weeks. The plating efficiency was defined by dividing the number of colonies by the number of plated cells. Plating efficiencies of control and paxilline-treated cells were 0.23 ± 0.001 and 0.22 ± 0.001 for T98G (n = 36) and 0.10 ± 0.003 and 0.06 ± 0.006 (n = 12) for U-87MG-Katushka cells, respectively. Survival fractions as calculated by dividing the plating efficiency of the irradiated cells by those of the unirradiated controls were fitted by the use of the linear quadratic equation.

Transfilter migration

The lower and upper chamber of a CIM-Plate 16 (Roche, Mannheim, Germany) were filled with 160 μl (lower chamber) and 100 μl (upper chamber) of RPMI-1640 medium containing 5% and 1% FCS, respectively, equilibrated at 37°C and 5% CO_2 for 30–60 min. The upper and lower chamber additionally contained SDF-1 (0 or 50 nM) and paxilline (0 or 5 μM in 0.1% DMSO). After CO_2 equilibration and resetting the impedance to zero, 100 μl of cell suspension containing 40.000 of unirradiated (SDF-1 experiments) or irradiated cells (0 or 2 Gy, 1–2 h after IR) in RPMI-1640/1% FCS were added to the upper chamber. After sedimentation and adherence of the cells (2–3 h after IR), migration was analyzed in real-time by measuring the impedance increase between electrodes which cover the lower surface of the filter membrane and the reference electrode in the lower chamber. Upon trans-filter migration, cells adhere to the filter electrode surface and increase the impedance. To compare between individual experiments the impedances were normalized to the 0.5 h values of the respective controls.

Quantitative RT-PCR

Messenger RNAs of fractionated irradiated (5 × 0 Gy or 5 × 2 Gy) U-87MG-Katushka and stably transfected T98G cells (see below) were isolated (Qiagen RNA extraction kit, Hilden, Germany) 24 h after the last IR fraction and reversely transcribed in cDNA (Transcriptor First Strand cDNA Synthesis Kit, Roche, Mannheim, Germany). BK K^+ channel-, CXCR4 chemokine receptor-, SDF-1 (CXCL12)-, matrix metalloproteinases MMP-2- and MMP-9-, and housekeeper β-actin (ACTB)-, pyruvate dehydrogenase beta (PDHB)-, and glyceraldehyde-3-phosphate dehydrogenase (GAPDH)-specific fragments were amplified by the use of SYBR Green-based

quantitative real-time PCR (QT00024157, QT00223188, QT00087591, QT00088396, QT00040040, QT01192646, QT00095431, and QT00031227 QuantiTect Primer Assay and QuantiFast SYBR® Green PCR Kit, Qiagen) in a Roche LightCycler Instrument. Abundances of the individual mRNAs were normalized to the geometrical mean of the three housekeeper mRNAs.

Western blotting

Whole protein lysates were prepared from semiconfluent irradiated (0 or 2 Gy, 2 h after IR) U-87MG-Katushka and stably transfected T98G cells (see below) using a buffer containing (in mM) 50 HEPES pH 7.5, 150 NaCl, 1 EDTA, 10 sodium pyrophosphate, 10 NaF, 2 Na_3VO_4, 1 phenylmethylsulfonylfluorid (PMSF) additionally containing 1% Triton X-100, 5 µg/ml aprotinin, 5 µg/ml leupeptin, and 3 µg/ml pepstatin (all Sigma-Aldrich), and separated by SDS-PAGE under reducing conditions. Segregated proteins were electro-transferred onto PVDF membranes (Roth, Karlsruhe, Germany). Blots were blocked in tris(hydroxymethyl) aminomethane-buffered saline (TBS) buffer containing 0.05% Tween 20 and 5% non-fat dry milk for 1 h at room temperature. The membranes were incubated overnight at 4°C with the following primary antibodies in TBS -Tween/5% milk against human CXCR4 (rabbit polyclonal antibody, #ab2074, 1:500 dilution, Abcam, Cambridge, UK), human HIF-1α (rabbit monoclonal, #61275, 1:1000 dilution, Active Motif, La Hulpe, Belgium) and human BK (rabbit polyclonal, #APC-107, 1:500 dilution, Alamone Labs, Jerusalem, Israel). Equal gel loading was verified by an antibody against β-actin (mouse anti-β-actin antibody, clone AC-74, Sigma #A2228 1:30,000). Antibody binding was detected with a horseradish peroxidase-linked goat anti-rabbit or horse anti-mouse IgG antibody (# 7074 and #7076, respectively; 1:2000 dilution in TBS-Tween/5% milk, Cell Signaling, Merck-Millipore, Darmstadt, Germany) incubated for 1 h at room temperature and enhanced chemoluminescence (ECL Western blotting analysis system, GE Healthcare/ Amersham-Biosciences, Freiburg, Germany).

Immunofluorescence microscopy of cultured cells

U-87MG-Katushka and T98G cells (0 or 2 Gy, 2 h after IR) were grown on object slides and irradiated with 0 or 2 Gy. Two hours after IR, cells were fixed for 15 min at room temperature with phosphate buffered saline (PBS)-containing 4% formaldehyde, 3 times rinsed with PBS for 5 min and blocked for 1 h at 21°C with PBS additionally containing 1% bovine serum albumin (BSA), 5% goat serum and 0.3% Triton X-100. Cells were then incubated with polyclonal rabbit anti-SDF-1 antibody (NBP1–19778, Novus Biologicals, R & D Systems Europe, Abingdon, UK) or rabbit IgG isotype control antibody (#12–370, Merck-Millipore, both 1 mg/ml) diluted (both 1:1000) in PBS containing 1% BSA and 0.3% Triton X-100. Thereafter, cells were rinsed 3 times for 5 min with PBS, incubated for 2 h at room temperature in the dark with goat FITC-conjugated anti-rabbit IgG antibody (1:1000, NB730-F, Novus Biologicals) diluted in PBS/1% BSA/0.3% Triton X-100, rinsed 3 times for 5 min with PBS, and coverslipped with 4',6-diamidino-2-phenylindole (DAPI) Vectashield Antifade Mounting Medium (Vector Laboratories, Loerrach, Germany).

Fura-2 Ca^{2+} imaging

Fluorescence measurements were performed using an inverted phase-contrast microscope (Axiovert 100; Zeiss, Oberkochen, Germany). Fluorescence was evoked by a filter wheel (Visitron Systems, Puchheim, Germany)-mediated alternative excitation at 340/26 or 387/11 nm (AHF, Analysentechnik, Tübingen, Germany). Excitation and emission light was deflected by a dichroic mirror (409/LP nm beam splitter, AHF) into the objective (Fluar x40/1.30 oil; Zeiss) and transmitted to the camera (Visitron Systems), respectively. Emitted fluorescence intensity was recorded at 587/35 nm (AHF). Excitation was controlled and data acquired by Metafluor computer software (Universal Imaging, Downingtown, PA, USA). The 340/380-nm fluorescence ratio was used as a measure of cytosolic free Ca^{2+} concentration ($_{free}[Ca^{2+}]_i$). U-87MG-Katushka and T98G cells were incubated with fura-2/AM (2 µM for 30 min at 37°C; Molecular Probes, Goettingen, Germany) in RPMI-1640/10% FCS medium. $_{free}[Ca^{2+}]_i$ was determined at 37°C during superfusion with NaCl solution (in mM: 125 NaCl, 32 HEPES, 5 KCl, 5 D-glucose, 1 $MgCl_2$, 2 $CaCl_2$, titrated with NaOH to pH 7.4) before and during stimulation with SDF-1 (50 nM) or conditioned NaCl solution harvested from irradiated cells. For conditioning, 250.000 cells were grown for 24 h in RPMI 1640/10% FCS. After further 24 h of serum depletion, cells were washed once with NaCl solution, overlayed with 1 ml of NaCl solution, irradiated (0 or 2 Gy) and further incubated for 2 h before harvesting the NaCl solution.

Orthotopic mouse model of human glioblastoma

Animal experiments were carried out according to the German animal protection law and approved by the local authorities. Fluorescent U-87MG-Katushka cells (Figure 8A) were inoculated stereotactically into the right striatum of 12 week old immunocompromised male and female NOD/SCID/IL2Rγ^{null} (NSG) mice. The skullcap was trepanated 2.6 mm laterally and 0.5 mm caudally of the bregma (as indicated in the drawing of Figure 8B) by the use of a dental driller and 30.000 U-87MG-Katushka cells (in 10 µl of FCS-free EMEM medium) were injected

in 3 mm depth from the dura surface into the right striatum. Starting at day 7, Isofluran-anaesthesized mice were immobilized under a 6 MV linear accelerator (LINAC SL25 Philips) and the right hemispheres were irradiated with daily fractions of 0 or 2 Gy 6 MV photons using mouse holders and shieldings as described in Figure 8E, 8F. On the days of radiation, paxilline (0 or 8 mg/kg BW i.p. in 70 µl 90% DMSO) was administered 6 h prior to and 6 h after each radiation fraction to some of the mice. In particular, 6 mice of the 5 × 0 Gy and 5 × 2 Gy control groups received vehicle alone while 14 mice were not i.p. injected. The data between the vehicle-receiving and non-receiving control mice did not differ in the 5 × 0 Gy or 5 × 2 Gy group and were pooled in each group. For dosimetry, Gafchromic 3 films (Ashland Inc., Covington, KY) placed in a mouse phantom (in 5 mm depth form the phantom surface) were exposed. By comparison with unshielded calibration films, dose distribution was defined by the film blackening inside and outside the target volume. For the dosimetry film shown in Figure 8G, background blackening (as defined by unexposed films) was subtracted.

Immunofluorescence microscopy and immunohistochemistry of brain sections

Three weeks (in pilot experiments one or two weeks) after tumor challenge, mice were sacrificed and brains were fixed (2% paraformaldehyd in phosphate buffered solution, PBS for 24 h), cryo-protected (30% sucrose in PBS for 24 h), frozen at –80°C in Richard-Allan Scientific™ Neg-50™ Frozen Section Medium (Thermo Scientific, Germany), and cryosectioned (20 µm). For glioblastoma cell migration, cryosections were directly coverslipped in Vectashield Antifade Mounting Medium with DAPI and Katushka and DAPI fluorescence was evaluated by conventional fluorescence microscopy. For each tumor, all emigrated cells were summarized to generate one data point. The total number of emigrated cells per tumor was then compared between all four groups (5 × 0 Gy- and 5 × 2 Gy-irradiated glioblastomas in absence and presence of systemical application of BK channel inhibitor paxilline).

For SDF-1 protein immunostaining, sections were post-fixed 15 min (4% paraformaldehyde in PBS) and processed identically to the protocol described above for the cultured cells. After mounting, SDF-1-specific FITC was analyzed by confocal fluorescence microscopy. Antibody specificity was confirmed by the isotype which didn't produce any considerable fluorescence staining (data not shown). For CXCR-4 staining, the brain sections were fixed and permeabilized with 100% icecold methanol for 10 min instead of PFA fixation. As primary antibody, an anti-CXCR4 antibody (rabbit polyclonal antibody, Abcam #ab2074) was used in a 1:100 dilution.

For BK channel staining (Figure 8I–8K), sections were washed three times for 5 min with PBS, fixed and permeabilized for 10 min with 100% icecold methanol, again washed with PBS for 5 min and blocked for one hour in blocking solution (PBS containing 1% BSA, 0,2% Glycin, 0,2% Lysin, 5% goat serum and 0,3% Triton X-100). Sections were incubated overnight (4°C) with rabbit anti $BKa_{(674–1115)}$ antibody [30], 1:500 in blocking solution and after washing three times for 5 min with PBS incubated for 1 h with the biotinylated secondary antibody, 1:200 (anti rabbit IgG, Vector Laboratories) in blocking solution. The staining was visualized with the alkaline phosphatase method and the sections were covered with Aquatex (Merck-Millipore). For positive and negative control hippocampus sections from a NSG mouse (Figure 8I) and a $BK^{-/-}$ mouse [30] (Figure 8K) were used, respectively.

BK knockdown

BK channels were down-regulated in T98G cells by transduction with a pool of five BK-specific MISSION® shRNA Lentiviral Transduction Particles and as a control with MISSION® pLKO.1-puro Empty Vector Control Transduction Particles (SHCLNV-NM_002247 and SHC001V, Sigma-Aldrich). Cells were transduced according to the provided experimental protocol positively transduced clones were selected by the use of 2 µg/ml puromycin in the culture medium. Down-regulation of BK was controlled by quantitative RT-PCR and immunoblotting (Figure 3G, insert).

SDF-1 ELISA

T98G cells (250.000) were seeded in 75 cm^2 cell culture flasks in RPMI-1640 medium containing 10% FCS and grown over night. Cells were washed with PBS and serum depleted for 24 h. Thereafter, cells were washed with PBS and overlaid with NaCl solution (see patch-clamp section) containing protease inhibitors (Roche, cOmplete Mini, EDTA-free, #04693159001). After 30 min incubation, cells were irradiated with 0 or 2 Gy. After further 2 h the medium was harvested and the SDF-1 concentration determined using an ELISA assay kit (R&D Systems, Human CXCL12/SDF-1 DuoSet ELISA, #DY350).

ACKNOWLEDGMENTS

We thank Heidrun Faltin, Ilka Müller and Maria Beer-Krön for excellent technical assistance, Savas Tsitsekidis for the dosimetry, and Andreas Hönes for constructing the mouse holders and lead shieldings.

GRANT SUPPORT

This work has been supported by a grant from the Wilhelm-Sander-Stiftung awarded to SH and PR (2011.083.1). LE was supported by a grant from the

Landesgraduierentförderungsgesetz, Baden-Württemberg. BS was supported by the DFG International Graduate School 1302 (TP T9 SH) and LK by the ICEPHA program of the University of Tübingen and the Robert-Bosch-Gesellschaft für Medizinische Forschung, Stuttgart.

CONFLICTS OF INTEREST

The authors declare no conflicts of interest.

REFERENCES

1. Johnson J, Nowicki MO, Lee CH, Chiocca EA, Viapiano MS, Lawler SE, Lannutti JJ. Quantitative analysis of complex glioma cell migration on electrospun polycaprolactone using time-lapse microscopy. Tissue Eng Part C Methods. 2009; 15:531–540.
2. Weber DC, Casanova N, Zilli T, Buchegger F, Rouzaud M, Nouet P, Vees H, Ratib O, Dipasquale G, Miralbell R. Recurrence pattern after [(18)F]fluoroethyltyrosine-positron emission tomography-guided radiotherapy for high-grade glioma: a prospective study. Radiother Oncol. 2009; 93:586–592.
3. Huber SM. Oncochannels. Cell Calcium. 2013; 53: 241–255.
4. Huber SM, Butz L, Stegen B, Klumpp L, Klumpp D, Eckert F. Role of ion channels in ionizing radiation-induced cell death. Biochim Biophys Acta. 2015; 1848:2657–2664.
5. Eke I, Storch K, Kastner I, Vehlow A, Faethe C, Mueller-Klieser W, Taucher-Scholz G, Temme A, Schackert G, Cordes N. Three-dimensional Invasion of Human Glioblastoma Cells Remains Unchanged by X-ray and Carbon Ion Irradiation *In Vitro*. Int J Radiat Oncol Biol Phys. 2012; 84:e515–23.
6. Greenfield JP, Cobb WS, Lyden D. Resisting arrest: a switch from angiogenesis to vasculogenesis in recurrent malignant gliomas. J Clin Invest. 2010; 120:663–667.
7. Zhou W, Xu Y, Gao G, Jiang Z, Li X. Irradiated normal brain promotes invasion of glioblastoma through vascular endothelial growth and stromal cell-derived factor 1alpha. Neuroreport. 2013; 24:730–734.
8. Pham K, Luo D, Siemann DW, Law BK, Reynolds BA, Hothi P, Foltz G, Harrison JK. VEGFR inhibitors upregulate CXCR4 in VEGF receptor-expressing glioblastoma in a TGFbetaR signaling-dependent manner. Cancer Lett. 2015; 360:60–67.
9. Sciaccaluga M, Fioretti B, Catacuzzeno L, Pagani F, Bertollini C, Rosito M, Catalano M, D'Alessandro G, Santoro A, Cantore G, Ragozzino D, Castigli E, Franciolini F, et al.CXCL12-induced glioblastoma cell migration requires intermediate conductance Ca2+-activated K+ channel activity. Am J Physiol Cell Physiol. 2010; 299:C175–184.
10. Tabatabai G, Frank B, Mohle R, Weller M, Wick W. Irradiation and hypoxia promote homing of haematopoietic progenitor cells towards gliomas by TGF-beta-dependent HIF-1alpha-mediated induction of CXCL12. Brain. 2006; 129:2426–2435.
11. Kioi M, Vogel H, Schultz G, Hoffman RM, Harsh GR, Brown JM. Inhibition of vasculogenesis, but not angiogenesis, prevents the recurrence of glioblastoma after irradiation in mice. J Clin Invest. 2010; 120:694–705.
12. Kozin SV, Kamoun WS, Huang Y, Dawson MR, Jain RK, Duda DG. Recruitment of myeloid but not endothelial precursor cells facilitates tumor regrowth after local irradiation. Cancer Res. 2010; 70:5679–5685.
13. Wang SC, Yu CF, Hong JH, Tsai CS, Chiang CS. Radiation therapy-induced tumor invasiveness is associated with SDF-1-regulated macrophage mobilization and vasculogenesis. PLoS One. 2013; 8:e69182.
14. Steinle M, Palme D, Misovic M, Rudner J, Dittmann K, Lukowski R, Ruth P, Huber SM. Ionizing radiation induces migration of glioblastoma cells by activating BK K^+ channels. Radiother Oncol. 2011; 101:122–126.
15. Woo SR, Ham Y, Kang W, Yang H, Kim S, Jin J, Joo KM, Nam DH. KML001, a telomere-targeting drug, sensitizes glioblastoma cells to temozolomide chemotherapy and radiotherapy through DNA damage and apoptosis. BioMed Res Int. 2014; 2014:747415.
16. Stegen B, Butz L, Klumpp L, Zips D, Dittmann K, Ruth P, Huber SM. Ca^{2+}-Activated IK K^+ Channel Blockade Radiosensitizes Glioblastoma Cells. Mol Cancer Res. 2015; 13:1283–1295.
17. Stupp R, Hegi ME, Mason WP, van den Bent MJ, Taphoorn MJ, Janzer RC, Ludwin SK, Allgeier A, Fisher B, Belanger K, Hau P, Brandes AA, Gijtenbeek J, et al. Effects of radiotherapy with concomitant and adjuvant temozolomide versus radiotherapy alone on survival in glioblastoma in a randomised phase III study: 5-year analysis of the EORTC-NCIC trial. Lancet Oncol. 2009; 10:459–466.
18. Wild-Bode C, Weller M, Rimner A, Dichgans J, Wick W. Sublethal irradiation promotes migration and invasiveness of glioma cells: implications for radiotherapy of human glioblastoma. Cancer Res. 2001; 61:2744–2750.
19. Desmarais G, Charest G, Fortin D, Bujold R, Mathieu D, Paquette B. Cyclooxygenase-2 inhibitor prevents radiation-enhanced infiltration of F98 glioma cells in brain of Fischer rat. Int J Radiat Biol. 2015:1–10.
20. Shankar A, Kumar S, Iskander A, Varma NR, Janic B, Decarvalho A, Mikkelsen T, Frank JA, Ali MM, Knight RA, Brown S, Arbab AS. Subcurative radiation significantly increases proliferation, invasion, and migration of primary GBM *in vivo*. Chin J Cancer. 2014;33:148–58.
21. Minniti G, Amelio D, Amichetti M, Salvati M, Muni R, Bozzao A, Lanzetta G, Scarpino S, Arcella A, Enrici RM. Patterns of failure and comparison of different target volume delineations in patients with glioblastoma treated with conformal radiotherapy plus concomitant and adjuvant temozolomide. Radiother Oncol. 2010; 97:377–381.

22. Chen L, Chaichana KL, Kleinberg L, Ye X, Quinones-Hinojosa A, Redmond K. Glioblastoma recurrence patterns near neural stem cell regions. Radiother Oncol. 2015; 116:294–300.

23. Heise N, Palme D, Misovic M, Koka S, Rudner J, Lang F, Salih HR, Huber SM, Henke G. Non-selective cation channel-mediated Ca^{2+}-entry and activation of Ca^{2+}/calmodulin-dependent kinase II contribute to G_2/M cell cycle arrest and survival of irradiated leukemia cells. Cell Physiol Biochem. 2010; 26:597–608.

24. Palme D, Misovic M, Schmid E, Klumpp D, Salih HR, Rudner J, Huber SM. Kv3.4 potassium channel-mediated electrosignaling controls cell cycle and survival of irradiated leukemia cells. Pflugers Arch. 2013; 465:1209–1221.

25. Klumpp D, Misovic M, Szteyn K, Shumilina E, Rudner J, Huber SM. Targeting TRPM2 channels impairs radiation-induced cell cycle arrest and fosters cell death of T cell leukemia cells in a Bcl-2-dependent manner. Oxid Med Cell Longev. 2016; 2016:8026702. doi: 10.1155/2016/8026702.

26. Zagzag D, Esencay M, Mendez O, Yee H, Smirnova I, Huang Y, Chiriboga L, Lukyanov E, Liu M, Newcomb EW. Hypoxia- and vascular endothelial growth factor-induced stromal cell-derived factor-1alpha/CXCR4 expression in glioblastomas: one plausible explanation of Scherer's structures. American J Pathol. 2008; 173:545–560.

27. Saur D, Seidler B, Schneider G, Algul H, Beck R, Senekowitsch-Schmidtke R, Schwaiger M, Schmid RM. CXCR4 expression increases liver and lung metastasis in a mouse model of pancreatic cancer. Gastroenterology. 2005; 129:1237–1250.

28. Peng H, Huang Y, Rose J, Erichsen D, Herek S, Fujii N, Tamamura H, Zheng J. Stromal cell-derived factor 1-mediated CXCR4 signaling in rat and human cortical neural progenitor cells. J Neurosci Res. 2004; 76:35–50.

29. Weaver AK, Olsen ML, McFerrin MB, Sontheimer H. BK channels are linked to inositol 1, 4, 5-triphosphate receptors via lipid rafts: a novel mechanism for coupling $[Ca^{2+}]_i$ to ion channel activation. J Biol Chem. 2007; 282:31558–31568.

30. Sausbier U, Sausbier M, Sailer CA, Arntz C, Knaus HG, Neuhuber W, Ruth P. Ca^{2+} -activated K^+ channels of the BK-type in the mouse brain. Histochem Cell Biol. 2006; 125:725–741.

31. Imlach WL, Finch SC, Dunlop J, Meredith AL, Aldrich RW, Dalziel JE. The molecular mechanism of "ryegrass staggers," a neurological disorder of K^+ channels. J Pharmacol Exp Ther. 2008; 327:657–664.

32. Knaus HG, McManus OB, Lee SH, Schmalhofer WA, Garcia-Calvo M, Helms LM, Sanchez M, Giangiacomo K, Reuben JP, Smith AB, 3rd and et al. Tremorgenic indole alkaloids potently inhibit smooth muscle high-conductance calcium-activated potassium channels. Biochemistry. 1994; 33:5819–5828.

33. Zhou Y, Lingle CJ. Paxilline inhibits BK channels by an almost exclusively closed-channel block mechanism. J Gen Physiol. 2014; 144:415–440.

34. Lee K, McKenna F, Rowe IC, Ashford ML. The effects of neuroleptic and tricyclic compounds on BKCa channel activity in rat isolated cortical neurones. Br J Pharmacol. 1997; 121:1810–1816.

35. Korpi ER, Kleinman JE, Costakos DT, Linnoila M, Wyatt RJ. Reduced haloperidol in the post-mortem brains of haloperidol-treated patients. Psychiatry Res. 1984; 11:259–269.

36. Huang CL, Ruskin BH. Determination of Serum Chlorpromazine Metabolites in Psychotic Patients. J Nerv Ment Dis. 1964; 139:381–386.

Published OnlineFirst June 3, 2015; DOI: 10.1158/1541-7786.MCR-15-0075

Cell Death and Survival

Molecular Cancer Research

Ca^{2+}-Activated IK K^+ Channel Blockade Radiosensitizes Glioblastoma Cells

Benjamin Stegen[1], Lena Butz[1,2], Lukas Klumpp[1,3], Daniel Zips[1], Klaus Dittmann[4], Peter Ruth[2], and Stephan M. Huber[1]

Abstract

Ca^{2+}-activated K^+ channels, such as BK and IK channels, have been proposed to fulfill pivotal functions in neoplastic transformation, malignant progression, and brain infiltration of glioblastoma cells. Here, the ionizing radiation (IR) effect of IK K^+ channel targeting was tested in human glioblastoma cells. IK channels were inhibited pharmacologically by TRAM-34 or genetically by knockdown, cells were irradiated with 6 MV photons and IK channel activity, Ca^{2+} signaling, cell cycling, residual double-strand breaks, and clonogenic survival were determined. In addition, the radiosensitizing effect of TRAM-34 was analyzed *in vivo* in ectopic tumors. Moreover, The Cancer Genome Atlas (TCGA) was queried to expose the dependence of IK mRNA abundance on overall survival (OS) of patients with glioma. Results indicate that radiation increased the activity of IK channels, modified Ca^{2+} signaling, and induced a G_2–M cell-cycle arrest. TRAM-34 decreased the IR-induced accumulation in G_2–M arrest and increased the number of γH2AX foci post-IR, suggesting that TRAM-34 mediated an increase of residual DNA double-strand breaks. Mechanistically, IK knockdown abolished the TRAM-34 effects indicating the IK specificity of TRAM-34. Finally, TRAM-34 radiosensitized ectopic glioblastoma *in vivo* and high IK mRNA abundance associated with shorter patient OS in low-grade glioma and glioblastoma.

Implications: Together, these data support a cell-cycle regulatory function for IK K^+ channels, and combined therapy using IK channel targeting and radiation is a new strategy for anti-glioblastoma therapy. *Mol Cancer Res; 13(9); 1283–95. ©2015 AACR.*

Introduction

Glioblastoma multiforme (GBM) represents the most common primary brain tumor in adults. The therapeutic concept combines resection of the tumor followed by adjuvant radiation therapy combined with simultaneous temozolomide chemotherapy. Although the administration of the alkylating cytostatic agent significantly prolongs overall survival (OS), the prognosis of patients with glioblastoma remains very poor, with a median survival time of less than 2 years (1).

The underlying radiobiological mechanisms of the poor radiation response of glioblastoma appear to include multiple factors. Among those are low cellular radiation sensitivity, high proportion of cancer stem cells, enhanced repopulation, protective tumor microenvironment, infiltration of the tumor by immune cells, and highly migratory phenotype of the GBM cells giving rise to infiltrative tumor growth. In addition, glioblastoma cells have been proposed to evade therapy by persisting in potential subventricular neural stem cell niches outside of the radiation target volume (2).

Glioblastoma cells functionally express high numbers of Ca^{2+}-activated IK K^+ channels (other names are hIKCa1, hKCa4, hSK4, KCa3.1) in their plasma membrane (3–6). Notably, IK channels are low expressed or even absent in human astrocytes (7) but upregulated during neoplastic transformation and malignant progression of the glioma (8). This suggests a specific function of these channels in glioblastoma tumorigenesis. As a matter of fact, IK channels have been demonstrated to be indispensable for glioblastoma cell migration (for review, see ref. 9). Accordingly, IK protein expression in the tumor significantly correlates with poor survival of the patients with glioma (10). Similar to glioblastoma, IK channels are upregulated in a variety of further tumor entities such as prostate (11), breast (12), and pancreatic cancer (13) as well as lymphoma (14) where they have been proven to control cell cycling and tumor growth.

In addition to tumor cell migration and proliferation, K^+ channel activity may contribute to radioresistance of tumor cells (for review, see refs. 15–17). Remarkably, the fungicide clotrimazole has been shown to impair glioblastoma growth *in vitro* and *in vivo* (18, 19) and to promote apoptotic cell death of irradiated glioblastoma cells *in vitro* (20). Because clotrimazole is a potent IK channel inhibitor, we tested in the present study for a functional significance of IK channels in the radioresistance of glioblastoma cells *in vitro*. We could show by physiologic and cell biologic means that ionizing radiation activates IK channels in glioblastoma cells. Channel activation, in turn, contributes to the cellular stress response. Accordingly, inhibition or silencing of IK channels resulted in impaired cell-cycle arrest and DNA repair and decreased the clonogenic survival of irradiated glioblastoma cells. In addition, pharmacologic targeting of IK channels radiosensitized glioblastoma grown ectopically in mice during fractionated radiation therapy.

[1]Department of Radiation Oncology, University of Tübingen, Tübingen, Germany. [2]Department of Pharmacology, Toxicology and Clinical Pharmacy, Institute of Pharmacy, University of Tübingen, Tübingen, Germany. [3]Dr. Margarete Fischer-Bosch-Institute of Clinical Pharmacology, Stuttgart, Germany. [4]Division of Radiobiology and Molecular Environmental Research, Department of Radiation Oncology, University of Tübingen, Tübingen, Germany.

Corresponding Author: Stephan M. Huber, Department of Radiation Oncology, Laboratory of Experimental Radiation Oncology, University of Tübingen, Hoppe-Seyler-Str. 3, Tübingen 72076, Germany. Phone: 49-0-7071-29-82183; Fax: 0-7071-29-4944; E-mail: stephan.huber@uni-tuebingen.de

doi: 10.1158/1541-7786.MCR-15-0075

©2015 American Association for Cancer Research.

Downloaded from mcr.aacrjournals.org on October 8, 2015. © 2015 American Association for Cancer Research.

Published OnlineFirst June 3, 2015; DOI: 10.1158/1541-7786.MCR-15-0075

Furthermore, a Cancer Genome Atlas (TCGA) query suggests an association between glioma IK mRNA abundance and progression-free survival (PFS) of patients with glioma.

Materials and Methods

Cell culture

Human T98G and U87MG glioblastoma cells were from the ATCC and were grown in 10% FCS-supplemented RPMI-1640 medium as described (21). The human SVGA fetal astrocyte cell line has been kindly provided by Professor Walter J. Atwood, Brown University (Providence, RI), and was maintained in 10% FCS-supplemented DMEM. Exponential growing T98G and U87 MG cells were irradiated with 6 MV photons (IR, single dose of 0, 2, 4, and 6 Gy) by using a linear accelerator (LINAC SL25 Philips) at a dose rate of 4 Gy/min at room temperature. Following irradiation, cells were postincubated in RPMI-1640/10% FCS medium for 2 to 6 hours (immunoblot, patch-clamp, fura-2 Ca^{2+} imaging), 24 hours (γH2AX immunofluorescence), 24 and 48 hours (flow cytometry), and 2 weeks (colony formation; ref. 21). In some experiments, cells were preincubated (0.5 hours) and postincubated after IR with the IK K^+ channel inhibitor TRAM-34 (10 μmol/L) or vehicle alone (0.1% DMSO). Transfected T98G cells were grown in RPMI-1640/10% FCS selection medium containing puromycin (2 μg/mL).

Immunofluorescence

Subconfluent T98G glioblastoma cells and SVGA fetal astrocytes grown on object slides (Millicell EZ SLIDES; Millipore) were fixed with 4% paraformaldehyde in PBS for 1 hour and washed three times for 5 minutes with PBS. Cells were blocked for 1 hour with PBS containing 0.3% Triton X-100, 5% normal goat serum, and washed for 15 minutes with PBS. Incubation with rabbit anti-IK antibody (H-120, SantaCruz Biotechnology, Inc.; sc-32949, 1:50) and rabbit IgG isotype control antibody (1:250, Millipore), respectively, in antibody dilution buffer (PBS, 0.3% Triton X-100, 1% BSA) was performed for 1 hour at room temperature. Cells were washed three times for 5 minutes in PBS and incubated for 2 hours at room temperature in the dark with FITC-conjugated goat anti-rabbit IgG antibody (1:500, Novus Biologicals). Cells were washed three times with PBS, and object slides were mounted with cover slips using the DNA-specific fluorochrome DAPI-containing ECTASHIELD mounting medium with DAPI (Vectashield, Vector Laboratories, BIOZOL).

Patch-clamp recording

Semiconfluent cells were irradiated with 0 Gy (SVGA, T98G) or 2 Gy (T98G). Whole-cell and on-cell currents were evoked by 9 to 11 (whole-cell) or 41 (on-cell) voltage square pulses (700 ms each) from −50 or 0 mV holding potential to voltages between −100 and +100 mV delivered in 5 or 20 mV increments. The liquid junction potentials between the pipette and the bath solutions were estimated according to previously published data (22), and data were corrected for the estimated liquid junction potentials. Cells were superfused at 37°C temperature with NaCl solution (125 mmol/L NaCl, 32 mmol/L HEPES, 5 mmol/L KCl, 5 mmol/L D-glucose, 1 mmol/L $MgCl_2$, 1 mmol/L $CaCl_2$, titrated with NaOH to pH 7.4). In the whole-cell experiment shown in Fig. 1, ionomycin (2.5 μmol/L) and TRAM-34 (1 μmol/L) or ionomycin (2.5 μmol/L), paxilline (5 μmol/L), and TRAM-34 (1 μmol/L, all from Sigma-Aldrich) were sequentially added to the bath solution. For this recording, a K-D-gluconate pipette solution was used containing: 140 mmol/L K-D-gluconate, 5 mmol/L HEPES, 5 mmol/L $MgCl_2$, 1 mmol/L K_2-EGTA, 1 mmol/L K_2-ATP, titrated with KOH to pH 7.4. In the on-cell experiments (Fig. 2), the pipette solution contained 0 or 0.01 mmol/L TRAM-34 in DMSO, 130 mmol/L KCl, 32 mmol/L HEPES, 5 mmol/L D-glucose, 1 mmol/L $MgCl_2$, 1 mmol/L $CaCl_2$, titrated with KOH to pH 7.4. Whole-cell and macroscopic on-cell currents were analyzed by averaging the currents between 100 and 700 ms of each square pulse.

Western blotting

Surface proteins of irradiated (0 and 2 Gy) T98G cells were enriched by the use of a cell surface protein isolation kit (Pierce) according to the supplied protocol. Whole protein lysates were prepared from stably transfected T98G cells (see below). Proteins were lysed in a buffer containing 50 mmol/L HEPES, pH 7.5, 150 mmol/L NaCl, 1 mmol/L EDTA, 10 mmol/L sodium pyrophosphate, 10 mmol/L NaF, 2 mmol/L Na_3VO_4, 1 mmol/L phenylmethylsulfonylfluoride (PMSF), additionally containing 1% triton X-100, 5 μg/mL aprotinin, 5 μg/mL leupeptin, and 3 μg/mL pepstatin, and separated by SDS-PAGE under reducing conditions. Segregated proteins were electrotransferred onto polyvinylidene difluoride (PVDF) membranes (Roth). Blots were blocked in TBS buffer containing 0.05% Tween-20 and 5% non-fat dry milk for 1 hour at room temperature. The membrane was incubated overnight at 4°C with the following primary antibodies in TBS-Tween/5% milk against IK (H-120, sc-32949 SantaCruz, 1:500) or the α_1 subunit of the Na^+ pump (Cell Signaling #3010, New England Biolabs; 1:500). Equal gel loading was verified by an antibody against β-actin (mouse anti-β-actin antibody, clone AC-74, Sigma #A2228; 1:20,000). Antibody binding was detected with a horseradish peroxidase–linked goat anti-rabbit or horse anti-mouse IgG antibody (Cell Signaling #7074 and #7076, respectively; 1:2,000 dilution in TBS-Tween/5% milk) incubated for 1 hour at room temperature, and enhanced chemoluminescence (ECL Western blotting analysis system, GE Healthcare/Amersham-Biosciences) of indicated protein levels were quantified by densitometry using ImageJ software (ImageJ 1.40g, NIH, Bethesda, MD).

Fura-2 Ca^{2+} imaging

Fluorescence measurements were performed using an inverted phase-contrast microscope (Axiovert 100; Zeiss). Fluorescence was evoked by a filter wheel (Visitron Systems)-mediated alternative excitation at 340/26 or 387/11 nm (AHF, Analysentechnik). Excitation and emission lights were deflected by a dichroic mirror (409/LP nm beamsplitter, AHF) into the objective (Fluar x40/1.30 oil; Zeiss) and transmitted to the camera (Visitron Systems), respectively. Emitted fluorescence intensity was recorded at 587/35 nm (AHF). Excitation was controlled and data acquired by Metafluor computer software (Universal Imaging). The 340/380-nm fluorescence ratio was used as a measure of cytosolic free Ca^{2+} concentration ($i[Ca^{2+}]_{free}$). T98G cells were irradiated (0 or 2 Gy) and loaded with fura-2/AM (2 μmol/L for 30 minutes at 37°C; Molecular Probes) in RPMI-1640/10% FCS medium. $i[Ca^{2+}]_{free}$ was determined 2 to 3 hours post-IR at 37°C during superfusion with NaCl solution (125 mmol/L NaCl, 32 mmol/L HEPES, 5 mmol/L KCl, 5 mmol/L D-glucose, 1 mmol/L $MgCl_2$, 2 mmol/L $CaCl_2$, titrated with NaOH to pH 7.4), during extracellular Ca^{2+} removal in EGTA-buffered NaCl solution (125 mmol/L NaCl,

Downloaded from mcr.aacrjournals.org on October 8, 2015. © 2015 American Association for Cancer Research.

Published OnlineFirst June 3, 2015; DOI: 10.1158/1541-7786.MCR-15-0075

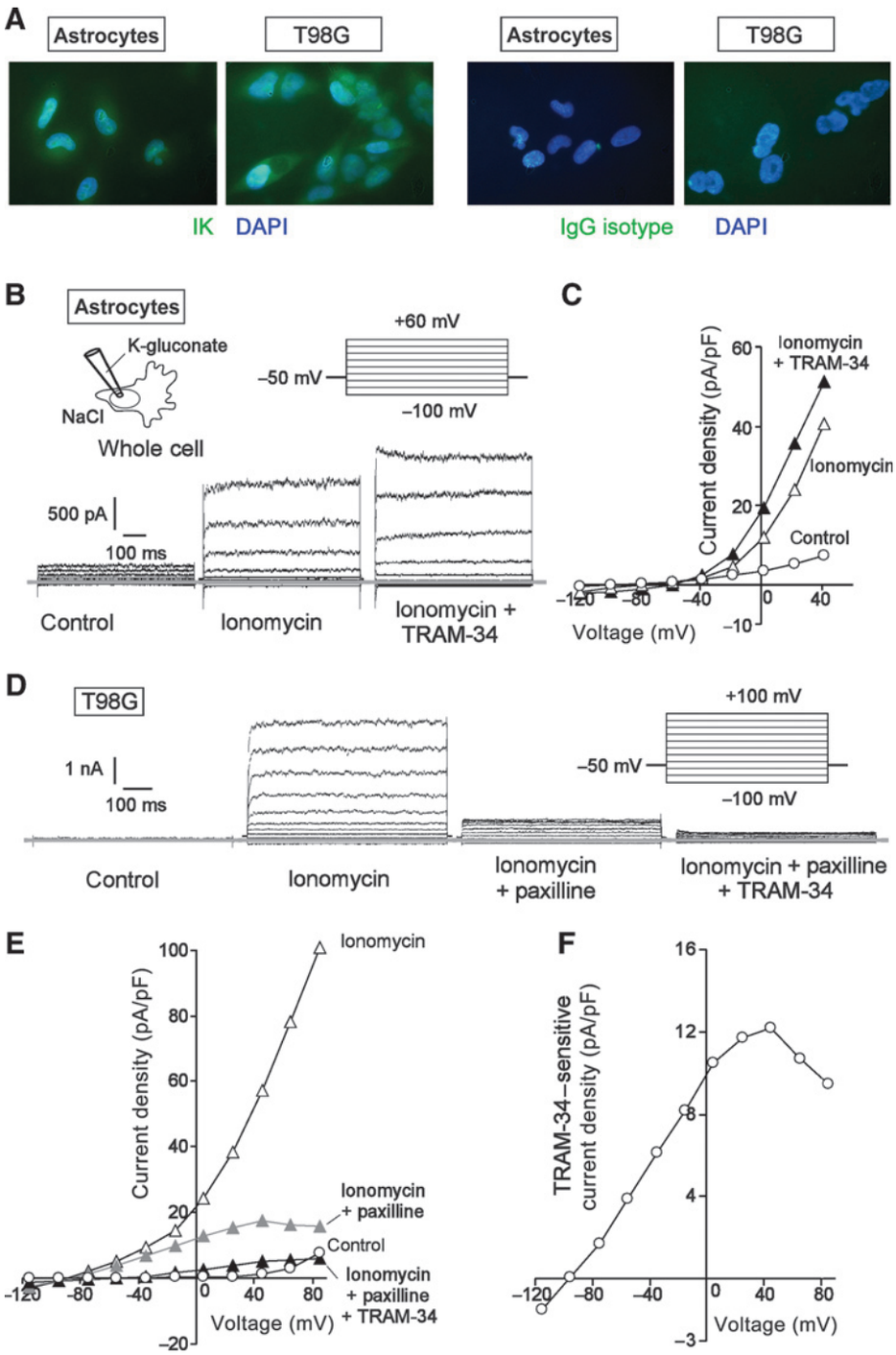

Figure 1.
T98G cells functionally express BK and IK K^+ channels. A, immunofluorescent micrographs of human astrocytes and T98G glioblastoma cells stained (green fluorescence) with an IK-specific antibody (left) or the IgG isotype control antibody (right). The nuclei were stained with the DNA-specific dye DAPI (blue). B, whole-cell current tracing of a human astrocyte recorded with K-gluconate pipette and NaCl bath solution before (first tracings) and after (second to third tracings) Ca^{2+} permeabilization of the plasma membrane with the Ca^{2+} ionophore ionomycin (2.5 μmol/L). Ca^{2+}-activated currents were recorded under control conditions (second tracings) or after bath application of the IK channel blocker TRAM-34 (1 μmol/L; third tracings; the inset in the middle shows the applied pulse protocol). C, dependence of the whole-cell current densities on voltage of the records shown in B. D, whole-cell current tracings of a T98G cell recorded as in B before (first tracings) and after (second to fourth tracings) Ca^{2+} permeabilization of the plasma membrane. Ca^{2+}-activated currents were recorded under control conditions (second tracings) or after bath application of the BK channel inhibitor paxilline (5 μmol/L, third tracings) and additional administration of the IK channel blocker TRAM-34 (1 μmol/L; fourth tracings; the inset on the right shows the applied pulse protocol). E, dependence of the whole-cell current densities on voltage of the records shown in D. F, TRAM-34–sensitive current density fraction as calculated by subtracting the current densities of E recorded with paxilline and TRAM-34 from those obtained with paxilline alone.

32 mmol/L HEPES, 5 mmol/L KCl, 5 mmol/L D-glucose, 1 mmol/L $MgCl_2$, 0.6 mmol/L EGTA, titrated with NaOH to pH 7.4), and during Ca^{2+} re-addition in $CaCl_2$-containing NaCl solution.

Flow cytometry

T98G cells were preincubated (0.25 hours), irradiated (0 or 2 Gy), and incubated for further 6 hours in RPMI-1640/10% FCS medium additionally containing the base analogue 5-ethynyl-2′-deoxyuridine (EdU; 5 μmol/L). EdU incorporation was analyzed by the use of a EdU flow cytometry kit (BCK-FC488, baseklick) after fixing the cells and co-staining the DNA with propidium iodide (PI; Sigma-Aldrich) according to the manufacturer's instructions. EdU-specific fluorescence and PI fluorescence were measured by flow cytometry (FACS Calibur, Becton Dickinson; 488 nm excitation wavelength) in fluorescence channel FL-1 (log scale, 515–545 nm emission wavelength) and FL-3 (linear scale, >670 nm emission wavelength), respectively. In additional experiments, T98G cells were preincubated (30 minutes),

Downloaded from mcr.aacrjournals.org on October 8, 2015. © 2015 American Association for Cancer Research.

Published OnlineFirst June 3, 2015; DOI: 10.1158/1541-7786.MCR-15-0075

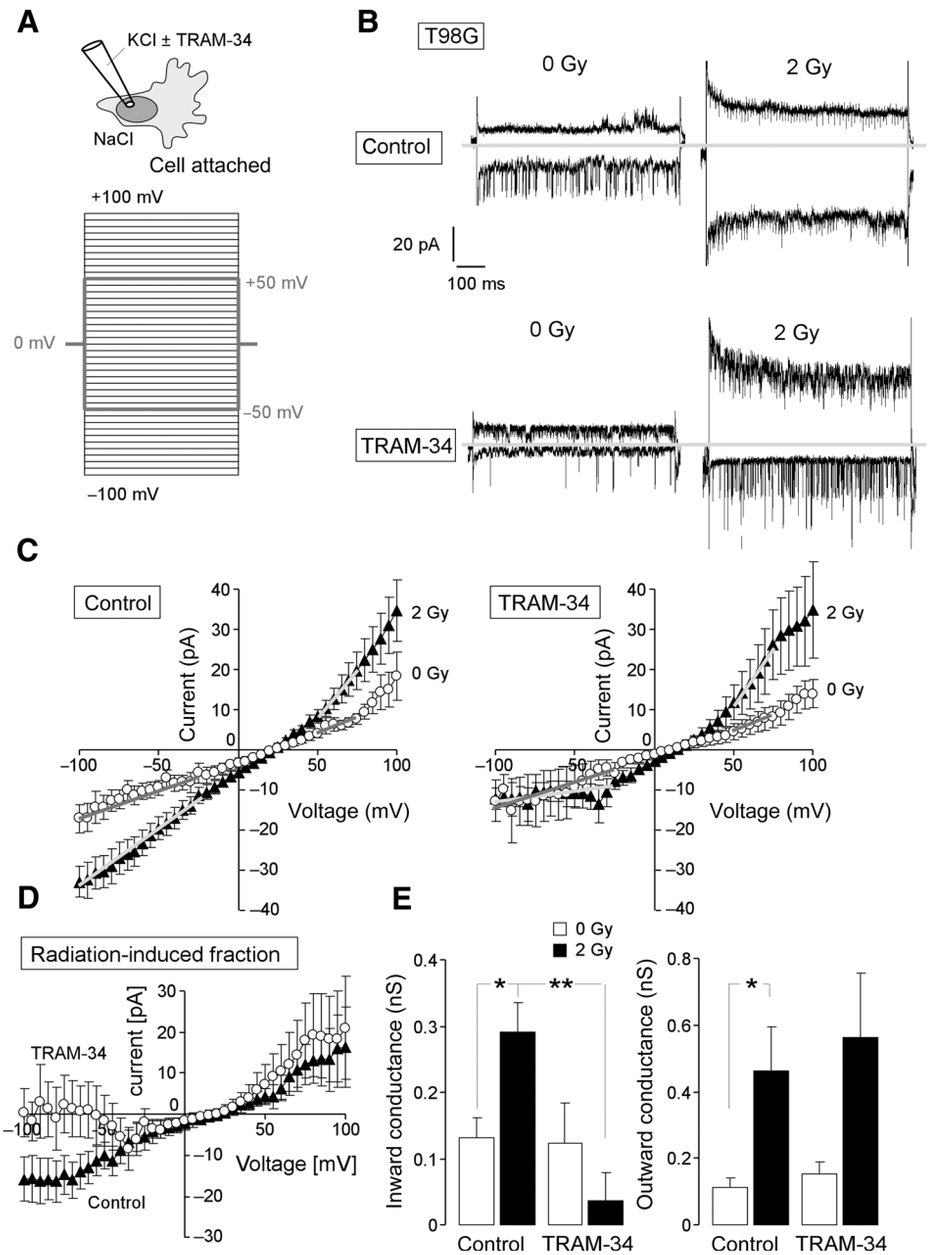

Figure 2.
IR increases the activity of IK K^+ channels. A, experimental setup: macroscopic on-cell currents were recorded from control and irradiated T98G cells with KCl pipette and NaCl bath solution applying the depicted pulse protocol. Currents obtained in the presence and absence of the IK channel inhibitor TRAM-34 (10 μmol/L) were compared between unpaired experiments. B, macroscopic on-cell current tracings recorded during voltage square pulses to −50 and +50 mV, respectively (as shown by the gray pulse protocol in A) from control (left) and irradiated (2 Gy) T98G cells with (lower traces) and without (upper traces) TRAM-34 in the pipette solutions. Note that the prominent single-channel current deflections are generated by BK K^+ channels, which are also activated by IR as reported (ref. 21; also evident from E, right). C, dependence of the mean macroscopic on-cell currents (±SE) on holding potential in control (open circles) and 2 Gy–irradiated T98G cells (2.5–5.5 hours after irradiation, closed triangles) recorded in the absence (left, $n = 26$–28) and presence (right, $n = 8$–9) of TRAM-34 in the pipette. D, mean (±SE) radiation-induced current fractions as calculated from the data in C for control (closed triangles) and TRAM-34-treated (open circles) T98G cells. E, mean (± SE) inward (left) and outward (right) conductance as calculated from the data in C by linear regression (voltage ranges are indicated by gray lines) for control (open bars) and irradiated (closed bars) T98G cells recorded in the absence (first and second bars) or presence of TRAM-34 (third and fourth bars; ** and * indicate $P \leq 0.01$ and $P \leq 0.05$, respectively, Kruskal–Wallis nonparametric ANOVA test).

irradiated (0, 2, 4, or 6 Gy), and incubated for further 24 or 48 hours in RPMI-1640/10% FCS medium additionally containing either TRAM-34 (10 μmol/L) or vehicle alone (0.1% DMSO). For cell-cycle analysis, cells were permeabilized and stained (30 minutes at room temperature) with PI solution (containing 0.1% Na citrate, 0.1% Triton X-100, 10 μg/mL PI in PBS), and the DNA amount was analyzed by flow cytometry in fluorescence channel FL-3 (linear scale). Data were analyzed with the FCS Express 3 software (De Novo Software).

γH2AX foci formation

T98G cells cultured on CultureSlides (Becton Dickinson) in RPMI-1640/10% FCS medium were irradiated (0 or 2 Gy) post-incubated for 24 hours in the presence of TRAM-34 (10 μmol/L) or vehicle alone (0.1% DMSO) and fixed with 70% ice-cold ethanol. For immunofluorescent analysis, cells were incubated with anti-γH_2AX antibody (Upstate, Millipore; clone JBW301; 1:500) at room temperature for 2 hours. Positive foci were visualized by incubation with a 1:500 dilution of Alexa488-labeled goat anti–mouse serum (Molecular Probes) for 30 minutes. CultureSlides were mounted in Vectashield/DAPI (Vector Laboratories) and evaluated by conventional fluorescence microscopy.

IK shRNA

IK was downregulated in T98G cells by stable transfection with IK-specific and—for control—nontargeting shRNA using MISSION pLKO.1 lentiviral transduction particles

Downloaded from mcr.aacrjournals.org on October 8, 2015. © 2015 American Association for Cancer Research.

Published OnlineFirst June 3, 2015; DOI: 10.1158/1541-7786.MCR-15-0075

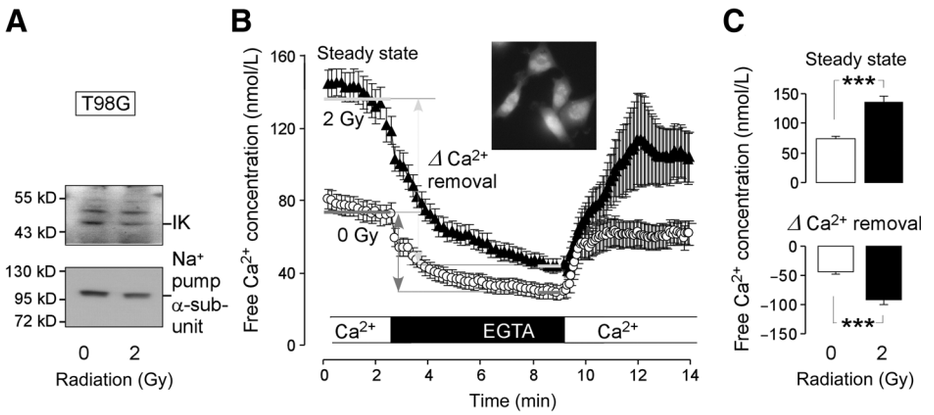

Figure 3.

IR modulates the cytosolic free Ca^{2+} concentration (i[Ca^{2+}]$_{free}$) but not the surface expression of IK channels in T98G cells. A, immunoblots of surface proteins from control (0 Gy) and irradiated T98G cells (2 Gy) probed against IK (top) and for loading control against the α_1 subunit of the Na^+ pump (bottom). B, time course of the mean (±SE) cytosolic free Ca^{2+} concentration (i[Ca^{2+}]$_{free}$) as measured by ratiometrical fura-2 Ca^{2+} imaging 3 to 5 hours after irradiation with 0 Gy (open circles; $n = 32$) or 2 Gy (closed triangles $n = 24$) during removal and re-addition of external Ca^{2+}. C, mean (±SE) steady-state i[Ca^{2+}]$_{free}$ (top, as indicated by gray lines at the beginning of the records in B) and mean (±SE) decrease in i[Ca^{2+}]$_{free}$ (bottom) upon removal of extracellular Ca^{2+} (as indicated by the gray arrows in B) in control (open bars) and irradiated cells (data from B; ***, $P \leq 0.001$, two-tailed t test).

(SHCLNV-NM_002250 and SHC002V, Sigma-Aldrich) according to the provided experimental protocol. Downregulation of IK was controlled by quantitative RT-PCR and immunoblotting (Fig. 7A and B).

Quantitative RT-PCR

mRNAs of stably transfected T98G cells were isolated (Qiagen RNA extraction kit) and reversely transcribed in cDNA (Transcriptor First Strand cDNA Synthesis Kit, Roche). IK K^+ channel and GAPDH-specific fragments were amplified by the use of SYBR Green–based quantitative real-time PCR (QT00003780 and QT01192646 QuantiTect Primer Assay and QuantiFast SYBR Green PCR Kit, Qiagen) in a Roche LightCycler Instrument.

Colony formation assay

To test for clonogenic survival, U87MG, parental T98G, and stably transfected T98G cells (clones #2 and #3) were irradiated (0, 2, 4, or 6 Gy) in RPMI-1640/10% FCS medium additionally containing TRAM-34 (10 μmol/L) or vehicle alone (0.1% DMSO). After 24 hours of incubation with the inhibitor/vehicle, cells were detached, 200 to 800 cells were reseeded in inhibitor-free medium on 3-cm wells and grown for further 2 to 3 weeks. The plating efficiency was defined by dividing the number of colonies by the number of plated cells. Survival fractions as calculated by dividing the plating efficiency of the irradiated cells by those of the unirradiated controls were fitted by the use of the linear quadratic equation.

Ectopic mouse model of human glioblastoma

All experiments were performed according to the German Animal Protection Law and approved by the local authorities (RP Tübingen, reference number PZ3/13). Human U87MG cells (500,000 cells in 100 μL PBS) were injected subcutaneously in the upper outer right hind limb of 8-week-old female $NMRI^{Nu/Nu}$ mice. Tumor growth was monitored at least 3 times per week by measuring tumor size in 3 dimensions using calipers. Upon reaching a tumor volume of around 150 μL, mice were randomly assigned to 4 treatment arms (control, fractionated radiation, TRAM-34, and TRAM-34 combined with fractionated radiation). Beginning with day 0, tumors were locally irradiated under isoflurane anesthesia at room temperature with 5 consecutive daily fractions of 0 (control) or 4 Gy 6 MV photons as described (23). Six hours before each radiation fraction, mice received intraperitoneal injections of the IK channel inhibitor TRAM-34 (0 or 120 mg/kg body weight in Mygliol). The drug TRAM-34 at the applied dose and local fractionated irradiation of the ectopic glioblastoma was well tolerated by the mice.

Querying TGCA datasets

Via the cBIOportal Web resource (24, 25), the provisional Glioblastoma-Multiforme and Lower-Grade-Glioma TCGA databases (http://cancergenome.nih.gov/) were queried for IK mRNA abundance of the tumor specimens and PFS of the patients with glioma. In lower grade glioma and glioblastoma, 14 to 22 of 116 to 346 tumor specimens with RNA Seq V2 mRNA data exhibited an IK mRNA abundance greater than a certain threshold. A threshold of the mean expression value + 2/3 z-score was used for both low-grade glioma and glioblastoma to define middle-rate and high IK mRNA abundance. The z-score of the IK mRNA abundance in an individual glioma specimen is calculated by the number of SDs the individual mRNA abundance differing from the mean value of all gliomas tumors that are diploid for the IK gene. In Fig. 9, PFS and OS of a low number of patients (n = 14–21) with tumors that exhibit an elevated IK mRNA abundance (i.e., above the mean value + 2/3 z-score) was compared with the majority of patients (n = 102–325) with gliomas that exhibit "middle-rate" IK mRNA abundance (i.e., varying within mean value ± 2/3 z-score). Statistical analysis was performed with the log-rank test.

Results

To assess IK protein expression in the embryonic astrocyte cell line SVGA and the glioblastoma cell lines T98G, exponential growing cells were fixed, immunostained with an IK-specific antibody or an IgG isotype control antibody, and analyzed by fluorescence microscopy. Figure 1A suggests higher IK protein abundance in T98G than in SVGA cells. To estimate the

Downloaded from mcr.aacrjournals.org on October 8, 2015. © 2015 American Association for Cancer Research.

Published OnlineFirst June 3, 2015; DOI: 10.1158/1541-7786.MCR-15-0075

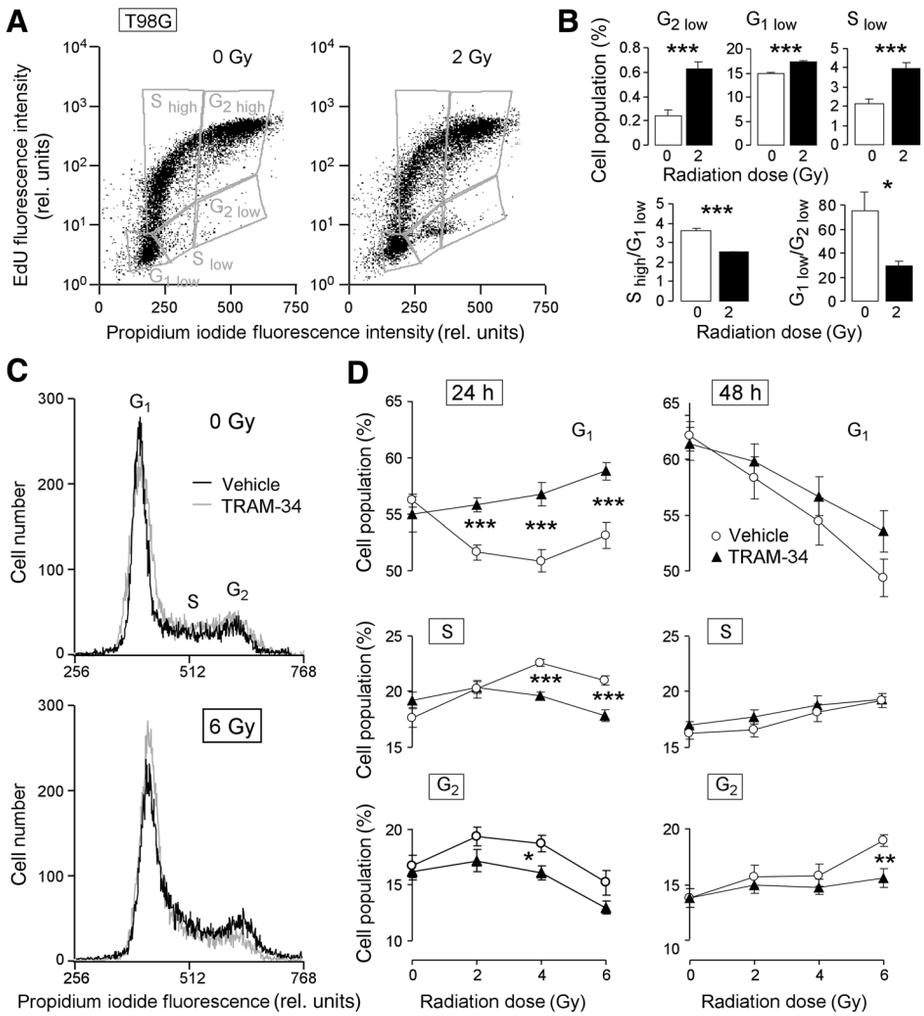

Figure 4.
The IK channel inhibitor TRAM-34 modifies cell-cycle control in irradiated T98G cells. A, dot blots showing EdU incorporation by irradiated (0 or 2 Gy as indicated) T98G cells. Immediately after irradiation cells were incubated for 6 hours with EdU (5 μmol/L) before co-staining with PI and analysis by flow cytometry. Gray gates show the different cell populations. B, mean percentage (±SE, $n = 6$) of irradiated (0 or 2 Gy) EdU-negative T98G cells arrested in G_2, G_1, or S phase of cell cycle (top line). Mean ratios (±SE, $n = 6$) of EdU-positive S-phase and EdU-negative G_1 phase populations (S_{high}/G_{1low}) as well as of EdU-negative G_1 and G_2 populations ($G_{1low}/G_{2\ low}$) in irradiated (0 or 2 Gy) cells as a measure of G_1–S transition and mitosis, respectively (bottom line). C, histograms of PI-stained T98G cells (Nicoletti protocol) recorded by flow cytometry 48 hours after IR with 0 Gy (top) or 6 Gy (bottom). Cells were preincubated (0.5 hours), irradiated, and postincubated in the absence (control, black line) or presence of TRAM-34 (10 μmol/L, gray line). D, mean percentage (±SE, $n = 9$) of irradiated (0, 2, 4, or 6 Gy) T98G cells residing 24 hours (left) or 48 hours (right) after IR in G_1 (top line), S (middle line), or G_2 phase of cell cycle (bottom line). Cells were pre- and postincubated as in A with vehicle alone (open circles) or with 10 μmol/L TRAM-34 (closed triangles; ***, **, and * indicate $P \leq 0.001$, $P \leq 0.01$, and $P \leq 0.05$, respectively, two -tailed (Welch-corrected) t test).

functionality of IK K^+ channels in SVGA, T98G, and a further glioblastoma cell line (U87MG), currents through the plasma membrane were recorded with the patch-clamp technique in whole-cell mode with physiologic bath and pipette solutions. Records were obtained before and after Ca^{2+} permeabilizing the plasma membrane with the Ca^{2+} ionophore ionomycin (2.5 μmol/L). To characterize the Ca^{2+}-stimulated current fraction, the BK K^+ channel inhibitor paxilline (5 μmol/L) and/or the IK K^+ channel inhibitor TRAM-34 (1 μmol/L) were added sequentially to the ionomycin-containing bathing solution. In SVGA astrocytes, ionomycin failed to induce outwardly rectifying whole-cell currents at voltages more negative than −20 mV in 6 of 6 tested cells suggestive of the absence of functional IK channel in the plasma membrane. Accordingly, bath application of TRAM-34 did not inhibit a fraction of the whole-cell currents. A representative experiment is depicted in Fig. 1B and C.

In sharp contrast, ionomycin activated a whole-cell outward current in T98G cells at all voltages more positive than K^+ equilibrium potential ($E_K \approx -90$ mV; Fig. 1D and E, open triangles). Paxilline inhibited about 80% of the outward current in Ca^{2+}-permeabilized T98G cells (Fig. 1D and E, gray filled triangles). Additional application of TRAM-34 blocked almost all of the remaining paxilline-insensitive current fraction (Fig. 1D and E, black filled triangles). This TRAM-34-sensitive current fraction (Fig. 1F) exhibited inward rectification with a conductance density of about 100 pS/pF at negative voltages and had a reversal potential close to E_K. Together, these data indicate functional expression of a Ca^{2+}-activated, inwardly rectifying K^+-selective and TRAM-34–sensitive current fraction, which is characteristic for an IK current (26) in T98G glioblastoma cells but not in the astrocyte cell line. Ca^{2+}-permeabilized U87MG cells showed similarly high IK channel activity albeit having lower paxilline-sensitive currents (data not shown).

To test whether IR induces changes in IK channel activity, T98G cells were irradiated with 2-Gy 6-MV photons by the use of a linear accelerator, postincubated for 2 to 6 hours, and recorded in cell-attached mode using a KCl solution in the pipette (Fig. 2A). IR stimulated an increase in the inward and outward fraction of the macroscopic cell–attached currents (Fig. 2B, top, and C, left). Importantly, when in unpaired experiments the IK channel inhibitor TRAM-34 (10 μmol/L) was added to the pipette solution (Fig. 2B, bottom, and C, right), an IR-stimulated inward current was no more detectable (Fig. 2C and D) indicative of an IR-stimulated IK current.

Reportedly, IR may modulate the Ca^{2+} signaling (for review, see ref. 15). To define signaling events upstream of IK channel

Downloaded from mcr.aacrjournals.org on October 8, 2015. © 2015 American Association for Cancer Research.

Published OnlineFirst June 3, 2015; DOI: 10.1158/1541-7786.MCR-15-0075

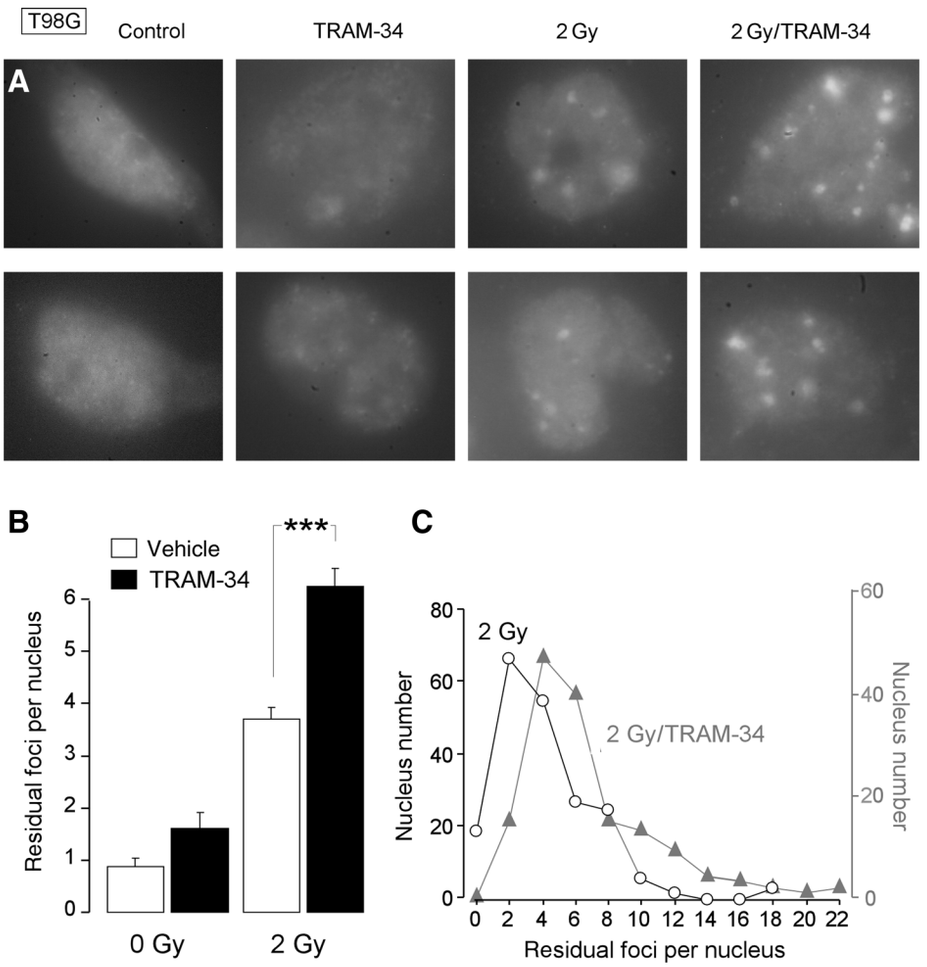

Figure 5.
IK channel inhibition increases the number of residual γH_2AX foci in T98G cells. A, immunofluorescent micrographs of T98G nuclei double-stained against γH_2AX and DNA (DAPI). Cells were fixed 24 hours after irradiation (0 or 2 Gy) and preincubation with TRAM-34 (0 or 10 μmol/L) as indicated. B, mean (±SE, $n = 30$–60 for 0 Gy and 150–200 for 2 Gy) numbers of residual γH_2AX foci per nucleus 24 hours after irradiation (0 or 2 Gy) and incubation with TRAM-34 (10 μmol/L) or vehicle. C, histograms of irradiated (black) and irradiated and TRAM-34–treated cells (gray, data from B) showing the distribution of residual γH_2AX foci counts (***, $P \leq 0.001$, Kruskal–Wallis nonparametric ANOVA test).

activation, cytosolic free Ca^{2+} concentration ($i[Ca^{2+}]_{free}$) was assessed by fura-2 Ca^{2+} imaging experiments in control and irradiated (2 Gy) T98G cells 3 to 5 h after IR. In addition, IK surface expression was analyzed in control and irradiated T98G cells by immunoblots of biotinylated and avidin-separated surface proteins probed against IK and—for loading control—against the α_1 subunit of the Na^+ pump. As shown in Fig. 3, the IR-induced increase in IK activity in T98G was probably due to IR-induced increase in $i[Ca^{2+}]_{free}$ (Fig. 3B and C) rather than to an elevated surface expression of IK channels (Fig. 3A). IR (2 Gy) induced a significant increase in steady-state $i[Ca^{2+}]_{free}$ (Fig. 3B and C, top). Upon removal and re-addition of extracellular Ca^{2+}, irradiated cells showed a larger drop-down and larger re-increase of $i[Ca^{2+}]_{free}$, respectively, as compared with unirradiated cells (Fig. 3B and C, bottom). This suggests that a shift in the Ca^{2+} leak/pump equilibrium of the plasma membrane accounted for the observed IR-induced $i[Ca^{2+}]_{free}$ increase.

K^+ channels have been shown to regulate the cell cycle in irradiated tumor cells (27). Therefore, we analyzed by flow cytometry, the incorporation of the base analogue EdU by irradiated (0 or 2 Gy) T98G cells within the first 6 hours after IR. Figure 4A shows the incorporated EdU in dependence on the DNA amount as defined by co-staining of the cells with PI as DNA-specific fluorescence dye. IR increased the cell populations residing in G_1, S, and G_2 phase in cell cycle with low EdU-specific fluorescence intensity (i.e., cells that did not incorporate EdU, Fig. 4B, top line). This points to an IR-induced G_1, S, and G_2–M arrest in T98G cells. In particular, IR decreased the ratios between cells in the S-phase that incorporated EdU (S_{high}) and the $G_{1\ low}$ population on the one hand and between the $G_{1\ low}$ and the $G_{2\ low}$ populations on the other (Fig. 4B, bottom line) indicative of a profound inhibition of G_1–S transition and mitosis in irradiated T98G cells.

To test for a function of IK channels in cell-cycle control, the effect of IR (0, 2, 4, or 6 Gy) in combination with IK inhibition by TRAM-34 on cell-cycle distribution of T98G cells was analyzed 24 and 48 hours after IR by PI staining in flow cytometry (Fig. 4C). Twenty-four hours after IR with 2 and 4 Gy, the G_1 population was decreased and the S and G_2 increased as compared to 0-hour values (open circles in Fig. 4D, left). This suggests that the G_1 arrest observed in the EdU incorporation experiments was short-living. In contrast, 24 hours after IR with 6 Gy, the accumulation in S and G_2 phase of cell cycle was blunted as compared with 2 or 4 Gy–irradiated cells suggestive of a sustained G_1 arrest induced in a fraction of cells at higher dose (open circles in Fig. 4D, left). However, 48 hours after IR, number of G_1 and G_2 residing cells decreased and increased, respectively, more or less linearly with increasing IR dose (open circles in Fig. 4B and D, right),

Downloaded from mcr.aacrjournals.org on October 8, 2015. © 2015 American Association for Cancer Research.

Published OnlineFirst June 3, 2015; DOI: 10.1158/1541-7786.MCR-15-0075

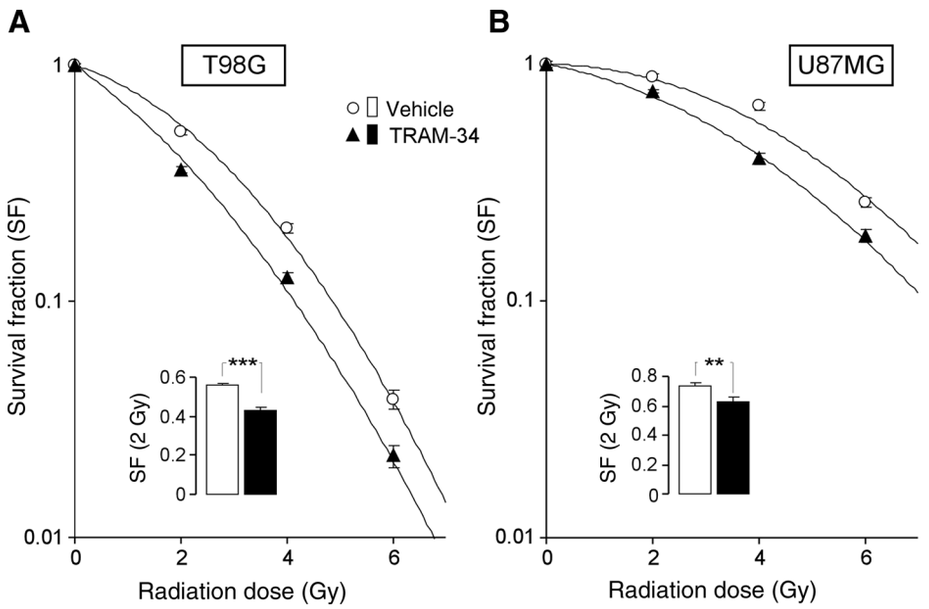

Figure 6.
IK inhibition radiosensitizes T98G and U87MG glioblastoma cells. A and B, mean survival fraction (±SE, $n = 8$) of irradiated (0, 2, 4, or 6 Gy) T98G (A) and U87MG cells (B). Cells were irradiated and postincubated (24 hours) in the presence of vehicle alone (open circles) or TRAM-34 (10 μL, closed triangles) before plating in inhibitor-free medium. The insets show the mean survival fractions (±SE, $n = 24$) upon irradiation with 2 Gy (SF_{2Gy}) in vehicle alone (open bars) and TRAM-34 (10 μmol/L, closed bars)-containing medium from a higher number of experiments (** and *** indicate $P \leq 0.01$ and $P \leq 0.001$, respectively, two-tailed t test).

confirming the transitory nature of the G_1 arrest. Importantly, the IK channel blocker TRAM-34 (10 μmol/L) delayed or even prevented the radiation-induced decrease of cell population in G_1 and accumulation in G_2 (Fig. 4D, closed triangles). Together, the data indicate functional significance of IK channels in cell-cycle control. Because only little effect of TRAM-34 on cell-cycle distribution was apparent in unirradiated cells (0 Gy in Fig. 4D), IK channels seem to regulate cell-cycle predominantly in cells undergoing genotoxic stress.

Next, we estimated the number of residual DNA double-strand breaks in T98G cells 24 hours after IR with 0 or 2 Gy by counting the γH_2AX foci in immunofluorescent micrographs (Fig. 5A). As shown in Fig. B (right), TRAM-34 (10 μmol/L) significantly increased the mean number of residual γH_2AX foci per nucleus from about 4 (vehicle control) to 6 (TRAM-34) 24 hours after IR with 2 Gy. Thereby, foci numbers seemed to be similarly elevated in nuclei with low, intermediate, and high foci counts as compared with the respective vehicle controls giving rise to a TRAM-34–induced right shift of the foci count/nucleus number histogram depicted in Fig. 5C. This right shift might be explained by a delay in DNA double-strand break repair in TRAM-34–treated cells.

Unirradiated cells showed a tendency of increased foci formation when incubated for 24 hours with TRAM-34 (Fig. 5B, left) that might hint to a genotoxic effect of TRAM-34. However, TRAM-34 (10 μmol/L) did not decrease the plating efficacy (0.25 ± 0.001, $n = 36$) when compared with the vehicle control (0.23 ± 0.001, $n = 36$) in delayed plating colony formation assays. Similarly, TRAM-34 did not decrease the plating efficacy of U87MG cells (0.56 ± 0.01 vs. 0.51 ± 0.01, $n = 36$), indicating that IK channel blockade does not impair the clonogenic survival of unirradiated glioblastoma cells. In irradiated T98G (Fig. 6A) and U87MG cells (Fig. 6B), in sharp contrast, TRAM-34 significantly decreased clonogenic survival with a radiosensitizer enhancement factor of about 1.4 (T98G) and 1.3 (U87MG) as determined for the survival fraction of 0.5. This suggests similar radiosensitizing effects of TRAM-34 in 2 human glioblastoma cell lines that differ in radiosensitivity (survival fractions at 2 Gy, SF_{2Gy}, of T98G and U87MG cells were $SF_{2Gy} = 0.56 \pm 0.01$ and $SF_{2Gy} = 0.74 \pm 0.02$, respectively; compare open bars in the insets of Fig. 6A and B).

To proof the IK specificity of the observed TRAM-34 effect on clonogenic survival, we knocked down IK channels in T98G cells by a lentiviral transduction with IK-specific and control shRNAs containing particles (Fig. 7A and B). The IK-depleted T98G clone #3 showed a higher percentage of cells residing in G_1 phase of cell cycle in flow cytometry than in the T98G control clone #2 suggestive of differing doubling times of the 2 clones. Within 24 hours, IR dose dependently and similarly decreased the fraction of cells residing in G_1 in both clones (Fig. 7C, left) and increased the population of cells accumulating in G_2 (Fig. 7C, right). Remarkably, TRAM-34 virtually abolished the IR-induced changes in cell-cycle distribution in the control clone #2 but had no apparent effect on IK-depleted clone #3.

To estimate whether the observed IK-mediated cell-cycle control in irradiated T98G cells might be required for DNA repair, we determined the number of residual γH_2AX foci in both T98G clones 24 hours after IR with 0 or 2 Gy. As shown in Fig. 7D and E, the IK-depleted clone #3 exhibited higher number of basal (0 Gy) and residual γH_2AX foci as compared with the control clone #2 suggestive of an impairment of DNA repair by IK knockdown. To test this assumption, the radioresistance of both clones was determined by delayed plating colony formation assay.

As a result, both T98G clones were more radioresistant than the parental T98G cell line (compare open circles in Fig. 7F and Fig. 6A). Notably, the IK-depleted clone #3 was significantly more radiosensitive ($SF_{2Gy} = 0.74 \pm 0.03$, $n = 12$) than the control clone #2 ($SF_{2Gy} = 0.83 \pm 0.02$, $n = 12$; $P = 0.02$, Welch-corrected two-tailed t test). Most importantly, TRAM-34 radiosensitized only the control clone #2 (Fig. 7F, left) but, again, had no effect on the IK-depleted clone #3 (Fig. 7F, right). Combined, these data indicate both IK-mediated radioresistance in human glioblastoma cell lines and target specificity of the IK channel blocker TRAM-34.

To test whether IK channel targeting may increase the efficacy of fractionated radiation in an *in vivo* ectopic glioblastoma mouse model, immunocompromised nude mice were challenged with

Downloaded from mcr.aacrjournals.org on October 8, 2015. © 2015 American Association for Cancer Research.

Published OnlineFirst June 3, 2015; DOI: 10.1158/1541-7786.MCR-15-0075

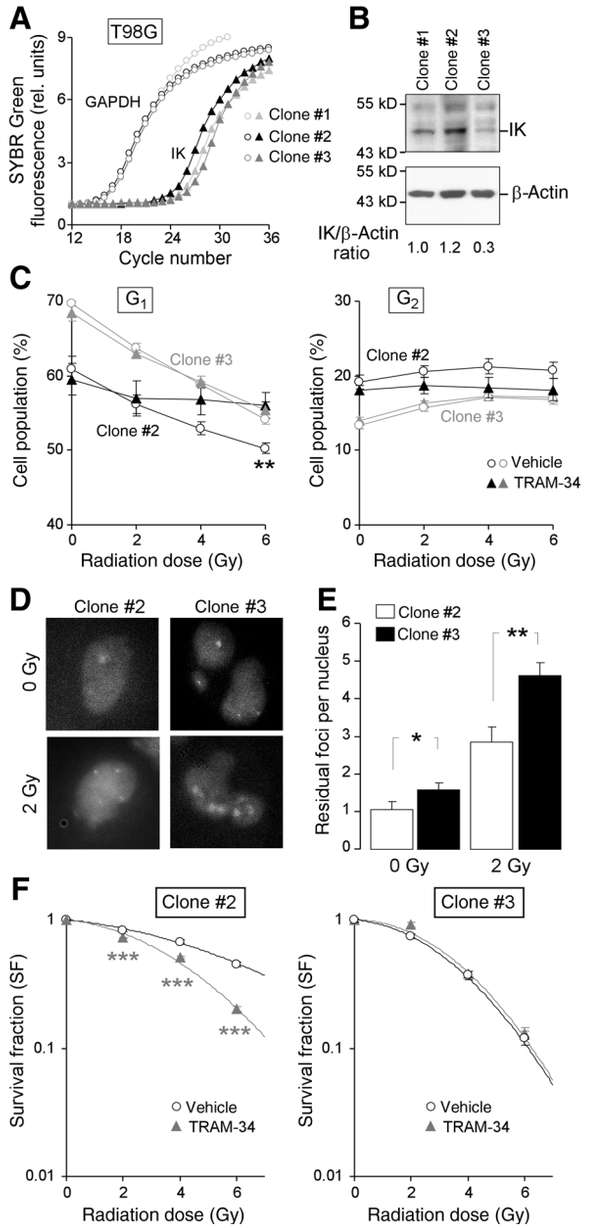

Figure 7.

TRAM-34 has no effect in IK-silenced T98G cells. A and B, abundances of IK mRNA and protein in T98G clones expressing control shRNAs (clones #1 and #2) and IK-specific shRNA (clone #3) as analyzed by quantitative RT-PCR (A) and immunoblotting (B). GAPDH served as housekeeper mRNA (A) and β-actin as loading control (B). C, mean percentage (±SE, $n = 9$) of irradiated (0, 2, 4, or 6 Gy) clone #2 (black) and clone #3 (gray) cells residing 48 hours after IR in G_1 (left) or G_2 phase of cell cycle (right). Cells were pre- and postincubated with vehicle alone (open circles) or with 10 μmol/L TRAM-34 (closed triangles). D, immunofluorescent micrographs of nuclei from T89G clone #2 (left) and clone #3 (right) double-stained against γH2AX and DNA (DAPI). Cells were fixed 24 hours after irradiation with 0 Gy (top) or 2 Gy (bottom) as indicated. E, mean (±SE, $n = 86$–199) numbers of residual γH2AX foci per nucleus of clone #2 (open bars) and clone #3 T98G cells (closed bars) 24 hours after irradiation with 0 (left) or 2 Gy (right). * and **, $P \leq 0.05$ and $P \leq 0.01$, respectively, Kruskal–Wallis nonparametric ANOVA test. F, mean survival fractions (±SE, $n = 12$) of clone #2 (left) and clone #3 (right) after irradiation with 0, 2, 4, or 6 Gy and combined treatment with TRAM-34 (10 μmol/L, filled triangles) or vehicle alone (open circles) as determined by delayed plating colony formation assay: plating efficacies were 0.31, 0.29, 0.18, and 0.14 for vehicle-treated clone #2, TRAM-34–treated clones #2, vehicle-treated clone #3, and TRAM-34–treated clones #3, respectively (*** and **, $P \leq 0.001$ and $P \leq 0.02$, respectively, two-tailed Welch-corrected t test).

human U87MG glioblastoma cells. When the ectopic glioblastoma has reached a volume of around 150 μL (Fig. 8A), mice were allocated to 4 treatment arms [control, $n = 5$; TRAM-34, $n = 4$; fractionated IR (fIR), $n = 9$; and TRAM-34/fIR, $n = 6$]. Figure 8B and C shows the tumor volume (V_t), normalized to the respective tumor volume at the start of treatment on day 0 (V_0), before, during (arrows), and after treatment with fIR (5×0 or 5×4 Gy) and TRAM-34 injections (5×0 or 5×120 mg/kg body weight) 6 hours prior to each IR fraction. One of 6 mice treated with combined fIR/TRAM-34 and 2 of 9 mice treated with fIR alone showed complete tumor remission. One of the latter did even not progress during treatment and could not be included in the calculation of the time to progression (i.e., the period between treatment start on day 0 and the time when the treated glioblastomas exceeded the initial volume, V_0). This time to progression is given for all treatment groups in Fig. 8 demonstrating that only the IR/TRAM-34 group exhibited significant longer time-to-progression periods than the control group.

The exponential growth of the ectopic glioblastoma can be illustrated by the linear relationship between the mean (±SE) logarithmized tumor volume [$\ln(V_t/V_0)$] and the time as depicted for the 4 treatment groups in Fig. 8E and F. The slope of these relationships [$\delta_{(\ln(Vt/V0)}/\delta_t$] as a measure of the exponential growth kinetics before and during the treatment as well as the treatment induced slope decline [$\Delta\delta_{(\ln(Vt/V0)}/\delta_t$] are given for the individual tumors in all 4 treatment groups in Fig. 8G–I. Only the fIR/TRAM-34 group showed a significant treatment-induced decrease in exponential growth as compared with the control group (Fig. 8I). Together, these *in vivo* experiments suggest both that TRAM-34 can be applied at pharmacologically relevant doses and that concomitant TRAM-34 chemotherapy may increase the efficacy of fractionated radiation therapy *in vivo*.

To explore the potential function of IK channels for the glioblastoma therapy resistance observed in the clinic, TCGA was queried using the provisional open access Glioblastoma-Multiforme and Lower-Grade-Glioma databases. As shown in Fig. 9, high IK mRNA abundance is associated with a shorter PFS (Fig. 9A) and OS (Fig. 9B) of patients with lower grade glioma and shorter OS (but not PFS, Fig. 9C) of patients with glioblastoma (Fig. 9D).

Discussion

The present study demonstrates IR-induced Ca^{2+} signaling and activation of Ca^{2+}-activated intermediate conductance IK K^+ channels in glioblastoma cells. The IR-stimulated IK channels, in turn, contribute to the stress response of the glioblastoma cells probably by adjusting the cell cycle. This IK channel-mediated stress response is required for the survival of the irradiated glioblastoma cells as evident from the fact that pharmacologic blockade of the IK channels radiosensitized the glioblastoma cells. In an astrocyte cell line, in contrast, functional IK channels were not apparent.

Downloaded from mcr.aacrjournals.org on October 8, 2015. © 2015 American Association for Cancer Research.

Published OnlineFirst June 3, 2015; DOI: 10.1158/1541-7786.MCR-15-0075

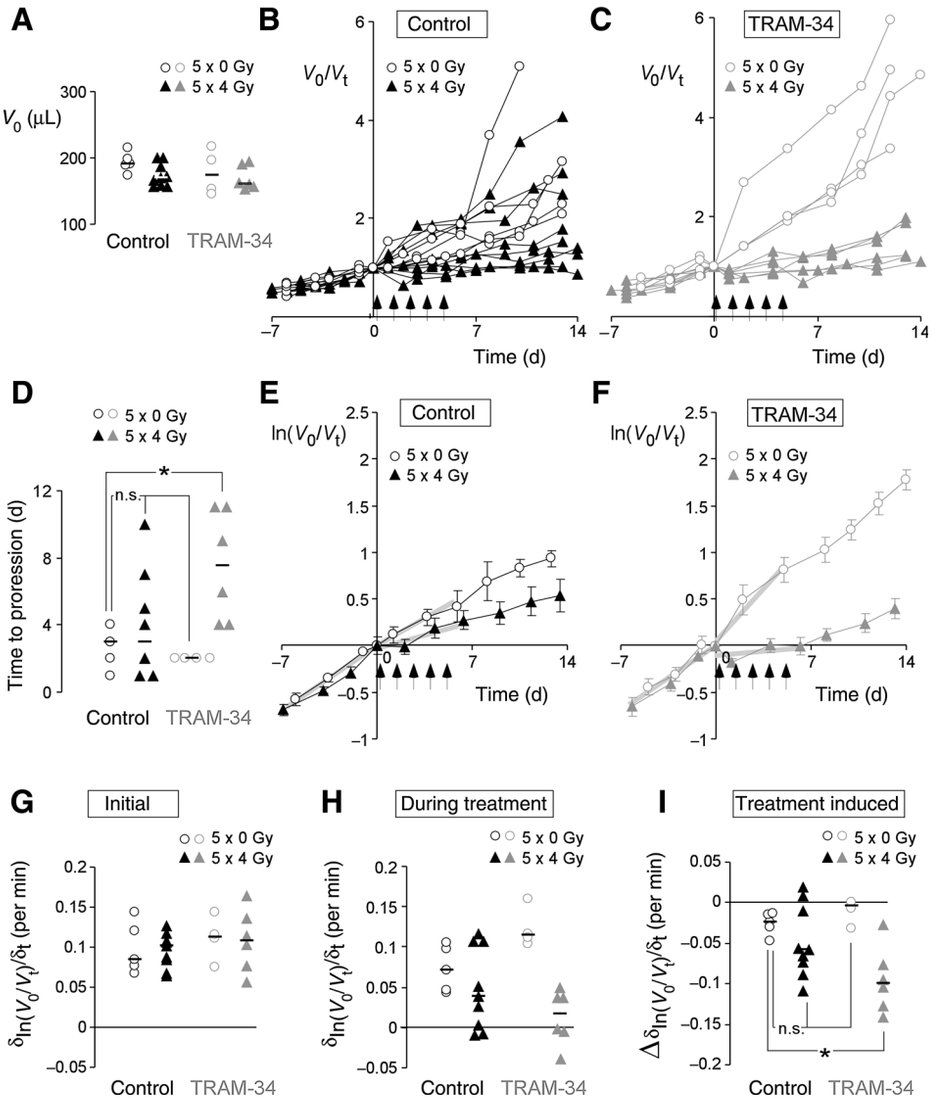

Figure 8.
TRAM-34 application concomitant to fractionated radiation delays ectopic tumor growth in the upper right hind limb of mice. A, volumes of ectopic human U87MG glioblastoma in immunocompromised nude mice at treatment start (day 0). B and C, time-dependent increase in normalized tumor volume (V_t/V_0). Tumors were irradiated with 5 fractions of 0 (open circles) or 4 Gy (closed triangles) on days 0 to 4. On these days, 0 (black symbols) or 120 mg/kg body weight TRAM-34 (gray symbols) were injected intraperitoneally 6 hours prior to radiation (arrows). D, time-to-tumor progression in the 4 treatment groups (one mouse in the radiation group with complete tumor remission did not show tumor progression and was excluded). E and F, time-dependent increase in mean (±SE, $n = 4$–9) logarithmized normalized tumor volume [$\ln(V_t/V_0)$, data from B and C] in the 4 treatment groups. G and H, slope [$\delta_{(\ln(Vt/V0)}/\delta_t$] of the time-dependent increase in logarithmized normalized tumor volume as a measure of exponential tumor growth kinetics before (days −7 to 0, G) and during treatment (days 0 to 8, H). Slopes are indicated by the thick gray lines in E and F. I, treatment-induced changes of $\delta_{(\ln(Vt/V0)}/\delta_t$ (the black line in A, D, and G–I and * in D and I indicate the median and $P \leq 0.05$, ANOVA, respectively).

IR-induced modifications of Ca^{2+} signaling and/or K^+ channel activity have been reported by our group in different tumor entities such as lung adenocarcinoma (28), leukemia cells (27, 29), or glioblastoma (21). In lung adenocarcinoma, K^+ channels contribute to an elevated glucose uptake by the irradiated cells. Increased amounts of glucose are probably needed to counteract energy crisis caused by DNA damage and to provide the carbohydrates required for histone acetylation during DNA decondensation (30). In leukemia, IR-induced co-activation of both Ca^{2+}-permeable channels and K^+ channels gives rise to Ca^{2+} signals that induce cell-cycle arrest via CaMKII-mediated inhibition of the mitosis-promoting factor cdc2. Notably, pharmacologic K^+ channel blockade overrides cell-cycle arrest of irradiated leukemia cells resulting in radiosensitization (27).

In the present study, irradiated cells exhibited an elevated steady state $i[Ca^{2+}]_{free}$ that was almost as double as high as the resting $i[Ca^{2+}]_{free}$ of unirradiated cells (see Fig. 3B and C). Glioblastoma cells functionally express STIM1/Orai1 store-operated Ca^{2+} channels (31) as well as TRPC1 and TRPM8 Ca^{2+}-permeable nonselective cation channels (32, 33), which might be candidates for augmented Ca^{2+} entry pathways in irradiated cells. A contribution of TRPM8 to the IR-induced Ca^{2+} signaling is suggested by the fact that TRPM8 knockdown impairs radioresistance and migration of glioblastoma cell lines (own unpublished observations).

In glioblastoma, IR-induced activation of BK K^+ channels is associated with radiogenic hypermigration of the tumor cells (for review, see refs. 15, 16). Like BK, IK channels have been demonstrated to essentially contribute to the mechanics of serum-induced (34), bradykinin-induced (6), and CXCL12 (SDF-1)-induced glioblastoma cell migration (35). In accordance with these *in vitro* data is the observation that the IK inhibitor TRAM-34 blocks the brain infiltration by xenografted human glioblastoma cells in orthotopic mouse models (36).

High IK channel expression has been associated with upregulation of "stemness" markers (8), and the glioblastoma "stem" cells have been suggested to express a highly migratory phenotype and to be primarily responsible for brain invasion (37, 38). As a matter of fact, IK channels have been demonstrated to mediate the migration of neuronal precursor cells, so-called neuroblasts,

Downloaded from mcr.aacrjournals.org on October 8, 2015. © 2015 American Association for Cancer Research.

Published OnlineFirst June 3, 2015; DOI: 10.1158/1541-7786.MCR-15-0075

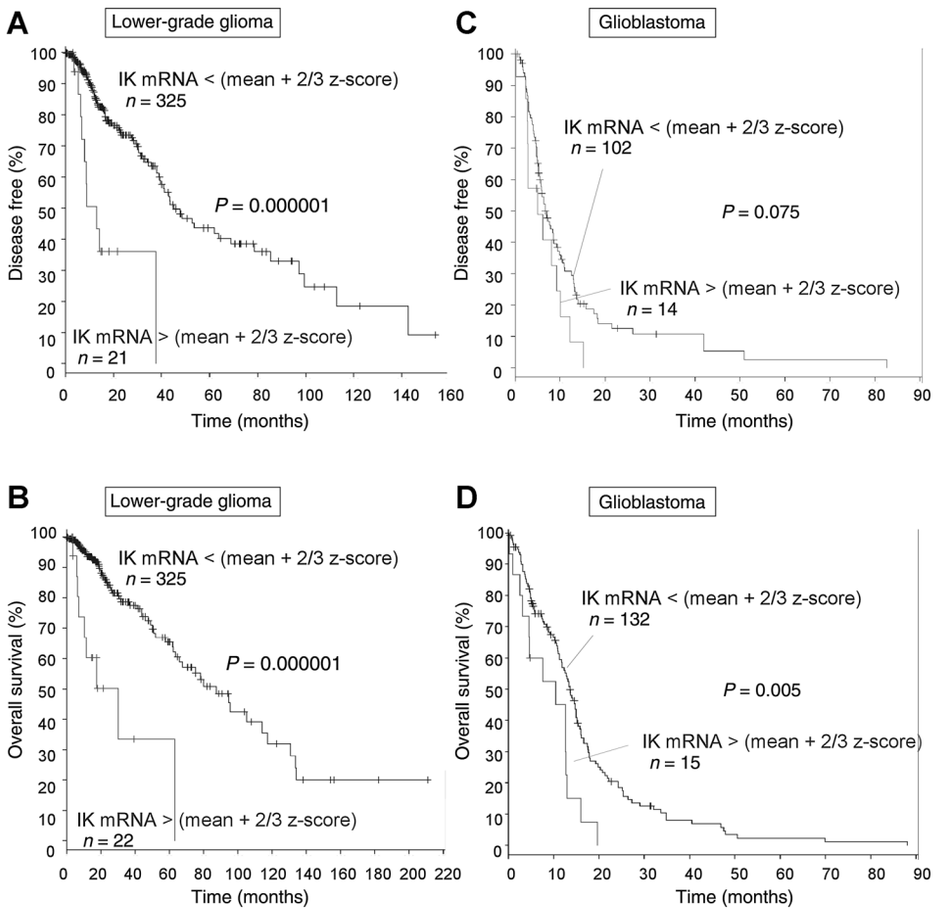

Figure 9.
IK mRNA abundance–dependent PFS (A, C) and OS (B, D) of patients with lower grade glioma (A, B) and glioblastoma (C, D). Data from TCGA. *P* values were calculated by the log-rank test.

along the rostral migratory stream to become interneurons in the olfactory bulb of normal adult mouse brain (39).

Glioblastoma "stem" cells are also thought to be more therapy-resistant than the bulk tumor mass of "differentiated" glioblastoma cells (for review, see ref. 15–17). The data of the present study on glioblastoma cell lines and on an ectopic mouse model suggest that IK channels may confer radioresistance besides promoting brain infiltration. Evidence for such an IK channel function in glioblastoma cells obtained *in vitro* has already been reported (20).

The potential dual function of IK channels for brain invasion and radioresistance of glioblastoma as suggested by the above-mentioned *in vitro* and animal studies might be reflected by recently reported retrospective clinical data. Querying the REMBRANDT patient gene data base of the National Cancer Institute has indicated an upregulation (1.5-fold greater than nontumor samples) of IK channel in more than 30% of the patients (10). Importantly, IK upregulation by the glioma correlates with a decreased survival of the patients (10). Likewise, querying the TCGA databases in the present study suggested that higher IK mRNA abundance in the glioma associates with shorter PFS (low-grade glioma) and OS (low-grade glioma and GBM) of patients with glioma. Subgroup analysis of the patients concerning, for example, tumor size, degree of surgical glioma resection, radiation therapy regimes, etc., could not be performed in the TCGA query and has not been reported in the REMBRANDT query (10), which limits the interpretation of the data. Nevertheless, provided that many patients of the databases received therapy regimes that comprise radiation therapy, the found associations might hint to a radioprotective function of IK channels in glioma.

IK channels might, therefore, become a highly attractive new target for anti-glioma therapy. IK channel targeting has been proposed for therapy of different diseases such as anemia (40, 41), in particular sickle cell anemia (42–45), Alzheimer disease (46), and various further inflammatory diseases (47). The TRAM-34 concentration (1–10 μmol/L) used in the present study is probably far above the plasma concentrations that might be reached in clinical trials. Senicapoc (ICA-17043), a further IK channel inhibitor, which is more potent than TRAM-34 ($IC_{50\text{-Senicapoc}}$, 11 nmol/L vs. $IC_{50\text{-TRAM-34}}$, 20 nmol/L), can be taken orally and has been shown to be safe in clinical trials (46). Moreover, a daily oral dose of 10-mg senicapoc resulted in mean plasma concentrations of 100 ng/mL (~0.3 μmol/L). Most importantly, senicapoc-containing plasma samples of the patients inhibited IK channels by up to 70% as assessed in tracer flux experiments (43). What is also important in this respect is the fact that GBM reportedly impairs the blood–brain barrier (BBB) by, for example, altering/replacing endothelial cells (48) and pericytes (49), suggesting that drugs like senicapoc or TRAM-34 may pass the BBB. In a mouse brain, a BBB passage of TRAM-34 could be directly demonstrated (36). Taken together, these data indicate that IK channel targeting is most probably feasible in a clinical setting. Higher drug levels at lower side effects might even be achieved in patients with glioblastoma by intracranial drug administration.

Downloaded from mcr.aacrjournals.org on October 8, 2015. © 2015 American Association for Cancer Research.

Published OnlineFirst June 3, 2015; DOI: 10.1158/1541-7786.MCR-15-0075

In conclusion, IK channels may promote beside a migratory and infiltrative phenotype also cellular radioresistance of glioblastoma cells. By doing so, IK channels contribute to those properties of GBM that most probably account for therapy failure associated with the very poor prognosis of patients. Importantly, pharmacologic IK channel targeting seems to be feasible in the clinic in combination with surgery and radiation therapy.

Disclosure of Potential Conflicts of Interest

No potential conflicts of interest were disclosed.

Authors' Contributions

Conception and design: D. Zips, K. Dittmann, P. Ruth, S.M. Huber
Development of methodology: B. Stegen, L. Butz, L. Klumpp, K. Dittmann, S.M. Huber
Acquisition of data (provided animals, acquired and managed patients, provided facilities, etc.): B. Stegen, L. Butz, L. Klumpp, S.M. Huber
Analysis and interpretation of data (e.g., statistical analysis, biostatistics, computational analysis): B. Stegen, L. Butz, D. Zips, P. Ruth, S.M. Huber
Writing, review, and/or revision of the manuscript: B. Stegen, L. Klumpp, D. Zips, S.M. Huber
Administrative, technical, or material support (i.e., reporting or organizing data, constructing databases): B. Stegen, L. Butz, S.M. Huber
Study supervision: P. Ruth, S.M. Huber

Acknowledgments

The authors thank Heidrun Faltin and Ilka Müller for excellent technical assistance.

Grant Support

This work was supported by a grant from the Wilhelm-Sander-Stiftung awarded to P. Ruth and S.M. Huber (2011.083.1). B. Stegen was supported by the DFG International Graduate School 1302 (TP T9 SH) and L. Klumpp by the Robert-Bosch-Stiftung as well as the ICEPHA program of the University of Tübingen.

Received February 11, 2015; revised April 28, 2015; accepted May 22, 2015; published OnlineFirst June 3, 2015.

References

1. Stupp R, van den Bent MJ, Hegi ME. Optimal role of temozolomide in the treatment of malignant gliomas. Curr Neurol Neurosci Rep 2005;5:198–206.
2. Evers P, Lee PP, DeMarco J, Agazaryan N, Sayre JW, Selch M, et al. Irradiation of the potential cancer stem cell niches in the adult brain improves progression-free survival of patients with malignant glioma. BMC Cancer 2010;10:384.
3. Fioretti B, Castigli E, Calzuola I, Harper AA, Franciolini F, Catacuzzeno L. NPPB block of the intermediate-conductance Ca2+-activated K+ channel. Eur J Pharmacol 2004;497:1–6.
4. Fioretti B, Castigli E, Micheli MR, Bova R, Sciaccaluga M, Harper A, et al. Expression and modulation of the intermediate- conductance Ca2+-activated K+channel in glioblastoma GL-15 cells. Cell Physiol Biochem 2006;18:47–56.
5. Fioretti B, Catacuzzeno L, Sforna L, Aiello F, Pagani F, Ragozzino D, et al. Histamine hyperpolarizes human glioblastoma cells by activating the intermediate-conductance Ca2+-activated K+ channel. Am J Physiol Cell Physiol 2009;297:C102–10.
6. Cuddapah VA, Turner KL, Seifert S, Sontheimer H. Bradykinin-induced chemotaxis of human gliomas requires the activation of KCa3.1 and ClC-3. J Neurosci 2013;33:1427–40.
7. Ishii TM, Silvia C, Hirschberg B, Bond CT, Adelman JP, Maylie J. A human intermediate conductance calcium-activated potassium channel. Proc Natl Acad Sci U S A 1997;94:11651–6.
8. Ruggieri P, Mangino G, Fioretti B, Catacuzzeno L, Puca R, Ponti D, et al. The inhibition of KCa3.1 channels activity reduces cell motility in glioblastoma derived cancer stem cells. PLoS One 2012;7:e47825.
9. Catacuzzeno L, Fioretti B, Franciolini F. Expression and Role of the Intermediate-Conductance Calcium-Activated Potassium Channel KCa3.1 in Glioblastoma. J Signal Transduct 2012;2012:421564.
10. Turner KL, Honasoge A, Robert SM, McFerrin MM, Sontheimer H. A proinvasive role for the Ca2+-activated K+ channel KCa3.1 in malignant glioma. Glia 2014;62:971–81.
11. Lallet-Daher H, Roudbaraki M, Bavencoffe A, Mariot P, Gackiere F, Bidaux G, et al. Intermediate-conductance Ca2+-activated K+ channels (IKCa1) regulate human prostate cancer cell proliferation through a close control of calcium entry. Oncogene 2009;28:1792–806.
12. Ouadid-Ahidouch H, Roudbaraki M, Delcourt P, Ahidouch A, Joury N, Prevarskaya N. Functional and molecular identification of intermediate-conductance Ca2+-activated K+ channels in breast cancer cells: association with cell cycle progression. Am J Physiol Cell Physiol 2004;287:C125–34.
13. Jager H, Dreker T, Buck A, Giehl K, Gress T, Grissmer S. Blockage of intermediate-conductance Ca2+-activated K+ channels inhibit human pancreatic cancer cell growth in vitro. Mol Pharmacol 2004;65:630–8.
14. Wang J, Xu YQ, Liang YY, Gongora R, Warnock DG, Ma HP. An intermediate-conductance Ca2+-activated K+ channel mediates B lymphoma cell cycle progression induced by serum. Pflugers Arch 2007;454:945–56.
15. Huber SM. Oncochannels. Cell Calcium 2013;53:241–55.
16. Huber SM, Butz L, Stegen B, Klumpp D, Braun N, Ruth P, et al. Ionizing radiation, ion transports, and radioresistance of cancer cells. Front Physiol 2013;4:212.
17. Huber SM, Butz L, Stegen B, Klumpp L, Klumpp D, Eckert F. Role of ion channels in ionizing radiation-induced cell death. Biochim Biophys Acta. 2014 Nov 15. pii: S0005-2736(14)00390-3.
18. Khalid MH, Shibata S, Hiura T. Effects of clotrimazole on the growth, morphological characteristics, and cisplatin sensitivity of human glioblastoma cells in vitro. J Neurosurg 1999;90:918–27.
19. Khalid MH, Tokunaga Y, Caputy AJ, Walters E. Inhibition of tumor growth and prolonged survival of rats with intracranial gliomas following administration of clotrimazole. J Neurosurg 2005;103:79–86.
20. Liu H, Li Y, Raisch KP. Clotrimazole induces a late G1 cell cycle arrest and sensitizes glioblastoma cells to radiation in vitro. Anticancer Drugs 2010;21:841–9.
21. Steinle M, Palme D, Misovic M, Rudner J, Dittmann K, Lukowski R, et al. Ionizing radiation induces migration of glioblastoma cells by activating BK K+ channels. Radiother Oncol 2011;101:122–6.
22. Barry PH, Lynch JW. Liquid junction potentials and small cell effects in patch-clamp analysis. J Membr Biol 1991;121:101–17.
23. Fotin-Mleczek M, Zanzinger K, Heidenreich R, Lorenz C, Kowalczyk A, Kallen KJ, et al. mRNA-based vaccines synergize with radiation therapy to eradicate established tumors. Radiat Oncol 2014;9:180.
24. Cerami E, Gao J, Dogrusoz U, Gross BE, Sumer SO, Aksoy BA, et al. The cBio cancer genomics portal: an open platform for exploring multidimensional cancer genomics data. Cancer Discov 2012;2:401–4.
25. Gao J, Aksoy BA, Dogrusoz U, Dresdner G, Gross B, Sumer SO, et al. Integrative analysis of complex cancer genomics and clinical profiles using the cBioPortal. Sci Signal 2013;6:pl1.
26. Huber SM, Tschop J, Braun GS, Nagel W, Horster MF. Bradykinin-stimulated Cl- secretion in T84 cells. Role of Ca2+-activated hSK4-like K+ channels. Pflugers Arch 1999;438:53–60.
27. Palme D, Misovic M, Schmid E, Klumpp D, Salih HR, Rudner J, et al. Kv3.4 potassium channel-mediated electrosignaling controls cell cycle and survival of irradiated leukemia cells. Pflugers Arch 2013;465:1209–21.
28. Huber SM, Misovic M, Mayer C, Rodemann HP, Dittmann K. EGFR-mediated stimulation of sodium/glucose cotransport promotes survival of irradiated human A549 lung adenocarcinoma cells. Radiother Oncol 2012;103:373–9.
29. Heise N, Palme D, Misovic M, Koka S, Rudner J, Lang F, et al. Non-selective cation channel-mediated Ca2+-entry and activation of Ca2+/calmodulin-dependent kinase II contribute to G2/M cell cycle arrest and survival of irradiated leukemia cells. Cell Physiol Biochem 2010;26:597–608.
30. Dittmann K, Mayer C, Rodemann HP, Huber SM. EGFR cooperates with glucose transporter SGLT1 to enable chromatin remodeling in response to ionizing radiation. Radiother Oncol 2013;107:247–51.

Downloaded from mcr.aacrjournals.org on October 8, 2015. © 2015 American Association for Cancer Research.

Published OnlineFirst June 3, 2015; DOI: 10.1158/1541-7786.MCR-15-0075

31. Motiani RK, Hyzinski-Garcia MC, Zhang X, Henkel MM, Abdullaev IF, Kuo YH, et al. STIM1 and Orai1 mediate CRAC channel activity and are essential for human glioblastoma invasion. Pflugers Arch 2013;465:1249–60.
32. Wondergem R, Ecay TW, Mahieu F, Owsianik G, Nilius B. HGF/SF and menthol increase human glioblastoma cell calcium and migration. Biochem Biophys Res Commun 2008;372:210–5.
33. Bomben VC, Sontheimer H. Disruption of transient receptor potential canonical channel 1 causes incomplete cytokinesis and slows the growth of human malignant gliomas. Glia 2010;58:1145–56.
34. Catacuzzeno L, Aiello F, Fioretti B, Sforna L, Castigli E, Ruggieri P, et al. Serum-activated K and Cl currents underlay U87-MG glioblastoma cell migration. J Cell Physiol 2011;226:1926–33.
35. Sciaccaluga M, Fioretti B, Catacuzzeno L, Pagani F, Bertollini C, Rosito M, et al. CXCL12-induced glioblastoma cell migration requires intermediate conductance Ca2+-activated K+ channel activity. Am J Physiol Cell Physiol 2010;299:C175–84.
36. D'Alessandro G, Catalano M, Sciaccaluga M, Chece G, Cipriani R, Rosito M, et al. KCa3.1 channels are involved in the infiltrative behavior of glioblastoma in vivo. Cell Death Dis 2013;4:e773.
37. Liu G, Yuan X, Zeng Z, Tunici P, Ng H, Abdulkadir IR, et al. Analysis of gene expression and chemoresistance of CD133+ cancer stem cells in glioblastoma. Mol Cancer 2006;5:67.
38. Nakada M, Nambu E, Furuyama N, Yoshida Y, Takino T, Hayashi Y, et al. Integrin alpha3 is overexpressed in glioma stem-like cells and promotes invasion. Br J Cancer 2013;108:2516–24.
39. Turner KL, Sontheimer H. KCa3.1 modulates neuroblast migration along the rostral migratory stream (RMS) in vivo. Cereb Cortex 2014;24:2388–400.
40. Foller M, Bobbala D, Koka S, Boini KM, Mahmud H, Kasinathan RS, et al. Functional significance of the intermediate conductance Ca2+-activated K +channel for the short-term survival of injured erythrocytes. Pflugers Arch 2010;460:1029–44.
41. Lang PA, Kaiser S, Myssina S, Wieder T, Lang F, Huber SM. Role of Ca2+-activated K+ channels in human erythrocyte apoptosis. Am J Physiol Cell Physiol 2003;285:C1553–60.
42. Ataga KI, Orringer EP, Styles L, Vichinsky EP, Swerdlow P, Davis GA, et al. Dose-escalation study of ICA-17043 in patients with sickle cell disease. Pharmacotherapy 2006;26:1557–64.
43. Ataga KI, Smith WR, De Castro LM, Swerdlow P, Saunthararajah Y, Castro O, et al. Efficacy and safety of the Gardos channel blocker, senicapoc (ICA-17043), in patients with sickle cell anemia. Blood 2008;111:3991–7.
44. Ataga KI, Stocker J. Senicapoc (ICA-17043): a potential therapy for the prevention and treatment of hemolysis-associated complications in sickle cell anemia. Expert Opin Investig Drugs 2009;18:231–9.
45. Ataga KI, Reid M, Ballas SK, Yasin Z, Bigelow C, James LS, et al. Improvements in haemolysis and indicators of erythrocyte survival do not correlate with acute vaso-occlusive crises in patients with sickle cell disease: a phase III randomized, placebo-controlled, double-blind study of the Gardos channel blocker senicapoc (ICA-17043). Br J Haematol 2011;153:92–104.
46. Maezawa I, Jenkins DP, Jin BE, Wulff H. Microglial KCa3.1 channels as a potential therapeutic target for Alzheimer's disease. Int J Alzheimers Dis 2012;2012:868972.
47. Lam J, Wulff H. The lymphocyte potassium channels Kv1.3 and KCa3.1 as targets for immunosuppression. Drug Dev Res 2011;72:573–84.
48. Wang R, Chadalavada K, Wilshire J, Kowalik U, Hovinga KE, Geber A, et al. Glioblastoma stem-like cells give rise to tumour endothelium. Nature 2010;468:829–33.
49. Cheng L, Huang Z, Zhou W, Wu Q, Donnola S, Liu JK, et al. Glioblastoma stem cells generate vascular pericytes to support vessel function and tumor growth. Cell 2013;153:139–52.

Downloaded from mcr.aacrjournals.org on October 8, 2015. © 2015 American Association for Cancer Research.

Published OnlineFirst June 3, 2015; DOI: 10.1158/1541-7786.MCR-15-0075

AACR American Association for Cancer Research

Molecular Cancer Research

Ca^{2+}-Activated IK K^{+} Channel Blockade Radiosensitizes Glioblastoma Cells

Benjamin Stegen, Lena Butz, Lukas Klumpp, et al.

Mol Cancer Res 2015;13:1283-1295. Published OnlineFirst June 3, 2015.

Updated version Access the most recent version of this article at: doi:10.1158/1541-7786.MCR-15-0075

Cited articles This article cites 48 articles, 11 of which you can access for free at: http://mcr.aacrjournals.org/content/13/9/1283.full.html#ref-list-1

E-mail alerts Sign up to receive free email-alerts related to this article or journal.

Reprints and Subscriptions To order reprints of this article or to subscribe to the journal, contact the AACR Publications Department at pubs@aacr.org.

Permissions To request permission to re-use all or part of this article, contact the AACR Publications Department at permissions@aacr.org.

Downloaded from mcr.aacrjournals.org on October 8, 2015. © 2015 American Association for Cancer Research.

Biochimica et Biophysica Acta 1848 (2015) 2657–2664

Contents lists available at ScienceDirect

Biochimica et Biophysica Acta

journal homepage: www.elsevier.com/locate/bbamem

Review

Role of ion channels in ionizing radiation-induced cell death☆

Stephan M. Huber [a,*], Lena Butz [a,b], Benjamin Stegen [a], Lukas Klumpp [a], Dominik Klumpp [a], Franziska Eckert [a]

[a] Department of Radiation Oncology, University of Tübingen, Germany
[b] Department of Pharmacology, Toxicology and Clinical Pharmacy, Institute of Pharmacy, University of Tübingen, Germany

ARTICLE INFO

Article history:
Received 31 July 2014
Received in revised form 30 October 2014
Accepted 5 November 2014
Available online 15 November 2014

Keywords:
Ion transport
Radiation
Cancer
Cell death
Therapy resistance
Ca^{2+}-activated K^+ channels

ABSTRACT

Neoadjuvant, adjuvant or definitive fractionated radiation therapy are implemented in first line anti-cancer treatment regimens of many tumor entities. Ionizing radiation kills the tumor cells mainly by causing double strand breaks of their DNA through formation of intermediate radicals. Survival of the tumor cells depends on both, their capacity of oxidative defense and their efficacy of DNA repair. By damaging the targeted cells, ionizing radiation triggers a plethora of stress responses. Among those is the modulation of ion channels such as Ca^{2+}-activated K^+ channels or Ca^{2+}-permeable nonselective cation channels belonging to the super-family of transient receptor potential channels. Radiogenic activation of these channels may contribute to radiogenic cell death as well as to DNA repair, glucose fueling, radiogenic hypermigration or lowering of the oxidative stress burden. The present review article introduces these channels and summarizes our current knowledge on the mechanisms underlying radiogenic ion channel modulation. This article is part of a Special Issue entitled: Membrane channels and transporters in cancers.

© 2014 Elsevier B.V. All rights reserved.

Contents

1. Introduction

Ionizing radiation kills or inactivates cells mostly by damaging the nuclear DNA and cell survival critically depends on successful repair of the DNA damage [1]. Ionizing radiation may lead to necrotic as well as apoptotic cell death depending on cell type, dose and fractionation protocols [2]. The major death pathway in this scenario in normal tissue cells is apoptosis. However, cancer cells which often have developed strategies to evade apoptosis [3] may either undergo (regulated) necrosis or reenter the cell cycle with accumulated DNA damages. During the subsequent cell divisions those cells will not be able to segregate the chromosomes and end up as multinucleated giant cells in mitotic catastrophe. Mitotic catastrophe again leads either to apoptotic or necrotic cell death. Another possible mechanism of radiation-induced death in cells with disturbed apoptosis machinery is excess autophagy. While autophagy is a survival strategy [4] excess autophagy overdigests the cytoplasm and cell organelles forcing the cell into apoptosis or necrosis [5].

Meanwhile, the evidence is overwhelming that ion channels fulfill pivotal functions in cell death mechanisms such as apoptosis (for review see the article by Annarosa Arcangeli in this special issue on "Membrane channels and transporters in cancers") as well as in stress response and survival strategies. Notably, tumor cells have been demonstrated to express a set of ion channels which is different to that of the parental normal cells. These channels may fulfill specific oncogenic functions in neoplastic transformation, malignant progression or tissue

☆ This article is part of a Special Issue entitled: Membrane channels and transporters in cancers.

* Corresponding author at: Department of Radiation Oncology, University of Tübingen, Hoppe-Seyler-Str. 3, 72076 Tübingen, Germany. Tel.: +49 7071 29 82183.
E-mail address: stephan.huber@uni-tuebingen.de (S.M. Huber).

http://dx.doi.org/10.1016/j.bbamem.2014.11.004
0005-2736/© 2014 Elsevier B.V. All rights reserved.

invasion and metastasis (for review see [1]). In addition, they may contribute to the cellular stress response for instance during fractionated radiation therapy and may confer radioresistance.

The present review intends to sum up data on ion channel function in the stress response to ionizing radiation. In particular, ion channels that may induce cell death in tumor cells and facilitate radiogenic cell killing are introduced. In addition, data on ion channels which, in contrast to the before mentioned, confer radioresistance are reviewed. Finally, ion channels of tumor cells that might contribute to acquired radioresistance, e.g. by promoting radiogenic hypermigration or transition into relatively radioresistant ***c***ancer ***s***tem (cell)-like ***c***ells (CSCs) are described. Prior to that, a brief introduction into radiotherapy and its radiobiological principles is given in the next paragraphs.

2. Radiotherapy

Radiation therapy together with surgery and systemic chemotherapy is the main pillar of anti-cancer treatment. About half of all cancer patients receive radiation therapy, half of all cures from cancer include radiotherapy [6]. Despite modern radiation techniques and advanced multimodal treatments, local failures and distant metastases often limit the prognosis of the patients, especially due to limited salvage treatments [7].

Ionizing radiation impairs the clonogenic survival of tumor cells mainly by causing double strand breaks in the DNA backbone. The number of double strand breaks increases linearly with the absorbed radiation dose. The intrinsic capacity to detoxify radicals formed during transfer of radiation energy to cellular molecules such as H_2O (giving rise to hydroxyl radicals, $^{\cdot}OH$) and the ability to efficiently repair DNA double strand breaks by non-homologous end joining or homologous recombination determines the radiosensitivity of a given tumor cell. Irradiated tumor cells which leave residual DNA double strand breaks un-repaired lose their clonogenicity meaning that these cells can not restore tumor mass (for review see [8]).

In addition to these intrinsic resistance factors, the microenvironment may lower the radiosensitivity of tumor cells. Hypoxic areas are frequent in solid tumors reaching a certain mass. Tumor hypoxia, however, decreases the efficacy of radiation therapy [9]. Ionizing radiation directly or indirectly generates radicals in the deoxyribose moiety of the DNA backbone. In a hypoxic atmosphere, cellular thiols can react with those DNA radicals resulting in chemical DNA repair. At higher oxygen partial pressure, in sharp contrast, radicals of the deoxyribose moiety are chemically transformed to strand break precursors [10]. By this mechanism, hypoxia increases radioresistance by a factor of two to three (oxygen enhancement ratio) [11].

Fractionated treatment regimens which improve recovery of the normal tissue after irradiation but not of the tumor have been established in radiotherapy [12]. In addition to limit normal tissue toxicity, killing of tumor mass by initial radiation fractions has been demonstrated to reoxygenate and thereby radiosensitize solid tumors during further fractionated radiotherapy. Beyond that, fractionated radiation regimens aim to redistribute tumor cells in a more vulnerable phase of the cell cycle in the time intervals between two fractions [13]. Accelerated repopulation of the tumor after irradiation is a frequently reported phenomenon. Possible mechanisms of accelerated repopulation include induction of CSCs: It has been proposed that radiation therapy induces CSCs to switch from an asymmetrical into a symmetrical mode of cell division; i.e., a CSC which is thought to normally divide into a daughter CSC and a lineage-committed progenitor cells is induced by the radiotherapy to divide symmetrically into two proliferative CSC daughter cells. This is thought to accelerate repopulation of the tumor after end of radiotherapy. Importantly, CSCs are thought be relatively radioresistant possibly due to i) high oxidative defense and, therefore, low radiation-induced insults, ii) activated DNA checkpoints resulting in fast DNA repair, and iii) an attenuated radiation-induced cell cycle redistribution [14].

Finally, fractionated radiation therapy, which applies fractions of sublethal radiation doses (usually 2 Gy per fraction), has been demonstrated in a variety of tumor entities *in vitro* and in animal models to stimulate hypermigration and hypermetastasis of tumor cells as well as infiltration of the tumor by CD11b-positive myeloid cells and subsequent vasculogenesis. It is tempting to speculate that radiogenic hypermigration boosts cellular interaction of tumor cells with non-tumor cells, e.g. endothelial cells. It has been proposed that CSCs lodge within perivascular niches where a complex regulatory network supports CSC survival [15]. As a matter of fact, CSCs but not non-CSCs gain radioresistance when transplanted orthotopically in mice [16] supporting the idea of a tumor microenvironment-dependent acquired radioresistance. Ion channels contribute to both, intrinsic and acquired radioresistance of tumor cells as discussed in the next paragraphs

3. Radiosensitizing ion channels

Member 2 of the melastatin family of transient receptor potential channel (TRPM2) is a Ca^{2+}-permeable nonselective cation channel. Heterologous expression of TRPM2 in human embryonic kidney cells [17] or A172 human glioblastoma cells [18] facilitates oxidative stress-induced cell death. Reactive oxygen species (ROS) have been demonstrated to trigger TRPM2 activation [19,20]. The principal activator, however, of TRPM2 is ADP-ribose (ADPR) that binds to a special domain located at the C-terminus of the channel [21,22]. Sources of ADPR are the mitochondria [23] or ADPR polymers. The latter are formed, e.g., during DNA repair by poly (ADP-ribose) polymerases (PARPs). ADPR is released from the ADPR polymers by glycohydrolases [21,24].

Expression of TRPM2 has been demonstrated in several tumor entities such as insulinoma [25], hepatocellular carcinoma [25], prostate cancer [26], lymphoma [27], leukemia [28] and lung cancer cell lines [29]. TRPM2 activity increases the susceptibility to cell death [30] probably by overloading cells with Ca^{2+} (Fig. 1A).

Remarkably, cancer cells may evade TRPM2-mediated cell death. In lung cancer cells, de-methylation of a GpC island within the TRPM2 gene gives rise to new promoters that regulate transcription of a non-functional truncated TRPM2 channel [29] and to a TRPM2 specific antisense RNA. This antisense RNA inhibits TRPM2 translation. Moreover, the truncated channel is non-functional and acts dominant negative, thus switching off the tumor-suppressing function of the full-length TRPM2 protein [29] (Fig. 1B).

The initially described member of the vanilloid family of TRP channels, the nociceptive and heat receptor TRPV1, is reportedly expressed in several tumor entities such as uveal melanoma [31], pancreatic [32] and prostatic neuroendocrine tumors [33], glioblastoma [34] and urothelial cancer of human bladder [35]. At least in the latter two tumor entities, TRPV1 exerts anti-oncogenic effects [35,36]. TRPV1 expression inversely correlates with glioma grading [34]. Remarkably, neural precursor cells have been demonstrated to induce ER stress-mediated cell death of glioblastoma cells by activating glioblastoma TRPV1 channels through secretion of endogenous vanilloids [37]. Along those lines is the observation that a TRPV1 antagonist promotes tumorigenesis in mouse skin [38].

Notably, targeting of TRPM2 and TRPV1 by RNA interference has been demonstrated to decrease gamma irradiation-induced formation of nuclear γH2AX foci and further DNA damage response in A549 lung adenocarcinoma cells [39]. Since γH2AX foci are used as a surrogate for DNA double strand breaks, one might speculate that TRPM2 or TRPV1 may amplify ionizing radiation-induced insults (Fig. 1). Another interpretation which has been favored by the author of the study [39] would be that activity of TRPM2 and TRPV1 is required for the formation of DNA repair complexes. In combination, the data hint to the possibility of radiosensitizing cancer cells by pharmacologically activating TRPM2 or TRPV1 channels. Whether this might become a promising new strategy of tumor radiosensitization has to await animal studies.

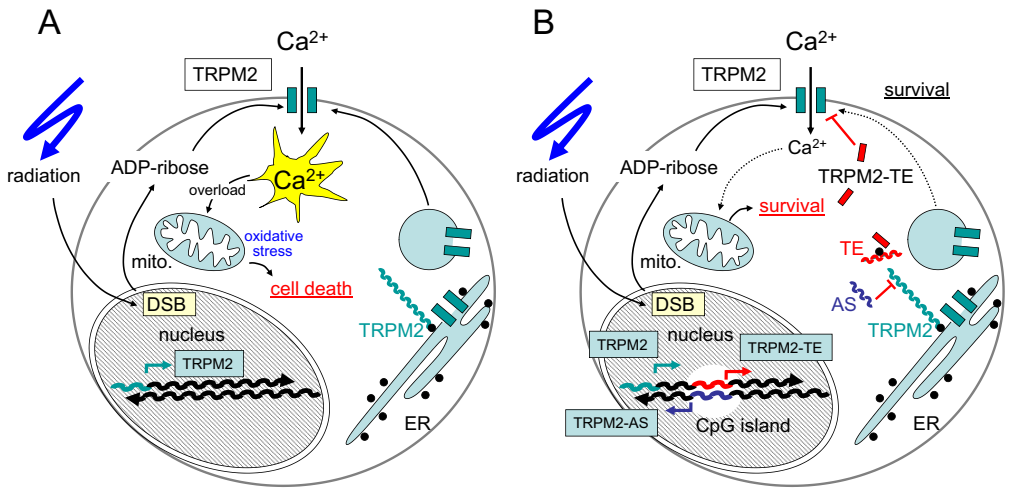

Fig. 1. Speculative mechanism of a putative TRPM2-mediated radiosensitization (A) and reported strategy [29] of lung cancer cells to avoid TRPM2-mediated susceptibility to cell death (B), for details see text. TRPM2-TE (TE): truncated TRPM2, TRPM2-AS (AS): TRPM2 antisense RNA, mito.: mitochondrion).

4. Ion channels conferring intrinsic radioresistance

DNA repair involves cell cycle arrest, chromatin relaxation and formation of repair complexes at the site of DNA damage. Moreover, radiation-induced formation of radicals requires activated radical detoxification pathways and increased oxidative defense to constrain the radiation-induced insults. All these processes of stress response lead to elevated ATP consumption which requires intensified energy supply. Recent *in vitro* observations suggest that these processes depend at least partially on radiation-induced ion channel activation.

Studies of our laboratory indicate that survival of irradiated human leukemia cells critically depends on Ca^{2+} signaling involving radiogenic activation of TRPV5/6-like nonselective cation and $K_v3.4$ voltage-gated K^+ channels [40,41]. The nonselective cation channels in concert with $K_v3.4$ generate radiogenic Ca^{2+} signals that contribute to G_2/M cell cycle arrest by CaMKII-mediated inhibition of the phosphatase cdc25B. Activity of the latter is required in these cells for release from radiation-induced G_2/M arrest via dephosphorylation and thereby activation of cdc2, a component of the mitosis promoting factor. Experimental interference with the radiogenic Ca^{2+} signals, e.g. by pharmacological inhibition or knock-down of $K_v3.4$ overrides cell cycle arrest resulting in increased apoptosis and decreased clonogenic survival of irradiated leukemia cells [40,41]. This radiosensitization by $K_v3.4$ targeting demonstrates the pivotal role of radiogenic $K_v3.4$ channel activation for cell cycle arrest and DNA repair.

Similar to leukemia cells, A549 lung adenocarcinoma cells reportedly respond to ionizing radiation with activation of K_v K^+ channels [42] and transient hyperpolarization of the plasma membrane. Later on, the membrane potential of the irradiated A549 cells strongly depolarizes. This depolarization is dependent on external glucose and inhibited by phlorizin, a sodium glucose cotransporter (SGLT) blocker. In parallel, irradiation induces phlorizin-sensitive ^{3}H-glucose uptake within few minutes after irradiation [43]. Combined, these data suggest that radiogenic activation of SGLT transporters and K_v K^+ channels cooperate in glucose fuelling of the irradiated A549 cells, the former by generating the glucose entry routes, the latter by increasing and maintaining the driving force for Na^+-coupled glucose entry. Glucose uptake by SGLTs is mainly driven by the inwardly directed electrochemical driving force for Na^+ which in turn is highly dependent on the K^+ channel-regulated membrane potential. SGLTs allow efficient glucose uptake even from a glucose-depleted microenvironment which is typical for malperfused solid tumors [44]. It is therefore not surprising that several tumor entities such as colorectal, pancreatic, lung, head and neck, prostate, kidney, cervical, breast, bladder and prostate cancer as well as chondrosarcomas and leukemia upregulate SGLTs [45–53].

SGLT has been shown to be in complex with the EGFR [50,53] and radiogenic SGLT activation depends on EGFR tyrosine kinase activity [43]. Importantly, radiogenic increase in glucose fuelling seems to be required for cell survival since the SGLT inhibitor phlorizin radiosensitizes A549 lung adenocarcinoma and FaDu head and neck squamous carcinoma cells [43].

Intracellular ATP concentration has been reported to drop in irradiated A549 cells indicative of an irradiation-caused energy crisis. Notably, recovery from radiation-induced ATP decline is EGFR/SGLT-dependent and associated with improved DNA-repair leading to increased clonogenic cell survival. This is evident from the fact that EGFR or SGLT blockade delays recovery of intracellular ATP concentration and histone modifications necessary for chromatin remodeling during DNA repair. *Vice versa*, inhibition of the histone H3 modification prevents chromatin remodeling as well as energy crisis [8]. Together, these data suggest that irradiation-associated interactions between SGLT1 and EGFR result in increased glucose uptake, which counteracts the energy crisis in tumor cells caused by chromatin remodeling required for DNA repair (Fig. 2) [8,43].

Besides plasma membrane ion channels, mitochondrial transport pathways have been shown to contribute to cellular stress response. Stress-induced upregulation of uncoupling proteins (UCPs) conveys hyperpolarization of the membrane potential across the inner mitochondrial membrane ($\Delta\Psi_m$,) and thereby formation of reactive oxygen species [54]. UCPs are reportedly upregulated in a number of aggressive human tumors (leukemia, breast, colorectal, ovarian, bladder, esophagus, testicular, kidney, pancreatic, lung, and prostate cancer) in which they are proposed to contribute to malignant progression (for review see [54]).

In addition to malignant progression, UCPs may alter the therapy sensitivity of tumor cells. UCP-2 expression has been associated with paclitaxel resistance of p53 wildtype lung cancer, CPT-11 resistance of colon cancer and gemcitabine resistance of pancreatic adenocarcinoma, lung adenocarcinoma, or bladder carcinoma. Accordingly, experimental targeting of UCPs has been demonstrated to sensitize tumor cells to chemotherapy *in vitro* (for review see [54]).

Notably, ionizing radiation induces up-regulation of UCP-2 expression in colon carcinoma cells [55] and in a radiosensitive subclone of B cell lymphoma [56], as well as UCP-3 expression in rat retina [57]. Radioprotection might result from lowering the radiation-induced burden of reactive oxygen species. As a matter of fact, multi-resistant subclones of leukemia cells reportedly show higher UCP-2 protein expression, lower $\Delta\Psi_m$, lower radiation induced formation of reactive oxygen species, and decreased DNA damage as compared to their parental sensitive cells [58].

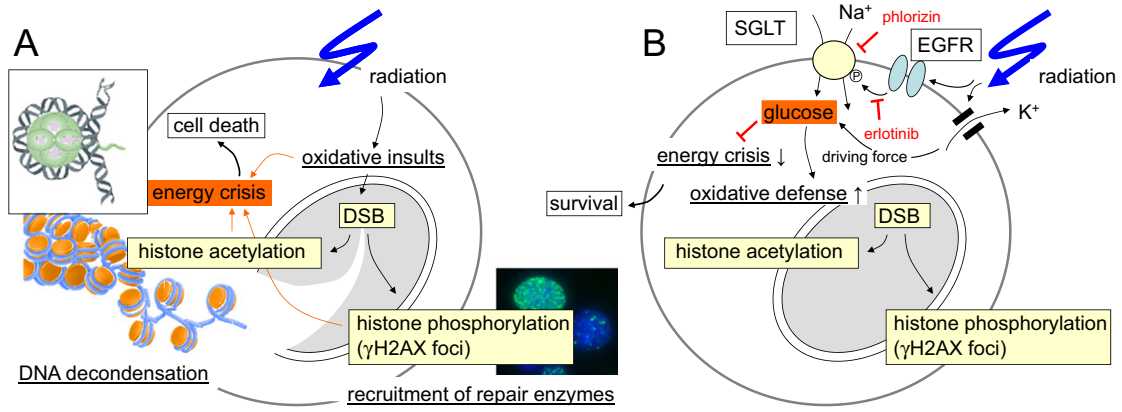

Fig. 2. Radiation-caused energy crisis (A) and functional significance of SGLT1-mediated glucose fueling for DNA repair and cell survival (B) of irradiated A549 lung adenocarcinoma cells (DSB: double strand breaks).

In summary, these data indicate that ion transports through channels may regulate processes that mediate intrinsic radioresistance. Only few laboratories worldwide including ours are working on the radiophysiology of tumor cells. The investigation of ion transports in irradiated cells therefore is at its very beginning and the few data available are mostly phenomenological in nature. The molecular mechanisms that underlie e.g. radiogenic channel activation are still ill-defined. Nevertheless, the data prove functional significance of ion transports and electrosignaling for the survival of irradiated tumor cells and might have translational implications for radiotherapy in the future.

5. Ion channels in acquired radioresistance

Microenvironmental stress such as hypoxia, interstitial nutrient depletion or low pH has been proposed to switch tumor cells from a "Grow" into a "Go" phenotype. By migration and tissue invasion "Go" tumor cells may evade the locally confined stress burden and resettle in distant and less hostile regions. Once resettled, tumor cells may readapt the "Grow" phenotype by reentering cell cycling and may establish tumor satellites in more or less close vicinity of the primary focus (for review see [54]).

In accordance with this hypothesis, sublethal ionizing irradiation as applied in single fractions of fractionated radiotherapy has been demonstrated *in vitro* and/or in rodent tumor models to induce migration, invasion and metastasis or spreading of cervix carcinoma [59], head and neck squamous cell carcinoma [60], lung adenocarinoma [61,62], colorectal carcinoma [62], breast cancer [62–64], meningioma [65], medulloblastoma [66] and glioblastoma. In particular, in glioblastoma the experimental evidence for such radiogenic hypermigration is meanwhile overwhelming [67–80]. Glioblastoma cells show a highly migrative phenotype that may "travel" large distances through the brain [81]. At least in theory, radiogenic hypermigration might, therefore, contribute to locoregional treatment failure by promoting emigration of tumor cells from the target volume during fractionated radiation therapy.

Migration and radiogenic hypermigration are well documented in glioma cells. They invade the surrounding brain parenchyma primarily by moving along axon bundles and the vasculature. During brain invasion along those tracks cells have to squeeze between very narrow interstitial spaces which requires effective local cell volume decrease and reincrease. Glioblastoma cells are capable of losing all unbound cell water [82]. The electrochemical driving force for this tremendous cell volume decrease is provided by an unusually high cytosolic Cl^- concentration (100 mM) [83,84] which is utilized as an osmolyte. During local regulatory volume decrease, extrusion of Cl^- and K^+ along their electrochemical gradients involves ClC-3 Cl^-- channels [85,86], Ca^{2+}-activated high conductance BK- [74,87,88] and intermediate

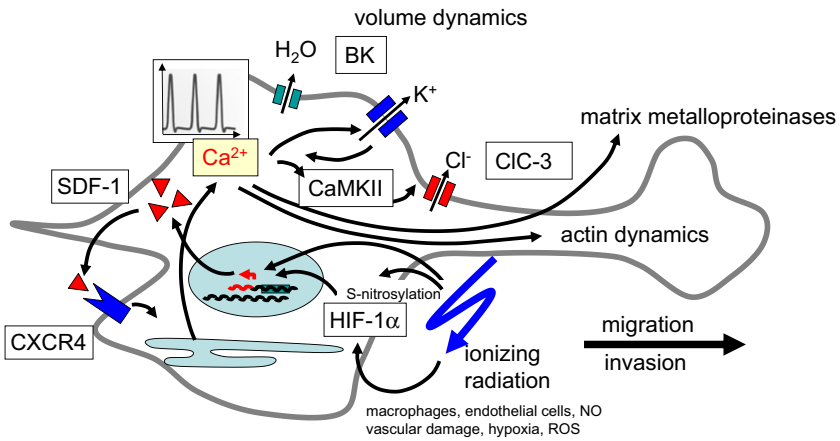

Fig. 3. Hypothetical signaling underlying radiogenic hypermigration of glioblastoma cells. SDF-1 is a HIF-1α target gene and hypoxia is a strong inductor of SDF-1 expression. IR-caused damage of the tumor vasculature and resultant tumor hypoxia has been proposed to induce SDF-1 expression [111]. Beyond that, ionizing radiation reportedly stimulates the generation of NO in tumor-associated macrophages leading to HIF-1α stabilization by S-nitrosylation [100]. Finally, radiation may directly stabilize HIF-1α as deduced from *in vitro* experiments (own unpublished results). SDF-1 induces Ca^{2+} signals through CXCR4 chemokine receptor that in turn contribute to the programming and mechanics of migration (for details see text) and possibly invasion, e.g., via calpain-dependent [112] activation of matrix metalloproteinases [113,114].

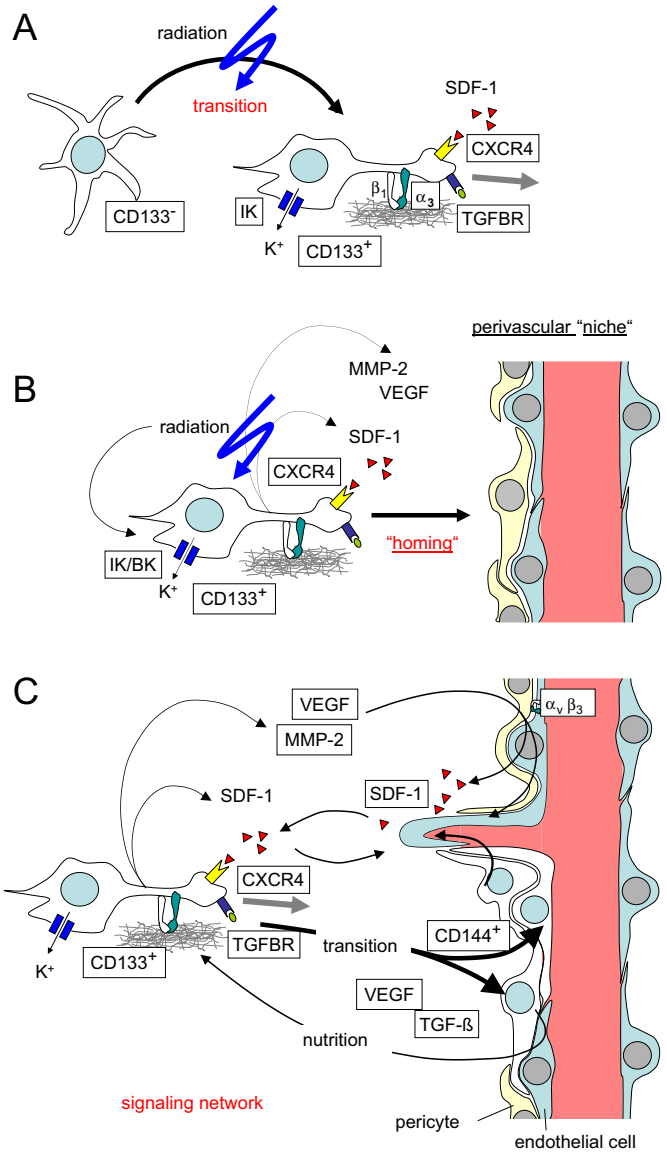

Fig. 4. Synopsis of the signaling network in glioblastoma conferring radioresistance and speculative role of ionizing radiation herein. A. Irradiation induces secretion of SDF-1 [80,95–97] and transition of $CD133^-$ "differentiated" glioblastoma cells to $CD133^+$ GSCs with up-regulated CXCR4 [106], β1/α3 integrins [108], TGFB2 receptor [115], TGF-β responsiveness [115], and IK Ca^{2+}-activated K^+ channel-dependent highly migratory and invasive phenotype [109] B. Irradiation promotes "homing" of GSCs to perivascular niches by stimulating cell migration. C. The reciprocal interaction between glioblastoma and endothelial cells strongly depends on matrix metalloproteinase-2 (MMP-2) expression by glioblastoma [114] and SDF-1 signaling of endothelial cells [110]. Importantly, irradiation induces upregulation of MMP-2 in glioblastoma cells (B) which is required for tissue invasion [67,71,72,79,114] and VEGF secretion (B) [71,75] which reportedly may promote angiogenesis [116]. In addition, transition of glioblastoma cells into endothelial cells [117] and pericytes [15] reconstruct the glioblastoma vasculature which supports both, vessel function and tumor growth.

conductance IK K^+ channels [86,89]. Inhibition of either of these channels attenuates glioblastoma cell migration or invasion [83,90–94] confirming their pivotal function in these processes.

Ionizing radiation has been demonstrated in our laboratory to activate BK K^+ channels in glioblastoma cells *in vitro* [74]. Radiogenic BK channel activity, in turn, is required for Ca^{2+}/calmodulin kinase II (CaMKII)- [74] and consecutive CaMKII-dependent ClC-3 channel activation (own unpublished observation and [85]). Inhibition of BK or CaMKII abolishes radiogenic hypermigration [74] indicating BK channel activation as key event of radiogenic hypermigration of glioblastoma cells. Radiogenic hypermigration is paralleled by radiogenic expression of the chemokine SDF-1 (stromal cell-derived factor-1, CXCL12) in different tumor entities including glioblastoma [80,95–97]. Glioblastoma cells reportedly express CXCR4 chemokine receptors and SDF-1 stimulates glioblastoma cell migration via CXCR4-mediated Ca^{2+} signaling [93]. CXCR4 receptors reportedly signal through phospholipase C and BK channels have been shown to be functionally coupled with IP_3 receptors in the ER [98] suggesting (and confirmed by own unpublished observations) that radiogenic SDF1/CXCR4 signaling is upstream of BK channel activation. SDF-1, in turn, is a target gene of the transcription factor HIF-1α which reportedly becomes stabilized, e.g. by S-nitrosylation, upon irradiation [95,99–101] (Fig. 3). Together, this gives a good example of radiogenic signaling which integrates biochemical signaling, electrosignaling (i.e., BK-dependent regulation of membrane potential) and Ca^{2+} signaling modules (more details are given in the legend to Fig. 3).

Ionizing radiation has been demonstrated to select stem (cell)-like glioblastoma cells (GSCs) or even induce transition of "differentiated" cancer cells to GSCs/CSCs in glioblastoma [102–104] and other tumor entities [14]. Notably, "stemness" is associated with SDF-1 secretion [105] and markedly increased CXCR4 chemokine expression [106]. Importantly, CXCR4 upregulation is required to maintain "stemness" of non-small cell lung cancer [107] and glioblastoma cells [105]. In accordance to CXCR4 upregulation, GSCs show a highly migratory/invasive phenotype [108,109]. Most importantly, this phenotype is highly dependent on the Ca^{2+}-activated IK K^+ channel [89,109]. Furthermore, IK channels have been demonstrated to be overexpressed in about one third of the glioma patients with IK protein expression correlating with poor patient survival [89].

Unexpectedly, a previous report demonstrated that *xeno*grafted $CD133^+$ stem-like subpopulations of glioblastoma exhibit a higher radioresistance than *xeno*grafted $CD133^-$ cells while radiosensitivity of both subpopulations does not differ *in vitro* [16]. This clearly indicates a function of the brain microenvironment for radioresistance. In particular, endothelial cells have been postulated to promote glioblastoma therapy resistance [110]. Part of the reported reciprocal interaction between glioblastoma cells and endothelial cells as well as of the complex signaling network in perivascular "niches" is schematically summarized in Fig. 4.

Albeit merely speculative, the idea that radiogenic hypermigration might promote "homing" of (CXCR4-highly-expressing stem-like) glioblastoma cells to perivascular niches is highly attractive. The subsequent reciprocal modifications of glioblastoma and endothelial cells might eventually induce radioresistance of glioblastoma cells. Together, these data suggest that radiogenic hypermigration might contribute to the apparently high radioresistance of glioblastoma cells either by promoting evasion from the radiation target volume or by stimulating the chemotaxis of glioblastoma cells to "radioprotective" perivascular niches.

6. Concluding remarks

The radiation physiology of cancer cells is yet a neglected research field. While the number of reports on ion channel function in neoplastic transformation, malignant progression or metastasis of cancer cells increases constantly only little is known about the role of ion channels in radiotherapy. The few data available strongly suggest that ionizing radiation-induced ion channel modifications are a common phenomenon. Importantly, these modifications impact on the stress response and survival of irradiated tumor cells. By modulating intracellular Ca^{2+} signals radiosensitive ion channels may directly crosstalk with the biochemical signaling of the DNA damage response. By driving local cell volume changes radiogenic ion channel modifications may promote cell migration and stress evasion of irradiated tumor cells. By stabilizing the membrane potential ionizing radiation-induced K^+ channel activity might facilitate Na^+-coupled glucose uptake providing the energy for DNA-repair. Finally, mitochondrial channels upregulated

by ionizing radiation might lower the oxidative insults associated with ionizing radiation. Given the aberrant and partly specific ion channel expression of tumor cells, a more profound understanding of the mechanisms underlying radiogenic ion channel modifications might be harnessed in the future to develop new strategies for the radiosensitization of tumors.

Acknowledgment

This work was supported by a grant from the Wilhelm-Sander-Stiftung awarded to SH (2011.083.1). BS and DK were supported by the DFG International Graduate School 1302 (TP T9 SH).

References

[1] S.M. Huber, Oncochannels, Cell Calcium 53 (2013) 241–255.
[2] M. Verheij, Clinical biomarkers and imaging for radiotherapy-induced cell death, Cancer Metastasis Rev. 27 (2008) 471–480.
[3] D. Hanahan, R.A. Weinberg, The hallmarks of cancer, Cell 100 (2000) 57–70.
[4] A. Apel, I. Herr, H. Schwarz, H.P. Rodemann, A. Mayer, Blocked autophagy sensitizes resistant carcinoma cells to radiation therapy, Cancer Res. 68 (2008) 1485–1494.
[5] S. Palumbo, S. Comincini, Autophagy and ionizing radiation in tumors: the "survive or not survive" dilemma, J. Cell. Physiol. 228 (2013) 1–8.
[6] German-Cancer-Aid, Information Booklet, http://www.krebshilfe.de/fileadmin/Inhalte/Downloads/PDFs/Blaue_Ratgeber/053_strahlen.pdf 2013.
[7] A.C. Muller, F. Eckert, V. Heinrich, M. Bamberg, S. Brucker, T. Hehr, Re-surgery and chest wall re-irradiation for recurrent breast cancer: a second curative approach, BMC Cancer 11 (2011) 197.
[8] K. Dittmann, C. Mayer, H.P. Rodemann, S.M. Huber, EGFR cooperates with glucose transporter SGLT1 to enable chromatin remodeling in response to ionizing radiation, Radiother. Oncol. (2013), http://dx.doi.org/10.1016/j.radonc.2013.03.016 (pii: S0167-8140(13)00145-X).
[9] H. Harada, How can we overcome tumor hypoxia in radiation therapy? J. Radiat. Res. 52 (2011) 545–556.
[10] P.M. Cullis, G.D.D. Jones, J. Lea, M.C.R. Symons, M. Sweeney, The effects of ionizing radiation on deoxyribonucleic acid. Part 5. The role of thiols in chemical repair, J. Chem. Soc. Perkin Trans. 2 (1987) 1907–1914.
[11] M. Langenbacher, R.J. Abdel-Jalil, W. Voelter, M. Weinmann, S.M. Huber, *In vitro* hypoxic cytotoxicity and hypoxic radiosensitization. Efficacy of the novel 2-nitroimidazole N, N, N-tris[2-(2-nitro-1H-imidazol-1-yl)ethyl]amine, Strahlenther. Onkol. 189 (2013) 246–254.
[12] B. Jones, R.G. Dale, A.M. Gaya, Linear quadratic modeling of increased late normal-tissue effects in special clinical situations, Int. J. Radiat. Oncol. Biol. Phys. 64 (2006) 948–953.
[13] T.M. Pawlik, K. Keyomarsi, Role of cell cycle in mediating sensitivity to radiotherapy, Int. J. Radiat. Oncol. Biol. Phys. 59 (2004) 928–942.
[14] F. Pajonk, E. Vlashi, W.H. McBride, Radiation resistance of cancer stem cells: the 4 R's of radiobiology revisited, Stem Cells 28 (2010) 639–648.
[15] L. Cheng, Z. Huang, W. Zhou, Q. Wu, S. Donnola, J.K. Liu, X. Fang, A.E. Sloan, Y. Mao, J.D. Lathia, W. Min, R.E. McLendon, J.N. Rich, S. Bao, Glioblastoma stem cells generate vascular pericytes to support vessel function and tumor growth, Cell 153 (2013) 139–152.
[16] M. Jamal, B.H. Rath, P.S. Tsang, K. Camphausen, P.J. Tofilon, The brain microenvironment preferentially enhances the radioresistance of $CD133^{+}$ glioblastoma stem-like cells, Neoplasia 14 (2012) 150–158.
[17] Y. Hara, M. Wakamori, M. Ishii, E. Maeno, M. Nishida, T. Yoshida, H. Yamada, S. Shimizu, E. Mori, J. Kudoh, N. Shimizu, H. Kurose, Y. Okada, K. Imoto, Y. Mori, LTRPC2 Ca^{2+}-permeable channel activated by changes in redox status confers susceptibility to cell death, Mol. Cell 9 (2002) 163–173.
[18] M. Ishii, A. Oyama, T. Hagiwara, A. Miyazaki, Y. Mori, Y. Kiuchi, S. Shimizu, Facilitation of H2O2-induced A172 human glioblastoma cell death by insertion of oxidative stress-sensitive TRPM2 channels, Anticancer Res. 27 (2007) 3987–3992.
[19] M. Naziroglu, A. Luckhoff, A calcium influx pathway regulated separately by oxidative stress and ADP-Ribose in TRPM2 channels: single channel events, Neurochem. Res. 33 (2008) 1256–1262.
[20] M. Naziroglu, A. Luckhoff, Effects of antioxidants on calcium influx through TRPM2 channels in transfected cells activated by hydrogen peroxide, J. Neurol. Sci. 270 (2008) 152–158.
[21] E. Fonfria, I.C. Marshall, C.D. Benham, I. Boyfield, J.D. Brown, K. Hill, J.P. Hughes, S.D. Skaper, S. McNulty, TRPM2 channel opening in response to oxidative stress is dependent on activation of poly(ADP-ribose) polymerase, Br. J. Pharmacol. 143 (2004) 186–192.
[22] F.J. Kuhn, I. Heiner, A. Luckhoff, TRPM2: a calcium influx pathway regulated by oxidative stress and the novel second messenger ADP-ribose, Pflugers Arch. 451 (2005) 212–219.
[23] A.L. Perraud, C.L. Takanishi, B. Shen, S. Kang, M.K. Smith, C. Schmitz, H.M. Knowles, D. Ferraris, W. Li, J. Zhang, B.L. Stoddard, A.M. Scharenberg, Accumulation of free ADP-ribose from mitochondria mediates oxidative stress-induced gating of TRPM2 cation channels, J. Biol. Chem. 280 (2005) 6138–6148.
[24] J. Eisfeld, A. Luckhoff, Trpm2, Handb. Exp. Pharmacol. (2007) 237–252.
[25] K. Inamura, Y. Sano, S. Mochizuki, H. Yokoi, A. Miyake, K. Nozawa, C. Kitada, H. Matsushime, K. Furuichi, Response to ADP-ribose by activation of TRPM2 in the CRI-G1 insulinoma cell line, J. Membr. Biol. 191 (2003) 201–207.
[26] X. Zeng, S.C. Sikka, L. Huang, C. Sun, C. Xu, D. Jia, A.B. Abdel-Mageed, J.E. Pottle, J.T. Taylor, M. Li, Novel role for the transient receptor potential channel TRPM2 in prostate cancer cell proliferation, Prostate Cancer Prostatic Dis. 13 (2010) 195–201.
[27] W. Zhang, I. Hirschler-Laszkiewicz, Q. Tong, K. Conrad, S.C. Sun, L. Penn, D.L. Barber, R. Stahl, D.J. Carey, J.Y. Cheung, B.A. Miller, TRPM2 is an ion channel that modulates hematopoietic cell death through activation of caspases and PARP cleavage, Am. J. Physiol. Cell Physiol. 290 (2006) C1146–C1159.
[28] W. Zhang, X. Chu, Q. Tong, J.Y. Cheung, K. Conrad, K. Masker, B.A. Miller, A novel TRPM2 isoform inhibits calcium influx and susceptibility to cell death, J. Biol. Chem. 278 (2003) 16222–16229.
[29] U. Orfanelli, A.K. Wenke, C. Doglioni, V. Russo, A.K. Bosserhoff, G. Lavorgna, Identification of novel sense and antisense transcription at the TRPM2 locus in cancer, Cell Res. 18 (2008) 1128–1140.
[30] S. McNulty, E. Fonfria, The role of TRPM channels in cell death, Pflugers Arch. 451 (2005) 235–242.
[31] S. Mergler, R. Derckx, P.S. Reinach, F. Garreis, A. Bohm, L. Schmelzer, S. Skosyrski, N. Ramesh, S. Abdelmessih, O.K. Polat, N. Khajavi, A.I. Riechardt, Calcium regulation by temperature-sensitive transient receptor potential channels in human uveal melanoma cells, Cell. Signal. 26 (2014) 56–69.
[32] S. Mergler, M. Skrzypski, M. Sassek, P. Pietrzak, C. Pucci, B. Wiedenmann, M.Z. Strowski, Thermo-sensitive transient receptor potential vanilloid channel-1 regulates intracellular calcium and triggers chromogranin A secretion in pancreatic neuroendocrine BON-1 tumor cells, Cell. Signal. 24 (2012) 233–246.
[33] S. Malagarie-Cazenave, N. Olea-Herrero, D. Vara, C. Morell, I. Diaz-Laviada, The vanilloid capsaicin induces IL-6 secretion in prostate PC-3 cancer cells, Cytokine 54 (2011) 330–337.
[34] C. Amantini, M. Mosca, M. Nabissi, R. Lucciarini, S. Caprodossi, A. Arcella, F. Giangaspero, G. Santoni, Capsaicin-induced apoptosis of glioma cells is mediated by TRPV1 vanilloid receptor and requires p38 MAPK activation, J. Neurochem. 102 (2007) 977–990.
[35] G. Santoni, S. Caprodossi, V. Farfariello, S. Liberati, A. Gismondi, C. Amantini, Antioncogenic effects of transient receptor potential vanilloid 1 in the progression of transitional urothelial cancer of human bladder, ISRN Urol. 2012 (2012) 458238.
[36] C. Amantini, P. Ballarini, S. Caprodossi, M. Nabissi, M.B. Morelli, R. Lucciarini, M.A. Cardarelli, G. Mammana, G. Santoni, Triggering of transient receptor potential vanilloid type 1 (TRPV1) by capsaicin induces Fas/CD95-mediated apoptosis of urothelial cancer cells in an ATM-dependent manner, Carcinogenesis 30 (2009) 1320–1329.
[37] K. Stock, J. Kumar, M. Synowitz, S. Petrosino, R. Imperatore, E.S. Smith, P. Wend, B. Purfurst, U.A. Nuber, U. Gurok, V. Matyash, J.H. Walzlein, S.R. Chirasani, G. Dittmar, B.F. Cravatt, S. Momma, G.R. Lewin, A. Ligresti, L. De Petrocellis, L. Cristino, V. Di Marzo, H. Kettenmann, R. Glass, Neural precursor cells induce cell death of high-grade astrocytomas through stimulation of TRPV1, Nat. Med. 18 (2012) 1232–1238.
[38] S. Li, A.M. Bode, F. Zhu, K. Liu, J. Zhang, M.O. Kim, K. Reddy, T. Zykova, W.Y. Ma, A.L. Carper, A.K. Langfald, Z. Dong, TRPV1-antagonist AMG9810 promotes mouse skin tumorigenesis through EGFR/Akt signaling, Carcinogenesis 32 (2011) 779–785.
[39] K. Masumoto, M. Tsukimoto, S. Kojima, Role of TRPM2 and TRPV1 cation channels in cellular responses to radiation-induced DNA damage, Biochim. Biophys. Acta 1830 (2013) 3382–3390.
[40] N. Heise, D. Palme, M. Misovic, S. Koka, J. Rudner, F. Lang, H.R. Salih, S.M. Huber, G. Henke, Non-selective cation channel-mediated Ca^{2+}-entry and activation of Ca^{2+}/calmodulin-dependent kinase II contribute to G2/M cell cycle arrest and survival of irradiated leukemia cells, Cell. Physiol. Biochem. 26 (2010) 597–608.
[41] D. Palme, M. Misovic, E. Schmid, D. Klumpp, H.R. Salih, J. Rudner, S. Huber, Kv3.4 potassium channel-mediated electrosignaling controls cell cycle and survival of irradiated leukemia cells, Pflugers Arch. (2013), http://dx.doi.org/10.1007/s00424-013-1249-5.
[42] S.S. Kuo, A.H. Saad, A.C. Koong, G.M. Hahn, A.J. Giaccia, Potassium-channel activation in response to low doses of gamma-irradiation involves reactive oxygen intermediates in nonexcitatory cells, Proc. Natl. Acad. Sci. U. S. A. 90 (1993) 908–912.
[43] S.M. Huber, M. Misovic, C. Mayer, H.P. Rodemann, K. Dittmann, EGFR-mediated stimulation of sodium/glucose cotransport promotes survival of irradiated human A549 lung adenocarcinoma cells, Radiother. Oncol. 103 (2012) 373–379.
[44] V. Ganapathy, M. Thangaraju, P.D. Prasad, Nutrient transporters in cancer: relevance to Warburg hypothesis and beyond, Pharmacol. Ther. 121 (2009) 29–40.
[45] J.A. Nelson, R.E. Falk, The efficacy of phloridzin and phloretin on tumor cell growth, Anticancer Res. 13 (1993) 2287–2292.
[46] N. Ishikawa, T. Oguri, T. Isobe, K. Fujitaka, N. Kohno, SGLT gene expression in primary lung cancers and their metastatic lesions, Jpn. J. Cancer Res. 92 (2001) 874–879.
[47] B.M. Helmke, C. Reisser, M. Idzko, G. Dyckhoff, C. Herold-Mende, Expression of SGLT-1 in preneoplastic and neoplastic lesions of the head and neck, Oral Oncol. 40 (2004) 28–35.
[48] L.C. Yu, C.Y. Huang, W.T. Kuo, H. Sayer, J.R. Turner, A.G. Buret, SGLT-1-mediated glucose uptake protects human intestinal epithelial cells against Giardia duodenalis-induced apoptosis, Int. J. Parasitol. 38 (2008) 923–934.
[49] V.F. Casneuf, P. Fonteyne, N. Van Damme, P. Demetter, P. Pauwels, B. de Hemptinne, M. De Vos, C. Van de Wiele, M. Peeters, Expression of SGLT1, Bcl-2 and p53 in primary pancreatic cancer related to survival, Cancer Invest. 26 (2008) 852–859.

[50] Z. Weihua, R. Tsan, W.C. Huang, Q. Wu, C.H. Chiu, I.J. Fidler, M.C. Hung, Survival of cancer cells is maintained by EGFR independent of its kinase activity, Cancer Cell 13 (2008) 385–393.

[51] N. Leiprecht, C. Munoz, I. Alesutan, G. Siraskar, M. Sopjani, M. Foller, F. Stubenrauch, T. Iftner, F. Lang, Regulation of Na^+-coupled glucose carrier SGLT1 by human papillomavirus 18 E6 protein, Biochem. Biophys. Res. Commun. 404 (2011) 695–700.

[52] E.M. Wright, D.D. Loo, B.A. Hirayama, Biology of human sodium glucose transporters, Physiol. Rev. 91 (2011) 733–794.

[53] J. Ren, L.R. Bollu, F. Su, G. Gao, L. Xu, W.C. Huang, M.C. Hung, Z. Weihua, EGFR-SGLT1 interaction does not respond to EGFR modulators, but inhibition of SGLT1 sensitizes prostate cancer cells to EGFR tyrosine kinase inhibitors, Prostate 73 (2013) 1453–1461.

[54] S.M. Huber, L. Butz, B. Stegen, D. Klumpp, N. Braun, P. Ruth, F. Eckert, Ionizing radiation, ion transports, and radioresistance of cancer cells, Frontiers in Physiology | Membrane Physiology and Membrane Biophysics 4 (2013) 212.

[55] A. Sreekumar, M.K. Nyati, S. Varambally, T.R. Barrette, D. Ghosh, T.S. Lawrence, A.M. Chinnaiyan, Profiling of cancer cells using protein microarrays: discovery of novel radiation-regulated proteins, Cancer Res. 61 (2001) 7585–7593.

[56] D.W. Voehringer, D.L. Hirschberg, J. Xiao, Q. Lu, M. Roederer, C.B. Lock, L.A. Herzenberg, L. Steinman, L.A. Herzenberg, Gene microarray identification of redox and mitochondrial elements that control resistance or sensitivity to apoptosis, Proc. Natl. Acad. Sci. U. S. A. 97 (2000) 2680–2685.

[57] X.W. Mao, J.D. Crapo, D.S. Gridley, Mitochondrial oxidative stress-induced apoptosis and radioprotection in proton-irradiated rat retina, Radiat. Res. 178 (2012) 118–125.

[58] M.E. Harper, A. Antoniou, E. Villalobos-Menuey, A. Russo, R. Trauger, M. Vendemelio, A. George, R. Bartholomew, D. Carlo, A. Shaikh, J. Kupperman, E.W. Newell, I.A. Bespalov, S.S. Wallace, Y. Liu, J.R. Rogers, G.L. Gibbs, J.L. Leahy, R.E. Camley, R. Melamede, M.K. Newell, Characterization of a novel metabolic strategy used by drug-resistant tumor cells, FASEB J. 16 (2002) 1550–1557.

[59] W.H. Su, P.C. Chuang, E.Y. Huang, K.D. Yang, Radiation-induced increase in cell migration and metastatic potential of cervical cancer cells operates via the K-Ras pathway, Am. J. Pathol. 180 (2012) 862–871.

[60] A.C. Pickhard, J. Margraf, A. Knopf, T. Stark, G. Piontek, C. Beck, A.L. Boulesteix, E.Q. Scherer, S. Pigorsch, J. Schlegel, W. Arnold, R. Reiter, Inhibition of radiation induced migration of human head and neck squamous cell carcinoma cells by blocking of EGF receptor pathways, BMC Cancer 11 (2011) 388.

[61] J.W. Jung, S.Y. Hwang, J.S. Hwang, E.S. Oh, S. Park, I.O. Han, Ionising radiation induces changes associated with epithelial–mesenchymal transdifferentiation and increased cell motility of A549 lung epithelial cells, Eur. J. Cancer 43 (2007) 1214–1224.

[62] Y.C. Zhou, J.Y. Liu, J. Li, J. Zhang, Y.Q. Xu, H.W. Zhang, L.B. Qiu, G.R. Ding, X.M. Su, S. Mei, G.Z. Guo, Ionizing radiation promotes migration and invasion of cancer cells through transforming growth factor-beta-mediated epithelial–mesenchymal transition, Int. J. Radiat. Oncol. Biol. Phys. 81 (2011) 1530–1537.

[63] S. Biswas, M. Guix, C. Rinehart, T.C. Dugger, A. Chytil, H.L. Moses, M.L. Freeman, C.L. Arteaga, Inhibition of TGF-beta with neutralizing antibodies prevents radiation-induced acceleration of metastatic cancer progression, J. Clin. Invest. 117 (2007) 1305–1313.

[64] D.M. Kambach, V.L. Sodi, P.I. Lelkes, J. Azizkhan-Clifford, M.J. Reginato, ErbB2, FoxM1 and 14-3-3zeta prime breast cancer cells for invasion in response to ionizing radiation, Oncogene 33 (2014) 589–598.

[65] O. Kargiotis, C. Chetty, V. Gogineni, C.S. Gondi, S.M. Pulukuri, A.P. Kyritsis, M. Gujrati, J.D. Klopfenstein, D.H. Dinh, J.S. Rao, uPA/uPAR downregulation inhibits radiation-induced migration, invasion and angiogenesis in IOMM-Lee meningioma cells and decreases tumor growth *in vivo*, Int. J. Oncol. 33 (2008) 937–947.

[66] S. Asuthkar, A.K. Nalla, C.S. Gondi, D.H. Dinh, M. Gujrati, S. Mohanam, J.S. Rao, Gadd45a sensitizes medulloblastoma cells to irradiation and suppresses MMP-9-mediated EMT, Neuro Oncol. 13 (2011) 1059–1073.

[67] C. Wild-Bode, M. Weller, A. Rimner, J. Dichgans, W. Wick, Sublethal irradiation promotes migration and invasiveness of glioma cells: implications for radiotherapy of human glioblastoma, Cancer Res. 61 (2001) 2744–2750.

[68] W. Wick, A. Wick, J.B. Schulz, J. Dichgans, H.P. Rodemann, M. Weller, Prevention of irradiation-induced glioma cell invasion by temozolomide involves caspase 3 activity and cleavage of focal adhesion kinase, Cancer Res. 62 (2002) 1915–1919.

[69] B. Hegedus, J. Zach, A. Czirok, J. Lovey, T. Vicsek, Irradiation and Taxol treatment result in non-monotonous, dose-dependent changes in the motility of glioblastoma cells, J. Neuro Oncol. 67 (2004) 147–157.

[70] S. Rieken, D. Habermehl, A. Mohr, L. Wuerth, K. Lindel, K. Weber, J. Debus, S.E. Combs, Targeting alphanubeta3 and alphanubeta5 inhibits photon-induced hypermigration of malignant glioma cells, Radiat. Oncol. 6 (2011) 132.

[71] A.V. Badiga, C. Chetty, D. Kesanakurti, D. Are, M. Gujrati, J.D. Klopfenstein, D.H. Dinh, J.S. Rao, MMP-2 siRNA inhibits radiation-enhanced invasiveness in glioma cells, PLoS One 6 (2011) e20614.

[72] S.Y. Kwak, J.S. Yang, B.Y. Kim, I.H. Bae, Y.H. Han, Ionizing radiation-inducible miR-494 promotes glioma cell invasion through EGFR stabilization by targeting p190B rhoGAP, Biochim. Biophys. Acta 1843 (2014) 508–516.

[73] A. Canazza, C. Calatozzolo, L. Fumagalli, A. Bergantin, F. Ghielmetti, L. Fariselli, D. Croci, A. Salmaggi, E. Ciusani, Increased migration of a human glioma cell line after *in vitro* CyberKnife irradiation, Cancer Biol. Ther. 12 (2011) 629–633.

[74] M. Steinle, D. Palme, M. Misovic, J. Rudner, K. Dittmann, R. Lukowski, P. Ruth, S.M. Huber, Ionizing radiation induces migration of glioblastoma cells by activating BK K^+ channels, Radiother. Oncol. 101 (2011) 122–126.

[75] W.J. Kil, P.J. Tofilon, K. Camphausen, Post-radiation increase in VEGF enhances glioma cell motility *in vitro*, Radiat. Oncol. 7 (2012) 25.

[76] I. Vanan, Z. Dong, E. Tosti, G. Warshaw, M. Symons, R. Ruggieri, Role of a DNA damage checkpoint pathway in ionizing radiation-induced glioblastoma cell migration and invasion, Cell. Mol. Neurobiol. 32 (2012) 1199–1208.

[77] W.T. Arscott, A.T. Tandle, S. Zhao, J.E. Shabason, I.K. Gordon, C.D. Schlaff, G. Zhang, P.J. Tofilon, K.A. Camphausen, Ionizing radiation and glioblastoma exosomes: implications in tumor biology and cell migration, Transl. Oncol. 6 (2013) 638–648.

[78] W. Zhou, Y. Xu, G. Gao, Z. Jiang, X. Li, Irradiated normal brain promotes invasion of glioblastoma through vascular endothelial growth and stromal cell-derived factor 1alpha, Neuroreport 24 (2013) 730–734.

[79] A. Shankar, S. Kumar, A. Iskander, N.R. Varma, B. Janic, A. Decarvalho, T. Mikkelsen, J.A. Frank, M.M. Ali, R.A. Knight, S. Brown, A.S. Arbab, Subcurative radiation significantly increases proliferation, invasion, and migration of primary GBM *in vivo*, Chin. J. Cancer 33 (2013) 148–158.

[80] S.C. Wang, C.F. Yu, J.H. Hong, C.S. Tsai, C.S. Chiang, Radiation therapy-induced tumor invasiveness is associated with SDF-1-regulated macrophage mobilization and vasculogenesis, PLoS One 8 (2013) e69182.

[81] J. Johnson, M.O. Nowicki, C.H. Lee, E.A. Chiocca, M.S. Viapiano, S.E. Lawler, J.J. Lannutti, Quantitative analysis of complex glioma cell migration on electrospun polycaprolactone using time-lapse microscopy, Tissue Eng. C Methods 15 (2009) 531–540.

[82] S. Watkins, H. Sontheimer, Hydrodynamic cellular volume changes enable glioma cell invasion, J. Neurosci. 31 (2011) 17250–17259.

[83] B.R. Haas, H. Sontheimer, Inhibition of the sodium-potassium-chloride cotransporter isoform-1 reduces glioma invasion, Cancer Res. 70 (2010) 5597–5606.

[84] C.W. Habela, N.J. Ernest, A.F. Swindall, H. Sontheimer, Chloride accumulation drives volume dynamics underlying cell proliferation and migration, J. Neurophysiol. 101 (2009) 750–757.

[85] V.A. Cuddapah, H. Sontheimer, Molecular interaction and functional regulation of ClC-3 by Ca^{2+}/calmodulin-dependent protein kinase II (CaMKII) in human malignant glioma, J. Biol. Chem. 285 (2010) 11188–11196.

[86] V.A. Cuddapah, K.L. Turner, S. Seifert, H. Sontheimer, Bradykinin-induced chemotaxis of human gliomas requires the activation of KCa3.1 and ClC-3, J. Neurosci. 33 (2013) 1427–1440.

[87] C.B. Ransom, H. Sontheimer, BK channels in human glioma cells, J. Neurophysiol. 85 (2001) 790–803.

[88] H. Sontheimer, An unexpected role for ion channels in brain tumor metastasis, Exp. Biol. Med. (Maywood) 233 (2008) 779–791.

[89] K.L. Turner, A. Honasoge, S.M. Robert, M.M. McFerrin, H. Sontheimer, A proinvasive role for the Ca^{2+}-activated K^+ channel KCa3.1 in malignant glioma, Glia 62 (2014) 971–981.

[90] N.J. Ernest, A.K. Weaver, L.B. Van Duyn, H.W. Sontheimer, Relative contribution of chloride channels and transporters to regulatory volume decrease in human glioma cells, Am. J. Physiol. Cell Physiol. 288 (2005) C1451–C1460.

[91] M.B. McFerrin, H. Sontheimer, A role for ion channels in glioma cell invasion, Neuron Glia Biol. 2 (2006) 39–49.

[92] L. Catacuzzeno, F. Aiello, B. Fioretti, L. Sforna, E. Castigli, P. Ruggieri, A.M. Tata, A. Calogero, F. Franciolini, Serum-activated K and Cl currents underlay U87-MG glioblastoma cell migration, J. Cell. Physiol. 226 (2010) 1926–1933.

[93] M. Sciaccaluga, B. Fioretti, L. Catacuzzeno, F. Pagani, C. Bertollini, M. Rosito, M. Catalano, G. D'Alessandro, A. Santoro, G. Cantore, D. Ragozzino, E. Castigli, F. Franciolini, C. Limatola, CXCL12-induced glioblastoma cell migration requires intermediate conductance Ca^{2+}-activated K^+ channel activity, Am. J. Physiol. Cell Physiol. 299 (2010) C175–C184.

[94] V.C. Lui, S.S. Lung, J.K. Pu, K.N. Hung, G.K. Leung, Invasion of human glioma cells is regulated by multiple chloride channels including ClC-3, Anticancer Res. 30 (2010) 4515–4524.

[95] G. Tabatabai, B. Frank, R. Mohle, M. Weller, W. Wick, Irradiation and hypoxia promote homing of haematopoietic progenitor cells towards gliomas by TGF-beta-dependent HIF-1alpha-mediated induction of CXCL12, Brain 129 (2006) 2426–2435.

[96] M. Kioi, H. Vogel, G. Schultz, R.M. Hoffman, G.R. Harsh, J.M. Brown, Inhibition of vasculogenesis, but not angiogenesis, prevents the recurrence of glioblastoma after irradiation in mice, J. Clin. Invest. 120 (2010) 694–705.

[97] S.V. Kozin, W.S. Kamoun, Y. Huang, M.R. Dawson, R.K. Jain, D.G. Duda, Recruitment of myeloid but not endothelial precursor cells facilitates tumor regrowth after local irradiation, Cancer Res. 70 (2010) 5679–5685.

[98] A.K. Weaver, M.L. Olsen, M.B. McFerrin, H. Sontheimer, BK channels are linked to inositol 1,4,5-triphosphate receptors via lipid rafts: a novel mechanism for coupling $[Ca^{2+}]_i$ to ion channel activation, J. Biol. Chem. 282 (2007) 31558–31568.

[99] C. Garcia-Moruja, J.M. Alonso-Lobo, P. Rueda, C. Torres, N. Gonzalez, M. Bermejo, F. Luque, F. Arenzana-Seisdedos, J. Alcami, A. Caruz, Functional characterization of SDF-1 proximal promoter, J. Mol. Biol. 348 (2005) 43–62.

[100] F. Li, P. Sonveaux, Z.N. Rabbani, S. Liu, B. Yan, Q. Huang, Z. Vujaskovic, M.W. Dewhirst, C.Y. Li, Regulation of HIF-1alpha stability through S-nitrosylation, Mol. Cell 26 (2007) 63–74.

[101] B.J. Moeller, Y. Cao, C.Y. Li, M.W. Dewhirst, Radiation activates HIF-1 to regulate vascular radiosensitivity in tumors: role of reoxygenation, free radicals, and stress granules, Cancer Cell 5 (2004) 429–441.

[102] M.J. Kim, R.K. Kim, C.H. Yoon, S. An, S.G. Hwang, Y. Suh, M.J. Park, H.Y. Chung, I.G. Kim, S.J. Lee, Importance of PKCdelta signaling in fractionated-radiation-induced expansion of glioma-initiating cells and resistance to cancer treatment, J. Cell Sci. 124 (2011) 3084–3094.

[103] C. Lagadec, E. Vlashi, L. Della Donna, C. Dekmezian, F. Pajonk, Radiation-induced reprogramming of breast cancer cells, Stem Cells 30 (2012) 833–844.
[104] K. Tamura, M. Aoyagi, N. Ando, T. Ogishima, H. Wakimoto, M. Yamamoto, K. Ohno, Expansion of CD133-positive glioma cells in recurrent de novo glioblastomas after radiotherapy and chemotherapy, J. Neurosurg. 119 (2013) 1145–1155.
[105] M. Gatti, A. Pattarozzi, A. Bajetto, R. Wurth, A. Daga, P. Fiaschi, G. Zona, T. Florio, F. Barbieri, Inhibition of CXCL12/CXCR4 autocrine/paracrine loop reduces viability of human glioblastoma stem-like cells affecting self-renewal activity, Toxicology 314 (2013) 209–220.
[106] G. Liu, X. Yuan, Z. Zeng, P. Tunici, H. Ng, I.R. Abdulkadir, L. Lu, D. Irvin, K.L. Black, J.S. Yu, Analysis of gene expression and chemoresistance of CD133^{+} cancer stem cells in glioblastoma, Mol. Cancer 5 (2006) 67.
[107] M.J. Jung, J.K. Rho, Y.M. Kim, J.E. Jung, Y.B. Jin, Y.G. Ko, J.S. Lee, S.J. Lee, J.C. Lee, M.J. Park, Upregulation of CXCR4 is functionally crucial for maintenance of stemness in drug-resistant non-small cell lung cancer cells, Oncogene 32 (2013) 209–221.
[108] M. Nakada, E. Nambu, N. Furuyama, Y. Yoshida, T. Takino, Y. Hayashi, H. Sato, Y. Sai, T. Tsuji, K.I. Miyamoto, A. Hirao, J.I. Hamada, Integrin alpha3 is overexpressed in glioma stem-like cells and promotes invasion, Br. J. Cancer 108 (2013) 2516–2524.
[109] P. Ruggieri, G. Mangino, B. Fioretti, L. Catacuzzeno, R. Puca, D. Ponti, M. Miscusi, F. Franciolini, G. Ragona, A. Calogero, The inhibition of KCa3.1 channels activity reduces cell motility in glioblastoma derived cancer stem cells, PLoS One 7 (2012) e47825.
[110] S. Rao, R. Sengupta, E.J. Choe, B.M. Woerner, E. Jackson, T. Sun, J. Leonard, D. Piwnica-Worms, J.B. Rubin, CXCL12 mediates trophic interactions between endothelial and tumor cells in glioblastoma, PLoS One 7 (2012) e33005.
[111] J.P. Greenfield, W.S. Cobb, D. Lyden, Resisting arrest: a switch from angiogenesis to vasculogenesis in recurrent malignant gliomas, J. Clin. Invest. 120 (2010) 663–667.
[112] H.S. Jang, S. Lal, J.A. Greenwood, Calpain 2 is required for glioblastoma cell invasion: regulation of matrix metalloproteinase 2, Neurochem. Res. 35 (2010) 1796–1804.
[113] C.M. Park, M.J. Park, H.J. Kwak, H.C. Lee, M.S. Kim, S.H. Lee, I.C. Park, C.H. Rhee, S.I. Hong, Ionizing radiation enhances matrix metalloproteinase-2 secretion and invasion of glioma cells through Src/epidermal growth factor receptor-mediated p38/Akt and phosphatidylinositol 3-kinase/Akt signaling pathways, Cancer Res. 66 (2006) 8511–8519.
[114] D.R. Maddirela, D. Kesanakurti, M. Gujrati, J.S. Rao, MMP-2 suppression abrogates irradiation-induced microtubule formation in endothelial cells by inhibiting alphavbeta3-mediated SDF-1/CXCR4 signaling, Int. J. Oncol. 42 (2011) 1279–1288.
[115] X.Z. Ye, S.L. Xu, Y.H. Xin, S.C. Yu, Y.F. Ping, L. Chen, H.L. Xiao, B. Wang, L. Yi, Q.L. Wang, X.F. Jiang, L. Yang, P. Zhang, C. Qian, Y.H. Cui, X. Zhang, X.W. Bian, Tumor-associated microglia/macrophages enhance the invasion of glioma stem-like cells via TGF-beta1 signaling pathway, J. Immunol. 189 (2012) 444–453.
[116] S. Bao, Q. Wu, S. Sathornsumetee, Y. Hao, Z. Li, A.B. Hjelmeland, Q. Shi, R.E. McLendon, D.D. Bigner, J.N. Rich, Stem cell-like glioma cells promote tumor angiogenesis through vascular endothelial growth factor, Cancer Res. 66 (2006) 7843–7848.
[117] R. Wang, K. Chadalavada, J. Wilshire, U. Kowalik, K.E. Hovinga, A. Geber, B. Fligelman, M. Leversha, C. Brennan, V. Tabar, Glioblastoma stem-like cells give rise to tumour endothelium, Nature 468 (2010) 829–833.

frontiers in
PHYSIOLOGY

REVIEW ARTICLE
published: 14 August 2013
doi: 10.3389/fphys.2013.00212

Ionizing radiation, ion transports, and radioresistance of cancer cells

Stephan M. Huber[1]*, Lena Butz[2], Benjamin Stegen[1], Dominik Klumpp[1], Norbert Braun[1], Peter Ruth[2] and Franziska Eckert[1]

[1] Department of Radiation Oncology, University of Tübingen, Tübingen, Germany
[2] Department of Pharmacology, Toxicology and Clinical Pharmacy, Institute of Pharmacy, University of Tübingen, Tübingen, Germany

Edited by:
Andrea Becchetti, University of Milano-Bicocca, Italy

Reviewed by:
Ildikò Szabò, University of Padova, Italy
Yinsheng Wan, Providence College, USA

***Correspondence:**
Stephan M. Huber, Department of Radiation Oncology, University of Tübingen, Hoppe-Seyler-Str. 3, 72076 Tübingen, Germany
e-mail: stephan.huber@uni-tuebingen.de

The standard treatment of many tumor entities comprises fractionated radiation therapy which applies ionizing radiation to the tumor-bearing target volume. Ionizing radiation causes double-strand breaks in the DNA backbone that result in cell death if the number of DNA double-strand breaks exceeds the DNA repair capacity of the tumor cell. Ionizing radiation reportedly does not only act on the DNA in the nucleus but also on the plasma membrane. In particular, ionizing radiation-induced modifications of ion channels and transporters have been reported. Importantly, these altered transports seem to contribute to the survival of the irradiated tumor cells. The present review article summarizes our current knowledge on the underlying mechanisms and introduces strategies to radiosensitize tumor cells by targeting plasma membrane ion transports.

Keywords: radiation therapy, cell cycle, DNA repair, ion channels

INTRODUCTION

Increasing pieces of evidence strongly indicate that ion transports across biological membranes fulfill functions beyond those described by classical physiology such as epithelial transports and neuronal or muscle excitability. More and more, it turns out that ion transports are involved in virtually all cell-biological processes. By modifying the chemistry, electricity and mechanics of cells, ion transports directly interact with cellular biochemistry and constitute signaling modules that are capable of altering protein function, gene expression (Tolon et al., 1996) and epigenetics (Lobikin et al., 2012). Moreover, ion transport-generating proteins such as ion channels have been identified to directly signal in macromolecular complexes with, e.g., surface receptors and downstream kinases (Arcangeli, 2011), or to directly bind to DNA as transcription factors (Gomez-Ospina et al., 2006).

Over the past two decades, ion transports came more and more in the focus of oncological research. Increasingly, data accumulate indicating tumor-suppressing as well as oncogenic functions of ion transport processes. In particular, ion transports have been identified as key regulators of neoplastic transformation, malignant progression, tissue invasion and metastasis (for review see Huber, 2013). Most recent data suggest that ion transports may also contribute to therapy resistance especially to radioresistance of tumor cells. The second chapter of this review article aims at giving an overview of those data. Since worldwide, only a handful of laboratories including ours are working in this research field only few data on ion transports in radioresistance are available and in most cases, the underlying molecular mechanisms of the observed phenomena remain ill-defined. Because tumor hypoxia is a major obstacle in radiotherapy, the second chapter also includes ion transports in the mitochondria that confer hypoxia resistance to normal tissue and probably also to tumor cells. At the end, this article provides some ideas how the acquired knowledge might be harnessed in the future for new strategies of anti-cancer therapy that combine ion transport-targeting and radiotherapy. To begin with, a brief introduction into radiotherapy and its radiobiological principles is given in the next paragraphs.

RADIOTHERAPY

According to the German Cancer Aid, 490,000 people in Germany are diagnosed with cancer every year (German-Cancer-Aid, 2013a) (data originating from February 2012), 218,000 die from their disease. About half of all cancer patients receive radiation treatment, half of all cures from cancer include radiotherapy (German-Cancer-Aid, 2013b). Radiotherapy is one of the main pillars of cancer treatment together with surgery and systemic therapy, mainly chemotherapy. Examples for curative radiotherapy without surgery are prostate (Eckert et al., 2013; Kotecha et al., 2013) and head and neck cancer (Glenny et al., 2010). Preoperative radiotherapy is applied in rectal cancer (Sauer et al., 2012), postoperative treatment in breast cancer (Darby et al.). Yet, also rare tumor entities like sarcoma and small cell carcinoma are treated with radiotherapy (Eckert et al., 2010a,b; Muller et al., 2012). Despite modern radiation techniques and advanced multimodal treatments local failures and distant metastases often limit the prognosis, especially due to limited salvage treatments (Muller et al., 2011; Zhao et al., 2012).

INTRINSIC AND HYPOXIC RADIORESISTANCE

Radiation therapy impairs the clonogenic survival of tumor cells mainly by causing double strand breaks in the DNA backbone. The number of double strand breaks increases linearly with the absorbed radiation dose (unit Gray, Gy). The intrinsic capacity

to repair these DNA damages by non-homologous end joining or homologous recombination determines how radio resistant a given tumor cell is. Irradiated tumor cells which leave residual DNA double strand breaks unrepaired lose their clonogenicity meaning that these cells cannot restore tumor mass. Ion transports may directly be involved in the cellular stress response to DNA damage by controlling cell cycle, metabolic adaptations or DNA repair and, thus, contribute to intrinsic radioresistance and the survival of the tumor cell.

Besides intrinsic factors, the microenvironment influences the radiosensitivity of a tumor. Hypoxic areas frequently occur in solid tumors. Hypoxic tumor cells, however, are somehow "protected" from radiotherapy [reviewed in Harada (2011)]. This is because ionizing radiation generates directly or indirectly radicals in the deoxyribose moiety of the DNA backbone. In a hypoxic atmosphere, thiols can react with those DNA radicals by hydrogen atom donation which results in chemical DNA repair. In the presence of oxygen, in contrast, oxygen fixes radicals of the deoxyribose moiety to strand break precursors (Cullis et al., 1987). This so called oxygen effect radiosensitizes tumor cells by a factor of two to three (oxygen enhancement ratio) as compared to the hypoxic situation (Langenbacher et al., 2013). Accordingly, patients with hypoxic tumors who undergo radiotherapy have a worse prognosis than those with normoxic tumors [e.g., cervical cancer (Fyles et al., 2002, 2006)]. Notably, ion transport processes have been identified as important players in the adaptation of tumor cells to a hypoxic microenvironment. Hence, ion transports via adaptation to hypoxia also indirectly contribute to the radioresistance of tumors.

In radiotherapy, fractionated treatment regimens have been established which may reoxygenate and thereby radiosensitize the irradiated tumor during therapy time. In addition, fractionated radiotherapy spaces out the single fractions in a way that allows DNA repair of normal tissue, that re-distribute cell cycle of the tumor cells in more sensitive phases and that minimize repopulation of the tumor during therapy. The next paragraphs will give an introduction to the underlying radiobiology.

FRACTIONATED RADIATION THERAPY. REPAIR, REOXYGENATION, REDISTRIBUTION, AND REPOPULATION

Early in historic development of radiotherapy fractionation was introduced as a means to limit side effects when giving therapeutic radiation doses (Bernier et al., 2004). Standard fractionation is defined as single doses of 1.8–2 Gy, once daily, 5 days per week.

The principal rationale for fractionation is based on the fact that recovery after radiation is better in normal tissue than in tumors, especially concerning late reacting tissues responsible for late side effects of radiotherapy (Jones et al., 2006) such as fibrosis, damage of spinal cord and brain, as well as most inner organs. Radiation with high single doses is only possible without increased side effects if the radiation field can be confined to the tumor (e.g., stereotactic radiotherapy of brain metastases [Rodrigues et al., 2013) and SBRT, stereotactic body radiation therapy (Grills et al., 2012)]. Yet, many situations in radiation oncology such as adjuvant treatment or irradiation of nodal regions require irradiation of significant volumes of normal tissue.

Alpha-beta ratios

Acute effects of ionizing irradiation on clonogenic cell survival *in vitro* as well as on late toxicity of the normal tissue in patients which underwent radiotherapy are described by the linear-quadratic model (Barendsen, 1982; Dale, 1985). The mathematical fit of the clonogenic survival (late toxicity) is calculated as follows: $N = N_0 \times E^{-(\alpha D - \beta D\hat{}2)}$ with N being the number of surviving cells (patients without late toxicity), N_0 being the initial number of cells (number of patients receiving radiotherapy), α [1/Gy] and β [1/Gy^2] being cell (tissue)-specific constants and D the delivered radiation dose. Low alpha-beta ratios (α/β) [Gy] as determined for many normal tissues indicate that dose fractionation in daily fractions of usually 2 Gy increases survival and decreases late toxicity as compared to a single equivalent dose. Tumors with high alpha-beta ratios, in contrast do not benefit from fractionation. For some tumors such as squamous cell carcinoma of the head and neck there is even a rationale for hyperfractionated radiotherapy with twice daily irradiation of 1.2–1.4 Gy per fraction [reviewed in Nguyen and Ang (2002)]. The theoretical advantage has been confirmed in clinical trials [e.g., EORTC trial 22791 in advanced head and neck cancer Horiot et al. (1992)]. Different fractionation schedules for distinct clinical situations are applied for example in whole-brain radiotherapy. In prophylactic radiation 2–2.5 Gy fractions are applied to limit neurocognitive deficits (Auperin et al., 1999; Le Pechoux et al., 2011; Eckert et al., 2012). For therapeutic radiation 3 Gy fractions or even 4 Gy fractions are preferred in a palliative setting and limited life expectancy to shorten the treatment time to 5 or 10 days (Lutz, 2007; Rades et al., 2007a,b).

Reoxygenation

As mentioned above, fractionated radiation may also lead to reoxygenation of the tumor during therapy (Withers, 1975; Pajonk et al., 2010). Blood vessels of tumors lack normal architecture and are prone to collapse whenever tissue pressure of the expanding tumor mass increases. This aggravates tumor malperfusion and accelerates intermittent or chronic tumor hypoxia. Being sublethal as related to the whole tumor, single radiation fractions in the range of 2 Gy kill a significant percentage of the tumor cells which give rise to tumor shrinkage. Shrinkage, in turn, is thought to increase blood and oxygen supply of the tumor by improving vessel perfusion and by increasing the ratio of vascularization and the residual tumor mass (Maftei et al., 2011; Narita et al., 2012). Increased oxygenation then reverses hypoxic radioresistance of the tumor and improves the therapeutic outcome of radiotherapy.

Redistribution and repopulation

The sensitivity to radiotherapy during cell cycle differs, being highest in M and lowest in late S phase of cell cycle (Pawlik and Keyomarsi, 2004). Often depending on p53 function, irradiated tumor cells accumulate in G_1 or G_2 phase of cell cycle to repair their DNA damages. In a radiation dose-dependent manner, irradiated cells are released from cell cycle arrest and re-enter cell

cycling and tumor repopulation. Importantly, repopulation after irradiation is often accelerated probably due to selection of more aggressive tumor cells (Marks and Dewhirst, 1991). Fractionated radiation regimes aim to re-distribute tumor cells in a more vulnerable phase of the cell cycle in the time intervals between two fractions and to impair repopulation (Pawlik and Keyomarsi, 2004).

CANCER STEM CELLS (CSCs)

Cancer stem cells (CSCs) may resist radiation therapy [for review see Pajonk et al. (2010)]. Mechanisms that might contribute to the relative resistance of CSCs as compared to the non-CSC cells of a given tumor include (i) higher oxidative defense and, therefore, lower radiation-induced insults, (ii) activated DNA checkpoints resulting in faster DNA repair, and (iii) an attenuated radiation-induced cell cycle redistribution. Fractionation regimes are designed that way that the macroscopically visible bulk of tumor cells (i.e., the non CSCs) and not the rare CSCs become redistributed into a more vulnerable phase of cell cycle between two consecutive fractions of radiotherapy. Finally, radiation therapy is thought to switch CSCs from an asymmetrical into a symmetrical mode of cell division; i.e., a CSC which normally divides into a daughter CSC and a lineage-committed progenitor cell is induced by the radiotherapy to divide symmetrically into two proliferative stem daughter cells. This is thought to accelerate repopulation of the tumor after end of radiotherapy (Pajonk et al., 2010).

In summary, fractionated radiotherapy may radio sensitize tumor cells by reoxygenation of the tumor and redistribution of the tumor cells in more vulnerable phases of cell cycle while protecting at the same time normal tissue if the alpha-beta ratio of the tumor exceeds that of the normal tissue. On the other hand, the applied fractionation protocols might spare CSCs due to their radiobiology that differs from that of the bulk of non-CSCs. Furthermore, single radiation fractions apply sublethal doses of ionizing radiation. Data from *in vitro* and animal studies suggest that sublethal doses of ionizing radiation may stimulate migration and tissue invasion of the tumor cells. Translated into the *in vivo* situation, this might imply that cells at the edge of solid tumors might be stimulated by the first radiation fractions to migrate out of the target volume of radiation resulting in survival of the evaded cells and tumor relapse. Moreover, if radiation fractions further induce tumor cell invasion into blood or lymph vessels, fractionated radiotherapy regimes might also boost metastases. As described in the next paragraphs, ion transports fulfill pivotal functions in cell migration especially in radiation-induced migration.

ION TRANSPORTS AND RADIORESISTANCE

Ion transports can be assessed by tracer-flux measurements, fluorescence microscopy/photometry using ion species-specific fluorescence dyes such as the Ca^{2+}-specific fluorochrome fura-2, as well as by electrophysiological means. The latter can be applied if ion transports are electrogenic. Measurements of ion transports during treatment with ionizing radiation are hardly feasible. Reported electrophysiological *in vitro* data on irradiated tumor cells indicate that radiation-induced transport modifications may occur instantaneously and may last up to 24 h post irradiation (Kuo et al., 1993). They further suggest that these modifications may be induced by doses used for single fractions in the clinic (Steinle et al., 2011). The following paragraphs summarize radiation-induced transport modifications as observed in *in vitro* studies on tumor cell lines and their putative contribution to the radioresistance of tumor cells. Whether these processes may indeed underlie therapy failure in tumor patients can only be answered if more data from tumor mouse models and clinical trials become available.

Tumor cells have been proposed to adapt either a "Grow" or a "Go" phenotype in dependence on changes in their microenvironment. When developing a certain mass, growing solid tumors are prone to become malperfused because of the insufficient tumor vasculature. As a consequence of malperfusion, microenvironmental stress by hypoxia, interstitial nutrient depletion, and low pH increases (Stock and Schwab, 2009; Hatzikirou et al., 2012) which is thought to trigger at a certain point the induction of the "Go" phenotype. By migration and tissue invasion "Go" tumor cells may evade the locally reined stress burden and resettle in distant and less hostile regions. Once re-settled, tumor cells may readapt the "Grow" phenotype by reentering cell cycling and may establish tumor satellites in more or less close vicinity of the primary focus. Moreover, this stress evasion may lead to metastases if the "Go" cells invade into blood or lymph vessels.

Migration and tissue invasion are directed by extracellular hapto- and chemotactic signals which trigger preset "Go" programs (Schwab et al., 2007, 2012). The latter comprise intracellular signaling, cellular motor functions including cell volume changes and cytoskeletal dynamics, as well as extracellular matrix digestion and reorganization. Ion transports have been suggested to contribute to all of these processes (Schwab et al., 2007, 2012). As a matter of fact, highly invasive and metastatic phenotypes of tumor cells often show aberrant activity of certain ion transports. The following paragraphs describe the role of these ion transports in particular of those across the plasma membrane using the example of glioblastoma cells.

MOTOR FUNCTION

Glioblastoma cells exhibit a highly migrative phenotype and "travel" long distances throughout the brain (Johnson et al., 2009). Primary foci of glioblastoma show, therefore, even at early stages of diagnosis a characteristic diffuse and net-like brain infiltration (Niyazi et al., 2011). Tumor margins are often not definable and complete surgical tumor resection as well as capture of all residual tumor cells by the radiation target volume is hardly possible (Weber et al., 2009). This results in therapy failure accompanied by very bad prognosis for the survival of the patient in almost all cases of glioblastoma (Niyazi et al., 2011). Glioblastoma cells typically migrate into the surrounding brain parenchyma primarily by using nerve bundles and the vasculature as tracks. The close vicinity to the vasculature has the advantage for the migrating glioblastoma cell of a continuous and sufficient supply of oxygen, nutrients, growth factors, chemokines, and cytokines (Montana and Sontheimer, 2011). Glioblastoma cells have to squeeze through very narrow interstitial spaces during their brain invasion along those tracks. This

requires highly effective local cell volume decrease and re-increase procedures. Notably, glioblastoma cells are capable to lose all unbound cell water leading to maximal cell shrinkage (Watkins and Sontheimer, 2011). Unusually high cytosolic Cl^- concentrations (100 mM) provide the electrochemical driving force for this tremendous cell volume decrease. The cytosolic Cl^- concentration is built up highly above its electrochemical equilibrium concentration by the Na/K/2Cl cotransporter NKCC1 (Haas and Sontheimer, 2010; Haas et al., 2011) allowing glioblastoma cells to utilize Cl^- as an osmolyte.

Local regulatory volume increase and decrease have been proposed to drive migration mechanics. The latter is generated by the loss of Cl^- and K^+ ions along their electrochemical gradients followed by osmotically obliged water fluxes. Involved transporters probably are ClC-3 Cl^- channels (Olsen et al., 2003; Cuddapah and Sontheimer, 2010; Lui et al., 2010), Ca^{2+}-activated high conductance BK (Ransom and Sontheimer, 2001; Ransom et al., 2002; Sontheimer, 2008) as well as intermediate conductance IK K^+ channels (Catacuzzeno et al., 2010; Sciaccaluga et al., 2010; Ruggieri et al., 2012) and AQP-1 water channels (Mccoy and Sontheimer, 2007; Mccoy et al., 2010). To a lower extent, K^+ and Cl^- efflux is probably also mediated by KCC1-generated cotransport (Ernest et al., 2005). These transports are crucial for glioblastoma migration since either transport blockade inhibits glioblastoma cell migration and invasion (Ernest et al., 2005; Mcferrin and Sontheimer, 2006; Catacuzzeno et al., 2010; Haas and Sontheimer, 2010; Lui et al., 2010; Sciaccaluga et al., 2010).

Notably, Ca^{2+}-activated BK (Ransom and Sontheimer, 2001; Liu et al., 2002; Ransom et al., 2002; Weaver et al., 2006) and IK K^+ channels (Ruggieri et al., 2012) are ontogenetically down-regulated or absent in mature glial cells but up-regulated with neoplastic transformation and malignant tumor progression as shown in expression studies in human glioma tissue. Moreover, glioblastoma cells up-regulate a unique splice variant of the BK channel (Liu et al., 2002) which exhibits a higher Ca^{2+} sensitivity than the other isoforms (Ransom et al., 2002) and is indispensable for glioblastoma proliferation *in vitro*. Similarly, ClC-3 Cl^- channels are mal-expressed in glioblastoma tissue where they traffic, in contrast to normal tissue, to the plasma membrane (Olsen et al., 2003). The predominant (surface) expression of ClC-3 and the BK splice variant by glioblastoma cells renders both channel types putative glioblastoma-specific therapeutic targets.

EVASION FROM RADIATION STRESS

External beam radiation may induce the "Go" phenotype in tumor cells similarly to the situation described for stress arising from an adverse tumor microenvironment (**Figure 1**). Ionizing radiation at doses used in single fractions during fractionated radiotherapy has been demonstrated *in vitro* and by a mouse study (Wild-Bode et al., 2001) to induce migration, invasion and spreading of head and neck squamous carcinoma (Pickhard et al., 2011), lung adenocarinoma (Jung et al., 2007; Zhou et al., 2011), meningioma (Kargiotis et al., 2008), medulloblastoma (Asuthkar et al., 2011), and glioblastoma cells (Wild-Bode et al., 2001; Wick et al., 2002; Badiga et al., 2011; Canazza et al., 2011; Rieken et al., 2011; Steinle et al., 2011; Kil et al., 2012; Vanan et al., 2012). The phenomenon of radiation-stimulated migration might be particularly relevant for highly migrating and brain-infiltrating glioblastoma cells.

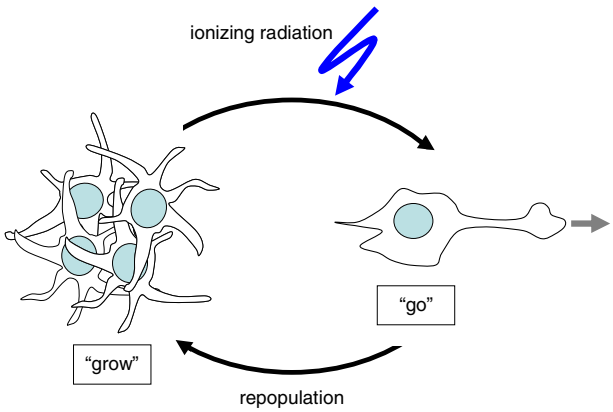

FIGURE 1 | Cellular stress such as ionizing radiation induces the switch from "Grow" to "Go" phenotype.

After macroscopic complete resection glioblastoma is usually treated by adjuvant radiotherapy of the tumor bed applying 54–60 Gy in daily fractions of 1.8–2 Gy combined with temozolomide (Stupp et al., 2005). The median progression-free survival after therapy ranges between 5 and 7 months (Stupp et al., 2005). The recurrence of glioblastoma is typically observed within the former target volume of the adjuvant fractionated radiotherapy. This might be due either to a high intrinsic radioresistance of the glioblastoma cells or to re-invasion of tumor cells into the area of the irradiated primary. One might speculate that this necrotic area, meanwhile cleared by phagocytes, offers optimal growth conditions for such re-invading tumor cells. In this latter scenario, re-invading cells might be recruited from glioblastoma (stem) cells pre-spreaded prior to radiotherapy onset in areas outside the target volume, or from cells that successfully evaded during radiation therapy.

Radiation-induced up-regulation of integrin- (Wild-Bode et al., 2001; Nalla et al., 2010; Canazza et al., 2011; Rieken et al., 2011), VEGF- (Sofia Vala et al., 2010; Badiga et al., 2011; Kil et al., 2012), EGF- (Kargiotis et al., 2008; Pickhard et al., 2011) or/and TGFbeta signaling (Canazza et al., 2011; Zhou et al., 2011) has been proposed to promote tumor cell migration. Downstream ion transport processes have been reported for glioblastoma cells (Steinle et al., 2011). In this study, BK K^+ channel activation and subsequent BK-dependent activation of the CaMKII kinase were identified as key triggers of radiation-induced migration (Steinle et al., 2011). Additionally, ClC-3 anion channels were identified as downstream targets of radiation-induced CaMKII activity (Huber, 2013). This suggests on the one hand motor function (i.e., volume decrease) of radiation-induced BK and ClC-3 currents, on the other hand, it points to a signaling function of BK channels in the programming of radiation-stimulated glioblastoma migration (**Figure 2**). Similar to the situation in migrating glioblastoma cells, radiation-induced plasma membrane K^+ currents and downstream CaMKII activation have been defined as key signaling events in cell cycle control of irradiated leukemia cells as introduced in the following paragraphs.

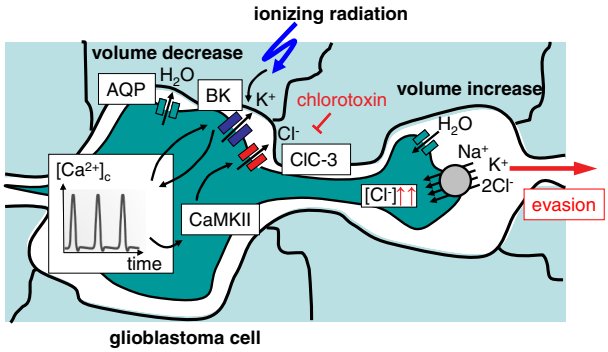

FIGURE 2 | Ionizing radiation (IR)-induced activation of BK K^+ channels results in evasion of glioblastoma cells from radiation stress. Activation of BK channels occurs upstream of CaMKII and ClC-3 Cl^- channels. The $Na^+/K^+/2Cl^-$ cotransporter accumulates Cl^- above its electrochemical equilibrium. Cl^- is used as osmolyte for volume decrease.

DNA REPAIR

Survival of irradiated tumor cells critically depends on DNA repair. This involves cell cycle arrest, elevated energy consumption, chromatin relaxation, and formation of repair complexes at the site of DNA damage. Recent *in vitro* observations suggest that radiation-induced ion transports may contribute to these processes in an indirect manner.

Cell cycle control

Survival of irradiated human leukemia cells depends on Ca^{2+} signaling. Radiation reportedly stimulates Ca^{2+} entry through TRPV5/6-like channels and subsequently activates CaMKII, which in turn fosters G_1/S transition, S progression and accumulation in G_2 phase of the cell cycle (Heise et al., 2010). Moreover, Ca^{2+} signaling in human leukemia cells has been demonstrated to be tightly regulated by voltage-gated $K_v3.4$ K^+ channels and translates into G_2/M cell cycle arrest by CaMKII-mediated inhibitory phosphorylation of the phosphatase cdc25B resulting in inactivation of the mitosis promoting factor and G_2/M arrest. Radiation activates Kv3.4 currents without changing the surface expression of the channel protein. Most importantly, inhibition of $K_v3.4$ by tetraethylammonium and blood-depressing substance-1 and substance-2 or silencing of the $K_v3.4$ channels by RNA interference prevents TRPV5/6-mediated Ca^{2+} entry, CaMKII activation, as well as cdc25B inactivation which results in release from radiation-induced G_2/M arrest, increased apoptosis, and decreased clonogenic survival. Thus, targeting of $K_v3.4$ radiosensitizes the leukemia cells demonstrating the pivotal role of this channel in cell cycle arrest required for DNA repair (Palme et al., 2013). Similar results have been obtained in prostate cancer cells, where TRPV6 inhibition by capsaicin resulted in radiosensitization (Klotz et al., 2011).

Glucose fueling and chromatin relaxation

In addition to cell cycle control, radiation-induced ion transports are proposed to improve glucose fueling of irradiated tumor cells. Fast proliferating tumor cells have a high metabolism at low external glucose and oxygen concentration in the usually chronically under-perfused growing tumor tissue. At the same time, many tumor cells cover their high energy requirements by anaerobic glycolysis with low ATP yield per metabolized glucose even under normoxic conditions. To sustain sufficient glucose fueling, tumor cells may up-regulate the Na^+/glucose cotransporter (SGLT). SGLTs are capable to take up glucose into the tumor cell even against a high chemical gradient (Ganapathy et al., 2009). Several tumor entities such as colorectal, pancreatic, lung, head and neck, prostate, kidney, cervical, mammary, and bladder cancer as well as chondrosarcomas and leukemia have indeed been shown to up-regulate SGLTs (Nelson and Falk, 1993; Ishikawa et al., 2001; Helmke et al., 2004; Casneuf et al., 2008; Weihua et al., 2008; Yu et al., 2008; Leiprecht et al., 2011; Wright et al., 2011). The inwardly directed Na^+ gradient and the voltage across the plasma membrane drive the electrogenic SGLT-generated glucose transport into the cell. The membrane voltage is tightly regulated by the activity of voltage gated K^+ channels which counteract SGLT-mediated depolarization.

Ionizing radiation has been demonstrated to activate EGF receptors (Dittmann et al., 2009). In addition, SGLT1 reportedly is in complex with and under the direct control of the EGF receptor (Weihua et al., 2008) suggesting radiation-induced SGLT1 modifications. As a matter of fact, ionizing radiation stimulates a long lasting EGFR-dependent and SGLT-mediated glucose uptake in A549 lung adenocarcinoma and head and neck squamous carcinoma cell lines (but not in non-transformed fibroblasts) as shown by ^{3}H-glucose uptake and patch-clamp, current clamp recordings (Huber et al., 2012). In the latter experiments, radiation-induced and SGLT-mediated depolarization of membrane potential was preceded by a transient hyperpolarization of the plasma membrane indicative of radiation-induced K^+ channel activation (Huber et al., 2012). Such radiation-induced increase in K^+ channel activity has been reported for several tumor cell lines including A549 lung adenocarcinoma cells (Kuo et al., 1993). In this cell line, radiation at doses between 0.1 and 6 Gy stimulates the activity of voltage gated K^+ channels within 5 min, which gradually declines thereafter. It is tempting to speculate that this radiation-stimulated K^+ channel activity counteracts the depolarization of the membrane potential caused by the SGLT activity shortly after radiation and sustains the driving force for Na^+-coupled glucose uptake (Huber et al., 2012).

Ionizing radiation may lead to necrotic as well as apoptotic cell death depending on cell type, dose, and fractionation (Verheij, 2008). In particular, necrotic cell death may be associated with ATP depletion (Dorn, 2013). Increased SGLT activity in irradiated tumor cells might contribute to ATP replenishment counteracting necrotic cell death. Such function has been suggested in irradiated A549 cells by experiments analyzing cellular ATP concentrations, chromatin remodeling, residual DNA damage, and clonogenic survival of irradiated tumor cells (Dittmann et al., 2013). The data demonstrate that radiation of A549 lung adenocarcinoma cells leads to a transient intracellular ATP depletion and to histone H3 modifications crucial

for both chromatin remodeling and DNA repair in response to irradiation.

Importantly, recovery from radiation-induced ATP crisis was EGFR/SGLT-dependent and associated with improved DNA-repair and increased clonogenic cell survival. The blockade of either EGFR or SGLT inhibited ATP level recovery and histone H3 modifications. *Vice versa*, inhibition of the acetyltransferase TIP60, which is essential for histone H3 modification, prevented chromatin remodeling as well as ATP crisis (Dittmann et al., 2013). Together, these data suggest that radiation-associated interactions between SGLT1 and EGFR result in increased glucose uptake, which counteracts the ATP crisis in tumor cells caused by chromatin remodeling. Importantly, the blockade of recovery from ATP crisis by SGLT1 inhibition may radio-sensitize tumor cells as demonstrated in lung adenocarcinoma and head and neck squamous carcinoma cell lines (Huber et al., 2012; Dittmann et al., 2013).

Formation of repair complexes

In addition to SGLT-generated glucose uptake, radiation-induced electrosignaling via transient receptor potential melastatin 2 (TRPM2) and vanilloid 1 (TRPV1) cation channels, has been shown to stimulate Ataxia telangiectasia mutated (ATM) kinase activation, histone 2AX (H2AX) phosphorylation, and γH2AX focus formation in A549 lung adenocarcinoma cells, processes required to recruit further repair proteins to the DNA double strand break (Masumoto et al., 2013). Furthermore, radiation-induced TRPM2 induces ATP release and P2Y signaling in A549 cells (Masumoto et al., 2013). Radiation-stimulated and $P2X_7$ receptor- and gap junction hemichannel connexin43-mediated ATP release has been suggested to signal in a paracrine manner to unirradiated bystander cells in the B16 melanoma model (Ohshima et al., 2012).

Combined, these recent data indicate that ion transports may regulate processes that mediate intrinsic radioresistance. The investigation of ion transports in radiobiology is at its very beginning and the few data available are mostly phenomenological in nature. The molecular mechanisms that underlie, e.g., regulation of DNA repair by ion transports are ill-defined. Nevertheless, the data prove functional significance of ion transports and electrosignaling for the survival of irradiated tumor cells and might have translational implications for radiotherapy in the future.

Similar to intrinsic radioresistance, the function of ion transports in hypoxia resistance and associated hypoxic radioresistance of tumor cells is not well-defined. The following paragraphs give a summary of what is known about mitochondrial transports and hypoxia resistance of normal tissue and how these findings might also apply for tumor cells.

MITOCHONDRIAL UNCOUPLING AND RESISTANCE TO HYPOXIA, CHEMO-, AND RADIOTHERAPY

Intermittent hypoxia is a common feature of vascularized solid tumors. The pathophysiologial aspects of hypoxia and reoxygenation are well-known from ischemia-reperfusion injuries observed in normal tissue. Reoxygenation-associated production of reactive oxygen species (ROS) is a major cause of the hypoxia/reoxygenation injury after myocardial, hepatic, intestinal, cerebral, renal and other ischemia and mitochondria have been identified as one of the main sources of ROS formation herein (Li and Jackson, 2002). Mitochondrial ROS formation mutually interacts with hypoxia/reoxygenation-associated cellular Ca^{2+} overload. Brief hypoxic periods induce an adaptation to hypoxia in several tissues which lowers ischemia-reperfusion injuries of subsequent ischemic insults (so-called ischemic preconditioning). Similar adaptations which involve alterations in mitochondrial ion transport have been proposed to confer hypoxia resistance of tumor cells.

Mitochondrial ROS formation

Activity and efficacy of the mitochondrial respiration chain are fine-tuned by the dependence of the ATP synthase (complex V) on the membrane potential $\Delta\Psi_m$, by the ATP/ADP ratio, as well as by reversible phosphorylation of the complexes I and IV (**Figure 3**) (Kadenbach, 2003). It is suggested that under physiological conditions (high ATP/ADP ratios), the membrane potential $\Delta\Psi_m$ is kept low [around −100 to −150 mV (Kadenbach, 2003)]. The efficacy of the respiratory chain at low $\Delta\Psi_m$ is high. At higher ATP demand or decreasing cellular ATP levels, cytochrome c oxidase (complex IV) is relieved from ATP blockade and $\Delta\Psi_m$ increases. High $\Delta\Psi_m$ values (up to −180 mV), however, lower the efficacy of cytochrome c oxidase (Kadenbach, 2003) and increase the probability of single electron leakage at complex I and III to molecular oxygen resulting in an increased $O_2{\cdot}^-$ production (**Figure 3**) (Korshunov et al., 1997; Skulachev, 1998; Kadenbach, 2003).

The respiratory chain is also regulated by the cytosolic ($[Ca^{2+}]_i$) and mitochondrial matrix free Ca^{2+} concentration ($[Ca^{2+}]_m$) in a complex manner (for review see Pizzo et al., 2012). The phosphatases that dephosphorylate (and thereby switch-off) the NADH oxidase and that relieve the ATP blockade of complex IV are inhibited by $[Ca^{2+}]_m$ and activated by $[Ca^{2+}]_i$, respectively (**Figure 3**). As a consequence, increase in $[Ca^{2+}]_m$ and $[Ca^{2+}]_i$ results in a higher $\Delta\Psi_m$ and a concurrently increased production of reactive oxygen species (Kadenbach, 2003).

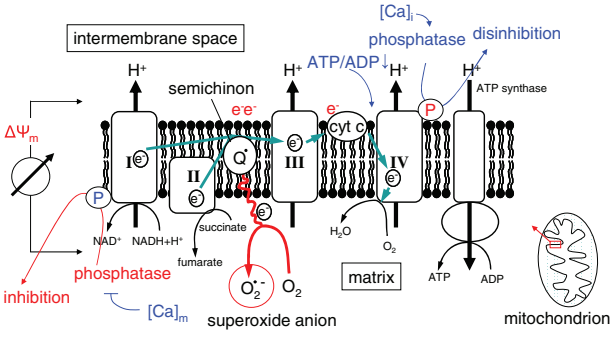

FIGURE 3 | Mitochondrial ROS formation in dependence on $\Delta\Psi_m$ (I, II, III, and IV, electron transport complexes I, II, III, and IV; Q: semiquinone radical; cyt C: cytochrome C). Ca^{2+} and the ATP/ADP ratio regulate the electron chain at complexes I and IV.

Hypoxia decreases the activity of the mitochondrial manganese superoxide dismutase (Mn-SOD) and of the cytochrome c oxidase. Depletion of the final electron acceptor, however, increases the formation of $O_2{\cdot}^-$ during reoxygenation by the enhanced leakage of single electrons from more proximal complexes of the respiration chain (for review see Li and Jackson, 2002; Sack, 2006). Lowered $O_2{\cdot}^-$-detoxifying capability combined with simultaneous elevated $O_2{\cdot}^-$ production results in a highly elevated $O_2{\cdot}^-$ concentration which, e.g., in hepatocytes increases 15-fold within 15 min of reoxygenation (Caraceni et al., 1995).

Hypoxia/reoxygenation-associated Ca^{2+} overload

Hypoxia-associated energy depletion and the concomitant impairment of plasma membrane Na^+ and Ca^{2+} pump activity lead to a decline of the chemical Na^+, Ca^{2+} and K^+ gradients across the plasma membrane and to the depolarization of the plasma membrane potential. In parallel, increased lactic acid fermentation during hypoxia increases the cytosolic proton concentration and lowers the intracellular pH. The proton extrusion machinery that is already active during hypoxia becomes massively activated during reoxygenation and restores a physiological pH by wash-out of lactic acid and activation of the sodium/hydrogen exchanger and sodium/bicarbonate symporter. The latter, Na^+-coupled transports, in turn, further increase the cytosolic Na^+ concentration to a level, where the low affinity high capacity sodium/calcium exchanger in the plasma membrane starts to operate in the reverse mode (i.e., to extrude Na^+ at the expense of Ca^{2+} uptake). At that time, reoxygenation-mediated oxidative stress (see above) stimulates further Ca^{2+} entry through Ca^{2+}-permeable channels in the plasma membrane and the release of Ca^{2+} from the endoplasmic reticulum resulting in an abrupt rise in $[Ca^{2+}]_i$ during the first minutes of reoxygenation. Cytosolic Ca^{2+} is buffered by $\Delta\Psi_m$-driven and uniporter-mediated Ca^{2+} uptake into the mitochondrial matrix which increases $[Ca^{2+}]_m$. Elevated $[Ca^{2+}]_m$ and $[Ca^{2+}]_i$ values, in turn, signal back to the respiratory chain by further increasing $\Delta\Psi_m$ (see above). Exceeding the Ca^{2+} threshold concentration in the matrix, $[Ca^{2+}]_m$ activates the permeability transition pore which leads to breakdown of $\Delta\Psi_m$, swelling of the mitochondrial matrix and eventually release of cytochrome c from the intermembrane space into the cytosol (Crompton, 1999; Rasola and Bernardi, 2011). By reversing the ATP synthase activity, into the ATPase proton pump mode, the F_0/F_1 complex in the inner mitochondrial delays the break-down of $\Delta\Psi_m$ at the expense of ATP hydrolysis. In addition to this ATP depletion, the loss of cytochrome c and the concurrent decline of the final electron acceptor (cytochrome c oxidase of complex IV) further increases the formation of $O_2{\cdot}^-$ by more proximal complexes. The pivotal role of membrane transports in this process is illustrated by the fact that inhibition of the sodium/hydrogen antiporter in the plasma membrane, the Ca^{2+} uniporter in the inner mitochondrial membrane, or Ca^{2+} channels in the endoplasmic reticulum (ER) decreases the hypoxia/reoxygenation injury *in vitro* (for review see Crompton, 1999; Li and Jackson, 2002; Sack, 2006; Yellon and Hausenloy, 2007).

Ischemic pre-conditioning

Cells can also adapt to repetitive periods of hypoxia. This so-called ischemic preconditioning has been demonstrated in the myocardium where it reduces ischemia-caused infarct size, myocardial stunning, and incidence of cardiac arrhythmias (Gross and Peart, 2003). Since mitochondrial ROS formation increases with increasing $\Delta\Psi_m$ (Korshunov et al., 1997; Skulachev, 1998; Kadenbach, 2003) lowering of the mitochondrial $\Delta\Psi_m$ is proposed to be a key adaptation event in ischemic preconditioning (Sack, 2006). Lowering of $\Delta\Psi_m$ reduces not only mitochondrial $O_2{\cdot}^-$ production but also the mitochondrial Ca^{2+} overload during reoxygenation (Gross and Peart, 2003; Prasad et al., 2009). The hypoxic preconditioning-associated reduction of $\Delta\Psi_m$ is in part achieved by up-regulation of ATP-sensitive (mitoKATP) and Ca^{2+}-activated (mitoKCa) K^+ channels in the inner mitochondrial membrane which short-circuit $\Delta\Psi_m$ (Murata et al., 2001; Gross and Peart, 2003; Prasad et al., 2009; Singh et al., 2012; Szabo et al., 2012). The uncoupling proteins-2 and -3 (UCP-2, -3) constitute two further proteins that have been suggested to play a role in counteracting cardiac hypoxia/reoxygenation injury and in hypoxic preconditioning in heart and brain (Mcleod et al., 2005; Sack, 2006; Ozcan et al., 2013). Activation of these proteins results in a modest depolarization of $\Delta\Psi_m$ by maximally 15 mV (Fink et al., 2002). High expression of UCP-3 has also been demonstrated in skeletal muscle where it suppresses mitochondrial oxidant emission during fatty acid-supported respiration (Anderson et al., 2007). Accordingly, overexpression of UCP-3 in cultured human muscle cells lowers $\Delta\Psi_m$, raises the ATP/ADP ratio, and favors fatty acid vs. glucose oxidation (Garcia-Martinez et al., 2001). Conversely, knockdown of UCP-3 increased the coupling between electron and proton transfer across the inner mitochondrial membrane and ROS production (Vidal-Puig et al., 2000; Talbot and Brand, 2005). UCP-3 protein is robustly up-regulated in chondrocytes (Watanabe et al., 2008) and skeletal muscle during hypoxia and the absence of UCP-3 exacerbates hypoxia-induced ROS (Lu and Sack, 2008). UCP-3 is not constitutively active. $O_2{\cdot}^-$ has been demonstrated to stimulate the activity of UCP-3 in skeletal muscle suggesting that UCP-3 is the effector of a feed back loop which restricts overshooting ROS production (Echtay et al., 2002).

Mitochondrial uncoupling in tumor cells

Recent studies suggest that UCPs are upregulated in a number of aggressive human cancers. In particular, over-expression of UCP2 has been reported in leukemia as well as in breast, colorectal, ovarian, bladder, esophagus, testicular, kidney, pancreatic, lung, and prostate cancer (Ayyasamy et al., 2011; Su et al., 2012). In human colon cancer, UCP2 mRNA and protein expression reportedly is increased by factor of 3–4 as compared to peritumoral normal epithelium. In addition, UCP2 expression gradually increases during the colon adenoma-carcinoma sequence (Horimoto et al., 2004) and is higher in clinical stages III and IV colon cancer than in stage I and II (Kuai et al., 2010). Similarly, UCP4 expression has been shown to correlate with lymph node metastases in breast cancer (Gonidi et al., 2011) and UCP1 expression in prostate cancer with disease progression from primary to bone metastatic cancers (Zhau et al., 2011). Moreover, postmenopausal breast

tumors with low estrogen receptor (ER) alpha to ER beta ratios that associate with higher UCP5 expression and higher oxidative defense have a poor prognosis (Sastre-Serra et al., 2013). Finally, ectopic expression of UCP2 in MCF7 breast cancer cells has been demonstrated to enhance proliferation, migration and matrigel invasion *in vitro* and to promote tumor growth *in viv*o (Ayyasamy et al., 2011). Together, these observations suggest that UCPs may contribute to the malignant progression of tumor cells.

In addition to malignant progression, UCPs may alter the therapy sensitivity of tumor cells. In specimens of human ovarian cancers carboplatin/paclitaxel-resistant cancers showed decreased UCP2 protein abundances as compared to the sensitive ones (Pons et al., 2012). Likewise, progression-free and overall survival of patients with inoperable lung cancer who received cisplatin-based chemotherapy was higher when tumors expressed high levels of UCP2 as compared to tumors with low UCP2 levels (Su et al., 2012). A possible explanation of the latter observation is that especially in lung tumors with mutated p53, cisplatin elicits oxidative stress that induces pro-survival signaling. High UCP2 expression, however, diminishes cisplatin-evoked oxidative stress and, in turn, decreases the pro-survival signals (Su et al., 2012).

In lung cancer cell lines with wildtype p53, in contrast, down-regulation of UCP2 results in significantly increased paclitaxel-induced cell death (Su et al., 2012). Similarly, overexpression of UCP2 in a human colon cancer cell line has been shown to blunt topoisomerase I inhibitor CPT-11-induced accumulation of reactive oxygen species and apoptosis *in vitro* and to confer CPT-11 resistance of tumor *xeno*grafts (Derdak et al., 2008). In addition, in pancreatic adenocarcinoma, non-small cell lung adenocarcinoma, and bladder carcinoma cell lines IC_{50} values of the anticancer drug gemcitabine increase with intrinsic UCP2 mRNA abundance. Furthermore, UCP2 overexpression strongly decreases gemcitabine-induced mitochondrial superoxide formation and protects cancer cells from apoptosis (Dalla Pozza et al., 2012). Finally, metabolic changes including UCP2 up-regulation and UCP2-mediated uncoupling of oxidative phosphorylation have been demonstrated in multidrug-resistant subclones of various tumor cell lines (Harper et al., 2002). Similarly, in acute myeloid leukemia cells, UCP2 up-regulation has been shown to foster the Warburg effect (i.e., anaerobic glycolysis in the absence of respiratory impairment) (Samudio et al., 2008).

UCP2 expression is stimulated by co-culturing of these leukemia cells with bone marrow-derived mesenchymal stromal cells (Samudio et al., 2008). Other stimuli of UCP expression/activity are hydrogen peroxide as shown for UCP5 in colon cancer cells (Santandreu et al., 2009) and gemcitabine chemotherapy as reported for UCP2 in pancreatic, lung and bladder cancer cell lines (Dalla Pozza et al., 2012). Collectively, these data suggest that tumor cells may acquire resistance to chemotherapy by up-regulation of UCPs and lowering of the therapy-evoked mitochondrial formation of reactive oxygen species (Robbins and Zhao, 2011).

Accordingly, experimental targeting of UCPs has been demonstrated to sensitize tumor cells to chemotherapy *in vitro*. For instance, genipin-induced inhibition or glutathionylation of UCP2 sensitizes drug-resistant leukemia subclones to chemotherapy with menadione, doxorubicin, or epirubicin (Mailloux et al., 2010; Pfefferle et al., 2012). Likewise, UCP2 inhibition by genipin or UCP2 mRNA silencing strongly enhances gemcitabine-induced mitochondrial superoxide generation and apoptotic cell death of pancreatic, lung and bladder cancer cell lines (Dalla Pozza et al., 2012). Moreover, UCP2 inhibition has been reported to trigger reactive oxygen species-dependent nuclear translocation of GAPDH and autophagic cell death in pancreatic adenocarcinoma cells (Dando et al., 2013) Together, this suggests that targeting UCPs might be a promising strategy to overcome resistance to anti-cancer therapies in the clinic. Notably, in an acute myeloid leukemia cell line, the cytotoxicity of cisplatin has been proposed to be in part mediated by cisplatin-dependent down-regulation of UCPs (Samudio et al., 2008) suggesting that established chemotherapy regimes already may co-target UCPs.

It is tempting to speculate that UCPs may also confer resistance to radiotherapy. One could hypothesize that UCPs adapt the tumor cells to a "relatively radioprotected" hypoxic microenvironment by decreasing hypoxia-associated mitochondrial formation of reactive oxygen species. Such UCP function in hypoxia resistance has been demonstrated for a lung adenocarcinoma cell line (Deng et al., 2012). Notably, radiation induces up-regulation of UCP2 expression as shown in colon carcinoma cells (Sreekumar et al., 2001) and in a radiosensitive subclone of B cell lymphoma (Voehringer et al., 2000). On the one hand, this UCP2 up-regulation might facilitate radiation-induced apoptosis induction by accelerating the break-down of $\Delta\Psi_m$ as proposed by the authors of these studies. On the other hand, radiation-induced UCP2 upregulation might be radioprotective by lowering the radiation-induced burden of reactive oxygen species. As a matter of fact, multi-resistant subclones of leukemia cells show higher UCP2 protein expression, lower $\Delta\Psi_m$, lower radiation induced formation of reactive oxygen species and decreased DNA damage as compared to their parental sensitive cells (Harper et al., 2002).

In summary, UCPs suppress the formation of $O_2{\cdot}^-$, a byproduct of the mitochondrial respiration chain and a major source of oxidative stress. In some cancers UCPs in particular UCP2 are highly upregulated and may contribute to the reprogramming of the cell metabolism that results in chemoresistance (for review see Baffy, 2010; Baffy et al., 2011) or even radioresistance. Moreover, recent studies imply that UCP2 may repress p53-mediated apoptosis providing a potential new mechanism of how UCP2 contributes to cancer development (Robbins and Zhao, 2011).

Together, these observations suggest that ion transport processes are critically involved in evasion from radiation stress, and intrinsic or hypoxic radioresistance. Since ion transport-mediated radioresistance might underlie failure of radiotherapy, concepts which combine ion transport targeting with radiotherapy hold promise for new therapy strategies in the future. A summary of how ion transport can be harnessed for anticancer therapy and how these therapy strategies might be combined with radiotherapy is given in the next paragraphs.

TARGETING ION TRANSPORTS IN RADIOTHERAPY

An important reason for the study of ion transports in the context of radiotherapy is the possible translation of the acquired knowledge into anti-cancer therapy. Many pharmacological modulators

of ion transports are already in clinical use or currently tested in clinical trials (Wulff and Castle, 2010). Moreover, tumors often over-express certain types of transport proteins.

These proteins such as the transient receptor melastatin 8 (TRPM8) non-selective cation channel in prostate cancer have been used in clinical trials as tumor-associated antigen for anti-tumor vaccination (Fuessel et al., 2006). Tumor promoting inflammation and anti-tumor immune effects are evolving fields of preclinical and clinical research (Hanahan and Weinberg, 2011). Preclinical evidence supports the thesis that tumors have to develop immune-evading capacities in order to grow into macroscopic, clinically detectable lesions (Koebel et al., 2007; Teng et al., 2008). Possible mechanisms are the secretion of cytokines and chemokines by cancer and tumor stroma cells (Vianello et al., 2006; Shields et al., 2010), the priming of infiltrating T-lymphocytes toward immunosuppressive regulatory T-cells and the recruitment of myeloid-derived suppressor cells and tumor-associated macrophages (Tanchot et al., 2013; Oleinika et al., 2013). Irradiation of tumors has been shown to impair on the one hand the immunosuppressive action of the tumor and on the other to induce so-called "immunogenic" cell death within the tumor with translocation of calreticulin to the plasma membrane, release of HMGB1 or ATP (Formenti and Demaria, 2013). Preclinical studies showed a synergistic effect of irradiation and several immunotherapeutic approaches such as dendritic cell injection (Finkelstein et al., 2012), anti-CTLA-4-antibody (Grosso and Jure-Kunkel, 2013), and vaccines (Chakraborty et al., 2004). Interestingly, for combination with anti-CTLA-4 antibody a synergistic effect could only be demonstrated for fractionated but not for single-dose irradiation (Demaria and Formenti, 2012).

In addition, over-expressed transport proteins in tumors can be harnessed to target drugs, cytokines, or radioactivity to the tumor cells (Hartung et al., 2011). One example is the specific surface expression of ClC-3 Cl^- channels by glioblastoma (and other tumor entities) which suggests ClC-3 as an excellent and highly specific target for anti-glioblastoma therapy. Chlorotoxin which is a 36 amino acid-long peptide from the venom of the scorpion *Leiurus quinquestriatus* has been found to inhibit ClC-3 and to preferentially bind to the cell surface of a variety of human malignancies. This specificity probably comes from the highly affine binding of chlorotoxin to a lipid raft-anchored complex of matrix metalloproteinase-2, membrane type-I MMP, and transmembrane inhibitor of metalloproteinase-2, as well as ClC-3 (Veiseh et al., 2007). Ongoing clinical trials successfully used ^{131}I-labeled chlorotoxin as glioblastoma-specific PET-tracer (Hockaday et al., 2005) and for targeted radiation of glioblastoma cells (Mamelak and Jacoby, 2007). Due to the low surface expression of ClC-3 in normal tissue, chlorotoxin exhibits little or no affinity to normal cells (Lyons et al., 2002). If the *in vitro* and mouse data on radiation-stimulated glioblastoma migration reflect indeed the *in vivo* situation in glioblastoma patients, a clinical setting might be envisaged in which radiation-induced glioblastoma spreading is prevented by combining radiotherapy with chlorotoxin blockade of ClC-3 channels.

CONCLUDING REMARKS

Interdisciplinary approaches linking radiobiology with physiology brought about the first peaces of evidence suggesting a functional significance of ion transport processes for the survival of irradiated tumor cells. The few reports published up to now on this topic are confined to phenomena occurring in the plasma membrane due to the methodological restrictions of studying these processes in the membranes of mitochondria, endoplasmic reticulum, or nuclear envelope. Intracellular membrane transports, however, might similarly impact tumor cell radiosensitivity. This is suggested by the notion that intracellular Cl^- channel CLIC1 protein expression regulates radiosensitivity in laryngeal cancer cells (Kim et al., 2010). However, the molecular mechanisms underlying, e.g., radiation-induced transport modifications, or downstream signaling events are far from being understood. Despite all these limitations, our current knowledge already clearly indicates that the observed transport processes may be crucial for the survival of the tumor and, thus, are worthwhile to spend further and more effort in this field which might lead to new strategies for cancer treatment in the future.

ACKNOWLEDGMENTS

This work has been supported by the Wilhelm-Sander-Stiftung (2011.083.1). Dominik Klumpp and Benjamin Stegen were supported by the DFG International Graduate School 1302 (TP T9).

REFERENCES

Anderson, E. J., Yamazaki, H., and Neufer, P. D. (2007). Induction of endogenous uncoupling protein 3 suppresses mitochondrial oxidant emission during fatty acid-supported respiration. *J. Biol. Chem.* 282, 31257–31266. doi: 10.1074/jbc.M706129200

Arcangeli, A. (2011). Ion channels and transporters in cancer. 3. Ion channels in the tumor cell-microenvironment cross talk. *Am. J. Physiol. Cell Physiol.* 301, C762–C771.

Asuthkar, S., Nalla, A. K., Gondi, C. S., Dinh, D. H., Gujrati, M., Mohanam, S., et al. (2011). Gadd45a sensitizes medulloblastoma cells to irradiation and suppresses MMP-9-mediated EMT. *Neuro Oncol.* 13, 1059–1073. doi: 10.1093/neuonc/nor109

Auperin, A., Arriagada, R., Pignon, J. P., Le Pechoux, C., Gregor, A., Stephens, R. J., et al. (1999). Prophylactic cranial irradiation for patients with small-cell lung cancer in complete remission. prophylactic cranial irradiation overview collaborative group. *N. Engl. J. Med.* 341, 476–484. doi: 10.1056/NEJM199908123410703

Ayyasamy, V., Owens, K. M., Desouki, M. M., Liang, P., Bakin, A., Thangaraj, K., et al. (2011). Cellular model of Warburg effect identifies tumor promoting function of UCP2 in breast cancer and its suppression by genipin. *PLoS ONE* 6:e24792. doi: 10.1371/journal.pone.0024792

Badiga, A. V., Chetty, C., Kesanakurti, D., Are, D., Gujrati, M., Klopfenstein, J. D., et al. (2011). MMP-2 siRNA inhibits radiation-enhanced invasiveness in glioma cells. *PLoS ONE* 6:e20614. doi: 10.1371/journal.pone.0020614

Baffy, G. (2010). Uncoupling protein-2 and cancer. *Mitochondrion* 10, 243–252. doi: 10.1016/j.mito.2009.12.143

Baffy, G., Derdak, Z., and Robson, S. C. (2011). Mitochondrial recoupling: a novel therapeutic strategy for cancer. *Br. J. Cancer* 105, 469–474.

Barendsen, G. W. (1982). Dose fractionation, dose rate and iso-effect relationships for normal tissue responses. *Int. J. Radiat. Oncol. Biol. Phys.* 8, 1981–1997. doi: 10.1016/0360-301690459-X

Bernier, J., Hall, E. J., and Giaccia, A. (2004). Radiation oncology: a century of achievements. *Nat. Rev. Cancer* 4, 737–747. doi: 10.1038/nrc1451

Canazza, A., Calatozzolo, C., Fumagalli, L., Bergantin, A., Ghielmetti,

F., Fariselli, L., et al. (2011). Increased migration of a human glioma cell line after *in vitro* CyberKnife irradiation. *Cancer Biol. Ther.* 12, 629–633. doi: 10.4161/cbt.12.7.16862

Caraceni, P., Ryu, H. S., Van Thiel, D. H., and Borle, A. B. (1995). Source of oxygen free radicals produced by rat hepatocytes during postanoxic reoxygenation. *Biochim. Biophys. Acta* 1268, 249–254. doi: 10.1016/0167-488900077-6

Casneuf, V. F., Fonteyne, P., Van Damme, N., Demetter, P., Pauwels, P., De Hemptinne, B., et al. (2008). Expression of SGLT1, Bcl-2 and p53 in primary pancreatic cancer related to survival. *Cancer Invest.* 26, 852–859. doi: 10.1080/07357900801956363

Catacuzzeno, L., Aiello, F., Fioretti, B., Sforna, L., Castigli, E., Ruggieri, P., et al. (2010). Serum-activated K and Cl currents underlay U87-MG glioblastoma cell migration. *J. Cell Physiol.* 226, 1926–1933. doi: 10.1002/jcp.22523

Chakraborty, M., Abrams, S. I., Coleman, C. N., Camphausen, K., Schlom, J., and Hodge, J. W. (2004). External beam radiation of tumors alters phenotype of tumor cells to render them susceptible to vaccine-mediated T-cell killing. *Cancer Res.* 64, 4328–4337. doi: 10.1158/0008-5472.CAN-04-0073

Crompton, M. (1999). The mitochondrial permeability transition pore and its role in cell death. *Biochem. J.* 341, 233–249.

Cuddapah, V. A., and Sontheimer, H. (2010). Molecular interaction and functional regulation of ClC-3 by Ca2+/calmodulin-dependent protein kinase II (CaMKII) in human malignant glioma. *J. Biol. Chem.* 285, 11188–11196. doi: 10.1074/jbc.M109.097675

Cullis, P. M., Jones, G. D. D., Lea, J., Symons, M. C. R., and Sweeney, M. (1987). The effects of ionizing radiation on deoxyribonucleic acid. Part 5. The role of thiols in chemical repair. *J. Chem. Soc., Perkin Trans. 2,* 1907–1914. doi: 10.1039/p29870001907

Dale, R. G. (1985). The application of the linear-quadratic dose-effect equation to fractionated and protracted radiotherapy. *Br. J. Radiol.* 58, 515–528. doi: 10.1259/0007-1285-58-690-515

Dalla Pozza, E., Fiorini, C., Dando, I., Menegazzi, M., Sgarbossa, A., Costanzo, C., et al. (2012). Role of mitochondrial uncoupling protein 2 in cancer cell resistance to gemcitabine. *Biochim. Biophys. Acta* 1823, 1856–1863. doi: 10.1016/j.bbamcr.2012.06.007

Dando, I., Fiorini, C., Pozza, E. D., Padroni, C., Costanzo, C., Palmieri, M., et al. (2013). UCP2 inhibition triggers ROS-dependent nuclear translocation of GAPDH and autophagic cell death in pancreatic adenocarcinoma cells. *Biochim. Biophys. Acta* 1833, 672–679. doi: 10.1016/j.bbamcr.2012.10.028

Darby, S., Mcgale, P., Correa, C., Taylor, C., Arriagada, R., Clarke, M., et al. (2011). Effect of radiotherapy after breast-conserving surgery on 10-year recurrence and 15-year breast cancer death: meta-analysis of individual patient data for 10, 801 women in 17 randomised trials. *Lancet* 378, 1707–1716. doi: 10.1016/S0140-673661629-2

Demaria, S., and Formenti, S. C. (2012). Radiation as an immunological adjuvant: current evidence on dose and fractionation. *Front. Oncol.* 2:153. doi: 10.3389/fonc.2012.00153

Deng, S., Yang, Y., Han, Y., Li, X., Wang, X., Li, X., et al. (2012). UCP2 inhibits ROS-mediated apoptosis in A549 under hypoxic conditions. *PLoS ONE* 7:e30714. doi: 10.1371/journal.pone.0030714

Derdak, Z., Mark, N. M., Beldi, G., Robson, S. C., Wands, J. R., and Baffy, G. (2008). The mitochondrial uncoupling protein-2 promotes chemoresistance in cancer cells. *Cancer Res.* 68, 2813–2819. doi: 10.1158/0008-5472.CAN-08-0053

Dittmann, K., Mayer, C., Kehlbach, R., Rothmund, M. C., and Peter Rodemann, H. (2009). Radiation-induced lipid peroxidation activates src kinase and triggers nuclear EGFR transport. *Radiother. Oncol.* 92, 379–382. doi: 10.1016/j.radonc.2009.06.003

Dittmann, K., Mayer, C., Rodemann, H. P., and Huber, S. M. (2013). EGFR cooperates with glucose transporter SGLT1 to enable chromatin remodeling in response to ionizing radiation. *Radiother. Oncol.* 107, 247–251. doi: 10.1016/j.radonc.2013.03.016

Dorn, G. W. 2nd. (2013). Molecular mechanisms that differentiate apoptosis from programmed necrosis. *Toxicol. Pathol.* 41, 227–234. doi: 10.1177/0192623312466961

Echtay, K. S., Roussel, D., St-Pierre, J., Jekabsons, M. B., Cadenas, S., Stuart, J. A., et al. (2002). Superoxide activates mitochondrial uncoupling proteins. *Nature* 415, 96–99. doi: 10.1038/415096a

Eckert, F., Alloussi, S., Paulsen, F., Bamberg, M., Zips, D., Spillner, P. et al. (2013). Prospective evaluation of a hydrogel spacer for rectal separation in dose-escalated intensity-modulated radiotherapy for clinically localized prostate cancer. *BMC Cancer* 13:27. doi: 10.1186/1471-2407-13-27

Eckert, F., Fehm, T., Bamberg, M., and Muller, A. C. (2010a). Small cell carcinoma of vulva: curative multimodal treatment in face of resistance to initial standard chemotherapy. *Strahlenther. Onkol.* 186, 521–524.

Eckert, F., Matuschek, C., Mueller, A. C., Weinmann, M., Hartmann, J. T., Belka, C., et al. (2010b). Definitive radiotherapy and single-agent radiosensitizing ifosfamide in patients with localized, irresectable soft tissue sarcoma: a retrospective analysis. *Radiat. Oncol.* 5, 55.

Eckert, F., Gani, C., Bamberg, M., and Muller, A. C. (2012). Cerebral metastases in extrapulmonary cell carcinoma: implications for the use of prophylactic cranial irradiation. *Strahlenther. Onkol.* 188, 478–483. doi: 10.1007/s00066-012-0084-5

Ernest, N. J., Weaver, A. K., Van Duyn, L. B., and Sontheimer, H. W. (2005). Relative contribution of chloride channels and transporters to regulatory volume decrease in human glioma cells. *Am. J. Physiol. Cell Physiol.* 288, C1451–1460. doi: 10.1152/ajpcell.00503.2004

Fink, B. D., Hong, Y. S., Mathahs, M. M., Scholz, T. D., Dillon, J. S., and Sivitz, W. I. (2002). UCP2-dependent proton leak in isolated mammalian mitochondria. *J. Biol. Chem.* 277, 3918–3925. doi: 10.1074/jbc.M107955200

Finkelstein, S. E., Iclozan, C., Bui, M. M., Cotter, M. J., Ramakrishnan, R., Ahmed, J., et al. (2012). Combination of external beam radiotherapy (EBRT) with intratumoral injection of dendritic cells as neo-adjuvant treatment of high-risk soft tissue sarcoma patients. *Int. J. Radiat. Oncol. Biol. Phys.* 82, 924–932. doi: 10.1016/j.ijrobp.2010.12.068

Formenti, S. C., and Demaria, S. (2013). Combining radiotherapy and cancer immunotherapy: a paradigm shift. *J. Natl. Cancer Inst.* 105, 256–265. doi: 10.1093/jnci/djs629

Fuessel, S., Meye, A., Schmitz, M., Zastrow, S., Linne, C., Richter, K., et al. (2006). Vaccination of hormone-refractory prostate cancer patients with peptide cocktail-loaded dendritic cells: results of a phase I clinical trial. *Prostate* 66, 811–821. doi: 10.1002/pros.20404

Fyles, A., Milosevic, M., Hedley, D., Pintilie, M., Levin, W., Manchul, L., et al. (2002). Tumor hypoxia has independent predictor impact only in patients with node-negative cervix cancer. *J. Clin. Oncol.* 20, 680–687. doi: 10.1200/JCO.20.3.680

Fyles, A., Milosevic, M., Pintilie, M., Syed, A., Levin, W., Manchul, L., et al. (2006). Long-term performance of interstial fluid pressure and hypoxia as prognostic factors in cervix cancer. *Radiother. Oncol.* 80, 132–137. doi: 10.1016/j.radonc.2006.07.014

Ganapathy, V., Thangaraju, M., and Prasad, P. D. (2009). Nutrient transporters in cancer: relevance to Warburg hypothesis and beyond. *Pharmacol. Ther.* 121, 29–40. doi: 10.1016/j.pharmthera.2008.09.005

Garcia-Martinez, C., Sibille, B., Solanes, G., Darimont, C., Mace, K., Villarroya, F., et al. (2001). Overexpression of UCP3 in cultured human muscle lowers mitochondrial membrane potential, raises ATP/ADP ratio, and favors fatty acid vs. glucose oxidation. *FASEB J.* 15, 2033–2035.

German-Cancer-Aid. (2013a). *Homepage*. Available online at: http://www.krebshilfe.de/krebszahlen.html

German-Cancer-Aid. (2013b). *Information Booklet*. Available online at: http://www.krebshilfe.de/fileadmin/Inhalte/Downloads/PDFs/Blaue_Ratgeber/053_strahlen.pdf.

Glenny, A. M., Furness, S., Worthington, H. V., Conway, D. I., Oliver, R., Clarkson, J. E., et al. (2010). Interventions for the treatment of oral cavity and oropharyngeal cancer: radiotherapy. *Cochrane Database Syst. Rev.* CD006387. doi: 10.1002/14651858.CD006387.pub2

Gomez-Ospina, N., Tsuruta, F., Barreto-Chang, O., Hu, L., and Dolmetsch, R. (2006). The C terminus of the L-type voltage-gated calcium channel Ca(V)1.2 encodes a transcription factor. *Cell* 127, 591–606. doi: 10.1016/j.cell.2006.10.017

Gonidi, M., Athanassiadou, A. M., Patsouris, E., Tsipis, A., Dimopoulos, S., Kyriakidou, V., et al. (2011). Mitochondrial UCP4 and bcl-2 expression in imprints of breast carcinomas: relationship with DNA ploidy and classical prognostic factors.

Pathol. Res. Pract. 207, 377–382. doi: 10.1016/j.prp.2011.03.007

Grills, I. S., Hope, A. J., Guckenberger, M., Kestin, L. L., Werner-Wasik, M., Yan, D., et al. (2012). A collaborative analysis of stereotactic lung radiotherapy outcomes for early-stage non-small-cell lung cancer using daily online cone-beam computed tomography image-guided radiotherapy. *J. Thorac. Oncol.* 7, 1382–1393. doi: 10.1097/JTO.0b013e318260e00d

Gross, G. J., and Peart, J. N. (2003). KATP channels and myocardial preconditioning: an update. *Am. J. Physiol. Heart Circ. Physiol.* 285, H921–H930.

Grosso, J. F., and Jure-Kunkel, M. N. (2013). CTLA-4 blockade in tumor models: an overview of preclinical and translational research. *Cancer Immun.* 13, 5.

Haas, B. R., Cuddapah, V. A., Watkins, S., Rohn, K. J., Dy, T. E., and Sontheimer, H. (2011). With-No-Lysine Kinase 3 (WNK3) stimulates glioma invasion by regulating cell volume. *Am. J. Physiol. Cell Physiol.* 301, C1150–C1160. doi: 10.1152/ajpcell.00203.2011

Haas, B. R., and Sontheimer, H. (2010). Inhibition of the sodium-potassium-chloride cotransporter isoform-1 reduces glioma invasion. *Cancer Res.* 70, 5597–5606. doi: 10.1158/0008-5472.CAN-09-4666

Hanahan, D., and Weinberg, R. A. (2011). Hallmarks of cancer: the next generation. *Cell* 144, 646–674. doi: 10.1016/j.cell.2011.02.013

Harada, H. (2011). How can we overcome tumor hypoxia in radiation therapy. *J. Radiat. Res.* 52, 545–556.

Harper, M. E., Antoniou, A., Villalobos-Menuey, E., Russo, A., Trauger, R., Vendemelio, M., et al. (2002). Characterization of a novel metabolic strategy used by drug-resistant tumor cells. *FASEB J.* 16, 1550–1557. doi: 10.1096/fj.02-0541com

Hartung, F., Stuhmer, W., and Pardo, L. A. (2011). Tumor cell-selective apoptosis induction through targeting of K(V)10.1 via bifunctional TRAIL antibody. *Mol. Cancer* 10, 109.

Hatzikirou, H., Basanta, D., Simon, M., Schaller, K., and Deutsch, A. (2012). 'Go or Grow': the key to the emergence of invasion in tumour progression. *Math. Med. Biol.* 29, 49–65. doi: 10.1093/imammb/dqq011

Heise, N., Palme, D., Misovic, M., Koka, S., Rudner, J., Lang, F., et al. (2010). Non-selective cation channel-mediated Ca2+-entry and activation of Ca2+/calmodulin-dependent kinase II contribute to G2/M cell cycle arrest and survival of irradiated leukemia cells. *Cell Physiol. Biochem.* 26, 597–608. doi: 10.1159/000322327

Helmke, B. M., Reisser, C., Idzko, M., Dyckhoff, G., and Herold-Mende, C. (2004). Expression of SGLT-1 in preneoplastic and neoplastic lesions of the head and neck. *Oral Oncol.* 40, 28–35. doi: 10.1016/S1368-837500129-5

Hockaday, D. C., Shen, S., Fiveash, J., Raubitschek, A., Colcher, D., Liu, A., et al. (2005). Imaging glioma extent with 131I-TM-601. *J. Nucl. Med.* 46, 580–586.

Horimoto, M., Resnick, M. B., Konkin, T. A., Routhier, J., Wands, J. R., and Baffy, G. (2004). Expression of uncoupling protein-2 in human colon cancer. *Clin. Cancer Res.* 10, 6203–6207. doi: 10.1158/1078-0432.CCR-04-0419

Horiot, J. C., Le Fur, R., N'guyen, T., Chenal, C., Schraub, S., Alfonsi, S., et al. (1992). Hyperfractionation versus conventional fractionation in oropharyngeal carcinoma: final analysis of a randomized trial of the EORTC cooperative group of radiotherapy. *Radiother. Oncol.* 25, 231–241. doi: 10.1016/0167-814090242-M

Huber, S. M. (2013). Oncochannels. *Cell Calcium*. 53, 241–255. doi: 10.1016/j.ceca.2013.01.001

Huber, S. M., Misovic, M., Mayer, C., Rodemann, H. P., and Dittmann, K. (2012). EGFR-mediated stimulation of sodium/glucose cotransport promotes survival of irradiated human A549 lung adenocarcinoma cells. *Radiother. Oncol.* 103, 373–379. doi: 10.1016/j.radonc.2012.03.008

Ishikawa, N., Oguri, T., Isobe, T., Fujitaka, K., and Kohno, N. (2001). SGLT gene expression in primary lung cancers and their metastatic lesions. *Jpn. J. Cancer Res.* 92, 874–879. doi: 10.1111/j.1349-7006.2001.tb01175.x

Johnson, J., Nowicki, M. O., Lee, C. H., Chiocca, E. A., Viapiano, M. S., Lawler, S. E., et al. (2009). Quantitative analysis of complex glioma cell migration on electrospun polycaprolactone using time-lapse microscopy. *Tissue Eng. Part C Methods* 15, 531–540. doi: 10.1089/ten.tec.2008.0486

Jones, B., Dale, R. G., and Gaya, A. M. (2006). Linear quadratic modeling of increased late normal-tissue effects in special clinical situations. *Int. J. Radiat. Oncol. Biol. Phys.* 64, 948–953. doi: 10.1016/j.ijrobp.2005.10.016

Jung, J. W., Hwang, S. Y., Hwang, J. S., Oh, E. S., Park, S., and Han, I. O. (2007). Ionising radiation induces changes associated with epithelial-mesenchymal transdifferentiation and increased cell motility of A549 lung epithelial cells. *Eur. J. Cancer* 43, 1214–1224. doi: 10.1016/j.ejca.2007.01.034

Kadenbach, B. (2003). Intrinsic and extrinsic uncoupling of oxidative phosphorylation. *Biochim. Biophys. Acta* 1604, 77–94. doi: 10.1016/S0005-272800027-6

Kargiotis, O., Chetty, C., Gogineni, V., Gondi, C. S., Pulukuri, S. M., Kyritsis, A. P., et al. (2008). uPA/uPAR downregulation inhibits radiation-induced migration, invasion and angiogenesis in IOMM-Lee meningioma cells and decreases tumor growth *in vivo*. *Int. J. Oncol.* 33, 937–947.

Kil, W. J., Tofilon, P. J., and Camphausen, K. (2012). Post-radiation increase in VEGF enhances glioma cell motility *in vitro*. *Radiat. Oncol.* 7, 25. doi: 10.1186/1748-717X-7-25

Kim, J. S., Chang, J. W., Yun, H. S., Yang, K. M., Hong, E. H., Kim, D. H., et al. (2010). Chloride intracellular channel 1 identified using proteomic analysis plays an important role in the radiosensitivity of HEp-2 cells via reactive oxygen species production. *Proteomics* 10, 2589–2604. doi: 10.1002/pmic.200900523

Klotz, L., Venier, N., Colquhoun, A. J., Sasaki, H., Loblaw, D. A., Fleshner, N., et al. (2011). Capsaicin, a novel radiosensitizer, acts via a TRPV6 mediated phenomenon. *J. Clin. Oncol.* 29(Suppl. 7; Abstr. 23).

Koebel, C. M., Vermi, W., Swann, J. B., Zerafa, N., Rodig, S. J., Old, L. J., et al. (2007). Adaptive immunity maintains occult cancer in an equilibrium state. *Nature* 450, 903–907. doi: 10.1038/nature06309

Korshunov, S. S., Skulachev, V. P., and Starkov, A. A. (1997). High protonic potential actuates a mechanism of production of reactive oxygen species in mitochondria. *FEBS Lett.* 416, 15–18. doi: 10.1016/S0014-579301159-9

Kotecha, R., Yamada, Y., Pei, X., Kollmeier, M. A., Cox, B., Cohen, G. N., et al. (2013). Clinical outcomes of high-dose-rate brachytherapy and external beam radiotherapy in the management of clinically localized prostate cancer. *Brachytherapy* 12, 44–49. doi: 10.1016/j.brachy.2012.05.003

Kuai, X. Y., Ji, Z. Y., and Zhang, H. J. (2010). Mitochondrial uncoupling protein 2 expression in colon cancer and its clinical significance. *World J. Gastroenterol.* 16, 5773–5778. doi: 10.3748/wjg.v16.i45.5773

Kuo, S. S., Saad, A. H., Koong, A. C., Hahn, G. M., and Giaccia, A. J. (1993). Potassium-channel activation in response to low doses of gamma-irradiation involves reactive oxygen intermediates in nonexcitatory cells. *Proc. Natl. Acad. Sci. U.S.A.* 90, 908–912. doi: 10.1073/pnas.90.3.908

Langenbacher, M., Abdel-Jalil, R. J., Voelter, W., Weinmann, M., and Huber, S. M. (2013). *In vitro* hypoxic cytotoxicity and hypoxic radiosensitization. Efficacy of the novel 2-nitroimidazole N, N, N-tris[2-(2-nitro-1H-imidazol-1-yl)ethyl]amine. *Strahlenther. Onkol.* 189, 246–254. doi: 10.1007/s00066-012-0273-2

Le Pechoux, C., Laplanche, A., Faivre-Finn, C., Ciuleanu, T., Wanders, R., Lerouge, D., et al. (2011). Clinical neurological outcome and quality of life among patients with limited small-cell cancer treated with two different doses of prophylactic cranial irradiation in the intergroup phase III trial (PCI99-01, EORTC 22003-08004, RTOG (0212). and IFCT 99-01). *Ann. Oncol.* 22, 1154–1163. doi: 10.1093/annonc/mdq576

Leiprecht, N., Munoz, C., Alesutan, I., Siraskar, G., Sopjani, M., Foller, M., et al. (2011). Regulation of Na(+)-coupled glucose carrier SGLT1 by human papillomavirus 18 E6 protein. *Biochem. Biophys. Res. Commun.* 404, 695–700. doi: 10.1016/j.bbrc.2010.12.044

Li, C., and Jackson, R. M. (2002). Reactive species mechanisms of cellular hypoxia-reoxygenation injury. *Am. J. Physiol. Cell Physiol.* 282, C227–241. doi: 10.1152/ajpcell.00112.2001

Liu, X., Chang, Y., Reinhart, P. H., Sontheimer, H., and Chang, Y. (2002). Cloning and characterization of glioma BK, a novel BK channel isoform highly expressed in human glioma cells. *J. Neurosci.* 22, 1840–1849.

Lobikin, M., Chernet, B., Lobo, D., and Levin, M. (2012). Resting potential, oncogene-induced tumorigenesis, and metastasis: the bioelectric basis of cancer *in vivo*. *Phys. Biol.* 9, 065002. doi: 10.1088/1478-3975/9/6/065002

Lu, Z., and Sack, M. N. (2008). ATF-1 is a hypoxia-responsive transcriptional activator of skeletal muscle mitochondrial-uncoupling protein 3. *J. Biol. Chem.* 283, 23410–23418. doi: 10.1074/jbc.M801236200

Lui, V. C., Lung, S. S., Pu, J. K., Hung, K. N., and Leung, G. K. (2010). Invasion of human glioma cells is regulated by multiple chloride channels including ClC-3. *Anticancer Res.* 30, 4515–4524.

Lutz, S. (2007). Palliative whole-brain radiotherapy fractionation: convenience versus cognition. *Cancer* 110, 2363–2365.

Lyons, S. A., O'neal, J., and Sontheimer, H. (2002). Chlorotoxin, a scorpion-derived peptide, specifically binds to gliomas and tumors of neuroectodermal origin. *Glia* 39, 162–173. doi: 10.1002/glia.10083

Maftei, C. A., Bayer, C., Shi, K., Astner, S. T., and Vaupel, P. (2011). Changes in the fraction of total hypoxia and hypoxia subtypes in human squamous cell carcinomas upon fractionated irradiation: evaluation using pattern recognition in microcirculatory supply units. *Radiother. Oncol.* 101, 209–216. doi: 10.1016/j.radonc.2011.05.023

Mailloux, R. J., Adjeitey, C. N., and Harper, M. E. (2010). Genipin-induced inhibition of uncoupling protein-2 sensitizes drug-resistant cancer cells to cytotoxic agents. *PLoS ONE* 5:e13289. doi: 10.1371/journal.pone.0013289

Mamelak, A. N., and Jacoby, D. B. (2007). Targeted delivery of antitumoral therapy to glioma and other malignancies with synthetic chlorotoxin (TM-601). *Expert Opin. Drug Deliv.* 4, 175–186. doi: 10.1517/17425247.4.2.175

Marks, L. B., and Dewhirst, M. (1991). Accelerated repopulation: friend or foe. Exploiting changes in tumor growth characteristics to improve the "efficiency" of radiotherapy. *Int. J. Radiat. Oncol. Biol. Phys.* 21, 1377–1383. doi: 10.1016/0360-301690301-J

Masumoto, K., Tsukimoto, M., and Kojima, S. (2013). Role of TRPM2 and TRPV1 cation channels in cellular responses to radiation-induced DNA damage. *Biochim. Biophys. Acta* 1830, 3382–3390. doi: 10.1016/j.bbagen.2013.02.020

Mccoy, E. S., Haas, B. R., and Sontheimer, H. (2010). Water permeability through aquaporin-4 is regulated by protein kinase C and becomes rate-limiting for glioma invasion. *Neuroscience* 168, 971–981. doi: 10.1016/j.neuroscience.2009.09.020

Mccoy, E., and Sontheimer, H. (2007). Expression and function of water channels (aquaporins) in migrating malignant astrocytes. *Glia* 55, 1034–1043. doi: 10.1002/glia.20524

Mcferrin, M. B., and Sontheimer, H. (2006). A role for ion channels in glioma cell invasion. *Neuron Glia Biol.* 2, 39–49. doi: 10.1017/S1740925X06000044

Mcleod, C. J., Aziz, A., Hoyt, R. F. Jr., Mccoy, J. P. Jr., and Sack, M. N. (2005). Uncoupling proteins 2 and 3 function in concert to augment tolerance to cardiac ischemia. *J. Biol. Chem.* 280, 33470–33476. doi: 10.1074/jbc.M505258200

Montana, V., and Sontheimer, H. (2011). Bradykinin promotes the chemotactic invasion of primary brain tumors. *J. Neurosci.* 31, 4858–4867. doi: 10.1523/JNEUROSCI.3825-10.2011

Muller, A. C., Eckert, F., Heinrich, V., Bamberg, M., Brucker, S., and Hehr, T. (2011). Re-surgery and chest wall re-irradiation for recurrent breast cancer: a second curative approach. *BMC Cancer* 11:197. doi: 10.1186/1471-2407-11-197

Muller, A. C., Gani, C., Weinmann, M., Mayer, F., Sipos, B., Bamberg, M., et al. (2012). Limited disease of extra-pulmonary small cell carcinoma. Impact of local treatment and nodal status, role of cranial irradiation. *Strahlenther. Onkol.* 188, 269–273. doi: 10.1007/s00066-011-0045-4

Murata, M., Akao, M., O'rourke, B., and Marban, E. (2001). Mitochondrial ATP-sensitive potassium channels attenuate matrix Ca(2+) overload during simulated ischemia and reperfusion: possible mechanism of cardioprotection. *Circ. Res.* 89, 891–898. doi: 10.1161/hh2201.100205

Nalla, A. K., Asuthkar, S., Bhoopathi, P., Gujrati, M., Dinh, D. H., and Rao, J. S. (2010). Suppression of uPAR retards radiation-induced invasion and migration mediated by integrin beta1/FAK signaling in medulloblastoma. *PLoS ONE* 5:e13006. doi: 10.1371/journal.pone.0013006

Narita, T., Aoyama, H., Hirata, K., Onodera, S., Shiga, T., Kobayashi, H., et al. (2012). Reoxygenation of glioblastoma multiforme treated with fractionated radiotherapy concomitant with temozolomide: changes defined by 18F-fluoromisonidazole positron emission tomography: two case reports. *Jpn. J. Clin. Oncol.* 42, 120–123. doi: 10.1093/jjco/hyr181

Nelson, J. A., and Falk, R. E. (1993). The efficacy of phloridzin and phloretin on tumor cell growth. *Anticancer Res.* 13, 2287–2292.

Nguyen, L. N., and Ang, K. K. (2002). Radiotherapy for cancer of the head and neck: altered fractionation regimens. *Lancet Oncol.* 3, 693–701. doi: 10.1016/S1470-204500906-3

Niyazi, M., Siefert, A., Schwarz, S. B., Ganswindt, U., Kreth, F. W., Tonn, J. C., et al. (2011). Therapeutic options for recurrent malignant glioma. *Radiother. Oncol.* 98, 1–14. doi: 10.1016/j.radonc.2010.11.006

Ohshima, Y., Tsukimoto, M., Harada, H., and Kojima, S. (2012). Involvement of connexin43 hemichannel in ATP release after gamma-irradiation. *J. Radiat. Res.* 53, 551–557. doi: 10.1093/jrr/rrs014

Oleinika, K., Nibbs, R. J., Graham, G. J., and Fraser, A. R. (2013). Suppression, subversion and escape: the role of regulatory T cells in cancer progression. *Clin. Exp. Immunol.* 171, 36–45. doi: 10.1111/j.1365-2249.2012.04657.x

Olsen, M. L., Schade, S., Lyons, S. A., Amaral, M. D., and Sontheimer, H. (2003). Expression of voltage-gated chloride channels in human glioma cells. *J. Neurosci.* 23, 5572–5582.

Ozcan, C., Palmeri, M., Horvath, T. L., Russell, K. S., and Russell, R. R. (2013). Role of uncoupling protein 3 in ischemia-reperfusion injury, arrhythmias and preconditioning. *Am. J. Physiol. Heart Circ. Physiol.* 304, H1192–H1200. doi: 10.1152/ajpheart.00592.2012

Pajonk, F., Vlashi, E., and Mcbride, W. H. (2010). Radiation resistance of cancer stem cells: the 4 R's of radiobiology revisited. *Stem Cells* 28, 639–648. doi: 10.1002/stem.318

Palme, D., Misovic, M., Schmid, E., Klumpp, D., Salih, H. R., Rudner, J., et al. (2013). Kv3.4 potassium channel-mediated electrosignaling controls cell cycle and survival of irradiated leukemia cells. *Pflugers Archiv* 465, 1209–1221. doi 10.1007/s00424-013-1249-5

Pawlik, T. M., and Keyomarsi, K. (2004). Role of cell cycle in mediating sensitivity to radiotherapy. *Int. J. Radiat. Oncol. Biol. Phys.* 59, 928–942. doi: 10.1016/j.ijrobp.2004.03.005

Pfefferle, A., Mailloux, R. J., Adjeitey, C. N., and Harper, M. E. (2012). Glutathionylation of UCP2 sensitizes drug resistant leukemia cells to chemotherapeutics. *Biochim. Biophys. Acta* 1833, 80–89. doi: 10.1016/j.bbamcr.2012.10.006

Pickhard, A. C., Margraf, J., Knopf, A., Stark, T., Piontek, G., Beck, C., et al. (2011). Inhibition of radiation induced migration of human head and neck squamous cell carcinoma cells by blocking of EGF receptor pathways. *BMC Cancer* 11:388. doi: 10.1186/1471-2407-11-388

Pizzo, P., Drago, I., Filadi, R., and Pozzan, T. (2012). Mitochondrial Ca(2)(+) homeostasis: mechanism, role, and tissue specificities. *Pflugers Arch.* 464, 3–17. doi: 10.1007/s00424-012-1122-y

Pons, D. G., Sastre-Serra, J., Nadal-Serrano, M., Oliver, A., Garcia-Bonafe, M., Bover, I., et al. (2012). Initial activation status of the antioxidant response determines sensitivity to carboplatin/paclitaxel treatment of ovarian cancer. *Anticancer Res.* 32, 4723–4728.

Prasad, A., Stone, G. W., Holmes, D. R., and Gersh, B. (2009). Reperfusion injury, microvascular dysfunction, and cardioprotection: the "dark side" of reperfusion. *Circulation* 120, 2105–2112. doi: 10.1161/CIRCULATIONAHA.108.814640

Rades, D., Kieckebusch, S., Lohynska, R., Veninga, T., Stalpers, L. J., Dunst, J., et al. (2007a). Reduction of overall treatment time in patients irradiated for more than three brain metastases. *Int. J. Radiat. Oncol. Biol. Phys.* 69, 1509–1513.

Rades, D., Lohynska, R., Veninga, T., Stalpers, L. J., and Schild, S. E. (2007b). Evaluation of 2 whole-brain radiotherapy schedules and prognostic factors for brain metastases in breast cancer patients. *Cancer* 110, 2587–2592.

Ransom, C. B., Liu, X., and Sontheimer, H. (2002). BK channels in human glioma cells have enhanced calcium sensitivity. *Glia* 38, 281–291. doi: 10.1002/glia.10064

Ransom, C. B., and Sontheimer, H. (2001). BK channels in human glioma cells. *J. Neurophysiol.* 85, 790–803.

Rasola, A., and Bernardi, P. (2011). Mitochondrial permeability transition in Ca(2+)-dependent apoptosis and necrosis. *Cell Calcium* 50, 222–233. doi: 10.1016/j.ceca.2011.04.007

Rieken, S., Habermehl, D., Mohr, A., Wuerth, L., Lindel, K., Weber, K., et al. (2011). Targeting alphanubeta3 and alphanubeta5 inhibits photon-induced hypermigration of malignant glioma cells. *Radiat. Oncol.* 6, 132. doi: 10.1186/1748-717X-6-132

Robbins, D., and Zhao, Y. (2011). New aspects of mitochondrial uncoupling proteins (UCPs) and their roles in tumorigenesis. *Int. J. Mol. Sci.* 12, 5285–5293. doi: 10.3390/ijms12085285

Rodrigues, G., Zindler, J., Warner, A., and Lagerwaard, F. (2013). Recursive partitioning analysis for the prediction of stereotactic radiosurgery brain metastases lesion

control. *Oncologist* 18, 330–335. doi: 10.1634/theoncologist.2012-0316

Ruggieri, P., Mangino, G., Fioretti, B., Catacuzzeno, L., Puca, R., Ponti, D., et al. (2012). The inhibition of KCa3.1 channels activity reduces cell motility in glioblastoma derived cancer stem cells. *PLoS ONE* 7:e47825. doi: 10.1371/journal.pone.0047825

Sack, M. N. (2006). Mitochondrial depolarization and the role of uncoupling proteins in ischemia tolerance. *Cardiovasc. Res.* 72, 210–219. doi: 10.1016/j.cardiores.2006.07.010

Samudio, I., Fiegl, M., Mcqueen, T., Clise-Dwyer, K., and Andreeff, M. (2008). The warburg effect in leukemia-stroma cocultures is mediated by mitochondrial uncoupling associated with uncoupling protein 2 activation. *Cancer Res.* 68, 5198–5205. doi: 10.1158/0008-5472.CAN-08-0555

Santandreu, F. M., Valle, A., Fernandez De Mattos, S., Roca, P., and Oliver, J. (2009). Hydrogen peroxide regulates the mitochondrial content of uncoupling protein 5 in colon cancer cells. *Cell Physiol. Biochem.* 24, 379–390. doi: 10.1159/000257430

Sastre-Serra, J., Nadal-Serrano, M., Pons, D. G., Valle, A., Garau, I., Garcia-Bonafe, M., et al. (2013). The oxidative stress in breast tumors of postmenopausal women is ERalpha/ERbeta ratio dependent. *Free Radic. Biol. Med.* 61C, 11–17. doi: 10.1016/j.freeradbiomed.2013.03.005

Sauer, R., Liersch, T., Merkel, S., Fietkau, R., Hohenberger, W., Hess, C., et al. (2012). Preoperative versus postoperative chemoradiotherapy for locally advanced rectal cancer: results of the German CAO/ARO/AIO-94 randomized phase III trial after a median follow-up of 11 years. *J. Clin. Oncol.* 30, 1926–1933. doi: 10.1200/JCO.2011.40.1836

Schwab, A., Fabian, A., Hanley, P. J., and Stock, C. (2012). Role of ion channels and transporters in cell migration. *Physiol. Rev.* 92, 1865–1913. doi: 10.1152/physrev.00018.2011.

Schwab, A., Nechyporuk-Zloy, V., Fabian, A., and Stock, C. (2007). Cells move when ions and water flow. *Pflugers Arch.* 453, 421–432. doi: 10.1007/s00424-006-0138-6

Sciaccaluga, M., Fioretti, B., Catacuzzeno, L., Pagani, F., Bertollini, C., Rosito, M., et al. (2010). CXCL12-induced glioblastoma cell migration requires intermediate conductance Ca2+-activated K+ channel activity. *Am. J. Physiol. Cell Physiol.* 299, C175–C184. doi: 10.1152/ajpcell.00344.2009

Shields, J. D., Kourtis, I. C., Tomei, A. A., Roberts, J. M., and Swartz, M. A. (2010). Induction of lymphoidlike stroma and immune escape by tumors that express the chemokine CCL21. *Science* 328, 749–752. doi: 10.1126/science.1185837

Singh, H., Stefani, E., and Toro, L. (2012). Intracellular BK(Ca) (iBK(Ca)) channels. *J. Physiol.* 590, 5937–5947. doi: 10.1113/jphysiol.2011.215533

Skulachev, V. P. (1998). Uncoupling: new approaches to an old problem of bioenergetics. *Biochim. Biophys. Acta* 1363, 100–124. doi: 10.1016/S0005-272800091-1

Sofia Vala, I., Martins, L. R., Imaizumi, N., Nunes, R. J., Rino, J., Kuonen, F., et al. (2010). Low doses of ionizing radiation promote tumor growth and metastasis by enhancing angiogenesis. *PLoS ONE* 5:e11222. doi: 10.1371/journal.pone.0011222

Sontheimer, H. (2008). An unexpected role for ion channels in brain tumor metastasis. *Exp. Biol. Med. (Maywood)* 233, 779–791. doi: 10.3181/0711-MR-308

Sreekumar, A., Nyati, M. K., Varambally, S., Barrette, T. R., Ghosh, D., Lawrence, T. S., et al. (2001). Profiling of cancer cells using protein microarrays: discovery of novel radiation-regulated proteins. *Cancer Res.* 61, 7585–7593.

Steinle, M., Palme, D., Misovic, M., Rudner, J., Dittmann, K., Lukowski, R., et al. (2011). Ionizing radiation induces migration of glioblastoma cells by activating BK K(+) channels. *Radiother. Oncol.* 101, 122–126. doi: 10.1016/j.radonc.2011.05.069

Stock, C., and Schwab, A. (2009). Protons make tumor cells move like clockwork. *Pflugers Arch.* 458, 981–992. doi: 10.1007/s00424-009-0677-8

Stupp, R., Van Den Bent, M. J., and Hegi, M. E. (2005). Optimal role of temozolomide in the treatment of malignant gliomas. *Curr. Neurol. Neurosci. Rep.* 5, 198–206. doi: 10.1007/s11910-005-0047-7

Su, W. P., Lo, Y. C., Yan, J. J., Liao, I. C., Tsai, P. J., Wang, H. C., et al. (2012). Mitochondrial uncoupling protein 2 regulates the effects of paclitaxel on Stat3 activation and cellular survival in lung cancer cells. *Carcinogenesis* 33, 2065–2075. doi: 10.1093/carcin/bgs253

Szabo, I., Leanza, L., Gulbins, E., and Zoratti, M. (2012). Physiology of potassium channels in the inner membrane of mitochondria. *Pflugers Arch.* 463, 231–246. doi: 10.1007/s00424-011-1058-7

Talbot, D. A., and Brand, M. D. (2005). Uncoupling protein 3 protects aconitase against inactivation in isolated skeletal muscle mitochondria. *Biochim. Biophys. Acta* 1709, 150–156.

Tanchot, C., Terme, M., Pere, H., Tran, T., Benhamouda, N., Strioga, M., et al. (2013). Tumor-infiltrating regulatory T cells: phenotype, role, mechanism of expansion in situ and clinical significance. *Cancer Microenviron.* 6, 147–157. doi: 10.1007/s12307-012-0122-y

Teng, M. W., Swann, J. B., Koebel, C. M., Schreiber, R. D., and Smyth, M. J. (2008). Immune-mediated dormancy: an equilibrium with cancer. *J. Leukoc. Biol.* 84, 988–993. doi: 10.1189/jlb.1107774

Tolon, R. M., Sanchez-Franco, F., Lopez Fernandez, J., Lorenzo, M. J., Vazquez, G. F., and Cacicedo, L. (1996). Regulation of somatostatin gene expression by veratridine-induced depolarization in cultured fetal cerebrocortical cells. *Brain Res. Mol. Brain Res.* 35, 103–110. doi: 10.1016/0169-328X(95)00188-X

Vanan, I., Dong, Z., Tosti, E., Warshaw, G., Symons, M., and Ruggieri, R. (2012). Role of a DNA damage checkpoint pathway in ionizing radiation-induced glioblastoma cell migration and invasion. *Cell Mol. Neurobiol.* doi: 10.1007/s10571–012-9846-y

Veiseh, M., Gabikian, P., Bahrami, S. B., Veiseh, O., Zhang, M., Hackman, R. C., et al. (2007). Tumor paint: a chlorotoxin:Cy5.5 bioconjugate for intraoperative visualization of cancer foci. *Cancer Res.* 67, 6882–6888. doi: 10.1158/0008-5472.CAN-06-3948

Verheij, M. (2008). Clinical biomarkers and imaging for radiotherapy-induced cell death. *Cancer Metastasis Rev.* 27, 471–480. doi: 10.1007/s10555-008-9131-1

Vianello, F., Papeta, N., Chen, T., Kraft, P., White, N., Hart, W. K., et al. (2006). Murine B16 melanomas expressing high levels of the chemokine stromal-derived factor-1/CXCL12 induce tumor-specific T cell chemorepulsion and escape from immune control. *J. Immunol.* 176, 2902–2914.

Vidal-Puig, A. J., Grujic, D., Zhang, C. Y., Hagen, T., Boss, O., Ido, Y., et al. (2000). Energy metabolism in uncoupling protein 3 gene knockout mice. *J. Biol. Chem.* 275, 16258–16266. doi: 10.1074/jbc.M910179199

Voehringer, D. W., Hirschberg, D. L., Xiao, J., Lu, Q., Roederer, M., Lock, C. B., et al. (2000). Gene microarray identification of redox and mitochondrial elements that control resistance or sensitivity to apoptosis. *Proc. Natl. Acad. Sci. U.S.A.* 97, 2680–2685. doi: 10.1073/pnas.97.6.2680

Watanabe, H., Bohensky, J., Freeman, T., Srinivas, V., and Shapiro, I. M. (2008). Hypoxic induction of UCP3 in the growth plate: UCP3 suppresses chondrocyte autophagy. *J. Cell Physiol.* 216, 419–425. doi: 10.1002/jcp.21408

Watkins, S., and Sontheimer, H. (2011). Hydrodynamic cellular volume changes enable glioma cell invasion. *J. Neurosci.* 31, 17250–17259. doi: 10.1523/JNEUROSCI.3938-11.2011

Weaver, A. K., Bomben, V. C., and Sontheimer, H. (2006). Expression and function of calcium-activated potassium channels in human glioma cells. *Glia* 54, 223–233. doi: 10.1002/glia.20364

Weber, D. C., Casanova, N., Zilli, T., Buchegger, F., Rouzaud, M., Nouet, P., et al. (2009). Recurrence pattern after [(18)F]fluoroethyltyrosine-positron emission tomography-guided radiotherapy for high-grade glioma: a prospective study. *Radiother. Oncol.* 93, 586–592. doi: 10.1016/j.radonc.2009.08.043

Weihua, Z., Tsan, R., Huang, W. C., Wu, Q., Chiu, C. H., Fidler, I. J., et al. (2008). Survival of cancer cells is maintained by EGFR independent of its kinase activity. *Cancer Cell* 13, 385–393. doi: 10.1016/j.ccr.2008.03.015

Wick, W., Wick, A., Schulz, J. B., Dichgans, J., Rodemann, H. P., and Weller, M. (2002). Prevention of irradiation-induced glioma cell invasion by temozolomide involves caspase 3 activity and cleavage of focal adhesion kinase. *Cancer Res.* 62, 1915–1919.

Wild-Bode, C., Weller, M., Rimner, A., Dichgans, J., and Wick, W. (2001). Sublethal irradiation promotes migration and invasiveness of glioma cells: implications for radiotherapy of human glioblastoma. *Cancer Res.* 61, 2744–2750.

Withers, H. R. (Ed). (1975). "The four R's of radiotherapy," in *Advances in Radiation Biology,* Vol. 5, ed J. T. A. H. Lett (New York, NY: Academic Press).

Wright, E. M., Loo, D. D., and Hirayama, B. A. (2011). Biology of human sodium glucose transporters. *Physiol. Rev.* 91, 733–794. doi: 10.1152/physrev.00055.2009

Wulff, H., and Castle, N. A. (2010). Therapeutic potential of KCa3.1 blockers: recent advances and promising trends. *Expert Rev. Clin. Pharmacol.* 3, 385–396. doi: 10.1586/ecp.10.11

Yellon, D. M., and Hausenloy, D. J. (2007). Myocardial reperfusion injury. *N. Engl. J. Med.* 357, 1121–1135. doi: 10.1056/NEJMra071667

Yu, L. C., Huang, C. Y., Kuo, W. T., Sayer, H., Turner, J. R., and Buret, A. G. (2008). SGLT-1-mediated glucose uptake protects human intestinal epithelial cells against Giardia duodenalis-induced apoptosis. *Int. J. Parasitol.* 38, 923–934. doi: 10.1016/j.ijpara.2007.12.004

Zhao, J., Du, C. Z., Sun, Y. S., and Gu, J. (2012). Patterns and prognosis of locally recurrent rectal cancer following multidisciplinary treatment. *World J. Gastroenterol.* 18, 7015–7020. doi: 10.3748/wjg.v18.i47.7015

Zhau, H. E., He, H., Wang, C. Y., Zayzafoon, M., Morrissey, C., Vessella, R. L., et al. (2011). Human prostate cancer harbors the stem cell properties of bone marrow mesenchymal stem cells. *Clin. Cancer Res.* 17, 2159–2169. doi: 10.1158/1078-0432.CCR-10-2523

Zhou, Y. C., Liu, J. Y., Li, J., Zhang, J., Xu, Y. Q., Zhang, H. W., et al. (2011). Ionizing radiation promotes migration and invasion of cancer cells through transforming growth factor-beta-mediated epithelial-mesenchymal transition. *Int. J. Radiat. Oncol. Biol. Phys.* 81, 1530–1537. doi: 10.1016/j.ijrobp.2011.06.1956

Conflict of Interest Statement: The authors declare that the research was conducted in the absence of any commercial or financial relationships that could be construed as a potential conflict of interest.

Received: 30 April 2013; paper pending published: 28 May 2013; accepted: 24 July 2013; published online: 14 August 2013.

*Citation: Huber SM, Butz L, Stegen B, Klumpp D, Braun N, Ruth P and Eckert F (2013) Ionizing radiation, ion transports, and radioresistance of cancer cells. Front. Physiol. **4**:212. doi: 10.3389/fphys.2013.00212*

This article was submitted to Frontiers in Membrane Physiology and Membrane Biophysics, a specialty of Frontiers in Physiology.

Copyright © 2013 Huber, Butz, Stegen, Klumpp, Braun, Ruth and Eckert. This is an open-access article distributed under the terms of the Creative Commons Attribution License (CC BY). The use, distribution or reproduction in other forums is permitted, provided the original author(s) or licensor are credited and that the original publication in this journal is cited, in accordance with accepted academic practice. No use, distribution or reproduction is permitted which does not comply with these terms.